Dissertation zur Erlangung des Doktorgrades
der Fakultät für Chemie und Pharmazie
der Ludwig-Maximilians-Universität München

The poly(A)-binding protein Nab2 functions in RNA polymerase III transcription

Luitpold Maximilian Reuter

aus

Regensburg, Deutschland

2015

Erklärung

Diese Dissertation wurde im Sinne von § 7 der Promotionsordnung vom 28. November 2011 von Frau Prof. Dr. Katja Sträßer betreut.

Eidesstattliche Versicherung

Diese Dissertation wurde eigenständig und ohne unerlaubte Hilfe erarbeitet.

München, 21.09.2015

L. Maximilian Reuter

Dissertation eingereicht am: 21.09.2015

1. Gutachterin / 1. Gutachter: Prof. Dr. Katja Sträßer

2. Gutachterin / 2. Gutachter: Prof. Dr. Klaus Förstemann

Mündliche Prüfung am: 03.11.2015

'The road not taken'

TWO roads diverged in a yellow wood,
And sorry I could not travel both
And be one traveler, long I stood
And looked down one as far as I could
To where it bent in the undergrowth;

THEN took the other, as just as fair,
And having perhaps the better claim,
Because it was grassy and wanted wear;
Though as for that the passing there
Had worn them really about the same,

AND both that morning equally lay
In leaves no step had trodden black.
Oh, I kept the first for another day!
Yet knowing how way leads on to way,
I doubted if I should ever come back.

I shall be telling this with a sigh
Somewhere ages and ages hence:
Two roads diverged in a wood, and I—
I took the one less traveled by,
And that has made all the difference.

Robert Frost, 1916

Für meine Familie

Summary

Gene expression and hence the fine-tuned and well-orchestrated transcription of genes is a fundamental process in living cells. Beside RNA polymerase II (RNAPII), which transcribes protein-coding genes and non-coding RNAs, RNA polymerase III (RNAPIII) synthesizes small RNAs, the most prominent being tRNAs. These RNAs are highly structured and have a central function in translation and cell metabolism. Although the basic mechanism of RNAPIII transcription is well understood, many molecular details of this transcription system remain elusive.

In the present study, we identified - by a genome-wide approach - that Nab2, a poly(A)-binding protein important for correct poly(A) tail length of mRNAs and nuclear mRNA export, is present at all RNAPIII-transcribed genes in the model organism *Saccharomyces cerevisiae*. Remarkably, this occupancy is specific for RNAPIII and independent of RNAPII. Analysis of the occupancy of Nab2 at RNAPIII-transcribed genes furthermore unveiled that it is dependent on active RNAPIII transcription. After generating a novel temperature-sensitive allele of *NAB2*, *nab2-34*, we could show that Nab2 is required for the occupancy of RNAPIII at its target genes.

In addition, we found that Nab2 directly interacts with RNAPIII and its precursor transcripts, suggesting a function of Nab2 in RNAPIII transcription. Importantly, impairment of Nab2 function causes an RNAPIII transcription defect *in vivo* and *in vitro* that can be rescued by the addition of recombinant Nab2. Stimulating the transcriptional activity of a minimal *in vitro* transcription system in a dose-dependent manner demonstrated that the function of Nab2 in RNAPIII transcription is direct.

Investigation of the molecular function of Nab2 in RNAPIII transcription revealed the involvement of the essential transcription initiation factor TFIIIB. Interestingly, the TFIIIB subunit Bdp1 and thus most likely the whole TFIIIB complex is less recruited to its target genes in our mutant *NAB2* strain. Consistently, Brf1, another TFIIIB subunit, interacted with Nab2 *in vivo*. Having found that TFIIIC was not affected by *nab2-34* nor did TFIIIC interact with Nab2, we studied how Nab2 specifically influences TFIIIB on RNAPIII genes. These experiments revealed that Nab2 increased the binding of TFIIIB to promoter DNA and is thus most likely required for efficient assembly and stability of the RNAPIII transcription initiation complex in *S. cerevisiae*.

Taken together, we discovered that Nab2, an important mRNA biogenesis factor, is a novel player required for full RNAPIII transcription by stabilizing TFIIIB and RNAPIII on promoter DNA.

Publications

Substantial parts of this thesis have been already published in:

Reuter, L.M., Meinel, D. M., and Sträßer, K., (2015), The poly(A)-binding protein Nab2 functions in RNA polymerase III transcription, *Genes & Development*, 29 (14), 1565-1575

In addition I contributed to the following publication:

Meier K., Mathieu E. L., Finkernagel F., Reuter L. M., Scharfe M., Doehlemann G., Jarek M., and Brehm A., (2012), LINT, a Novel dL(3)mbt-Containing Complex, Represses Malignant Brain Tumour Signature Genes, *PLOS Genetics*, 8 (5), e1002676

Abbreviations

Amino acids are abbreviated according to the standard single or three letter code. The nucleotides Adenine, Cytosine, Guanine, Thymine, and Uracil are abbreviated A, C, G, T, and U, respectively. Standard unit prefixes are used when needed. The abbreviations used throughout this study are listed below in an alphabetical order:

α	Anti	EMSA	Electromobility shift assay
aa	Amino acid	ER	Endoplasmic reticulum
°C	Celsius	FACT	Facilitates chromatin transcription
AID	Auxin-inducible degron		
APS	Ammonium persulfate	6-FAM	6-carboxyfluorescein
ARE	AU-rich element	Fig.	Figure
bp	Base pair	gDNA	Genomic DNA
C-	Carboxy-terminal	GFP	Green fluorescent protein
CBP	Calmodulin binding peptide	GST	Glutathione-S-transferase
		h	Hour
cDNA	CopyDNA	HEK293	A human embryonic kidney cell line
ChIP	Chromatin Immunoprecipitation	HeLa	A human cervical cancer derived cell line (Henrietta Lacks)
CPF	Cleavage and Polyadenylation factor		
CRAC	Crosslinking and analysis of cDNA	HEPES	4-(2-hydroxyethyl)-1-piperazineethanesulfonic acid
Da	Dalton		
DAPI	4′,6-Diamidin-2-phenylindole	HMG	High mobility group
		hnRNP	Heterogenous nuclear ribonucleoprotein
ddH$_2$O	Double-distilled water		
DEPC	Diethylpyrocarbonate	Ig	Immunoglobuline
DMSO	Dimethyl sulfoxide	IPTG	Isopropyl β-D-1-thiogalactopyranoside
DNA	Desoxyribonucleic acid		
dNTP	Desoxynucleoside triphosphate	M	Molar
		MCS	Multiple Cloning Site
ds	Double stranded	min	Minute
DTT	Dithiothreitol	mRNA	Messenger RNA
EDTA	Ethylene diamine tetra acetic acid	mRNP	Messenger ribonucleoprotein
EM	Electron microscopy	ncRNA	Non-coding RNA

N-	Amino-terminal	SANT	Transcription regulation
NLS	Nuclear localization		domain (Swi3, Ada2, N-
	sequence		Cor and TFIIIB)
nt	Nucleotides	SCF	Skp1, Cullin, and F-box
NTP	Nucleoside triphosphate	SD	Standard devitation
OD	Optical density	SRP	Signal recognition particle
ORF	Open reading frame	ss	Single stranded
PABP	Poly(A)-binding protein	SUMO	Small ubiquitin-like
PAF	Polymerase associating		modifier
	factor	Tab.	Table
PAGE	Polyacrylamide gel	TAE	Tris-acetate-EDTA
	electrophoresis	TAP	Tandem affinity
PAR-CLIP	Photoactivatable-		purification
	Ribonucleoside-Enhanced	TBE	Tris-borate EDTA
	Crosslinking and	TEMED	Tetramethyl-
	Immunoprecipitation		ethylenediamine
PBS	Phosphate buffered saline	TEV	Tobacco etch virus
PCG	Protein coding gene		cleavage site
PCR	Polymerase chain reaction	TF	Transcription factor
PDB	Protein Data Bank	tgm	tRNA gene-mediated
PEG	Polyethylene glycol		silencing
pH	Potentia hydrogenii	THSC	Thp1-Sac3-Sus1-Cdc31
poly(A)	Poly adenosine	TPR	Tetratricopeptide repeat
RBP	RNA binding protein	TREX	Transcription and Export
RNA	Ribonucleic acid	TRIS	Tris(hydroxyl-
RNAP	DNA dependent RNA		methyl)aminomethane
	polymerase	tRNA	Transfer RNA
RNase	Ribonuclease	ts	Temperature-sensitive
RNP	Ribonucleoprotein	qPCR	Quantitative PCR
rpm	Rounds per minute	U	Unit of enzyme activity,
RGG	Arginine-glycine-glycine		conversion of 1 µmol
	repeats		substrate min^{-1}
RRM	RNA recognition motif	v/v	Volume per volume
RSC	Remodel the Structure of	w/v	Weight per volume
	Chromatin	wt	Wild-type
RT	Room temperature	Zn	Zinc
s	Seconds	Znf	Zinc finger

Table of contents

1. Introduction

1.1 Gene expression

In eukaryotes, transcription of genes requires the orchestrated activity of three DNA dependent RNA polymerases. Each of these polymerases serves a specific class of genes. RNA polymerase II (RNAPII) transcribes the most complex set of genes, which yields thousands of different protein-coding messenger RNAs (mRNAs) but also microRNAs (miRNAs), small nuclear RNAs (snRNAs), and small nucleolar RNAs (snoRNAs). In contrast to this huge and diverse number of genes, RNA polymerase I (RNAPI) transcribes genes coding for the 5.8S, 18S, and 28S ribosomal RNA (rRNA). Moreover, RNA polymerase III (RNAPIII) transcribes tRNA genes and other small noncoding RNA genes, such as the RNA of the Signal recognition particle (SRP), the 5S rRNA or the RNA subunit of RNase P.

1.2 mRNA biogenesis and export

The compartmentalization of eukaryotic cells into nucleus and cytoplasm necessitates export and import pathways that facilitate the movement of molecules into and out of the nucleus. The export of mRNA, one of the main products of RNA polymerase II (RNAPII), is a crucial step in gene expression. However, before the transcripts can be transported to the cytoplasm, where they are translated into proteins, several processing steps have to occur (See Fig. 1).

1.2.1 Three platforms provide the recruitment of mRNA binding proteins

When RNAPII travels along the gene and synthesizes mRNA, the C-terminal domain (CTD) of its biggest subunit Rpb1 is heavily and dynamically phosphorylated. It thereby acts as a platform orchestrating the recruitment of proteins that are involved in transcription, RNA processing, export or chromatin remodeling (Zhang et al. (2012) and references therein). The coordinated recruitment of factors is achieved by different phosphorylation patterns of mainly serine 2, 5, 7, and tyrosine 1 of the highly conserved heptapeptide repeat YSPTSPS. For example, in yeast 26 of these repeats are present in Rpb1 (Buratowski, 2009; Mayer et al., 2010; Zhang et al., 2012). In addition to the CTD of Rpb1, two other recruitment platforms have been described: First, the C-terminal region of Spt5 (CTR) and, second, the nascent mRNA itself (reviewed in Meinel and Strasser (2015)).

Spt5 is a general transcription elongation factor that can be phosphorylated at the C-terminal repeats similar to RNAPII (Yamada et al., 2006). In yeast, phosphorylation of these repeats by the kinase Bur1 leads to the recruitment of the PAF complex (Polymerase associated factor, Liu et al. (2009)), which is known to be a platform for chromatin remodeling enzymes, such as the histone H3K4 methylating Set1/COMPASS complex (Li et al., 2007). Besides the interaction with chromatin regulating enzymes and complexes (*e.g.* Set1 or FACT), interactions of Spt5 with general transcription elongation factors such as TFIIF or TFIIS, as well as with the mRNA capping enzyme or the pre-mRNA cleavage factor I (CFI) were identified, pointing out the general role of Spt5 as an auxiliary platform for mRNA binding proteins (Lindstrom et al., 2003; Mayer et al., 2012).

The nascent RNA, as it emerges from RNAPII, is accessible for mRNA binding proteins that recognize specific motifs. As an example, the Cleavage and Polyadenylation Specificity Factor (CPSF) recognizes the A-rich positioning element on the RNA directly, directing the 3' cleavage of transcripts (Mandel et al. (2008) and references therein). Other proteins with affinity to RNA are recruited to the nascent transcript early after or during synthesis, such as Nab2, which binds to the mRNA body and poly(A) tails of the maturated 3'-end of the mRNA, and Npl3, which binds RNA with a slight preference for G+U-rich RNAs but mostly in a non-sequence specific way (Anderson et al., 1993; Deka et al., 2008; Marfatia et al., 2003).

The three introduced recruitment platforms do not act independently of each other, but are combined to efficiently recruit core components of the maturation machinery to the nascent RNA. As an example, the CFI subcomplex of CPF (Cleavage and Polyadenylation Factor), may be recruited simultaneously by the S2-phosphorylated CTD of RNAPII, the CTR of Spt5, and a poly(A) sequence within the RNA (Mayer et al., 2012). Another concept of recruiting protein complexes to the RNA is the initial interaction of one subunit via the described platforms. Then the complex assembles by interaction with the previously bound subunit. This has been described for the U1 snRNP that initially recruits subunits of the spliceosome to the nascent mRNA but leaves the pre-catalytic spliceosome (Matera and Wang, 2014). A more complex example for this is the Pcf11-Yra1 interaction. Pcf11, a 3'-end processing factor, is recruited to the S2-phosphorylated CTD and RNA (Hollingworth et al., 2006). It then promotes basis for Yra1 binding, which is necessary for coupling 3'-end processing with mRNA export via its interaction with Mex67 and hence for recruitment of the conserved exporter complex (Johnson et al., 2009; Strasser and Hurt, 2000).
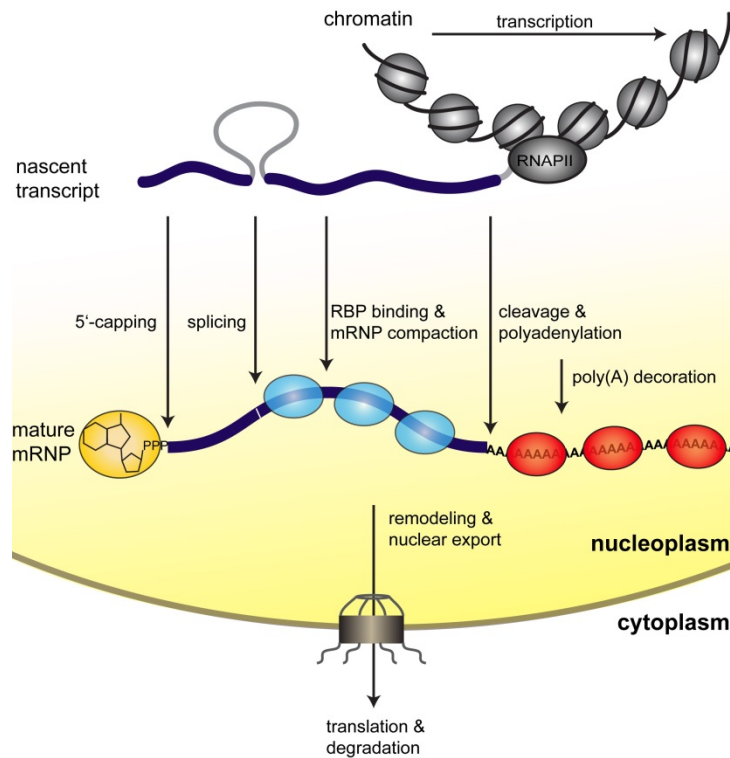
Fig. 1: Different steps in mRNP biogenesis. Co-transcriptionally, the nascent mRNA protruding from the transcribing polymerase is capped at its 5'-end, spliced, cleaved, and polyadenylated at the poly(A) site. These processes go hand in hand with a rich decoration of several mRNA binding proteins that remodel the maturating RNA until an export competent mRNP is formed. The mRNP complex is transported through the nuclear pore complex into the cytoplasm, where it will be translated and eventually degraded. Colored circles: different proteins / protein complexes acting on the nascent RNA or DNA. Figure modified after Meinel and Strasser (2015).

The proteins recruited to the mRNA can be involved in a variety of modifications, *e.g.* 5'-capping, splicing, 3'-end processing, which are summed up as mRNA processing. Later maturation steps are RBP binding and subsequently mRNP formation, followed by export to the cytoplasm (see Fig. 1).

1.2.2   mRNA processing and mRNP formation

The first maturation step that occurs as soon as the first 15-30 nucleotides of the nascent pre-mRNA exit the RNA polymerase is 5'-capping. Here, a three step process is utilized to produce a functional cap by (i) removing the 5'-γ-phosphate group of the first transcribed nucleotide, (ii) transferring a guanosine monophosphate nucleotide (GMP, after hydrolysis of pyrophosphate from GTP) to the 5'-end of the RNA, and (iii) finally by methylation of the N-7 atom of the guanosine (reviewed in Topisirovic et al. (2011)). This process is carried out by the 'capping enzymes', which are recruited to the S5-phosphorylated CTD of RNAPII at an

early step of the transcription cycle. The mature cap (m^7GpppN) is recognized and bound in yeast by the cap binding complex (Cbp 20 and Cbp 80). It has been shown that the cap structure has pivotal roles for the fate of mRNAs, as capped mRNAs are spliced more efficiently (Edery and Sonenberg, 1985) and binding of the general translation initiation factor eIF4E, the first step of cap-dependent translation, directs the ribosome to the mRNA (Sonenberg and Hinnebusch, 2009).

Also co-transcriptionally, the nascent mRNA is spliced. This is an essential process that removes intronic sequences from the mRNA. It is also thought to be a quality control step, as incorrectly spliced mRNAs (*e.g.* retention of inefficiently spliced introns) are subjected to exosomal pre-mRNA decay (Lemieux et al. (2011) reviewed in Schneider and Tollervey (2013)). Recognizing the 5'-splice site by base pairing with the U1 snRNA, the U1 snRNP binds as the first component. Now, a highly ordered and ATP-dependent assembly of the spliceosome commences and multiple RNA-protein interactions are required to build an activated spliceosome. Subsequently, the RNA is cleaved, a lariat structured intron is released and the exons are ligated (reviewed in Matera and Wang (2014)). Although only roughly 5% of all genes in *Saccharomyces cerevisiae* contain single introns, they account for nearly 30% of synthesized RNAs. This is due to the over-representation of introns in genes coding for ribosomal proteins and other highly transcribed genes, such as actin (Spingola et al., 1999). This highlights the importance of splicing even in the relative simple model organism *S. cerevisiae*.

A later step in mRNA biogenesis and mRNP formation is 3'-end processing. Briefly, the transcribed RNA is cleaved, released from the RNA polymerase II, and a poly(A) tail is produced subsequently.

The first step in 3'-end formation is cleavage of the nascent RNA. The CPF complex (Cleavage and Polyadenylation Factor) consisting of more than 20 proteins is recruited to a canonical cleavage site, partially through the interaction with the RNA and the S2-phosphorylated CTD of RNAPII (see CFI complex above and reviewed in (2013); Zhao et al. (1999)). The cleavage site in yeast is defined by a single pyrimidine, which is followed by multiple adenosines and located between an up- and downstream U-rich element (Mandel et al., 2008; Zhao et al., 1999).

   After the mRNA is cut, the poly(A) polymerase Pap1, which is also a subunit of CPF, produces a poly(A) tail. During synthesis, poly(A)-binding proteins (PABPs) bind to the growing tail thereby stabilizing it (Mandel et al., 2008). Not only the occupancy of proteins like Nab2 or Pab1 on poly(A) tails, which both are thought to stabilize the mRNA, but also the length of the produced poly(A) tail is crucial for mRNA stability (Amrani et al. (1997); Mandel

et al. (2008); Soucek et al. (2012) and references therein). After initial polyadenylation of the mRNA, the yeast poly(A) nuclease complex (PAN) trims the poly(A) tail to a length of 60-80 nucleotides (nt) (up to 200-300 nt in humans) (Mandel et al. (2008) and references therein). In addition, binding of Nab2 to the mature mRNA regulates the poly(A) tail length by preventing readenylation (Kelly et al., 2010; Viphakone et al., 2008).

Recent findings show that Rrp6, a 3'-5' exonuclease component of the nuclear exosome can displace Nab2 by direct interaction and subsequently leads to mRNA decay (Schmid et al., 2012). In general, errors in the correct 3'-end processing are recognized and defective RNAs are degraded by the exosome (reviewed in Parker (2012); Schneider and Tollervey (2013)).

As described above, a variety of RNA binding proteins (RBPs) is binding to the nascent mRNA during and after transcription with modular structural motifs and different RNA-sequence affinities and specificities. Forming an mRNP, these proteins regulate mRNA translation, mRNP localization and eventually its degradation. By the use of modern techniques, such as PAR-CLIP or coupling of mRNP purification with mass spectrometry, hundreds of proteins and their binding-sites have been identified to bind to mRNPs in *S. cerevisiae* or higher eukaryotic cells (Baejen et al., 2014; Baltz et al., 2012; Castello et al., 2012; Mitchell et al., 2013). Also, the temporospatial binding could now be investigated, which highlighted mRNPs as highly dynamic macromolecular particles that are tailored to the individual function and fates of the bound transcript, *i.e.* from synthesis to decay (Baejen et al., 2014; Tuck and Tollervey, 2013). An interesting observation is that besides the classical RBPs with known RNA binding motifs, many new proteins were found to bind these RNAs, even without encoding a classical RNA-binding motif. They are rather a heterogeneous group of proteins, such as enzymes (*e.g.* kinases or ubiquitin proteases), that might be activated by RNA or lead to a local modification or remodeling of the mRNP as a second independent function (Castello et al., 2012; Mitchell et al., 2013).

In addition to RNA binding proteins, large ncRNAs have been found to bind to and act on mRNA and mRNP complexes in higher eukaryotic cells. They can function as post-transcriptional regulators, *e.g.* during splicing by influencing the binding of SR-proteins (serine-/arginine rich) to the mRNA (Yoon et al. (2013) and references therein). Furthermore, they were described to regulate mRNA stability and translational activity by recruiting proteins or impeding the binding of proteins to the RNA (Faghihi et al. (2008); Yoon et al. (2012) and reviewed in Yoon et al. (2013)).

Altogether, the above mentioned mechanisms lead to a very complex picture of the assembly of mature RNAs and mRNPs. The customized mix of mRNA decorated with proteins and

regulatory ncRNAs provides tunable sets of messenger ribonucleoprotein complexes that fulfill the various needs of cells depending on their surrounding environment.

1.2.3 Nuclear export of mRNPs

After successful processing of the mRNA, the protein decorated mRNP needs yet to be exported. In order to promote efficient export, these export-competent mRNPs interact with export adapter proteins, *e.g.* Mex67-Mtr2 and NPC-associated factors (NPC: Nuclear pore complex) to initiate mRNA export (Rodrigues et al., 2001; Strasser and Hurt, 2000; Sträßer et al., 2002). The NPC spans the nuclear envelope and facilitates nucleocytoplasmic transport. With an approximate size of 40-60 MDa in yeast and up to 125 MDa in vertebrates, it is one of the biggest proteinaceous particles in the cell. It has an eight-fold rotational symmetry that creates a pore with an approximate diameter of 40 nm. In addition, filaments on each site reach out about 50-80 nm into the cytoplasm and nucleoplasm, respectively, creating the nuclear basket at the nuclear side. NPC proteins, also called nucleoporins or Nups, are the building blocks of the NPC. Structural Nups create a scaffold for other proteins temporarily binding to the NPC, such as Yrb2 or Nup2, as well as FG-nucleoporins (Dilworth et al., 2001; Dilworth et al., 2005; Floer and Blobel, 1996). The latter are rich in FG-repeats (phenylalanine-glycine repeats), highly conserved among eukaryotic evolution and have pivotal roles in NPC barrier formation, transport selection, and present docking stations for transportable complexes (reviewed in Aitchison and Rout (2012), Bjork and Wieslander (2014) and Hurt and Beck (2015)).

The nuclear pore not only serves as a gate, providing regulated transport into and out of the nucleus. It has been reported for several model organisms, including *S. cerevisiae*, that the NPC has an additional role in gene expression as it influences the sub-nuclear localization of transcriptionally active gene regions by interacting with chromatin and the mRNA export machinery (reviewed in Burns and Wente (2014). These processes, which are thought to physically couple transcription to the nuclear pore, are summed up in the hypothesis of 'gene gating' (Blobel (1985), Burns and Wente (2014) and references therein).

Mlp1 (Myosin like protein 1) is one example of the Mlp protein family that act as docking platforms for export competent mRNPs. In addition, this pre-export binding serves as a final quality check for malformed or unspliced mRNAs (Fasken et al., 2008; Strambio-de-Castillia et al., 1999; Vinciguerra et al., 2005). At this stage, the mRNP has undergone a vast number of remodeling events, as described above and has also been decorated with proteins involved in export.

The subdivision of cells in cytoplasm and nucleus necessitated the development of proteins that link transcriptional processes to mRNA export. One of the key players in coupling transcription to mRNA export is the highly conserved TREX complex that is already co-transcriptionally loaded onto the mRNA in a length dependent manner (Meinel et al., 2013). It is composed of the heteropentameric subcomplex THO (Hpr1, Mft1, Tex1, Tho2 and Thp2) that is complemented by Gbp2, Hrb1, Sub2, and Yra1 as shown in Chavez et al. (2000); Sträßer et al. (2002) and Figure 2. Only recently, it was shown that the Hpr1 subunit of the THO complex can be sumoylated on its C-terminus by Siz1 and Siz2, thereby regulating its recruitment to the nascent mRNP.
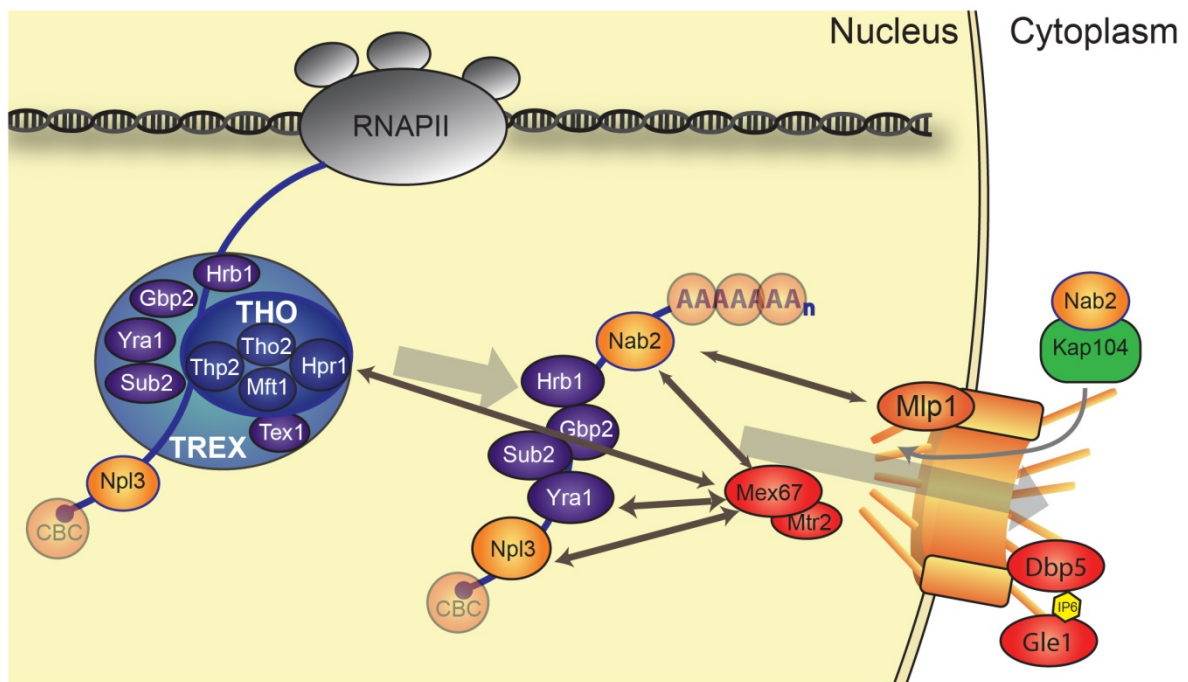
Fig. 2: The mRNA export machinery. As RNAPII transcribes through its target gene, the THO/TREX complex gets recruited to the nascent mRNA via interaction with the S2-/S5-diphosphorylated CTD of RNAPII and the mRNA. After release and remodeling of the mRNA, the heterodimer Sub2-Yra1 recruits the canonical exporter Mex67/Mtr2. In addition, alternative adaptors like Nab2 and Npl3 help to load the exporter onto the mRNP (see text for details). After passing the NPC, the mRNP is again remodeled on the cytoplasmic side of the NPC by Dbp5 and the shuttling exporters are released from the mRNP. In addition, the reimport of released Nab2 by its karyopherin Kap104 into the nucleus is depicted. Figure modified after Chanarat et al. (2012).

The sumolyation is rather needed for the expression of stress-inducible genes, as the bulk mRNA export was not affected in a non-sumoylatable *HPR1* mutant (Bretes et al., 2014).

As a next step in mRNA export, the conserved heterodimer Sub2-Yra1 recruits the conserved mRNA exporter Mex67-Mtr2 to the mRNA, which directly facilitates export of the mRNA through the NPC (Stewart (2010) and references therein, Strasser and Hurt (2000); Strasser and Hurt (2001); Sträßer et al. (2002); Stutz et al. (2000)). At the NPC, Mex67

interacts with the FG-nucleoporins and is released in an ATP-dependent manner on the cytoplasmic site by the IP_6-activated (Inositol hexakisphosphate) DEAD box helicase Dbp5, which is bound to the cytoplasm-localized Nup Gle1 (Lund and Guthrie, 2005; Noble et al., 2011; Tran et al., 2007). An alternative mechanism to recruit Mex67-Mtr2 to the mRNA is proposed by the ubiquitinylation of the THO subunit Hpr1 (Gwizdek et al., 2006; Hobeika et al., 2009). Although this is only shown for some genes yet, the above mentioned observations of proteins being recruited in a non-sequential order may point out the presence of a central and complex packing station. In this model, recruitment of remodeling factors and the export machinery, as well as mRNP compaction already happen during transcription (Meinel and Strasser, 2015). This theory is underlined by findings, such as that Mex67 was found to play a role in 3'-end processing (Qu et al., 2009) or the vast amount of proteins that interact with the CTD, but are required for different other processes than RNA synthesis. Examples are the capping enzyme (Hossain et al., 2013), the TREX complex (Meinel et al., 2013), or the THSC (Thp1-Sac3-Sus1-Cdc31-Sem1) complex (Pascual-García et al., 2008) to name but a few.

Besides the exporter Mex67-Mtr2, other proteins associate with the mRNA and support its export. Examples for this kind of alternative mRNA export adaptors are Nab2 and Npl3. Npl3 is one of three SR-like proteins (serine-/arginine-rich) in *S. cerevisiae* and functions in multiple RNA-related processes such as transcription, splicing, and mRNA export ((Santos-Pereira et al., 2014) and references therein). It binds to the RNA by interacting with the S2-phosphorylated CTD of Rpb1 (RNAPII), is crucial for preserving genome integrity by inhibiting R-loop formation (DNA-RNA hybrids with a displaced DNA strand), and does not leave the mRNA until it is exported (Santos-Pereira et al. (2013), Santos-Pereira et al. (2014) and references therein). The dephosphorylation of mRNP-associated Npl3 by the nuclear phosphatase Glc7 leads to subsequent release of 3'-end processing factors and recruitment of Mex67-Mtr2, which then promotes the export of mRNPs (Gilbert and Guthrie, 2004). The role of the poly(A)-binding protein Nab2 in mRNA export is described below (see Introduction,1.3.2).

In addition to the TREX complex, the THSC complex (also termed TREX-2) is an additional conserved, multi-subunit complex that plays important roles in mRNA export and gene tethering to the NPC (Luna et al. (2009) and references therein). In *S. cerevisiae*, it consists of Thp1, Sac3, Sem1, Sus1 and Cdc31, and its structure is partially resolved as different subunits of THSC have been co-crystalized (Ellisdon et al., 2012; Jani et al., 2009; Jani et al., 2014). It tethers the TREX complex and Mex67 close to the NPC, as revealed by genetic interaction of *YRA1* and *SAC3* and strong defects in mRNA export upon mutations in *e.g.* Sac3 or Thp1 (Fischer et al. (2002) and reviewed in Luna et al. (2009)). Only very recently,

THSC was found to interact with the Mediator complex via Med31/Med7 and to influence Ser5 phosphorylation of RNAPII, thereby providing another link between transcription and mRNA export (Schneider et al., 2015).

The combination of multiple processes, leading to a mature mRNA that is translated in the cytoplasm is controlled and intertwined at different steps (see above). Many of the mentioned events seem not to take place consecutively, but rather occur simultaneously or in an RNA customized order (Meinel and Strasser, 2015). Thus, transcription is linked to mRNA processing, mRNP formation, and mRNA export in a much more complex way than anticipated before.

1.3 The poly(A)-binding protein Nab2

One of the many proteins that are recruited to the nascent mRNA is Nab2 (Nuclear abundant poly(A) RNA binding 2, see above). It was originally discovered in a screen for proteins that bind to nuclear polyadenylated RNAs in *S. cerevisiae* by UV crosslinking and oligo(dT)-Sepharose purification of RNPs (Anderson et al., 1993). It consists of 525 amino acids (58 kDa) and has essential functions in mRNA export and poly(A) tail length control (Anderson et al., 1993; Green et al., 2002; Hector et al., 2002). Nab2 is present along the whole open reading frame of protein-coding genes as determined by single chromatin immunoprecipitation (ChIP) experiments and genome-wide experiments, *e.g.* ChIPs hybridized to high density tiling arrays (Gonzalez-Aguilera et al., 2011; Meinel et al., 2013).

As a member of the poly(A)-binding protein family (PABPs), Nab2 binds specifically to the poly(A) tail and the body of mRNAs during or shortly after their polyadenylation (Kelly et al. (2010); Tuck and Tollervey (2013); Soucek et al. (2012) and references therein). After passage through the NPC, Nab2 is released from the mRNP complex through the earlier mentioned RNA helicase Dbp5 and cycles back to the nucleus (Hodge et al., 1999; Noble et al., 2011; Tran et al., 2007). The interaction with components of the TREX (Yra1) and THSC (Thp1) complexes, as well as Mex67 in yeast and the shuttling of Nab2 with the mRNA suggest Nab2 as a key component in the tightly intertwined system of transcription, processing, mRNP formation, and export of mRNA (Batisse et al., 2009; Gallardo et al., 2003).

Four major domains have been characterized in Nab2 (see Fig. 3A). The N-terminal domain (amino acids 1-97) assembles in a five alpha-helix bundle with a PWI-like (proline-tryptophane-isoleucine) fold and is necessary for the physical interaction with Mlp1 (Grant et al., 2008; Green et al., 2003; Marfatia et al., 2003). Mlp1, as a representative of Mlp proteins

(see above), is located at the nucleoplasmic site of the NPC and is thought to act as a control step through binding to mRNPs before export of mature mRNP complexes can occur (Fasken et al., 2008; Green et al., 2003; Strambio-de-Castillia et al., 1999). The direct interaction of Nab2 with the C-terminal globular domain of Mlp1 is mediated by a hydrophobic patch surrounding Phe73 (see Fig. 4A, F73). Deletion or mutagenesis of this residue results in disruption of the Mlp1-Nab2 interaction *in vitro* and nuclear accumulation of polyadenylated mRNAs *in vivo* (Fasken et al., 2008). In addition, the F73D mutant shows genetic interactions with *MEX67* and *YRA1*, which supports the hypothesis of Nab2 binding to Mlp1 as an important step in mRNA export (Fasken et al., 2008).
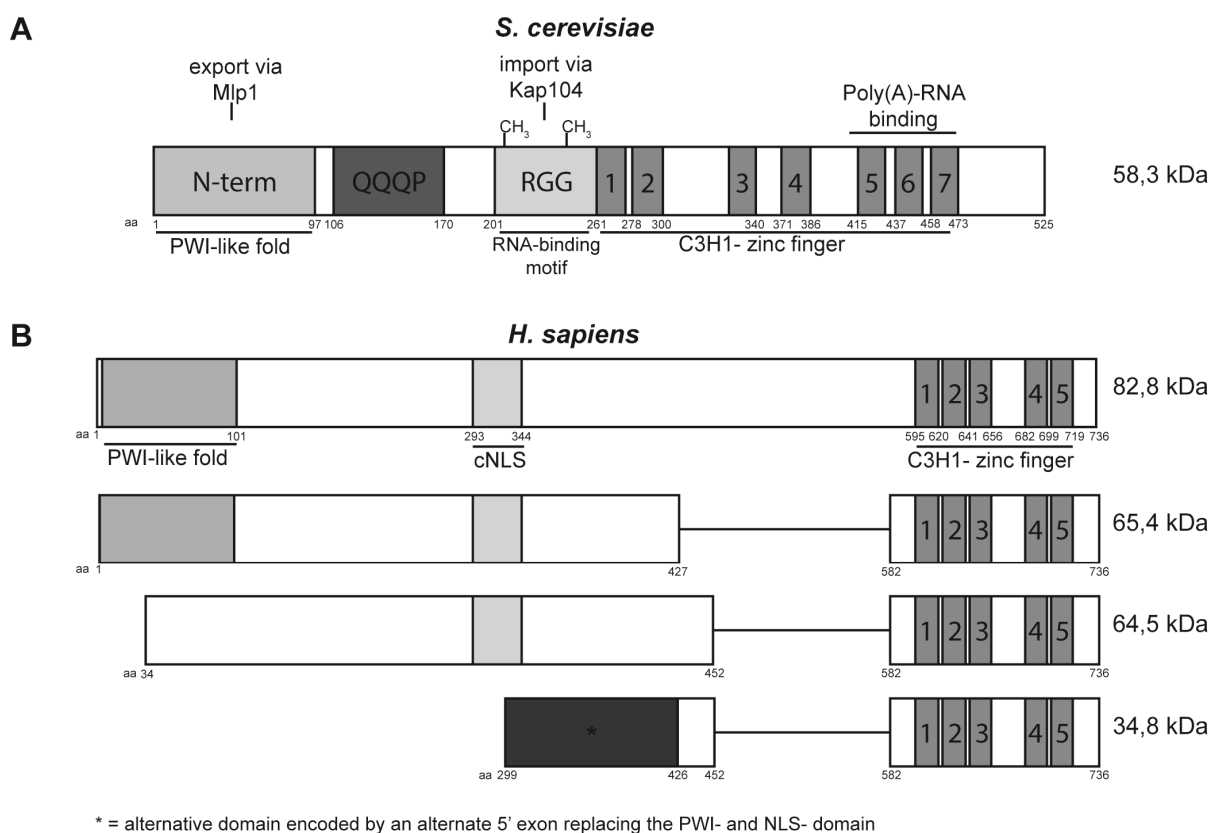
Fig. 3: A schematic view of the Nab2 domain structure. (A) The domain structure of Nab2 and the corresponding functions are indicated. The N-terminal domain is required for Mlp1 interaction, facilitating the export of Nab2. The QQQP-domain has an unknown function. The RGG-domain is necessary for import/ export of Nab2 and gets methylated by Hmt1. The C-terminal domain is structured into of two zinc finger repeats comprising three and four zinc fingers in series. This domain is crucial for poly(A) RNA binding. **(B)** The human orthologue of Nab2 and domain structures are presented. Most conserved domains are the nuclear localization domain and the zinc fingers. These have been implicated in poly(A) tail length control and are present in each expressed isoform. Isoforms are arranged according to their size (Isoform 1: 82.8 kDa, isoform 2: 65.4 kDa, isoform 3: 64.5 kDa and the cytoplasmic isoform 4: 34.8 kDa). Isoform 3short is not presented.

Another important interface at the N-terminus of Nab2 is located around the Tyr34 residue, as it is necessary to bind Gfd1. Gfd1, a protein involved in enhancing mRNA export, interacts with Gle1 and Nab2 on the cytoplasmic site of the NPC.

The interaction of Gfd1 with Nab2 is important for the Dbp5 remodeling activity at the last step of mRNA export and mRNP disassembly (see Introduction, 1.3.2 and Suntharalingam et al. (2004); Zheng et al. (2010)).

The second domain of Nab2 (amino acids 100-144) contains multiple QQQP (glutamine-proline) repeats with so far unknown function and deletion of which shows no growth defect (Marfatia et al., 2003).

Similar to other proteins that bind to mRNA and are known to be involved in RNA metabolism, the third domain of Nab2 contains an RGG-domain (arginine-glycine-glycine, amino acids 201-260), a classical RNA recognition motif (RRM) in metazoans and yeast, with a total of four RGG repeats (Birney et al., 1993; Green et al., 2002). However, several studies showed that Nab2 does not bind to RNA with this domain compared to many other proteins (reviewed in Rajyaguru and Parker (2012)). It rather functions as a nuclear localization sequence (NLS), through which Nab2 binds to its importin Kap104 and is thus important for the import of cytoplasmic Nab2. No alternative importin for Nab2 was identified, as a Kap104 depletion results in a rapid cytoplasmic shift of Nab2 from the nucleus (Aitchison et al., 1996; Green et al., 2002; Lee and Aitchison, 1999; Marfatia et al., 2003; Truant et al., 1998).
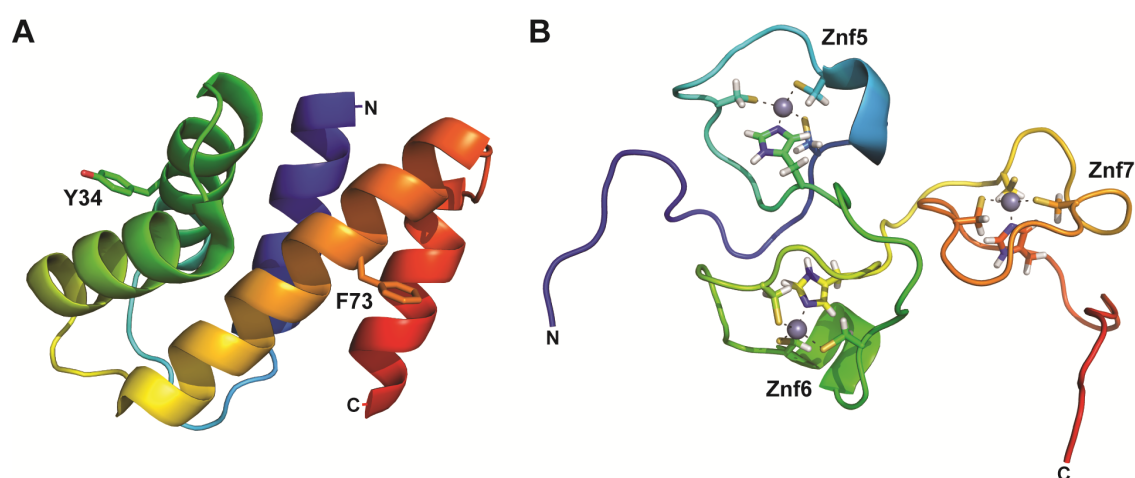
Fig. 4: Structural data for *S. cerevisiae* Nab2. (A) The crystal structure of the N-terminus of Nab2 is presented. It consists of a five alpha-helix bundle with a PWI-fold and interacts with Mlp1 to promote nuclear export of mRNPs. The important residues Y34 and F73 are indicated and discussed in the text. **(B)** The solution structure of zinc finger 5-7 of Nab2 by NMR spectroscopy is shown. Each zinc atom (grey dots) is coordinated in one CCCH-zinc finger by three cysteines in a planar way and perpendicular by a single histidine. The figure was generated using PyMol software from the PDB files (A) [2V75] (Grant et al., 2008) and (B) [2LHN] (Brockmann et al., 2012), available at the RSCB Protein data base.

The sequence within Nab2 that interacts with Kap104 is known and was crystalized together with the human karyopherin homologue Kapβ2 (Soniat et al. (2013) PDB file [4JLQ]).

In addition, Hmt1, a SAM-dependent type I protein-arginine methylase, acts on arginine residues of several hnRNPs (*e.g.* Hrp1 or Npl3) and also targets the RGG-domain of

Nab2 (see Fig. 3A and Gary et al. (1996); Green et al. (2002); Shen et al. (1998). Deletion of Hmt1 results in nuclear retention of Nab2 and mRNA, whereas removal of the RGG-domain has no influence on the export, indicating the binding of an unknown nuclear factor to Nab2 preventing its export when Nab2 is not methylated (Green et al., 2002; Marfatia et al., 2003). This presents the methylated RGG domain as a second prerequisite for an export competent Nab2 offering an additional step for mRNP quality control.

The C-terminal part of Nab2 is composed of seven zinc fingers that can be divided in two repeats of three (amino acids 415-473) and four zinc fingers in series (amino acids 261-386, see Fig. 3A), which furthermore are structurally independent subdomains (Martinez-Lumbreras et al., 2013). Zinc fingers are small protein folds that usually consist of 2-3 cysteines and 1-2 histidines that tetrahedraly coordinate one Zn^{2+} atom. Some proteins only contain a single zinc finger, but usually at least two or more serial zinc fingers occur. Around 14 classes of zinc fingers were identified so far with varying functions, such as DNA or RNA binding, but also interactions with lipids or proteins have been described (Carballo et al. (1998) and reviewed in Hall (2005); Matthews and Sunde (2002)).

The zinc fingers (ZnF) in Nab2 are C_3H_1-type ($CX_5CX_{4-6}CX_3H$, see Fig. 4B) zinc fingers, which have been shown to bind to RNA motifs *in vivo* (Hall (2005); Kelly et al. (2007) and reviewed in Soucek et al. (2012)). This domain is crucial for the binding of Nab2 to poly(A) RNA *in vitro* and *in vivo* (Anderson et al., 1993; Marfatia et al., 2003). Complete or partial deletion of the zinc fingers results in inviability, hyperadenylated mRNAs, and a severely reduced binding of poly(A) RNA *in vitro* (Hector et al., 2002; Marfatia et al., 2003). Furthermore, the zinc finger domain was proposed to bind RNA in a 3'-5' manner and to be involved in protein-protein interactions on RNA *e.g.* in self-recognition, as described for the mammalian PABN1 protein (Eckmann et al., 2011; Kuhn et al., 2009; Martinez-Lumbreras et al., 2013). Here, the growing poly(A) tail is recognized by PABN1 and other PABN1 molecules are recruited via protein-protein interactions and specificity for poly(A) RNA. It still remains to be shown whether this is true for Nab2.

Interestingly, the affinity of the two zinc finger arrays to poly(A) RNA is different as revealed by *in vivo* crosslinking of zinc finger deletion mutants to poly(A) RNA and *in vitro* binding studies (Kelly et al., 2007; Marfatia et al., 2003). Full length Nab2 binds poly(A)$_{25}$ RNA *in vitro* with an approximated K_d of ~30 nM. When ZnF 5-7 were deleted from the protein, the K_d was reduced about 60 fold to ~2 µM. This defined the last three zinc fingers as the main poly(A)RNA binding site of Nab2, as the first four zinc fingers were only weakly binding to tested RNAs and deletion of which resulted in a modest reduction of Nab2 / poly(A) RNA interaction (Kelly et al., 2007; Marfatia et al., 2003).

The high specificity of Nab2 to poly(A) RNA is further underlined by the fact that other

tested RNA sequences (*e.g.* poly(N), poly(G), RNA oligonucleotides like UAUU) could not compete Nab2 from poly(A) RNA *in vitro* (Kelly et al., 2010; Kelly et al., 2007). Nevertheless, poly(G), poly(U) but not poly(C) can be bound by Nab2 (Anderson et al., 1993). An unspecific binding to RNA, as well as to the bodies of mRNAs *in vivo* was also described (Kelly et al., 2007; Tuck and Tollervey, 2013). This led to the conclusion that ZnF 5-7 of Nab2 are necessary and sufficient for the high affinity binding of Nab2 to poly(A) RNA in yeast.

Moreover, the C-terminal part of Nab2 interacts with Pub1 (poly(U)-binding protein 1), which predominantly localizes to the cytoplasm, thereby recruiting it to the mRNA. Together with Nab2, it is important for regulating mRNA stability, especially for transcripts that contain ARE-like (AU-rich elements) elements (Apponi et al., 2007).

1.3.1 Regulation of poly(A) tails

While Nab2 is recruited to the nascent mRNA during transcription elongation of protein coding genes (Meinel et al., 2013), it has also been found to associate with the 3'-end processing machinery by genetic interaction with *RNA15*, the CFIA cleavage factor, and physically contacting the cleavage factor I subunit Hrp1 (Soucek et al. (2012) and references therein). This is further supported by the fact that Nab2 was found to support 3'-end processing reactions of purified CFIA, CFIB, and CPF *in vitro* and thus having a role in 3'-end processing (Dheur et al., 2005; Hector et al., 2002).

The control of poly(A) tail length is mainly achieved by a combination of the RGG-domain and a part of the zinc fingers ZnF 5-7 of Nab2 by inhibiting readenylation of trimmed poly(A) tails. This inhibition is thought to be accomplished by limiting the accessibility of mRNA 3'-ends to modifications (Hector et al., 2002; Viphakone et al., 2008). In line with this, it is thought that Nab2 can cover poly(A) units of around 20 nt *in vitro* (Viphakone et al., 2008). In addition, it was shown that Rrp6, a nuclear exosome subunit, can displace Nab2 from poly(A) tails and may lead to poly(A) RNA turnover (Schmid et al., 2012). A similar mechanism was described for the *Schizosaccharomyces pombe* orthologue of Nab2 (Grenier St-Sauveur et al., 2013). Only recently, it was shown that Nab2 can protect early mRNAs from degradation by the exosome. Rapid depletion of Nab2 caused a general loss of poly(A) mRNAs that can be partially restored after long-term depletion of Nab2 (Schmid et al., 2015). Being a central player in regulating poly(A) tails during early and late stages of mRNP biogenesis, Nab2 has a well-defined role in 3'-end processing of mRNAs in *S. cerevisiae* and potentially other organisms (Kelly et al., 2014).

1.3.2   **Nab2 mediates export of mature mRNPs**

Being processed and decorated with a variety of proteins, the mature mRNP can interact with the export machinery. One key step in this process is the recruitment of Mex67-Mtr2 to the mRNP (see 1.2.2). Nab2 was found to be directly interacting with Mex67, which is enhanced by the TREX subunit and export adapter Yra1 (couples TREX to the exporter Mex67-Mtr2) (Iglesias et al., 2010). Interestingly, Yra1 becomes dispensable for this interaction, when either *NAB2* or *MEX67* were overexpressed. Furthermore, Yra1 gets ubiquitinylated by Tom1 at the nuclear side of the NPC and leaves the mRNP before export, supported by the fact that Yra1 is not a shuttling factor (Iglesias et al., 2010; Strasser and Hurt, 2000; Stutz et al., 2000).

Nab2 also seems to interact with the THSC/TREX-2 complex, as overexpression of *NAB2* rescues the mRNA export defect in Δ*thp1* cells (Gallardo et al., 2003). Together with the fact that Mex67-Mtr2 additionally interacts with Sac3 of THSC/TREX-2 (see above and Fischer et al. (2002)), it was suggested that Nab2 and THSC/TREX-2 act synergistically on the same biological pathway (Gallardo et al., 2003).

Finally, reaching the nuclear face of the NPC, Nab2 interacts with Mlp1 (see 1.3) and the mRNA is exported (Grant et al., 2008). On the cytoplasmic side, Nab2 interacts with Gfd1 and is disassembled from the mRNP by Dbp5 (see 1.2.2, 1.3 and Hodge et al. (1999); Lund and Guthrie (2005); Suntharalingam et al. (2004); Tran et al. (2007)).

1.3.3   **Nab2 is conserved from yeast to humans**

Orthologues of Nab2 have been identified in many organisms including *Homo sapiens* (ZC3H14), *Mus musculus* (MSUT-2), *Rattus norvegicus* (ZC3H14), *Caenorhabditis elegans* (SUT-2), *Drosophila melanogaster* (dNab2), and *S. pombe* (nab2)*,* showing its conservation throughout evolution (Anderson et al., 1993; Guthrie et al., 2011; Guthrie et al., 2009; Leung et al., 2009; Pak et al., 2011; Yoon, 2009). The overall function of Nab2 in poly(A) tail length control seems to be conserved within these different organisms, as poly(A) RNA binding of orthologues have been shown in *H. sapiens*, *M. musculus*, *R. norvegicus*, and *D. melanogaster* (Kelly et al., 2007; Pak et al., 2011). To prove that orthologues of Nab2 have similar functions, it was shown that human ZC3H14 can functionally substitute dNab2 in fly neuronal tissue (Kelly et al., 2014). Furthermore, Nab2 is required for correct poly(A) tail length in *D. melanogaster* and probably in *H. sapiens* (Kelly et al., 2014; Pak et al., 2011).

Being ubiquitously expressed in human, *ZC3H14* exists in at least four different isoforms (see Fig. 3B). Isoforms 1, 2, 3 and 3short contain predicted classical nuclear localization signals (cNLS) and localize to the nucleus, whereas isoform 4 contains an

alternative first exon lacking the NLS and consequently localizes to the cytoplasm (Leung et al., 2009). Besides the cNLS, every isoform contains an array of zinc finger domains in the C-terminus, probably mediating poly(A) tail binding (Leung et al., 2009). Interestingly, mutations in ZC3H14 (*e.g.* R154Stop) cause a form of non-syndromic autosomal recessive intellectual disability (NS-ARID) in humans and abnormal behavior in *Drosophila*, where Nab2 is needed for neuronal function (Pak et al., 2011). Even more, a recent study identified Nab2 as a supporting factor for correct axiogenic development of mushroom body neurons in *D. melanogaster* (Kelly et al., 2015).

In summary, the known data present Nab2 as an essential protein in mRNA processing and export throughout evolution. It binds to the poly(A) tails of mRNA, interacts with Mex67-Mtr2, the NPC-associated factor Mlp1 and shuttles to the cytoplasm. When reaching the cytoplasm Dbp5 gets recruited to the mRNP and remodels it, thereby releasing Nab2. Finally, it is reimported into the nucleus where it can undergo another round of mRNA export.

1.4   RNA polymerase III transcribes tRNA and other ncRNA genes

RNAPIII is necessary for transcription of a small set of highly expressed, infrastructural RNAs, such as tRNAs, the 5S rRNA or the RNA of the signal recognition particle (*SCR1*), and other small non-coding RNAs, which *e.g.* function in tRNA splicing or maturation (reviewed in Dieci et al. (2007)). The majority of products, the tRNAs and the 5S rRNA, serve in translation by either providing activated amino acids to the ribosome or being an integral component of the large ribosomal 60S subunit (reviewed in Ciganda and Williams (2011); Pang et al. (2014)).

1.4.1   The RNA polymerase III transcription apparatus

RNAPIII is composed of a total number of 17 subunits, of which five subunits (Rpc160, Rpc128, Rpc40, Rpc19 and ABC23) build up its core structure. Five proteins are present in all RNA polymerases (ABC27, 23, 14.5, 10α, and 10β) and eight subunits are RNAPIII specific, from which five do not have RNAPI or RNAPII paralogues (Rpc31, Rpc34, Rpc37, Rpc53, and Rpc82). However, four of these RNAPIII subunits (all except Rpc31) were identified as 'permanently recruited' homologues of RNAPII general transcription factors (e.g. Rpc34 and Rpc82 show homologies to TFIIE α and β (Carter and Drouin, 2010; Kuhn et al., 2007). Thus, many RNAPIII subunits show evolutionary conservation to RNAPI and RNAPII as well as to subunits of archaeal and bacterial polymerases (reviewed in Gabrielsen and Sentenac (1991); Geiduschek and Kassavetis (2001); Memet et al. (1988); Werner et al.

(2009)). Several other subunits join the above mentioned core to finally enable the complex to be recruited to its target genes (Wang and Roeder, 1997). A few years ago, the structure of RNAPIII was solved by cryo-electron microscopy and single-particle analysis at 9.9 Å resolution and at 16.5 Å resolution in the elongating form, showing the incoming DNA duplex as well as the exit pathway of the newly synthesized RNA (see Fig. 6B and Fernandez-Tornero et al. (2010); Fernandez-Tornero et al. (2007)).

General transcription by RNAPIII is dependent on the three transcription factors TFIIIA, TFIIIB and TFIIIC. TFIIIB is a tripartite complex composed of Tbp (TATA-box binding protein), Bdp1 (B double prime 1), and Brf1 or 2 (TFIIB related factor 1 or 2). TFIIIC is the most complex transcription factor with total of six subunits (See below and Acker et al. (2013); Schramm and Hernandez (2002)).

Similar to RNAPII genes, the TSS of tRNA genes in yeast is free of nucleosomes and flanked by two highly positioned nucleosomes (-1 and +1 with a distance of each ~150-200bp from the TSS) that contain the H2A histone variant H2A.Z, a marker for open chromatin at the 5'-end of RNAPII transcribed genes (Kumar and Bhargava, 2013; Lieb and Clarke, 2005; Mahapatra et al., 2011). As tRNA genes are rather small, the nucleosome free region mostly covers the whole gene body (reviewed in Bhargava (2013)). Together with the H2A.Z histone variant, nucleosomes closely located to transcribed tRNA genes show classical euchromatic histone modifications in humans, such as H3K4 tri-methylation and H3K4/9/23/27 acetylation (Moqtaderi and Struhl, 2004). These open structures are prerequisites for the high transcription rate, necessary to produce sufficient amount of tRNAs and ncRNAs in the exponentially growing cell. An estimation revealed that cells need approximately 3-6 million tRNAs per cell cycle/ division (Dieci et al., 2013).

1.4.2 RNAPIII promoter elements

Transcription by RNAPIII is initiated at three distinct types of promoters, which are highly diverse and have a relatively small number of cis-acting elements. These are located largely intragenically, and require only two or three transcription factors (TFs) for minimal transcriptional activity (see Fig. 5 and Acker et al. (2013); Orioli et al. (2012); White (2011) and references therein). In general, TFIIIC recruits TFIIIB to the transcription start site at type 1 (with help of TFIIIA) and 2 promoters, whereas type 3 promoters use a different mechanism.

The most common RNAPIII promoters are type 2 promoters that mainly drive transcription of the ~274 nuclear tRNA genes in *S. cerevisiae*, but are also present upstream of the *SCR1* (RNA of the signal recognition particle), *SNR52* (coding for a C/D box small nucleolar RNAS), and *RPR1* (coding for the RNA of RNase P) genes (see Fig. 5 for type 2 promoter

and Dieci et al. (2007); Guffanti et al. (2006); Hani and Feldmann (1998)). A typical type 2 promoter consists of an A and a B box, which together recruit TFIIIC. Their transcribed sequences also build up the universally conserved D- and TψC-loops of the tRNA structure (see Fig. 8B, Introduction 1.5, and Orioli et al. (2012)). The A box is a precisely located sequence element 12-20 bp downstream of the transcription start site (TSS) with a flexible consensus sequence of $T_8RGYnnAnnnG$ (the number indicates the nucleotide position in respect to the canonical and mature tRNA sequence) that itself is insufficient to recruit TFIIIC to the DNA, but indispensable for TFIIIB recruitment and hence precise transcription initiation (Geiduschek and Kassavetis, 2001; Marck et al., 2006).

In contrast, the B box mostly functions as an activator and has a consensus sequence of $G_{52}WTCRAnnC$ (the number indicates the nucleotide position in respect to the canonical and mature tRNA sequence) (Marck et al., 2006). Its location is relatively flexible, as intronic sequences are usually interspersed between the A and B boxes (Orioli et al., 2012). In addition, the promoters of the *SCR1* and the *SNR6* genes contain TATA boxes located 5' of the transcription start sites (see Fig. 5 and Dieci et al. (2002); Eschenlauer et al. (1993)). The type 2 promoter structure of the *SNR6* gene is an exception, as the B box is located around 120 bp downstream of the gene (Eschenlauer et al., 1993). In addition, it was shown that this gene can be transcribed in the absence of TFIIIC *in vitro* (Joazeiro et al., 1994).

Type 1 promoters are exclusively present at the genes encoding the 5S rRNA, named *RN5S* in mammalians and *RDN5* in yeast. A typical type 1 promoter has three internally located DNA elements: The A box, the intermediate element (IE), and the C box, which together constitute the Internal Control Region (ICR, see Fig. 5) and span around 50 bp on the DNA. During initiation at type 1 promoters, TFIIIA binds to the ICR and recruits TFIIIC (Rothfels et al. (2007) and Layat et al. (2013) and references therein).

In contrast to type 1 and 2 promoters, type 3 promoters are relatively rare and all their elements lie 5' of the transcription start site: a distal sequence element (DSE), a proximal sequence element (PSE) and a TATA box (reviewed in Dieci et al. (2007); Orioli et al. (2012)). Type 3 promoters are only present in metazoan genomes, *e.g.* at the U6 snRNA gene. The DSE recruits the transcription factors Oct1 and STAF, whereas the PSE recruits the conserved multi-subunit SNAPc complex, which in turn binds TFIIIB and recruits it together with the TATA box to the promoter (Dumay-Odelot et al. (2010); Schramm and Hernandez (2002) and references therein). Notably, the promoter of the *S. cerevisiae* U6 snRNA gene, *SNR6,* is of type 2 (instead of type 3 in metazoans) and contains an upstream TATA box in addition to the canonical A and B box (Brow and Guthrie, 1990; Eschenlauer et al., 1993).
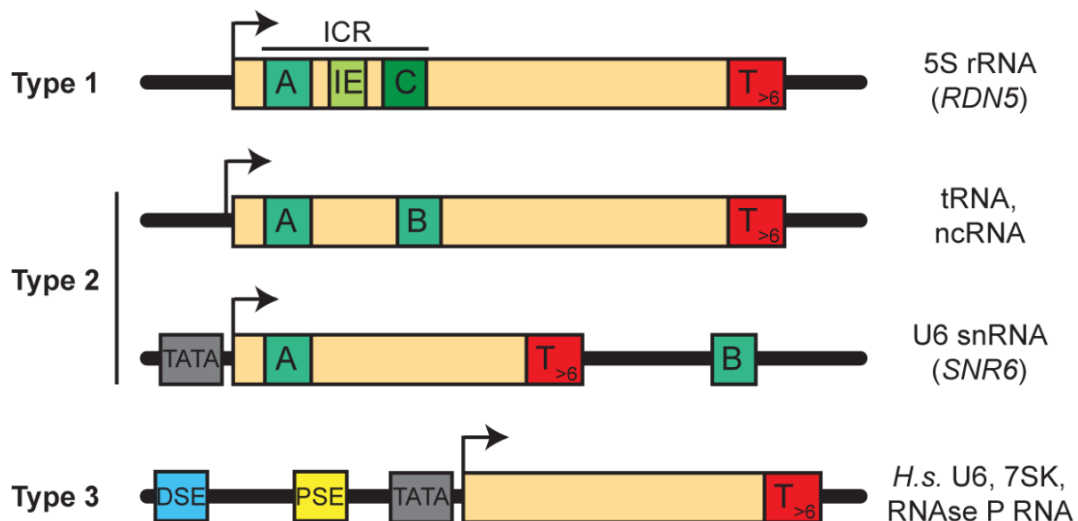
Fig. 5: Schematic representation of RNAPIII promoter types. The three different promoter types and the approximate positions of promoter elements that drive expression of RNAPIII genes are depicted. The solid black bar represents flanking DNA regions, orange boxes the mature product, blue, green and yellow boxes show different promoter elements (A: A box, B: B box, C: C box, IE: interspersed element, ICR: Internal Control Region, DSE: distal sequence element and PSE: proximal sequence element) and red boxes mark the site of transcription termination (T-stretches). The arrows indicate the transcription start sites and note that gene sizes and distances are not in scale. Gene names on the right are representatives for each type of promoter.

After assembling the pre-initiation complex (PIC), TFIIIB recruits RNAPIII to the gene at all three types of promoters (Acker et al. (2013) and references therein).

1.4.3 The RNAPIII transcription factor TFIIIA

In yeast, TFIIIA is a single DNA-binding protein (Tfc2) with a molecular weight of ~40 kDa (Wang and Weil, 1989), is highly conserved from yeast to human, and consists mostly of C_2H_2 zinc finger repeats (Acker et al., 2013; Layat et al., 2013). Using these ZnFs, TFIIIA contacts the ICR element at the 5S rRNA gene and TFIIIC. Furthermore, it has been reported that TFIIIA binds to the 5S rRNA with high specificity and thereby either protects the RNA from degradation or forms a storage RNP (7S RNP) that accumulates the 5S rRNA for later ribosomal biogenesis (reviewed in Layat et al. (2013)).

1.4.4 The RNAPIII transcription factor TFIIIB

The transcription factor TFIIIB is the key player that ultimately recruits RNA polymerase III to its target genes. TFIIIB is also responsible for opening the double-stranded DNA and thus for establishing a closed pre-initiation complex and the transcription bubble (Acker et al. (2013) and references therein and Kassavetis et al. (2001)).

TFIIIB is a heterotrimeric complex consisting of the TATA-box binding protein (Tbp), Brf1 (TFIIB related factor 1), and Bdp1 (B double prime 1) (see Fig. 6A, Geiduschek and

Kassavetis (2001) and references therein). DNA binding of TFIIIB to TATA-box containing genes is mediated by Tbp (~27 kDa). Interestingly, RNA polymerase III promoters are the most prominent binding targets for this general transcription factor that is also required in RNAPII PIC formation (Kim and Iyer, 2004). Once bound, Tbp sharply bends the DNA and this bending is preserved during TFIIIB assembly. Brf1 (~67 kDa) joins the Tbp-DNA complex, then called B', and binds Tbp tightly via a large interacting surface that extends from the N-terminus of Tbp to the other site of the bent complex (see Fig. 6A, blue structure). This strong and very stable association of Tbp with class III gene promoters together with Brf1 is thought to contribute to the high levels of RNAPIII transcription in cells (reviewed in Acker et al. (2013); Geiduschek and Kassavetis (2001)).
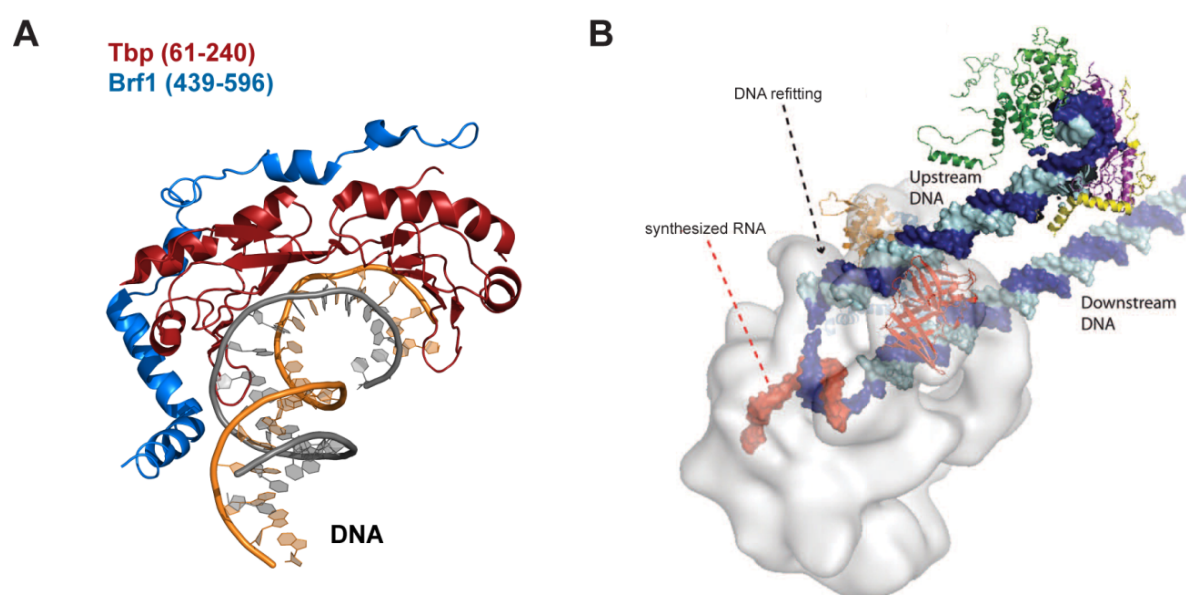
Fig. 6: Structural data for the RNAPIII transcription machinery. (A) Tbp binds directly to the DNA (non-transcribed strand in grey, transcribed strand in orange) and interacts tightly with Brf1 (blue). The very large binding surface of Brf1 extends from the N-terminus of Tbp over the saddle-like structure that binds the DNA. The same region within Brf1 was mapped to interact with Bdp1 (not shown). The figure was generated using PyMol software from the PDB file [1NGM], (Juo et al., 2003). **(B)** The RNAPIII cryo EM structure with modeled DNA (light and dark blue), RNA (red), TBP (purple), and Brf1 (green and yellow) is shown during transcription elongation phase (modified after Fernandez-Tornero et al. (2011)). Interestingly, the fitted DNA accumulates a U-shaped structure, instead of an, as earlier proposed, L-like shape (Fernandez-Tornero et al., 2011).

In contrast, TFIIIB is recruited to TATA-less RNAPIII genes in a mostly TFIIIC dependent manner via initial Brf1 recruitment to TFIIIC subunits together with Tbp (see below and Chaussivert et al. (1995); Deprez et al. (1999)), as well as (Male et al. (2015); Rameau et al. (1994) and Geiduschek and Kassavetis (2001) and references therein). Furthermore, RNAPIII is finally recruited to the assembled PIC on the respective RNAPIII gene by Brf1 (Brun et al., 1997; Werner et al., 1993).

In higher cells, two homologues of Brf1 exist (Brf1 and Brf2). Brf1 is necessary and sufficient for transcription of type 1 and 2 promoter driven RNAPIII genes, whereas Brf2 is needed for expression of type 3 promoter containing genes (Schramm and Hernandez, 2002).

Bdp1 (~68 kDa), the last subunit in joining TFIIIB, is only weakly associated, but nevertheless mandatory for transcriptional activity *in vitro* (Geiduschek and Kassavetis, 2001). The interaction of Bdp1 with Brf1 was mapped to a 66 amino acid long stretch at the C-terminus of Bdp1 (aa 410-476) that also comprises a SANT domain, the only sequence in Bdp1 with homology to other proteins (Kassavetis et al., 2006). Interestingly, the domain within Brf1 needed for Bdp1 interaction overlaps with the crystalized Tbp binding domain (see Fig. 6A) and presents Brf1 as a two-sided adhesive structure. Consistent with this is the finding that a $Brf1_N$-Tbp-$Brf1_C$ fusion protein can replace Brf1 *in vivo* (Kassavetis et al., 2005).

1.4.5 The RNAPIII transcription factor TFIIIC

The *S. cerevisiae* TFIIIC complex has an approximate mass of ~520 kDa and is composed of the six subunits Tfc1, Tfc3, Tfc4, Tfc6, Tfc7, and Tfc8, which are further organized into two globular domains called τA (Tfc1, Tfc4 and Tfc7) and τB (Tfc3, Tfc6 and Tfc8). The domain names reflect the binding of each domain to either the A or B box promoter element (reviewed in Geiduschek and Kassavetis (2001)). Only recently, the first model of the overall TFIIIC architecture was reported, also showing how τA (Tfc4) and τB (Tfc3) interact (Male et al., 2015). Binding to the DNA is most likely mediated via the subunits Tfc1 and Tfc3, as suggested by UV crosslinks of TFIIIC and DNA (Ducrot et al., 2006; Gabrielsen et al., 1989). Tfc4 (τA) and Tfc8 (τB) have additional roles, as these subunits contact TFIIIB and therefore are crucial for its recruitment via interacting with Brf1 (N-terminal 580 aa containing TPR motifs) and Tbp on the one hand and Bdp1 on the other hand. As Bdp1 competes with Tfc3 for binding to Tfc4 and B', it might induce a break or a conformational change within TFIIIC, potentially leading to its partial displacement from the DNA (Male et al., 2015). In addition, interactions with RNAPIII subunits, *e.g.* Rpc53 and ABC10α, are described (Chaussivert et al. (1995); Deprez et al. (1999); Male et al. (2015) and reviewed in Geiduschek and Kassavetis (2001); Schramm and Hernandez (2002)).

TFIIIC is mostly involved during PIC formation and initiation of transcription on class III genes. It was suggested that TFIIIC leaves the DNA after transcription initiation, as only low levels of TFIIIC are present at transcribed genes (compared to TFIIIB and RNAPIII) and TFIIIB alone is sufficient to enable transcription on shorter genes (*i.e.* tRNA genes) *in vitro* (Dieci and Sentenac, 1996; Kassavetis et al., 1990). On the other hand, TFIIIC was shown to function in transcription reinitiation and/or elongation (Ferrari et al. (2004) and reviewed in Acker et al. (2013)). Which of these hypotheses or whether a combination of both holds true still remains to be shown, although the role of TFIIIC, depending on the local genomic

environment seems to be more complex than just being crucial for initial recruitment of TFIIIB.

Interestingly, TFIIIC was found to bind to isolated B boxes in the genome of *S. cerevisiae* and *H. sapiens* without other components of the RNAPIII machinery (Moqtaderi and Struhl, 2004; Moqtaderi et al., 2010). Being genomic association sites for TFIIIC, these isolated B boxes are discussed to be *cis*-acting elements for RNAPII transcription or, more general, to serve as 'bookmarks' for maintaining or delimiting chromatin states on the genomic landscape (Donze (2012); Kleinschmidt et al. (2011); Orioli et al. (2012) and references therein). Evidence for this was shown in *S. pombe*, where TFIIIC, bound to isolated B boxes, is involved in boundary formation against heterochromatin spreading (Noma et al., 2006). Although RNAPII and RNAPIII do not occupy the same set of genes in yeast (Venters et al., 2011), a crosstalk of RNAPII and RNAPIII transcription systems was shown in higher cells (Barski et al., 2010; Raha et al., 2010). Additionally, it was found that a TFIIIC bound B-box can negatively regulate transcription of a TFIIIC subunit (Kleinschmidt et al., 2011). Taken together, these observations point to additional TFIIIC-DNA association modes, which participate in chromatin organization and extend the possibility for RNAPII–RNAPIII crosstalks (Orioli et al., 2012).

1.4.6 **The RNAPIII transcription cycle and termination**

After the PIC has formed at the promoter site of RNAPIII genes, RNAPIII is assembled over the TSS and the transcription bubble is opened. Initiation occurs and often -as with other polymerases- short, abortive transcripts are produced (Bhargava and Kassavetis, 1999). Once a stable elongation complex is formed, transcription proceeds through the gene body with a speed of 60-75 nt/s and a reinitiation interval of ~1.2 s (French et al., 2008). Although still prone to pausing and back-tracking (note that TFIIIA and TFIIIC bind intragenic, but do not affect overall transcription speed (0.2 sec delay for passing TFIIIC; Matsuzaki et al. (1994); Wolffe et al. (1986)), productive transcription advances until a simple T-rich repeat on the non-template strand is reached (Fig. 7; Acker et al. (2013); Geiduschek and Kassavetis (2001) and references within).

This poly(dT) stretch has been identified as the universal terminator for RNAPIII at every gene, irrespective of the promoter, other *cis*-elements, or *trans*-acting factors (Arimbasseri et al. (2013) and references therein). This signal is usually located ~20 bp downstream of the 3'-end of the mature RNA sequence. Depending on the organism, a minimum T-stretch (a series of thymidines in the DNA) of four (vertebrates) to six T residues (*S. cerevisiae*) is necessary to induce cleavage of the product and termination (reviewed in Arimbasseri et al. (2013); Orioli et al. (2012)). This mechanism is reminiscent of the factor independent, intrinsic termination in bacteria (reviewed in Santangelo and Artsimovitch

(2011)), but even requires less sequence elements. For example, a hairpin 5'-located of the oligo(dA) stretch is not required for efficient termination in *S. cerevisiae* (Arimbasseri et al., 2014).

Transcription termination of the 17-subunit RNAPIII holoenzyme is dependent on the three intrinsic subunits Rpc53, Rpc37, and Rpc11 recognizing 5-7 thymidine residues on the non-template strand, thereby forming a pre-termination complex (PTC) (see Fig. 7, step 2&3). These complexes are highly conserved and Rpc57 as well as Rpc37 share homology to the auxiliary factor TFIIF of RNAPII, whereas Rpc11 is homologous to TFIIS and Rpb9 (Arimbasseri and Maraia (2015); Chedin et al. (1998) and reviewed in Arimbasseri et al. (2013)). A very recent study by Arimbasseri and Maraia showed how transcription is terminated on a molecular level (Arimbasseri and Maraia, 2015). Recognition of four Us (four uridines in the nascent RNA) by the subcomplex Rpc53/37 and Rpc11 leads to transformation of the elongating complex to a PTC.
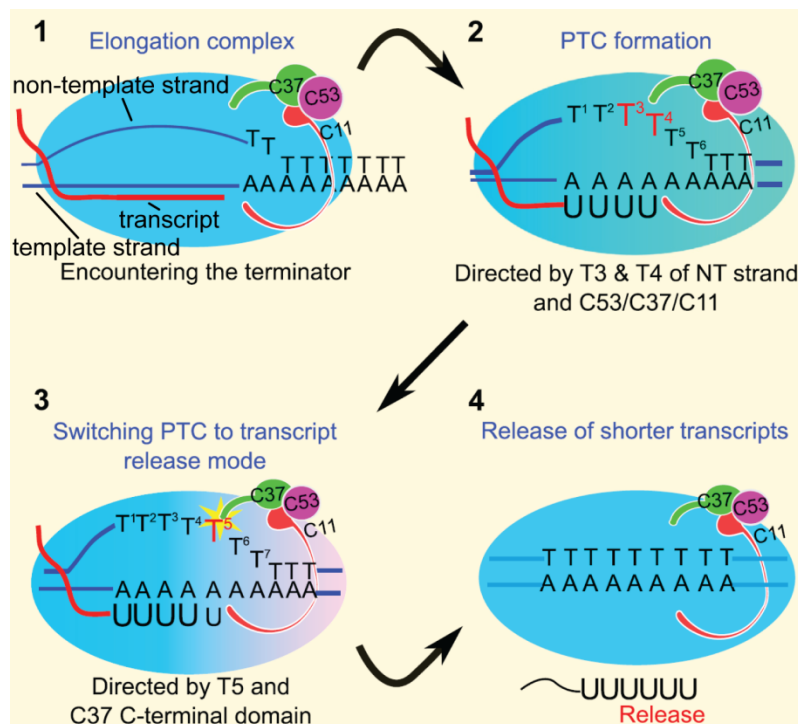
Fig. 7: RNAPIII termination mechanism. (1) The RNA polymerase III (blue) with the subcomplex C53/37 (ruby/green) and C11 (red) encounters the terminator. (2) The elongating complex is destabilized and the PTC is formed by recognition of T_3/T_4 through C53/37. (3) Synthesis of >4Us and recognition of T_5 on the non-template strand leads to switching from the PTC to transcript release mode. Cleavage of the nascent transcript is dependent and mediated by the C11 subunit and finally (4) the nascent transcript is released. Figure modified after Arimbasseri and Maraia (2015).

Upon addition of subsequent Us, the T_5-stretch and Rpc37 are important for switching the polymerase to a transcript release compatible mode (see Fig. 7, step 3). Release of the transcript occurs after transcript cleavage, which is dependent on the C11 subunit (Fig. 7,

step 4 and Chedin et al. (1998)). Albeit transcription can be alternatively terminated in an Rpc53/37 and Rpc11-independent manner when a minimum of eight U residues are synthesized, most RNAPIII terminators contain seven or less Ts preferring an Rpc53, Rpc37 and Rpc11 dependent termination mechanism (Arimbasseri and Maraia, 2013; Rijal and Maraia, 2013). The possibility of this termination factor independent termination and the efficient release of RNAs consisting of small U stretches (1-4Us) without a non-template strand points toward a termination mechanism initially activated by the weak rU:dA hybrid (see Fig. 7 and Arimbasseri and Maraia (2015)). Especially this kind of hybrid is very unstable and was proposed to be very important in general transcription termination throughout evolution (Martin and Tinoco, 1980). As with many essential processes in the cell, important steps are not coupled to the function of a single protein. The same is true for transcription termination, as one of the first proteins that interact with the nascent tRNA, Lhp1 with its human homologue La, was found to be important for the release of new transcripts and re-initiation of the transcription cycle (Maraia et al., 1994). It was first described as a chaperone for RNAs transcribed by RNAPIII and binds to them sequence- and length-specific to oligo(U) sequences of the RNA (reviewed in Arimbasseri et al. (2013); Maraia (2001)). This and other proteins, such as Rpc1 and Rpc2, Tfc6 or the human PC4 (Sub1 in *S. cerevisiae*), NF1 or TFIIICβ have been proposed to aid in transcription termination of RNAPIII (Acker et al. (2013) and references therein).

1.4.7 **RNAPIII recycling is required for multiple rounds of transcription**

The need of tRNAs and other ncRNAs in the cell is high, as rRNAs and tRNAs represent up to 95% of cellular RNA (~10% tRNA; White (2005)). Therefore, efficient transcription mechanisms had to be evolved to meet these high requirements. One way to do so is entitled 'facilitated recycling', in which a polymerase that transcribed a gene is committed predominantly to reinitiation on the same gene, thereby circumventing the slow steps of initiation. Hence, a new transcription cycle is completed up to 10-fold faster than the initial round of transcription, but only when a proper termination signal is present (Dieci and Sentenac, 1996). Interestingly, recycling RNAPIII is also approximately 10-fold less sensitive to Heparin treatment, which sequesters the polymerase from the gene by occupying the DNA binding site of RNA polymerases (Dieci and Sentenac, 1996).

Without facilitated recycling, RNAPIII is released from the gene into a free pool of RNAPIII after completing a full round of transcription (see Fig. 8A, 1). As a new round of transcription again requires the formation of the initiation factors and recruitment of the polymerase, which is the rate-limiting step, synthesis levels are comparably low. In contrast, facilitated recycling does not result in free polymerase, but rather tethers a single polymerase to a gene (see Fig. 8A, 2) (Dieci and Sentenac, 1996; Ferrari et al., 2004). However the

complete mechanism of how the polymerase is transferred back to the promoter to reinitiate transcription (see Fig. 8A) still remains elusive.

It is anticipated that the polymerase never leaves the vicinity of the promoter during transcription of the small tRNA genes. As the DNA is bent by TFIIIB and TFIIIC (bending not shown in Fig. 8A) into a potential gene loop, it is thought that the polymerase is reloaded on the same promoter. The still assembled PIC then promotes another round of transcription (Dieci et al., 2013; Dieci and Sentenac, 1996; Ferrari and Dieci, 2008; Ferrari et al., 2004; Leveillard et al., 1991). Although, *in vitro* a basic reinitiation only relies on the presence of TFIIIB, TFIIIC is needed for efficient transcription reinitiation especially of long RNAPIII genes (>300 bp) (Ferrari et al., 2004). In addition, it is discussed in the field, whether Rpc11 has a function in fostering reinitiation (Dieci et al., 2013). Furthermore, it was reported for *H. sapiens* that facilitated recycling protects the RNA polymerase III from repression by Maf1, the conserved, negative regulator of RNAPIII (Cabart et al., 2008).
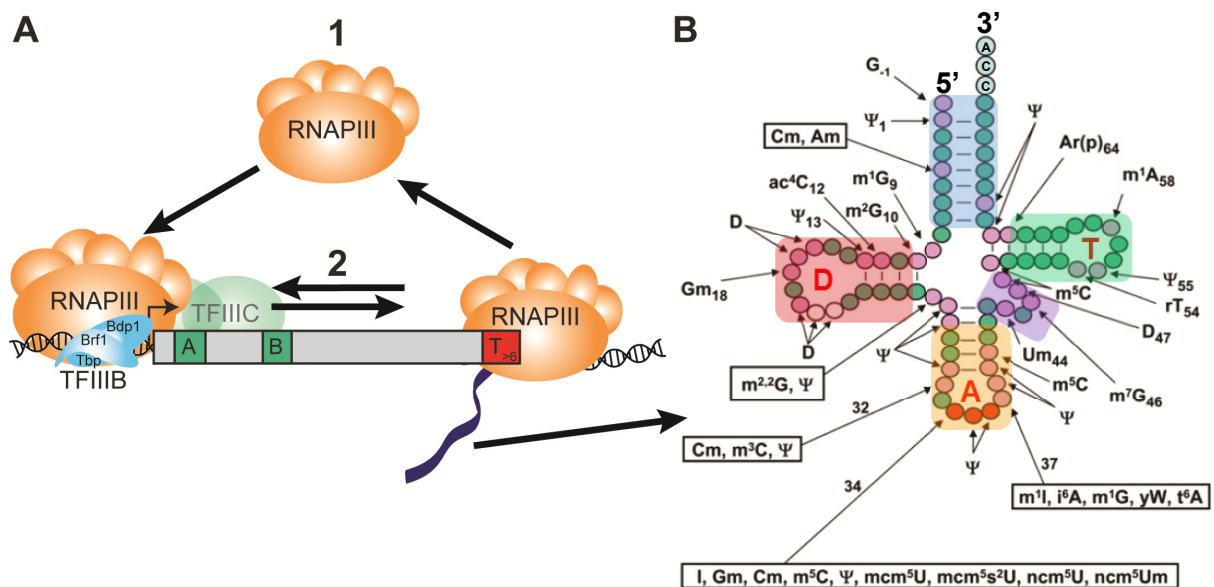
Fig. 8: Recycling of RNAPIII and tRNA structure. (A) A model of the reinitiating RNAPIII is depicted. (1) Classical initiation/ reinitiation from a free pool of RNAPIII. (2) Facilitated recycling by reloading the nearby polymerase to the same gene promoter with an intact PIC. Especially for long genes, TFIIIC is required for efficient reinitiation. See text for details. **(B)** Secondary cloverleaf structure and schematic of modifications of tRNA is shown. (D): D-loop, (A): Anticodon loop, (T): TψC-loop, blue area: acceptor stem, red area: D-arm, orange area: anticodon arm, purple area: variable loop and green area: T-loop. Unmodified bases (green circles), modified bases (pink), additional bases (white), the anticodon (red) and the CCA end (blue) are depicted. The 5'- and 3'-ends of the tRNA are highlighted. See text for details. Figure modified after Phizicky and Hopper (2010).

1.5 tRNA and tRNA metabolism

1.5.1 tRNA structure and function

After the nascent tRNA transcripts are released from the polymerase, they usually contain 5'-leader and 3'-trailer sequences and optionally introns (22% of all tRNA genes in yeast) that need to be removed to yield the typical 75-90 nt, long-living tRNAs that are present in all kingdoms of life. Forming the typical L-like tertiary structure, its secondary structure is often visualized as the known cloverleaf structure (see Fig. 8B). In this structure, five main domains can be recognized. These include (1) a relatively unmodified acceptor stem (Fig. 8B, blue area) that is extended with CCA bases on the 3'-end, where eventually an amino acid is coupled to by aminoacyl tRNA synthetases and (2) the D-loop (Fig. 8B, red area), which is important for tRNA recognition by aminoacyl tRNA synthetases together with the anticodon (Shimada et al., 2001). Furthermore, an (3) A-loop is present (Fig. 8B, orange area) that includes the important anticodon and hence is crucial for decoding the genetic information on the mRNA by providing the correct amino acid to the nascent peptide chain. A (4) variable loop (Fig. 8B, purple area) and the (5) TψC-loop (Fig. 8B, green area) that binds to the 5S rRNA of the large subunit of the ribosome complete the secondary cloverleaf structure of tRNAs (Grummt et al. (1974) and Hopper (2013); Hopper and Huang (2015); Phizicky and Hopper (2010) and references therein). The most important function of this structural RNA is to serve in translation, linking the genetic information of the nucleic acid sequence to the amino acids that are incorporated into the nascent polypeptide.

1.5.2 tRNA maturation, export and degradation

Being synthesized as precursors, tRNAs undergo a variety of maturation events. Post-transcriptionally, the 5'-leaders and 3'-trailers (Fig. 9, purple extensions on tRNA) are cleaved, respectively. The nucleolar RNase P complex consists of nine proteins (Pop1, Pop3-8, Rpp1 and Rpp2) and the *RPR1* RNA, which is transcribed by RNAPIII (Lee et al. (1991) and reviewed in Xiao et al. (2002)). Recognizing at least two structural domains of pre-tRNAs (acceptor stem and the TψC-loop), RNase P is mostly sufficient to generate mature 5'-ends of tRNAs (Schon (1999) and references therein). In contrast to that, 3'-end maturation is more complex and involves the endonuclease RNase Z, the 3'-5' exonuclease Rex1, and molecular chaperone Lhp1 (La in *H. sapiens*) (reviewed in Hopper (2013)). After trimming of the 3'-end, the CCA residues are added to every tRNA by the tRNA nucleotidyl transferase Cca1 (and its isoforms) (Aebi et al., 1990; Martin and Hopper, 1994). This is a prerequisite for the aminoacylation of tRNAs, which is conducted by aminoacyl tRNA synthetases through covalently attaching a specific amino acid to the ribose of the last 3'-A

base of the selected tRNA under ATP consumption (reviewed in Pang et al. (2014)). In addition, this process is one of the key fidelity steps for correct translation, as it defines the amino acid that will be inserted into a translated protein dependent on a specific codon. Hence, some synthetases have evolved amino acid editing mechanisms (Pang et al., 2014).

In addition to these terminal processing events, intron-containing tRNAs have to be spliced before they can function in translation. They are first exported by Los1 after the initial modifications took place (see above and Fig. 9, green area) or leave the nucleus as pre-tRNAs (Fig. 9, blue area), as the splicing occurs on the cytoplasmic surface of mitochondria. In yeast, the splicing machinery consists of three parts: (i) the tRNA splicing endonuclease complex (Sen complex), (ii) the tRNA ligase (Trl1), and (iii) the 2' phosphotransferase (Tpt1) (reviewed in Hopper and Huang (2015); Phizicky and Hopper (2010)). Subsequently, tRNAs are aminoacylated either in the cytoplasm or after their reimport into the nucleus (Fig. 9).
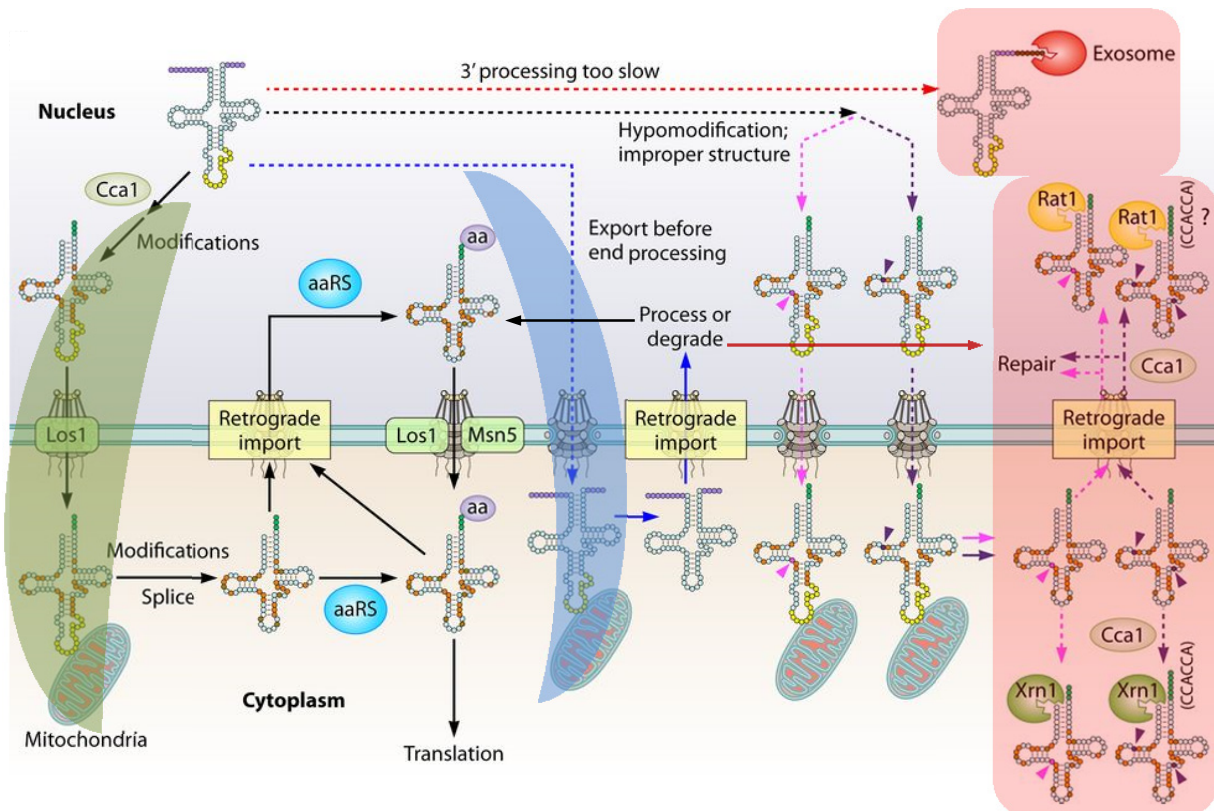
Fig. 9: tRNA quality control overview. Intron-containing tRNA modification and control pathways are depicted. Green area: Correct tRNA modification and export. Intron-containing tRNAs are spliced on the outer surface of the mitochondria, reimported, aminoacylated, and re-exported to serve in translation. Non-intron containing tRNAs are aminoacylated in the nucleus in addition before export. Blue area: Same as in green area, but tRNAs are exported prior to end processing, spliced, reimported, and eventually processed or degraded. Red area: The various ways of tRNA degradation in the cytoplasm and the nucleus are shown. Black arrows: maturation pathways, red arrows: degradation pathways, pink arrows: hypomodified tRNAs, green boxes: proteins involved in tRNA export, aaRS: aminoacyl-tRNA synthetases. See text for details. Figure modified after Hopper and Huang (2015).

Here, additional processing occurs or defective / non-correctly spliced tRNAs are degraded (Phizicky and Hopper, 2010). In addition to the mentioned sequence alterations, a plethora of base modifications are known for tRNAs. In total, up to 85 modifications have been described in all kingdoms (25 in yeast) and usually a combination of 7-17 of these are found in each mature tRNA (see Fig. 8B and El Yacoubi et al. (2012); Phizicky and Hopper (2010) and references therein). These include acetylation, isopentenylation, methylation, pseudouridylation (ψ), or uridine thiolation of pre-tRNA, to name but a few. These base modifications play important roles mostly in codon-anticodon recognition, translation fidelity, correct tRNA positioning inside the ribosome or tRNA stability (Phizicky and Hopper (2010) and references therein).

tRNA degradation is also highly regulated, depending on the stage of tRNA life. If the tRNA processing is too slow, or hypomodification is recognized, an oligo(dA) tail will be attached to the 3'-end of the tRNA and it is degraded by the exosome (Fig. 9, upper red area, Parker (2012) and references therein). The 5'-3' exonucleases Rat1 and the cytoplasmic Xrn1 function in later stages of tRNA life, once the tRNA is matured but is lacking specific modifications that cannot be repaired (Fig. 9, lower red area).

The latter mechanism, named rapid tRNA decay (RTD), requires Met22, a methionine biosynthetic enzyme, to efficiently break down tRNAs (Chernyakov et al., 2008).

1.6   tRNA associated diseases

Evidence exists that tRNAs function in a variety of cellular pathways, such as stress response, gene expression, regulation of apoptosis by binding to cytochrome C or translation regulation by cleavage of tRNAs into tiRNA after heat shock (Mei et al. (2010); Yamasaki et al. (2009) and reviewed in Raina and Ibba (2014)). Furthermore, several diseases have been identified to be caused by defects in tRNA biology. For example, tRNA levels are often upregulated in cancer, impaired aminoacylation causes neurological or mitochondrial diseases like Charcot-Marie-Tooth syndrome or ataxia. Conversely, it has also been described that reduced tRNA levels can lead to neonatal death or hypoplasia, especially during development (reviewed in Kirchner and Ignatova (2015)). Interestingly, incorrect or insufficient processing of tRNAs has also been linked to Amyotrophic Lateral Sclerosis (ALS) or Parkinson's Disease (PD) (Anderson and Ivanov (2014) and references therein). In addition, an emerging role for tRNA halves and processing products (*e.g.* for the 5'-leader or the 3'-trailer) in varying cellular processes is discussed in the field (Deng et al. (2015); Haussecker et al. (2010), Anderson and Ivanov (2014) and references therein).

1.7   Additional RNAPIII transcription factors and effectors

As already outlined above, efficient synthesis of RNAPIII products is crucial for many different processes in the cell, especially for protein biosynthesis, *i.e.* providing the structural 5S rRNA and tRNAs. Therefore, an understanding of regulatory factors that fine-tune RNAPIII transcription is important. Biochemical and genome-wide studies have identified several factors influencing the expression of class III genes, in addition to TFIIIB and TFIIIC. To mention but a few, Maf1, Dst1 (TFIIS), Sub1, Myc, Rb and p53 have been identified to function in RNA polymerase III transcription (Ghavi-Helm et al. (2008); Pluta et al. (2001); Tavenet et al. (2009) and Acker et al. (2013); White (2005) and references therein).

Maf1, as mentioned above, is a key negative regulator of RNAPIII transcription. It represses transcription by RNAPIII in response to stress conditions (Roberts et al., 2006). Additionally, a Δ*maf1* deletion strain shows accumulation of pre-tRNAs in the nucleus. This is due to non-mature transcripts that saturate the tRNA exporter Los1 (Karkusiewicz et al., 2011). Upon various stress conditions, Maf1 is dephosphorylated, imported into the nucleus, and can interact with RNAPIII. Co-localizing genome-wide with RNAPIII, Maf1 inhibits steps before and after the PIC formation (Pluta et al., 2001; Roberts et al., 2006; Vannini et al., 2010).

Dst1/ TFIIS is a general elongation factor in yeast and helps RNAPII to read through transcription blocks by stimulating the nascent transcript cleavage activity of RNAPIII at arrest sites (Ubukata et al., 2003). In addition to that, Dst1 was identified to bind to all RNAPIII transcribed genes in yeast and mouse, to function in RNAPIII transcription, and to be involved in start site selection (Carriere et al., 2012; Ghavi-Helm et al., 2008). Another RNAPII auxiliary factor identified in RNAPIII transcription is Sub1 and its human homologue PC4. Sub1/ PC4 was first identified as a coactivator of RNAPII and is required for cellular processes such as transcription, DNA repair and replication (Conesa and Acker (2010) and references therein). Genome-wide data revealed that Sub1 binds to RNAPIII genes, interacts with the transcription machinery and helps efficient initiation and reinitiation of RNAPIII transcription *in vitro* (Tavenet et al., 2009).

Furthermore, chromatin modifying enzymes and remodeling complexes have been proposed to influence RNAPIII transcription. Detailed mechanisms are not known yet, but remodeling complexes are thought to adapt and maintain the local chromatin state (euchromatin) and to keep tRNA genes free from nucleosomes (Kumar and Bhargava (2013) and Acker et al. (2013); Bhargava (2013) and references therein). In good accordance with the nucleosome free region of tRNA genes, RSC (Remodel the Structure of Chromatin), an ATP-dependent chromatin remodeling complex, interacts with RNAPIII and was found to be necessary for a low density of nucleosomes in this region (Bhargava (2013) and references therein). Moreover, RSC promotes the recruitment of the FACT complex (Facilitates

Chromatin Transcription) to the *SUP4* gene for keeping it nucleosome-free (Mahapatra et al., 2011). A factor potentially interacting with RSC is Nhp6. Nhp6 delineates the two highly homologues and functionally redundant proteins Nhp6A and Nhp6B that bind to DNA in a sequence-unspecific manner via their HMG (high mobility group) B domains and modulate chromatin structure (reviewed in Acker et al. (2013). It was described that Nhp6 enhances transcription of *SNR6* genes *in vitro* and is necessary for transcriptional initiation fidelity of some RNAPIII genes (Kassavetis and Steiner, 2006; Kruppa et al., 2001). Strikingly, Δ*nhp6* mutants, *i.e.* in which Nhp6 is lost from RNAPIII genes, display changed chromatin structure over the TATA box of *SNR6*. Furthermore, barrier activity against heterochromatin spreading over a tested tRNA gene is compromised (Braglia et al., 2007; Lopez et al., 2001; Venters et al., 2011).

Many more proteins have been implicated in RNAPIII transcription, *e.g.* Fkh1, Reb1, or Yap6. These proteins are transcriptional effectors of RNAPII and were identified in genome-wide binding analyses (Venters et al., 2011). Unfortunately, their function in RNAPIII transcription remains elusive, just as their potential to link the RNAPII and RNAPIII transcription systems. Another example is Yox1, which is a homeodomain-containing transcriptional repressor that binds to tRNA genes and intergenic regions in close proximity (Horak et al., 2002; Kaufmann, 1993). As before, no exact role for this protein has been revealed in RNAPIII transcription yet.

1.8   Aims and Scope

The correct and efficient expression of tRNAs and other ncRNAs by RNA polymerase III is a crucial and highly regulated process. Nearly a decade ago, the first complete recombinant reconstituted RNAPIII transcription system was described and it was found that this system has only low transcription rates, compared to isolated, transcription active cell fractions (Ducrot et al., 2006). This strongly highlights the necessity of additional proteins that help the polymerase to effectively produce tRNAs and other ncRNAs. In the last decade, genome-wide studies indeed led to the discovery of several proteins in varying species with a function in RNAPIII transcription, whereas the detailed molecular mechanisms often still remain elusive (reviewed in Acker et al. (2013)).

Serendipitously, when investigating the genome-wide localization of the THO/TREX complex and other proteins involved in nuclear mRNP biogenesis, the poly(A)-binding protein Nab2 was found to occupy all tRNA and other ncRNA gene loci examined (Meinel, 2013).

Nab2 was originally identified as an essential nuclear polyadenylated RNA-binding

protein, in particular important for poly(A) tail length control and export of mRNAs (Anderson et al. (1993) and reviewed in Soucek et al. (2012)). Binding to the mRNA occurs shortly after transcription or during 3'-end processing and Nab2 accompanies the mRNP to the cytoplasm, where it leaves the mRNA and travels back to the nucleus. Additionally, orthologues of Nab2 have been identified throughout evolution from yeast to humans (see Kelly et al. (2014); Pak et al. (2011) and Introduction, 1.3.3). Hence, it was surprising to find an mRNP biogenesis factor that occupies RNAPIII genes.

The localization of Nab2 to RNAPIII genes raised the question whether Nab2 functions in RNAPIII transcription and if so, which function would be fulfilled by Nab2. Hence, starting from the genome-wide data, the first aim of this PhD project was to identify whether Nab2 is functioning in RNAPIII transcription. As a starting point, the first task of this project was the generation of a new conditional allele of *NAB2* or a functional degron to deplete Nab2 fast from cells. This mutant could subsequently be used to investigate the potential function of Nab2 in RNAPIII transcription. Furthermore, it was investigated whether Nab2 interacts physically with RNAPIII. Co-occupancies should be confirmed on single target genes.

Having identified Nab2 being required for the synthesis of wild-type tRNA levels, the second aim was to investigate the molecular mechanism of how Nab2 can stimulate RNAPIII transcription. For this, specific assays, such as whole-cell extract based, as well as fully reconstituted *in vitro* transcription assays were set up and performed to detect a stimulation of Nab2 on the transcriptional output. In addition, the involvement of the transcription initiation factors TFIIIB and TFIIIC was tested.

2. Material and Methods

2.1 Material

2.1.1 Chemicals and consumables

If not stated otherwise, chemicals and consumables were purchased from the following companies: Agilent Technologies (Waldbronn, Germany), Applichem GmbH (Darmstadt, Germany), Applied Biosciences (Darmstadt, Germany), Beckman Coulter (Krefeld, Germany), Bio-Rad (Hercules, USA), Biozym (Hess. Oldendorf, Germany), Carl Roth (Karlsruhe, Germany), Diagenode (Liege, Belgium), Eppendorf (Hamburg, Germany), Fermentas (St. Leon-Rot, Germany), Formedium (Norwich, UK), Fujifilm Corporation (Tokyo, Japan), GE Healthcare Europe (Freiburg, Germany), Gilson (Bad Camberg, Germany), Hartmann Analytic GmbH (Braunschweig, Germany), Invitrogen (Karlsruhe, Germany), Jena Bioscience GmbH (Jena, Germany), Life Technologies (Carlsbad, USA), Macherey&Nagel (Düren, Germany), MembraPure (Bodenheim, Germany), Merck Biosciences (Darmstadt, Germany), Millipore (Molsheim, France), Mobitec (Göttingen, Germany), Molecular Probes (Eugene, USA), Nanoprobes (Yaphank, USA), NEB (Frankfurt, Germany), Neolab (Heidelberg, Germany), Open Biosystems (Huntsville, USA), Promega (Mannheim, Germany), Qiagen (Hilden, Germany), Quantifoil Micro Tools GmbH (Jena, Germany) Roche (Mannheim, Germany), Sarstedt (Nümbrecht, Germany), Serva (Heidelberg, Germany), Sigma (Taufkirchen, Germany), Spectrum Europe B.V. (Breda, Netherlands), Stratagene (Amsterdam, Netherlands), Thermo Scientific (Munich, Germany), VWR (Ismaning, Germany).

2.1.2 Equipment

The used equipment is listed in Table 1.

Table 1: Equipment

Name	Supplier
AEKTA Purifier	GE Healthcare (Freiburg, Germany)
BAS IP SR2040 E	Fujifilm (Tokyo, Japan
Bioruptor UCL 200 Diagenode	(Liege, Belgium)
Beckman DU650 spectrophotometer	Beckman Coulter (Krefeld, Germany)
ChemoCam Imager ECL HR 16-3200	Intas, (Göttingen, Germany)
CME microscope	Leica (Buffalo, USA)
CO8000 Cell Density Meter	WPA (Cambridge, UK)
Dissection microscope MSM 400	Singer Instruments (Somerset, UK)

Electrophoresis Power Supply Consort E835	Neolab (Heidelberg, Germany)
Eppendorf centrifuge 5415D, 5424R	Eppendorf (Hamburg, Germany)
Gel iX20	Intas (Göttingen, Germany)
Heating oven	BINDER GmbH (Tuttlingen, Germany)
Heidolph shaker duomax 1030	Neolab (Heidelberg, Germany)
Hybaid Mini Oven	Thermo Fisher Scientific (Munich, Germany)
Innova 44 shaking incubator	New Brunswick Scientific (Nürtingen)
Incubator shaker ISF-1-V	Adolf Kühner AG (Basel, Switzerland)
Laser Scanning microscope	Zeiss LSM510
Mini-Protean II system, Mini Trans-Blot Cell	Bio-Rad Laboratories (Herucles, USA)
Model 583 gel dryer	Bio-Rad Laboratories (Herucles, USA)
Morgagni transmission electron microscope	FEI (Hillsboro, USA)
Multitron Pro / Labotron shaker	Infors HT (Einsbach, Germany)
Optima TM L-90 K and L80 ultracentrifuge	Beckman Coulter (Krefeld, Germany)
Optimax TR developing machine	MS Laborgeräte (Dielheim, Germany)
Pipetboy acu	INTEGRA Biosciences AG (Zizers, Switzerland)
pH 211 Microprocessor pH meter	HANNA instruments (Woonsocket, USA)
Poros HS 50 10/100	Life Technologies (Carlsbad, USA)
Pulverisette	Fritsch (Idar-Oberstein, Germany)
Rotanda 46R, 460R	Hettich (Tuttlingen, Germany)
Rotator, Vortex Genie2	Neolab (Heidelberg, Germany)
Semi Dry Blot Apparatus	Peqlab (Erlangen, Germany)
SLC 6000, GS3, SW34 rotor	Thermo Fisher Scientific (Munich, Germany)
Spectrophotometer ND-1000	Thermo Fisher Scientific (Munich, Germany)
Sonifier 250	Branson (Danbury, USA)
Sorvall Evolution RC, RC 5B Plus	Thermo Fisher Scientific (Munich, Germany)
StepOnePlus Real Time PCR System	Applied Biosystems (Darmstadt, Germany)
Sunrise Microplate Absorbance Reader	Tecan Group Ltd. (Männedorf, Switzerland)
Superose 6 10/300 GL	GE Healthcare (Freiburg, Germany)
SW-22 shaking waterbath	Julabo (Seelbach, Germany)
SW32, SW40 rotor	Beckman Coulter (Krefeld, Germany)
T3 Thermocycler	Biometra (Göttingen, Germany)
Thermomixer compact, BioPhotometer	Eppendorf (Hamburg, Germany)
Trans-Blot Cell	Bio-Rad Laboratories (Herucles, USA)
Trans-Blot Semidry Blotter	Bio-Rad Laboratories (Herucles, USA)
Typhoon FLA-9500 / 9400	GE Healthcare (Freiburg, Germany)
Unichromat 1500	Uniequip (Martinsried, Germany)
Universal Analytical Balance	Satorius (Göttingen, Germany)
UV Crosslinker FB-UVXL-1000	Fisher Scientific (Hampton, USA)
Vakulab S3000	MMM GmbH (Planegg, Germany)

2.1.3 **Media and buffers**

Media and buffers were prepared with MilliQ water (Merck, Darmstadt, Germany) and autoclaved (120°C, 20 min). Heat sensitive solutions and buffers used in chromatography were sterile-filtered (0.22 μm) prior to use. Glassware was washed, dried and eventually autoclaved as stated above. Specific buffers for experiments are mentioned in section 2.2.

Table 2: Media

Media	Composition
'Lysogeny' Broth (LB)	1% (w/v) tryptone; 0.5% (w/v) yeast extract; 0.5% (w/v) NaCl; (2% (w/v) agar for plates)
Synthetic complete dropout medium (SDC)	0.67% (w/v) yeast nitrogen base; 0.06% (w/v) complete synthetic mix of aa; drop out as required; 2% (w/v) glucose; when required 0.1% (w/v) 5-FOA was added; (2% (w/v) agar plates)
Sporulation medium (YPA)	2% (w/v) peptone; 1% (w/v) potassium acetate; 1% (w/v) yeast extract; 2% (w/v) agar
Yeast full medium (YPD)	2% (w/v) peptone; 2% (w/v) glucose; 1% (w/v) yeast extract; (2% (w/v) agar for plates)
HEK293T cell medium	Dulbecco's minimal essential medium supplemented with 10% fetal bovine serum, 1x L-glutamine and penicillin/streptomycin

Table 3: Buffers

Buffer	Composition
5x Bradford reagent	0.05% (w/v) Coomassie Brilliant Blue G-250, 25% Ethanol, 42.5% Phosphoric acid
Coomassie stain solution	0.25% (w/v) Coomassie Brilliant Blue R-250, 30% (v/v) ethanol, 10% (v/v) acetic acid
Destain solution	30% (v/v) ethanol, 10% (v/v) acetic acid
6x DNA loading dye	40% (w/v) sucrose, 0.25% bromphenol blue, 0.25% xylene cyanole FF,
1x Formamide loading buffer	90% (v/v) Formamide, 1x TBE buffer, 0.05% bromphenol blue, 0.05% xylene cyanole FF
Phosphate-buffered saline (PBS)	137 mM NaCl, 2,7 mM KCl, 20 mM NaH_2PO_4, 10 mM Na_2HPO_4 (pH 7.5)
Protease inhibitor (100x)	8 ng/ml Leupeptin, 137 ng/ml Pepstatin A, 17 ng/ml PMSF, 0.33 mg/ml Benzamidine, solved in 100% EtOH (p.a.)
4x SDS sample buffer	0.2 M Tris-HCl (pH 6.8); 40% (v/v) glycerol, 8% (w/v) SDS, some mg of bromophenol blue, 0.1M DTT
SDS-PAGE running buffer	25 mM Tris, 0.1% (w/v) SDS, 0.19 mM glycine
4x separating SDS-gel buffer	3 M Tris, 0.4% (w/v) SDS, pH 8.8 (HCl)
4x stacking SDS-gel buffer	0.5 M Tris, 0.4% (w/v) SDS, pH 6.8 (HCl)

20x SSC buffer	300 mM sodium citrate (pH 7), 3M NaCl
50x TAE	2 M Tris, 100 mM EDTA, pH 8.0; 1 M acetic acid
TE (1x)	1 mM EDTA, 10 mM Tris-HCl, pH 8.0
Tris-buffered saline(TBS)	137 mM NaCl, 2.7 mM KCl, 12.5 mM Tris-HCl (TBS-T: add 0.1% (v/v) Tween-20)
Wet blotting buffer	25 mM Tris, 192 mM glycine, 10% methanol
10x KNOP buffer	500 mM Tris-HCl (pH 9.2), 160 mM $(NH_4)_2SO_4$, 22.5 mM $MgCl_2$

2.1.4 Organisms

2.1.4.1 Yeast strains and cultivation

Wild-type strains were initially purchased from Euroscarf (Frankfurt, Germany). If not stated otherwise, cultures were grown in YPD at 30°C and shaking at 230 rpm. Lists with strains and organisms used in this study can be found in the tables below.

Table 4: *Saccharomyces cerevisiae* Strains

Strain	Genotype	Reference
BY4741	*MATa; his3Δ1; leu2Δ0; met15Δ0; ura3Δ0*	Euroscarf
RS453	*MATa; ade2-1; his3-11,15; ura3-52; leu2-3,112; trp1-1; can1-100; GAL+*	Euroscarf
W303	*MATa; ura3-1; trp1-1; his3-11,15; leu2-3,112; ade2-1; can1-100; GAL+*	Euroscarf
Δmod5	*MATa; mod5::kanMX4; his3Δ1; leu2Δ0; met15Δ0; ura3Δ0*	Euroscarf
BDP1-TAP	*MATa; BDP1-TAP::TRP1; ade2-1; his3-11,15; ura3-52; leu2-3,112; trp1-1; can1-100; GAL+*	this study
BRF1-HA	*MATa; BRF1-HA::HIS3mx6; ade2-1; his3-11,15; ura3-52; leu2-3,112; trp1-1; can1-100; GAL+*	this study
HPR1-TAP	*MATa; HPR1-TAP::URA3; his3Δ1; leu2Δ0; met15Δ0; ura3Δ0*	(Meinel et al., 2013)
NAB2-AID	*MATa; NAB2-AID::kanMX6; ura3-1; trp1-1; his3-11,15; leu2-3,112; ade2-1; can1-100; GAL+; ura3::pNHK53*	this study
NAB2 shuffle	*MATa ;nab2::HIS3; ura3-1; trp1-1; his3-11,15; leu2-3,112; ade2-1; can1-100; GAL+; pRS316-NAB2*	this study
NAB2 shuffle BDP1-TAP	*MATa ;nab2::HIS3; BDP1-TAP::TRP1; ura3-1; trp1-1; his3-11,15; leu2-3,112; ade2-1; can1-100; GAL+; pRS316-NAB2*	this study
NAB2 shuffle RPC160-TAP	*MATa; nab2::HIS3; RPC160-TAP::TRP1; ura3-1; trp1-1; his3-11,15; leu2-3,112; ade2-1; can1-100; GAL+; pRS316-NAB2*	this study
NAB2 shuffle TFC1-TAP	*MATa ;nab2::HIS3; TFC1-TAP::TRP1; ura3-1; trp1-1; his3-11,15; leu2-3,112; ade2-1; can1-100; GAL+; pRS316-NAB2*	this study

Nab2-TAP	*MATa; NAB2-TAP::TRP1; ade2-1; his3-11,15; ura3-52; leu2-3,112; trp1-1; can1-100; GAL+*	this study
Nab2-TAP BRF1-HA	*MATa; NAB2-TAP::TRP1; BRF1-HA::HIS3mx6; ade2-1; his3-11,15; ura3-52; leu2-3,112; trp1-1; can1-100; GAL+*	this study
Nab2-TAP TFC8-HA	*MATa; NAB2-TAP::TRP1; TFC8-HA::HIS3mx6; ade2-1; his3-11,15; ura3-52; leu2-3,112; trp1-1; can1-100; GAL+*	this study
NAB2-TAP RPC160-HA	*MATa; NAB2-TAP::TRP1; RPC160-HA::HIS3mx6; ade2-1; his3-11,15; ura3-52; leu2-3,112; trp1-1; can1-100; GAL+*	this study
RPA190-TAP	*MATa; RPA190-TAP::TRP1; his3-11,15; ura3-52; leu2-3,112; trp1-1;can1-100; GAL+*	this study
RPB3-TAP	*MATa; RPB3-TAP::HIS3; his3Δ1; leu2Δ0; met15Δ0; ura3Δ0*	(Meinel et al., 2013)
RPC25 (YPH500)	*MATα; ura3-52; lys2-801_amber, ade2-101_ochre; trp1-Δ63; his1-Δ200; leu2-Δ1*	(Zaros and Thuriaux, 2005)
RPC25 NAB2-TAP	*MATα; NAB2-TAP::TRP1; ura3-52; lys2-801_amber, ade2-101_ochre; trp1-Δ63; his1-Δ200; leu2-Δ1*	this study
RPC25 RPC160-TAP	*MATα; RPC160-TAP::TRP1; ura3-52; lys2-801_amber, ade2-101_ochre; trp1-Δ63; his1-Δ200; leu2-Δ1*	this study
rpc25-S100P (DS3-6b)	*MATa; ura3-52; trp1-Δ63; his3-Δ200; leu2; rpc25-S100P*	(Zaros and Thuriaux, 2005)
rpc25-S100P NAB2-TAP	*MATa; NAB2-TAP::TRP1; ura3-52; trp1-Δ63; his3-Δ200; leu2; rpc25-S100P*	this study
rpc25-S100P RPC160-TAP	*MATa; RPC160-TAP::TRP1; ura3-52; trp1-Δ63; his3-Δ200; leu2; rpc25-S100P*	this study
RPC160-HA	*MATa; RPC160-HA::HIS3mx6; ade2-1; his3-11,15; ura3-52; leu2-3,112; trp1-1; can1-100; GAL+*	this study
RPC160-TAP	*MATa; RPC160-TAP::TRP1; ade2-1; his3-11,15; ura3-52; leu2-3,112; trp1-1; can1-100; GAL+*	this study
RPC160-TAP NAB2-AID	*MATa; RPC160-TAP::TRP1; ura3::pNHK53; NAB2-AID::kanMX6; ade2-1; his3-11,15; ura3-52; leu2-3,112; trp1-1; can1-100; GAL+*	this study
TFC1-TAP	*MATa; TFC1-TRP1::TRP1; ade2-1; his3-11,15; ura3-52; leu2-3,112; trp1-1; can1-100; GAL++*	this study
TFC8-HA	*MATa; TFC8-HA::HIS3mx6; ade2-1; his3-11,15; ura3-52; leu2-3,112; trp1-1; can1-100; GAL+*	this study
YMS721	*MATα; his3Δ1; leu2Δ0; met15Δ0; ura3Δ0; can1Δ::STE2pr-spHIS5; lyp1Δ::STE3pr-LEU2*	(Breslow et al., 2008)

2.1.4.2 Mammalian cell culture

HEK293T cells were grown at 37°C with 5% CO_2 in supplemented DMEM medium and used for transfection with *ZC3H14* in peGFP-N3 using Lipofectamine 2000 (Invitrogen).

2.1.4.3 *E. coli*

E. coli strains were grown in LB medium, supplemented with the corresponding antibiotic, at 37°C, 180 rpm and used for molecular cloning and production of recombinant proteins originated from humans or yeast according to standard molecular biology procedures.

Table 5: *E . coli* Strains

Strain	Genotype	Reference
Escherichia coli DH5α	F⁻ endA1 glnV44 thi-1 recA1 relA1 gyrA96 deoR nupG Φ80dlacZΔM15 Δ(lacZYA-argF)U169 hsdR17(r_K^- m_K^+) λ–	Woodcock et al. (1989)
Escherichia coli BL21 (DE3)	F⁻ *ompT hsdS*$_B$(r_B^- m_B^-) *gal dcm* (DE3)	Studier and Moffatt (1986)
Escherichia coli Rosetta™ (DE3)pLysS	F⁻ *ompT hsdS*$_B$(r_B^- m_B^-) *gal dcm* (DE3) pLysSRARE2 (Cam^R)	Novagen®

2.1.5 Oligonucleotides

Used oligonucleotides are listed in Tables 6 to 9 and were synthesized by Thermo Fisher Scientific (Ulm, Germany) or Biolegio (Njimegen, Netherlands).

Table 6: Oligonucleotide Sequences used for Genomic Tagging

Name	Sequence (5′–3′)
Bdp1-HA fw	GACAATGAGGATAATGAAGGAAGTGAAGAAGAGCCTGAGATTGAT CAACGTACGCTGCAGGTCGAC
Bdp1-HA rev	GTTGTGCTATTTATCCATTATGTATGCATATAAATGTCTCTTAATCG ATGAATTCGAGCTCG
Nab2-TAP fw	GCAAACCAGTTTTACGCACCAAGAACAAGATACGGAAATGAACTCC ATGGAAAAGAGAAG
Nab2-TAP rev	GGTGTCTTCCATCAAAAGGGTCACAGGAACATGAATTTCGTTCCTA CGACTCACTATAGGG
Rpc160-TAP fw	GCGATGTCTATTTGAAAGTCTCTCAAATGAGGCAGCTTTAAAAGCG AACTCCATGGAAAAGAGAAG
Rpc160-TAP rev	GGTTTTTATCATGTAGTTTTATATGTATAAATACGTTAAATGACTGT GGTAGTACGACTCACTATAGGG
3_NAB2AID-rev	AAAAGGGTCACAGGAACATGAATTTCGTTCCGTGATTTTAATAGTA ATCATTAATCGATGAATTCGAGCTCG

4_NAB2AID-fw	CTCCTCCGCAAACCAGTTTTACGCACCAAGAACAAGATACGGAAAT GAACCGTACGCTGCAGGTCGAC
5_Rpc160HA -fw	AGCGATGTCTATTTGAAAGTCTCTCAAATGAGGCAGCTTTAAAAGC GAACCGTACGCTGCAGGTCGAC
6_Rpc160HA-rev	GTAGAAAATAATACAAATGCTATAAAAAAGTTTAAAAACGACTACT TTAATCGATGAATTCGAGCTCG
113_LHP1-HA-fw	CAAAAGAGGACTCTTCTGCCATTGCCGATGACGATGAGGAGCACA AGGAGCGTACGCTGCAGGTCGAC
114_LHP1-HA-rev	TATGCTATGATAATGAGATACGAGAACCAGAAGAAACACAAGAATC AATCGATGAATTCGAGCTCG
128_Bdp1-TAP-fw	GGATAATGAAGGAAGTGAAGAAGAGCCTGAGATTGATCAATCCAT GGAAAAGAGAAGATGG
129_Bdp1-TAP-rev	GTGCTATTTATCCATTATGTATGCATATAAATGTCTCTTATACGACT CACTATAGGGCGAATTG
130_Tfc1-TAP-fw	TGAAAAGCGAGCTCAAGGGATTTGTTGATGAAGTCGATCTGTCCAT GGAAAAGAGAAGATGG
131_Tfc1-TAP-rev	GGCATATTTTGATATTGAAATAAAAGAAAACCTACTTATTATACGAC TCACTATAGGGCGAATTG
186_Brf1_HA_for	CAAGTTTCTCCAAGAAGATTAATTACGACGCCATTGACGGTTTGTT TAGGCGTACGCTGCAGGTCGAC
187_BRf1_HA-rev	CTTTATTTCCGTTCCCTTTTTCCTTCCTAGGGTTGATTACCTAAACG TTAATCGATGAATTCGAGCTCG
205_Tfc8-HA-fw	AAAGATTTAATGAAATAAGCGTATATTGTGGAACAACGCTGGAAGT TATGCGTACGCTGCAGGTCGAC
206_Tfc8-HA-rev	TATGACTACTTTTTATATCTGCAAGTAATTCTTTGTCTCTTGTATCCT TAATCGATGAATTCGAGCTCG

Table 7: Oligonucleotide Sequences used for Cloning

Name	Sequence (5′–3′)
27_Nab2aa526_rev	TAAGCGGCCGCTCAGTTCATTTCCGTATCTTG
26_seq*NAB2*_fw	ATCGCGCAACAGCAACCTC
60_Nab2_rev	ATTGGATCCGTTCATTTCCGTATCTTG
35_Nab2aa1_fw	ATTGGATCCATGTCTCAAGAACAGTACAC
28_Nab2aa101_rev	TAAGCGGCCGCTCATTGTCCCAAGCTTTGC
29_Nab2aa180_rev	TAAGCGGCCGCTCAGGATGGAGTTGCAGG
30_Nab2aa183_fw	ATTGGATCCATGGCCTTTTCCGGCGTTGTTAAC
31_Nab2aa261_rev	TAAGCGGCCGCTCAACGCCCCTCTTTCTTG
32_Nab2aa262_fw	ATTGGATCCATGTGCAGATTGTTTCCTCAC
58_Nab2aa399_fw	ATTGGATCCAGCCAGAAGAAAGCAGCTCC
59_Nab2aa398_rev	ATTGCGGCCGCTCATATTGGTTTTACTTCC
66_Nab2aa330_rev	ATTGCGGCCGCTCACCTTTTTGCCGCCAAT
67_Nab2aa328_fw	ATTGGATCCGCAAAAAGGAAACCGG
120_Zc3h14rev97aa	CATGCGGCCGCTCATGAAGGCACGTTACTATC
123_Zc3h14rev97aa	ATTGGATCCATGGAGATCGGCACC
135_Zc3h14-GFP_fw	ATTCTCGAGATGGAGATCGGCACC
136_Zc3h14-GFP_rev	TTAGGATCCTTCGCTGGTTTGAGG
145_*SUP4*-200_fw	ATTGCGGCCGCTTTCTAATTCCGTTG

146_*SUP4*+197_rev	ATTCTCGAGTTCAAGCGCACTTTTAG
154_Bdp1-His_fw	ATTGAATTCATGAGTAGTATTG
155_Bdp1-His_rev	ATTGCGGCCGCTTGATCAATCTCAGGCT
156_Brf1-His_fw	ATTGAGCTCATGCCAGTGTGTAAG
157_Brf1-His_rev	ATTGCGGCCGCCCTAAACAAACCGTC
158_Tbp-His_fw	ATTGAATTCATGGCCGATGAGGAAC
159_Tbp-His_rev	ATTGCGGCCGCCATTTTTCTAAATTCAC
167_*URA3*_fw	GCGGAGCTCTCAATTCATCATTTT
168_*URA3*_rev	TCAAAGCTTGCGGCCGCTAGCCACGTTCTTTAATAG
169_*SUP4*_fw	GTGGCTAGCTTTCTAATTCCGTTG
170_*SUP4*_rev	TAAAAGCTTGCGGCCGCATAATAACTCTTCG
1449_*NAB2*	ATTCTCGAGGTCACCGTTGTCGGAGAGTT
1450_*NAB2*	ATTGCGGCCGCTCAGCAAGAGAAGCAAGATTAGG
1542_*NAB2*mutPCRfw	CCAGGGTTTTCCCAGTCA
1543_*NAB2*mutPCRrev	ACTTTATGCTTCCGGCTCCT

Table 8: Oligonucleotide Sequences used for qPCR

Name	Sequence (5'–3')
*PMA1*_fw	CGATGACGCTGCATCTGAA
*PMA1*_rev	CCGTGATTAGATTGTAGTTCTTCGATT
RT_5S-2-fw	AAGATTGCAGCACCTGAGTTTCG
RT_5S-2-rev	ATGTCTGGACCCTGCCCTCATAT
RT_*RPR1*-fw	ATGGTACGCTGTGGTGCTC
RT_*RPR1*-rev	CCATAGGTGGGGATCCTTTCT
RT_SNR6-fw	GTCATCTTCCTGGACCTCATGTGA
RT_SNR6-rev	AGGGGAACTGCTGATCATCTCTGT
RT_*YER*-fw	TGCGTACAAAAAGTGTCAAGAGATT
RT_*YER*-rev	ATGCGCAAGAAGGTGCCTAT
46_RT-*tK*-fw	CTTGTTGGCGCAATCGGTAG
47_RT-*tK*-rev	GGGCTCGAACCCCTAACCTT
99_*SCR1*-1fw	CCAGGACATCCATAGCTTGTG
100_*SCR1*-1rev	ATGAAAAGTTCCTGGCGATG
101_*SCR1*-2fw	CATCGCCAGGAACTTTTCAT
102_*SCR1*-2rev	ACAGCCTAGCACAATTGGAA
103_*SCR1*-3fw	CTTTCTGGTGGGATGGGATA
104_*SCR1*-3rev	TTTACGACGGAGGAAAGACG
105_*SCR1*-4fw	GTCCTGGGCAGAGCTGTCT
106_*SCR1*-4rev	AAGGTGGAGCCCCTAAGGA
107_*SCR*1-5fw	ACCGCTGTTAGGGGAGTTTT
108_*SCR1*-5rev	CCAAATTAAACCGCCGAAG
109_*SCR1*-6fw	CGGTGCCATCAGGATTTACT
110_*SCR1*-6rev	CTTCCAACATCCCTCATTGG
111_*SCR1*-7fw	TTTTCGAATATAAATGACGATTGG
112_*SCR1*-7rev	TGTCGCTACTCACTCTACAACCA

Table 9: Oligonucleotide Sequences used for EMSA

Name	Sequence (5′–3′)
160_TA-30B6-fw	GCTGAAATCTCTTTTTCAATTGCTCCGGTGTATAAAGCCGCGGTCCCTTACTCTTTCTTCAACAATTAAATACTC
161_TA-30B6-rev	GAGTATTTAATTGTTGAAGAAAGAGTAAGGGACCGCCCCTTTATTGACCGGAGCAATTGAAAAGAGATTTCAGC
196_Scr_TA 1+_fw	ATCGTAGATACTGAGTACTCACATCGTCAAGATCACAAGACTATGCACTAGTCACGTCACGTCATAGACTAGATA
197_Scr_TA 1+_rev	TATCTAGTCTATGACGTGACGTGACTAGTGCATAGTCAAGTGATCAAGACGATGTGAGTACTCAGTATCTACGAT
198_Scr_TA 1-_rev	TATCTAGTCTATGACGTGACGTGACTAGTGCATAGTCTTGTGATCTTGACGATGTGAGTACTCAGTATCTACGAT
199_Scr_TA 2+_fw	GACTATCTAGACTGCGATCTCAATCTTCGAAGCTTACAAGTATCACCTATGCATTCAAGTTGCAACGTACTGCAT
200_Scr_TA 2+_rev	ATGCAGTACGTTGCAACTTGAATGCATAGGTGATACAAGTAAGCAACGAAGATTGAGATCGCAGTCTAGATAGTC
201_Scr_TA 2-_rev	ATGCAGTACGTTGCAACTTGAATGCATAGGTGATACTTGTAAGCTTCGAAGATTGAGATCGCAGTCTAGATAGTC

Table 10: Oligonucleotide Sequences used for Northern Blotting

Name	Sequence (5′–3′)
34_*tI(UAU)*L_Northern	TGCTTTTAAAGGCCTGT
73_*RPR1*_Northern	TCCTTCTGTAAACAGG
78_*SNR6*_Northern	GTTCATCCTTATGCAGGGGA
80_*SNR14*_Northern	ACACAATCTCGGACGAATCC

2.1.6 **Plasmids**

Used plasmids are listed in Table 11.

Table 11: Plasmids

Name	Description	Source
pAC1038	Δ*N-NAB2-GFP*, *CEN*, *LEU2*	(Green et al., 2002)
pAC1152	Δ*N-NAB2* (*nab2-1*), *CEN*, *LEU2*	(Marfatia et al., 2003)
pAC2307	*nab2-C437S*, *CEN*, *LEU2*	(Kelly et al., 2007)
pBluescriptIIKS-*SNR6*	the genomic *SNR6* locus including 117 bp upstream and 253 bp downstream was cloned into pBluescriptIIKS	(Brow and Guthrie, 1990)

pBluescriptIIKS-*SUP4*	the genomic *SUP4* locus including 200 bp upstream and 197 bp downstream was cloned into pBluescriptIIKS	this study
pBluescriptIIKS-*tA*	the coding region of *tRNA^{Ala}(UGC)E* was cloned in pBluescriptII KS	this study
pBS1479	plasmid for genomic TAP-tagging with the *TRP1-KL* marker	Euroscarf
peGFP-N3	Neomycin, Ampicillin, C-term GFP tag, CMV promoter	Conzelmann lab
peGFP-N3-ZC3H14	peGFP-N3 with inserted ZC3H14	This study
pET21a-*BDP1*	pET21a plus full length *BDP1*	this study
pET21a-*BRF1*	pET21a plus full length *BRF1*	this study
pET21a-*NAB2*	pET21a plus full length *NAB2*	this study
pET21a-*TBP*	pET21a plus full length *TBP*	this study
pGex-6p-1	Vector for IPTG-inducible GST-protein production	GE Healthcare
pGex-6P-1-*NAB2*	pGex-6p-1 plus Nab2 (aa 1-525)	this study
pGex-6P-1-*NAB2*-B	pGex-6p-1 plus Nab2 (aa 1-261)	this study
pGex-6P-1-*NAB2*-C	pGex-6p-1 plus Nab2 (aa 1-180)	this study
pGex-6P-1-*NAB2*-D	pGex-6p-1 plus Nab2 (aa 1-101)	this study
pGex-6P-1-*NAB2*-E	pGex-6p-1 plus Nab2 (aa 102-525)	this study
pGex-6P-1-*NAB2*-F	pGex-6p-1 plus Nab2 (aa 183-525)	this study
pGex-6P-1-*NAB2*-G	pGex-6p-1 plus Nab2 (aa 262-525)	this study
pGex-6P-1-*NAB2*-H	pGex-6p-1 plus Nab2 (aa 262-398)	this study
pGex-6P-1-*NAB2*-I	pGex-6p-1 plus Nab2 (aa 399-525)	this study
pGex-6P-1-*ZC3H14*	pGex-6p-1 plus ZC3H14 (aa1-97)	this study
pMK43	AID, Vector to introduce IAA17 tag plus kanMX selection	(Nishimura et al., 2009)
pNHK53	AID, Vector coding *Os*TIR1 and fully integratable in *ura3* locus	(Nishimura et al., 2009)
pRS314, pRS315, pRS316	*E. coli*, yeast shuttle vectors	(Sikorski and Hieter, 1989)
pRS314-*NAB2*	the ORF of *NAB2* including 532 bp 5' and 311 bp 3' was cloned into pRS314	this study
pRS315-*NAB2*	the ORF of *NAB2* including 532 bp 5' and 311 bp 3' was cloned into pRS315	this study
pRS315-*nab2-34*	*nab2-34* inserted by homologous recombination after mutagenic PCR of the *NAB2* ORF	this study
pRS316-*NAB2*	the ORF of *NAB2* including 532 bp 5' and 311 bp 3' was cloned into pRS316	this study
pYM15	plasmid for genomic HA tagging with the *HIS3mx6* marker	Euroscarf

2.1.7 **Antibodies**

Used antibodies are listed in Table 12.

Table 12: Antibodies

Name	Source	Dilution	Supplier
Peroxidase anti-Peroxidase	rabbit, monoclonal	1:5,000	Sigma (P1291)
anti-CBP	rabbit, polyclonal	1:2,000	OpenBiosystems (CAB1001)
anti-GFP	mouse, monoclonal	1:2,000	Förstemann lab
anti-HA	rat, monoclonal	1:1,000	Roche (1-867-423)
anti-His	mouse, monoclonal	1:1,000	ABM (G020)
anti-Nab2	mouse, monoclonal	1:10,000	Swanson lab (3F2)
anti-PGK-1	mouse, monoclonal	1:10,000	Molecular probes (A6457)
Anti-ZC3H14 #2	rabbit, polyclonal	1:1,000	Pineda, Sträßer lab
anti-rabbit-HRPO	goat, monoclonal	1:3,000	Bio-Rad Laboratories (#170-6515)
anti-mouse-HRPO	goat, monoclonal	1:3,000	Bio-Rad Laboratories (#170-6516)
anti-rat-HRPO	goat, monoclonal	1:5,000	Sigma (A9037)

2.2 **Methods**

2.2.1 **Standard methods**

Standard molecular cloning techniques including growth of bacteria, DNA subcloning, restriction enzyme digestion, dephosphorylation of DNA, DNA ligation, small scale DNA isolation and DNA analysis on 1% (w/v) agarose gels in 1x TAE were performed according to standard procedures as described in Sambrook and Russel (2001). Whenever a kit or commercially available enzymes were applied, procedures were carried out as written in the manufacturer's instructions. For plasmid isolation from *E. coli*, the NucleoBond® PC100 (Macherey & Nagel) or NucleoSpin® Plasmid QuickPure kit (Macherey & Nagel) was used. Gel extraction of DNA, clean up after crosslink reversal or restriction digesion were carried out using the NucleoSpin® PCR and Gel Clean-up kit (Macherey & Nagel). All plasmids in this study were confirmed by restriction digestion and sequencing (MWG, Eurofins or GATC Biotech). Enzymes were either purchased from Fermentas or NEB (New England Biolabs). Ethidium bromide (VWR) or DNA Stain G (Serva) was used to stain DNA and RNA agarose gels according to the manufacturer's instructions.

2.2.2 **PCR**

Depending on the planned cloning, either KNOP-Polymerase Mix (integration of DNA in yeast, regular cloning) or a high fidelity polymerase was used.

2.2.2.1 **KNOP-Polymerase-mix**

Taq-DNA Polymerase (5 U/µL, Fermentas or NEB), Vent Polymerase (2 U/µL, NEB), and 50% glycerol were mixed prior to PCR in a ratio of 10:7:8. A typical PCR reaction per tube is shown in Table 13. Usually, a minimum of 300 µL of PCR product was used for integration into yeast cells. Therefore, the PCR product was purified and concentrated by phenol-chloroform extraction and a chloroform wash. The DNA was precipitated with 3 volumes 100% ethanol, 1/10 volume 3 M NaOAc (pH 5.2) and incubation of at least 20 min at -20°C. After washing once with 70% ethanol, the DNA was dried and resuspended in 10 µL 1x TE.

Table13: KNOP PCR Mix and Program

Amount [µL]		Temperature	Time [min]	
0.5	Each primer (100 µM)	94°C	2	
1	Template (1-250 ng)	94°C	1	
8	dNTP (2.5 mM)	50°C	0.5	35x
10	10x KNOP buffer	68°C	2.5	
2	KNOP Polymerase mix	68°C	10	
78	H$_2$O			
100	Total volume			

2.2.2.2 **Phusion high-fidelity PCR master-mix**

For high-fidelity amplification of DNA, the Phusion High-Fidelity PCR Master-Mix (NEB) was utilized. PCRs were carried out in a total volume of 20 µL and a typical reaction mixture is shown in Table 14. The PCR products were directly subjected to agarose gel analysis or restriction digestion after clean-up.

Table 14: High-Fidelity PCR Mix and Program

Amount [µL]		Temperature	Time	
1	Each primer (10 µM)	98°C	60 sec	
1	Template (1-250 ng)	94°C	30 sec	
10	2x Phusion PCR Master-Mix	48-58°C	25 sec	35x
7	H$_2$O	72°C	15 sec/kbp	
20	Total volume	72°C	300 sec	

2.2.2.3 Error prone PCR

Error Prone PCR (epPCR) was applied for generation of randomly mutagenized *NAB2*. Hereby, a standard KNOP polymerase mix PCR (see Material and Methods, 2.2.2.1) was modified to further decrease the inherently low fidelity of the *Taq* Polymerase. This was accomplished by adding 2.5 mM $MnCl_2$, increasing the $MgCl_2$ concentration to 5 mM and changing dNTP concentrations to 1 mM dCTP, dGTP, dTTP and 0.5 mM dATP.

2.2.3 Yeast culture

2.2.3.1 Cultivation of *S. cerevisiae*

Yeast strains were cultivated either on solid agar plates (at 30°C, if not stated otherwise) or in liquid culture (at 30°C and 250 rpm, if not stated otherwise), containing full media or synthetic complete drop-out media (SC). Cell densities in liquid culture were measured in a spectrophotometer at a wavelength of 600 nm. One optical density unit (OD_{600}) corresponds to approximately 2.5×10^7 cells.

2.2.3.2 Genomic tagging of *S. cerevisiae*

Genomic integration of tags was done essentially as described before (Janke et al. (2004); Puig et al. (2001). In brief, PCR reactions were prepared by amplifying the desired tag and a marker or an antibiotic resistance gene. The 5'- and 3'-ends of the PCR products contained sequence homologies to the 3'-end of the target gene to be tagged. By exploiting homologous recombination in yeast, the tag sequences were integrated in frame excluding the stop codon of the target gene.

2.2.3.3 Dot spots

To test for potential growth defects, mutant strains were analyzed using dot spots. Therefore, one loop of freshly grown cells was mixed in 1 mL of ddH_2O and diluted 4 times, each 10 fold. 5-10 µL of these dilutions were spotted on the respective media plate, air dried and incubated for up to 5 days under different conditions (*e.g.* temperature, chemicals).

2.2.3.4 Mating

In order to construct the conditional allele of *NAB2*, haploid wild-type strains had to be mated. For mating, freshly grown cells were mixed on a YPD medium plate and incubated several hours. Cells were checked for 'shmooing' under a light microscope (Leica) and

diploid cells were picked with a micromanipulator (Singer Instruments) and incubated on YPD medium plates.

2.2.3.5 Sporulation and tetrad dissection

To gain haploid strains from diploid progenitor cells, sporulation of yeast cells was conducted. Therefore, freshly grown yeast cells were restreaked on YPA sporulation media plates. These plates contain only a few nutritional substances and a non-fermentable carbon source so that yeast cells undergo meiosis to form spores. Here, the genetic information is divided into haploid spores, enclosed in a tetrade. These can be examined visually under a light microscope (Leica) and dissected using a micromanipulator (Singer Instruments). Prior to dissection, the outer cell wall was digested with 10 μL Zymolyase 20T (MP Biomedicals). Tetrades with four growing spores were restreaked and tested for growth on auxotrophic maker plates to check for the correct segregation of markers.

2.2.3.6 Yeast gene deletion

To delete or disrupt a gene in *S. cerevisiae*, it is necessary to partially or completely replace the coding region of this gene. Typically, this is done by exploiting naturally occurring homologous recombination in yeast and thereby replacing a target gene with an auxotrophic marker or an antibiotic resistance gene. A PCR reaction was set up containing primers that carry homologous sequences to the promoter and the 3'-downstream region of the gene to be deleted. The disruption cassettes can either be amplified from plasmid collections (*e.g.* PCR toolbox by Janke and colleagues (Janke et al., 2004) or from DNA of the corresponding, commercially available BY deletion strain (Euroscarf). PCR products were transformed and growing yeast cells were selected on selective media plates.

2.2.3.7 Transformation of yeast cells

For genomic integration of DNA or plasmid transformation, a 50 mL yeast culture was grown to mid-log phase (OD$_{600}$: 0.6-0.8), harvested (3600 rpm, 3 min) and washed once with ddH$_2$O and 0.5 mL of solution I (see Table 15). Cells were resuspended in 0.25 mL solution I and 50 μL of this cell suspension was mixed with 300 μL solution II, 1-5 μg of DNA and 5 μL of single stranded carrier DNA (2 mg/mL). After incubation for 30 min on a rotating wheel, a 10 min heat shock at 42°C was conducted and cells were incubated on ice for 3 min. 1 mL of ddH$_2$O was added to remove the PEG solution and cells were pelleted (3600 rpm, 3 min, RT). When transforming plasmids, the cells were directly spread on selective media plates. For integrations into the genome, cells were incubated in 1 mL of YPD for 1-5 h on a rotating

wheel prior to spreading on selective media plates. Cells were typically incubated for 2-4 days at 30°C.

Table 15: Reagents for Yeast Transformation

Solution I	Solution II
10 mM Tris-HCl (pH 7.5)	10 mM Tris-HCl (pH 7.5)
1 mM EDTA	1 mM EDTA
100 mM LiOAc	100 mM LiOAc
	40% (v/v) PEG-4000

2.2.3.8 Yeast whole cell extracts

To verify the successful genomic integration of protein tags, whole cell extracts were prepared from fresh yeast cells growing on plate. Therefore, a white loop of cells was suspended in 40 µL 1x SDS sample buffer and approximately 30 µL of glass beads. Repeated (3 times) vortexing for 1 min and boiling at 95°C for 2 min was sufficient to lyse the cells and these lysates were loaded directly on a SDS-PAA gel and subjected to Western Blot analysis.

For protein quantification, denaturing whole cell extracts were prepared as described previously (Knop et al., 1996). 5 OD_{600} of cells growing logarithmically were harvested and washed once with water. After resuspension in 0.5 mL H_2O and 150 µL pre-treatment solution, cells were incubated 20 min on wet ice, followed by addition of 0.15 mL 55% trichloroacetic acid (TCA, w/v) to precipitate total protein and 20 min incubation on ice. After 30 min centrifugation at maximum speed, the pellet was resuspended in up to 100 µL 1x SDS sample buffer and neutralized using 5-10 µL of 1 M Tris base. Samples were then subjected to SDS-PAGE and further analysis.

2.2.3.9 Allele identification (*nab2-34*)

The *S. cerevisiae NAB2* ORF was deleted using a PCR based strategy. The *HISMx6* locus was amplified from the pYM15 plasmid with 50 bp flanking sequences that are homologous to the 5'- and 3'-end of the *NAB2* coding sequence. The PCR product was subsequently transformed into a diploid wildtype yeast strain (W303). Heterozygous *HIS*[+] transformants were selected and again transformed with a centromeric plasmid encoding the complete *NAB2* ORF, 500 bp flanking region each and the *URA3* locus (pRS316_*NAB2*). Yeast cells being both His[+] and Ura[+] were then sporulated and tetrads dissected. Retrieved spores, the shuffle strain, were tested on growth on selective media to confirm the constructed strain.

To generate the desired conditional allele, random mutagenesis PCR (epPCR) was performed. Resulting PCR fragments were transformed together with a linearized plasmid (pRS315_*NAB2*; cut with NotI and XhoI) encoding the *LEU2* gene. This so called plasmid gap repair is used to incorporate the different PCR fragments into a desired DNA molecule in yeast (Chekanova, 2003; Lundblad and Zhou, 2001; Puig et al., 2001; Sträßer et al., 2002). Transformants, grown on media lacking leucine, were plated on plates containing 5-Fluoroorotic Acid to shuffle out the *URA3*-containing plasmid. Colonies were then tested for thermo-sensitivity at 18, 25, and 37°C. One allele identified that way, the *nab2-34*, was used in this study. It was further isolated from yeast, transformed into *E.coli* and sequenced. To confirm that the observed phenotype was due to the mutated ORF of *NAB2*, the isolated plasmid was transformed again into the shuffle strain and tested for growth deficiencies.

2.2.4 Protein purifications

2.2.4.1 Tandem affinity purification

Tandem affinity purification (TAP) was essentially done as in Sträßer et al. (2002). The fused and endogenously expressed tag is comprised of two affinity tags (Protein A and Calmodulin binding peptide) that are used to specifically purify the desired protein and interacting proteins from yeast. In this study, all strains were tagged C-terminally, to purify either RNAP complexes or Nab2.

Lysates were prepared from 2 L yeast cultures grown to an OD_{600} of 3.0 - 3.5 using a planetary mill (Fritsch) and glass beads at 4°C (ratio: 1 pellet volume, 1 volume TAP-buffer and 2 volumes of glass beads). After a two-step centrifugation (4000 rpm, 10 min at 4°C and 100,000 g for 1 h at 4°C) the lysate was bound to 0.4 mL pre-equilibrated IgG Sepharose 6 Fast Flow (GE Healthcare) slurry for one hour at 4°C. If needed, DNase I or RNase A was added to remove nucleic acid contaminations following extensive washing with TAP-buffer, the bound proteins were eluted by TEV cleavage for 1 h and 20 min on a rotating wheel at 16°C in TAP-buffer.

Table 16: TAP-buffer

TAP buffer
50 mM Tris-HCl pH 7.5
100 mM NaCl
1.5 mM $MgCl_2$
0.15% NP-40 (w/v)
1 mM DTT
1x protease inhibitor

Further purification was achieved by binding the TEV eluate to Calmodulin Sepharose (Agilent Technologies) for 1 h at 4°C. During binding and washing the TAP-buffer was supplemented with 2 mM $CaCl_2$. Elution was done in 50 mM Tris-HCl pH 7.5, 5 mM EGTA for 15 min at 37°C. Finally, eluted proteins were precipitated by addition of TCA to a final concentration of 10% (v/v) and incubated for 20 min on ice. After pelleting the precipitated proteins for 20 min at 13000 rpm at 4°C, the pellet was resuspended in 60 µL 1x SDS sample buffer and neutralized using 1 M Tris base.

For *in vivo* interaction analysis of Nab2 with RNAPIII, proteins were purified using both tags (with RNase and DNase). For *in vitro* interaction assays and fully reconstituted *in vitro* transcription assays, proteins were purified with TAP-buffer containing 800 mM NaCl until the TEV eluate and treated with RNase/ DNase.

2.2.4.2 Recombinant Nab2 purification

In order to purify recombinant Nab2 from *E.coli*, the complete *NAB2* ORF was introduced into both pGex6-P1 and pET21a. Proteins were produced in *E. coli* Bl21 DE3 at 37°C, 200 rpm with addition of 0.3 mM isopropyl-1-thio-β-D-galactopyranoside (IPTG) at an OD_{600} of 0.6 for 3 hours. Cells from 200 mL culture were harvested, washed, resuspended in NETN 1000 buffer (50 mM Tris-HCl pH 7.5, 1 M NaCl, 1 mM EDTA, 10 µM $ZnCl_2$, 2 mM DTT, 1x protease inhibitors and 1% NP-40), lysed using sonication and centrifuged for 15 min at 13,500 rpm and 4°C in a SS-34 rotor. Lysates were bound either to Glutathione coupled or Ni-NTA resin and purified according to the manufacturer's protocol.

GST-fused Nab2 was either stored coupled to beads in 1x PBS/40% (v/v) glycerol or eluted using the 'PreScission protease' that cuts within the linker region between the GST-tag and Nab2. When purifying His_6-tagged protein, a buffer change was applied after regular washing to equilibrate the beads in chromatography buffer (Buffer A) before elution. Elution from Ni-NTA was done using 250 mM Imidazol and eluate fractions were subjected to ion exchange chromatography.

For further purification of Nab2-His_6, ion exchange chromatography was conducted on an Äkta purifier system (GE Healthcare) under standard conditions as described in the manufacturer's instructions in combination with a Frac-950 automatic fraction collector. Samples were centrifuged and filtrated (0.45 µm) prior to loading on the chromatography system. Columns used for this were either a Poros HS 20 µm 4.6/100 (Life Technologies) or a MonoS 5/50 GL (GE Healthcare) column. Flow rates were usually 1 to 2 mL/min, always considering the maximum pressure of the column, read out as the total system backpressure

generated by chromatography system. The collected fraction size was 0.5 mL and eluates were checked on SDS-PAGE for protein content. A usual run contained the following steps:

Table 17: Ion Exchange Chromatography of Nab2

Block	Settings
Equilibration	5-10 CV of Buffer A
Loading	Injecting > 1 loop volume
Washing	2 CV of Buffer A
Elution	**3 step gradient to 100% buffer B:** **1**. 10 CV linear gradient to 29% buffer B **2**. 5 CV step gradient to 60% buffer B **3**. 5 CV linear gradient to 100 % buffer B
Cleaning	5 CV of Buffer A and H_2O

Table 18: Ion Exchange Buffer

Buffer A	Buffer B
50 mM MES pH 6.5	50 mM MES pH 6.5
20 mM NaCl	1M NaCl
10 µM $ZnCl_2$	10 µM $ZnCl_2$
2 mM DTT	2 mM DTT

A desalting and a buffer exchange step was subsequently applied to the peak fractions containing Nab2. A maximum of 2.5 mL of eluate was pooled and loaded on a pre-equilibrated PD-10 desalting column (GE Healthcare). In brief, 25 mL of PD-10 buffer was used to equilibrate the column by gravity flow at 4°C, 2.5 mL of eluate was loaded and allowed to enter the bed completely. Elution was done with 3.5 mL of PD-10 buffer and 0.5 mL fractions were collected. These were again checked on a SDS-PAA gel, fractions containing Nab2 were aliquoted, flash frozen, and stored at -80°C until use.

Table 19: PD-10 Buffer

PD-10 buffer
20 mM Tris-HCl pH 8.0
90 mM KCl
10% glycerol
5 mM $MgCl_2$
10 µM $ZnCl_2$

2.2.4.3 **Bdp1 purification**

Bdp1-His$_6$ was expressed in *E. coli* BL21 DE3 (250 mL) and induced with 1 mM IPTG for 3 h at 37°C. Purification was essentially done as described in Kumar et al. (1997). 1 g of cells was resuspended in 3 mL of lysis buffer (Table 20) and incubated for 30 min on ice. 0.1% Tween-20 (w/v) was added, and the mixture was sonicated 5 x 30 sec (25% output). The lysate was diluted twofold with lysis buffer containing 1 M NaCl, but lacking EDTA and lysozyme. Again, the lysate was sonicated 5 x 30 sec (25% ouput), followed by centrifugation at 22,000 g for 30 min and 4°C. MgCl$_2$ and imidazole were added (7mM and 10 mM) and the lysate was loaded on a 2 mL Ni-NTA agarose column equilibrated with buffer D500. After 1 h incubation at 4°C, the column was washed with 5 mL buffer D500, 6 mL buffer D500 plus 30 mM imidazole and proteins were eluted with 6 mL of buffer D500 supplemented with 100 mM imidazole. Peak fractions were diluted to 250 mM NaCl in bufferD and loaded on a Mono S 5/50 GL column (GE Healthcare, 1 mL), which was installed in an Äkta purifier system (GE Healthcare) and equilibrated in buffer D with 250 mM NaCl. After washing the column, Bdp1 fractions were eluted from the column with a linear NaCl gradient (15 CV, 0.5 mL fractions) from 250-1000 mM NaCl in buffer D. Peak fractions were collected and stored at – 80°C in high salt buffer.

Table 20: Bdp1 Purification Buffers

Lysis buffer	Buffer D500
50 mM Tris (pH 8.0)	20 mM HEPES (pH 7.9)
0.1 mM EDTA	500 mM NaCl
5% glycerol (v/v)	7 mM MgCl$_2$
10 mM β-mercaptoethanol	0.01% Tween-20 (w/v)
300 µg/mL lysozyme	10 mM β-mercaptoethanol
1x protease inhibitors	10% glycerol (v/v)

2.2.4.4 **Brf1 purification**

Brf1-His$_6$ was expressed in *E. coli* BL21 DE3 Rosetta (250 mL) and induced with 1 mM IPTG for 3 h at 37°C. Purification was essentially done as described previously in Kassavetis et al. (1998). Lysis was done under native conditions as mentioned above (see Material and Methods, 2.2.4.3). The sedimented pellet was resuspended in buffer A (5 mL) and again centrifuged (30 min, 16,800 rpm, 4°C, JA20). The supernatant fluid was applied to 2.5 mL Ni-NTA agarose (Qiagen) and mixed for 30 min at 4°C. The column was washed with 10 mL of buffer A and subsequently developed with buffer B (each 5 mL) at pHs 6.7, 6.3, 5.9, 5.7, 5.5, 5.1, and 4.9. Peak fractions (pH 6.7-5.9) were dialyzed (Spectra/Por 2, 10mm) for 2 h each

at 4°C in buffer D500 (see Table 20) with decreasing urea concentrations (3, 1.5, 0.75, and 0 M), but without $ZnSO_4$.

Table 21: Brf1 Purification Buffers

Buffer A	Buffer B
50 mM Tris (pH 8.0)	100 mM Na_2HPO_4
6 M guanidine HCl	7 M Urea
0.1% Tween-20 (w/v)	7 mM β-mercaptoethanol
7 mM β-mercaptoethanol	1x protease inhibitors
10% glycerol (v/v)	adjust pH with H_3PO_4
1x protease inhibitors	

2.2.4.5 **Tbp purification**

Tbp-His$_6$ was expressed in *E. coli* BL21 DE3 (250 mL) and induced with 0.1 mM IPTG for 14 h at 22°C. Cells were lysed in 10-20 mL LB200 (Table 22), supplemented with 20 mM imidazole, sonified for 10 min (30% output, 40% duty cycle) and treated with lysozyme (100 µg/mL). The lysate was centrifuged and applied to 0.5 mL pre-equilibrated Ni-NTA agarose beads (Qiagen) and incubated for 1 h at 4°C. After extensive washing with four times LB200 buffer for each 5 min at 4°C, the bound proteins were eluted five times with LB200 supplemented with 250 mM imidazole. Peak elution fractions were pooled and loaded on a HiTrap Heparin HP column (GE Healthcare, 1 mL), which was installed in an Äkta purifier system (GE Healthcare). After washing the column, Tbp fractions were eluted from the column with a linear NaCl gradient (10 CV, 0.5 mL fractions) from 200-1000 mM NaCl. 2.5 mL of peak fractions were then subjected to a PD-10 desalting column (GE Healthcare) and eluted with buffer used in *in vitro* transcription or EMSA (see Material and Methods 2.2.6, 2.2.7, and 2.2.8.1).

Table 22: LB200 Buffer

LB200 buffer
50 mM Tris-HCl (pH 7.5)
200 mM NaCl
0.05 % NP-40 (w/v)
1 mM EDTA
2 mM DTT
1x protease inhibitors

2.2.4.6 GST protein production and purification

Recombinantly produced proteins were expressed according to standard procedures. In general, production of proteins in *E.coli* BL21 DE3 (0.1-0.5 L) was induced at an OD_{600} of 0.6-0.8 by adding 0.3 mM IPTG and expression was allowed for 3 h at 37°C. The harvested bacteria were resuspended in 10-20 mL NETN 1000 (see Material and Methods, 2.2.3.2), supplemented with 1 mM DTT and 1x protease inhibitors, and lysed by sonification (4 x 30 sec, 25% output). 30 min incubation with lysozyme (100 µg/mL) on ice was applied when needed. After clearing of the lysate (15 min, 13,500 rpm, 4°C, SS-34/JA-20 rotor), GST proteins were bound to Glutathione Sepharose 4B (200-400µL, GE Healthcare) for 1 h at 4°C on a rotating wheel. After three times washing with NETN 1000, proteins coupled to beads were treated according to the subsequent experiments. For generation of antibodies, the GST proteins were eluted with 15 mM glutathione in a low salt buffer; for pulldown experiments, proteins were washed with a low salt buffer and stored in 40% buffer / 60% glycerol at -20°C; for purification of the pure protein, the 'PreScission protease' was used to cleave the linker between GST and the protein of interest.

2.2.5 Molecular biology methods

2.2.5.1 Chromatin immunoprecipitation (ChIP)

To analyze the association of proteins to their target genes or genomic regions, Chromatin immunoprecipitation (ChIP) was performed. ChIP assays were conducted according to Chanarat et al. (2011); Meinel et al. (2013). In summary, *S. cerevisiae* strains were grown in appropriate media to mid-exponential phase (OD_{600} = 0.8) and cross-linked with 1% formaldehyde for 20 min at RT with mild agitation. Cells harboring thermosensitive alleles were shifted for indicated amounts of time to the restrictive temperature and treated the same way at the permissive temperature in parallel. Whereas for *nab2-34*, a shifting time of three hours to 37°C was sufficient, the *rpc25-S100P* allele was shifted 6-10 hours to 37°C. The cross-linking was stopped by addition of 0.25 M glycine and incubation for 5 min at RT. The cells were then harvested (3600 rpm, 3 min and RT), washed three times in 1x TBS, and flash frozen in liquid nitrogen until use. Pellets were thawn on ice, resuspended in 0.8 mL of FA-Lysis buffer (see Table 23) and mixed with equal amounts of glass beads. Cell lysis was done by vortexing the cells at maximum output for 7 times with each 3 min vortexing and 2 min break on ice. Lysates were sonicated using a Bioruptor (Diagenode) for 3 times 15 minutes with 5 min breaks on ice to yield chromatin size between 0.25 – 0.5 kbp. The lysate was cleared by centrifugation twice (5 min and 15 min, 13,000 rpm at 4°C), before a 10 µL aliquot was saved as input sample. The remaining sample was incubated with 15 µL

magnetic beads (Invitrogen) coupled with IgG (for TAP-tagged proteins) or a specific antibody against the protein of interest. After 2.5 h of incubation at 20°C, beads were collected and washed with 800 µL of buffer (2x FA–Lysis (low salt), 2x FA-Lysis (high salt), 2x TLEND and 1x TE). Next, DNA was eluted from beads using ChIP elution buffer (140 µL) and vigorous shaking at 65°C. Beads were collected and the supernatant was mixed with 80 µL 1x TE and 10 µL Proteinase K (10 mg/mL). Input samples were mixed with 80 µL 1x TE, 80 µL ChIP elution buffer and 10 µL Proteinase K. Finally, the reversal of crosslinks was incubated for 2 h at 37°C, followed by 12 -16 h of incubation at 65°C. Samples were purified using the 'PCR clean up' Kit (Macherey & Nagel) according to the manufacturer's instructions.

Table 23: Buffers for ChIP

FA–Lysis (low salt)	FA-Lysis (high salt)
50 mM HEPES (pH 7.5)	50 mM HEPES (pH 7.5)
150 mM NaCl	500 mM NaCl
1 mM EDTA	1 mM EDTA
1% Triton x-100 (w/v)	1% Triton x-100 (w/v)
0.1% SDS (w/v)	0.1% SDS (w/v)
0.1% Sodium Deoxycholate (w/v)	0.1% Sodium Deoxycholate (w/v)
1x protease inhibitors	

TLEND	ChIP Elution
10 mM Tris-HCl (pH 8.0)	50 mM Tris-HCl (pH 7.5)
250 mM LiCl	10 mM EDTA
1 mM EDTA	1% SDS (w/v)
0.5% NP-40 (w/v)	
0.5% Sodium Deoxycholate (w/v)	

2.2.5.2 qPCR

qPCR is a method for the relative quantification of DNA. It combines the standard amplification of a specific DNA, as in regular PCR, with sensitive fluorescent dye detection. Here, SYBR green was used as a dye that intercalates into the DNA after amplification and thereby enhances its fluorescent properties. For quantification of the purified DNA, the StepOnePlus[TM] cycler (Applied Biosystems) was used with the Applied Biosystems Power Sybr Green PCR Master Mix as recommended by the manufacturer's instructions. When possible, Primer express 3.0 software (Applied Biosystems) was used for primer design. To determine the primer efficiencies, standard curves were used. Each tested sample or

controls (H_2O, standard curves) were pipetted as technical duplicates. Specificity of the used primers was verified by melting curve analysis of the amplicon products obtained at the qPCR run. For calculation of the enrichments, a non-transcribed region (NTR) on Chromosome V (174131-174200) was applied. A typical qPCR run is displayed in Table 24, a list of qPCR primers is given in Table 8. A qPCR reaction contained 0.1 µL (100 pmol/µL) of each primer, 5 µL 2x Power Sybr Green PCR Master Mix, 2.3 µL of ddH_2O and 2.5 µL of diluted DNA. Usually, the purified DNA was diluted 1:20 prior to analysis of RNAPIII or Nab2 ChiPs.

Table 24: qPCR program

Step	Temperature	Time	
Initial Denaturation	95°C	10 min	
Denaturation	95°C	15 sec	45 Cycles
Annealing/ Elongation	60°C	60 sec	
	95°C	15 sec	
	60°C	60 sec	
Melting curve	60°C - 95°C	continuously	0.3 °C
	95°C	15 sec	

Ct values (<u>c</u>ycle <u>t</u>hreshold) were calculated by the StepOne™ Software (v2.2.2) (Applied Biosystems) as the number of cycles necessary for the fluorescent signal to reach a set threshold level. Occupancies were calculated as enrichments of the tested gene (YFG) relative to the mentioned NTR with the following formula (comparative Ct method): $(E^{\wedge}(C_T^{IP} - C_T^{INP}))_{NTR} / (E^{\wedge}(C_T^{IP} - C_T^{INP})_{YFG})$ as described by Livak and Schmittgen (2001).

2.2.5.3 ChIP-chip data

ChIP-chip datasets of Nab2-TAP, TAP-Npl3, TAP-Tho2, Rpb3-TAP cells were used from Meinel et al. (2013). ChIP-chip datasets of Rpc160-TAP cells were performed by Cornelia Burkert-Kautzsch during this study. The ChIP-chip data was normalized according to Meinel et al. (2013). Data normalization and analysis was carried out by Dominik M. Meinel using R (CRAN). The meta profiles for tRNA genes were calculated by averaging the occupancies of all intron-less tRNA. To analyze the significance of the Pearson's correlation coefficient for the peak occupancies at protein coding or tRNA genes for Nab2 and Rpb3 or Nab2 and Rpc160, the correlation coefficients of 100,000 random permutations of the data sets were calculated and compared to the correlation coefficient of the not permutated dataset.

2.2.5.4 **Nab2 CRAC data**

The Nab2 CRAC data from Tuck and Tollervey (2013) was inspected for Nab2 binding to the different RNAPIII transcripts using Integrated Genome Browser (Nicol et al., 2009) and R (CRAN, by Dominik M. Meinel). For the CRAC tRNA meta profile, the reads for all intronless tRNAs smaller than 76 bp were averaged and plotted vs. the position relative to the first nucleotide of the tRNA gene.

2.2.5.5 **RNA extraction**

When working with RNA, general precautions were taken to provide an RNase-free environment and only DEPC treated water (Diethylpyrocarbonate) was used for all buffers. Total RNA was extracted from cells growing in mid-log phase (A_{600} 0.6-0.8), cultivated in YPD and harvested at 30°C or after a shift to 37°C for indicated times using 300 µL of 10 mM Tris-HCl buffer (pH 8.0), 1 mM EDTA, 100 mM NaCl, 1% SDS (w/v) and 2% Triton X-100 (w/v). 300 µL glass beads and 300 µL phenol/chloroform solution were added and cells were lysed by vortexing at maximum intensity. After centrifugation (13,200 rpm, 5 min, RT) the RNA was washed once with chloroform and precipitated with 3 volumes 100% ethanol, 1/10 volume 3 M NaOAc (pH 5.2) and incubation of at least 20 min at -20°C. The samples were centrifuged (13,200 rpm, 4°C and 15 min) afterwards, pellets were dried and the extracted RNA was dissolved in RNase-free water. Subsequently, contaminating DNA was digested (DNase, 10 U/100 µL) in presence of an RNase inhibitor (80 U/100 µL) for at least 15 min at 37°C. Finally, RNA concentration was measured using a NanoDrop ND-1000 (Thermo Scientific) and integrity was tested on 2% (w/v) agarose denaturing formaldehyde gels.

2.2.5.6 **Northern blotting**

5-10 µg of total RNA was mixed with at least an equal amount of formamide loading dye (95% Formamide, 0.1% TAE, bromophenol blue and xylene cyanol), heated to 65°C for 5 min and separated by electrophoresis on 6 or 9% polyacrylamide gels with 6 M Urea and 1x TAE for 45 min and 200 V. After blotting onto a Nylon membrane (Trans-Blot,Biorad) for 20 V, 45 mA and 60 min in 1xTAE, the RNA was crosslinked to the membrane with UV radiation (254 nm, 1,200 µJ, UV Crosslinker, Fisher Scientific). All following steps were performed in a hybridization oven (Hybaid Mini Oven, Thermo Fisher). The blot was pre-hybridized in Church buffer (0.5 M $NaHPO_4$ (pH 7.2), 1 mM EDTA, and 7% SDS (w/v)) for 1 h at 37°C, then radiolabeled oligonucleotides were hybridized to the blot in the same buffer overnight at 37°C. After washing 3 times with 2x SSC buffer and 0.1% SDS for each 15 min at 37°C, the blots were dried and exposed overnight to a storage phosphor screen and

analyzed by a phosphoimager (Typhoon 9400, Amersham Bioscience). Quantifications were done using ImageQuant 5.2. If necessary, blots could be stripped by boiling in 0.1% SDS (w/v) and shaking incubation for 5 min. Afterwards, pre-hybridization was performed again before probing with new oligonucleotides. Hybridized oligonucleotides were labeled with 10 µCi [γ-^{32}P]-ATP (SRP-310, Hartmann Analytic) using the polynucleotide kinase (Fermentas) and purified by Micro Bio-Spin 30 columns (Biorad) following the manufacturer's instructions. Oligonucleotides used are listed in Table 10.

2.2.6 Transcription assays

2.2.6.1 Whole cell extract *in vitro* transcription assay

Whole cell extracts for transcription assays and *in vitro* transcription were done essentially as described in Schultz et al. (1992); Schultz et al. (1991). Yeast cells were grown in 2 L of YPD to an OD_{600} of 1.5, harvested, and frozen in liquid N_2. Other than described in their protocol, higher transcriptional activity was achieved, when the frozen pellet was crushed in a precooled mortar (on wet ice and rinsed with liquid N_2) constantly bathed in liquid N_2. The fine ground pellet powder was weighted and 15% of extraction buffer (v/w) was added. After 20 min of incubation on ice, the yeast sorbet was centrifuged (100,000 g, 1 h at 4°C) in a SW-55 rotor (Beckmann Coultier) and dialyzed 3 times (500 mL each) for 1 h at 4°C against dialysis buffer. Protein amount was measured in a Bradford assay (see Material and Methods, 2.2.14) and extracts were frozen in liquid N_2.

For *in vitro* transcription assays (20 µL), 30 µg of whole cell extract was mixed with 4 µL 5x transcription buffer complemented with 1 mM DTT, 200 ng of α-amanitin, 20 U of RiboLock RNase inhibitor, 500 nM ATP, CTP, UTP, 50 nM GTP, 100 ng of plasmid template and 5 µCi of [α-^{32}P] GTP (FP-208, Hartmann Analytic). The reaction was incubated for 30 min on either 25°C or 37°C and stopped with 180 µL stop buffer (0.1 M NaOAc, 10 mM EDTA, 0.5% SDS (w/v) and 5 µg/mL tRNA). In case of add back experiments, Nab2 was added at last in varying amounts. After phenol/chloroform extraction and ethanol precipitation, the dried RNA pellets were resuspended in formamide loading buffer, ran on a 9% polyacrylamide gel with 6M Urea in 1x TAE buffer. Gels were dried in a geldryer (Model 583 gel dryer, Biorad) for at least 1 h at 80°C and exposed overnight to a storage phosphor screen and analyzed by a phosphoimager (Typhoon 9400, Amersham Bioscience). Quantifications were done using ImageQuant 5.2.

Table 25: *In Vitro* Transcription Buffers

Extraction buffer	Dialysis buffer	5x transcription buffer
100 mM HEPES (pH 7.9)	20 mM HEPES (pH 7.9)	100 mM HEPES (pH 7.9)
245 mM KCl	100 mM KCl	400 mM KCl
5 mM EGTA	5 mM $MgCl_2$	25 mM $MgCl_2$
1 mM EDTA	1 mM EDTA	5 mM EDTA
2 mM DTT	20% glycerol	10% glycerol
1x protease inhibitors	2 mM DTT	
	1x protease inhibitors	

2.2.7   Fully reconstituted *in vitro* transcription assays

2.2.7.1   Reconstituted specific transcription assay

To test for a specific effect of a protein in the transcription events of RNAPIII, reconstituted specific transcription assays were performed as described by Huet and colleagues (Huet et al., 1996). A reaction (40 µL) contained 100 ng of template plasmid, 10 U RNase inhibitor (RiboLock, Fermentas), 1 mM DTT, 0.6 mM of each ATP, CTP, GTP and 0.03 mM UTP, 10 µCi [α-^{32}P] UTP (SRP-210, Hartmann Analytic) in 1x IVT buffer (Table 26). Proteins were added in the following order: 50-100 ng Tbp (see Material and Methods, 2.2.4.5), 80-100 ng Brf1 (see Material and Methods, 2.2.4.4), 100 ng Bdp1 (see Material and Methods, 2.2.4.3), 50-150 ng TFIIIC (see Material and Methods, 2.2.4.1), 50-100 ng RNAPIII (see Material and Methods, 2.2.4.1) and varying amounts of Nab2 (0-500 ng, see Material and Methods, 2.2.4.2). The order of mixture was: DNA, TFIIIC, TFIIIB (Tbp, Brf1 and Bdp1), Nab2 and RNAP III. After a 30 min incubation at 25°C, the reaction was stopped by addition of 60 µL of 2% SDS (w/v) in H_2O and subsequent phenol/ chloroform extraction. The RNA was precipitated with 1/10 volume of 3 M NaOAc (pH 5.5) and 3 volumes of 100% EtOH and incubated for 1 h at -20°C. After centrifugation (>20 min, 13.200 rpm and 4°C), the RNA was washed once with 70% EtOH and centrifuged for 5 min at max. speed at RT. The dried pellet was dissolved in 10 µL of formamide loading buffer, heated to 85°C for 2 min and cooled on wet ice for 2 min. The samples were subjected to electrophoresis in a 10% (v/v) polyacrylamide gel containing 8 M Urea at 300 V for 20-25 min in 0.5x TBE. The gel was disassembled, dried for 2 h in a geldryer (Model 583 gel dryer, Biorad) on Whatman paper, exposed overnight to a storage phosphor screen and analyzed by a phosphoimager (FLA 9500, (GE Healthcare)) and Image Quant TL (GE Healthcare).

Table 26: IVT Buffer

IVT buffer (1x)
20 mM HEPES (pH 7.9)
90 mM KCl
5 mM MgCl$_2$
0.1 mM EDTA
10% glycerol (v/v)

➔ prepared as 4x

2.2.7.2 **17-mer assay**

To investigate a role of Nab2 in transcription initiation of RNAPIII, 17-mer assays were essentially done as described in Dieci and Sentenac (1996). Briefly, transcription reactions were set up containing 250 ng *SUP4* tRNA (pBSKII-*SUP4*), 50-100 ng affinity purified TFIIIC (see Material and Methods, 2.2.4.1), 40 ng Tbp (see Material and Methods, 2.2.4.5), 50 ng Brf1 (see Material and Methods, 2.2.4.4), and 100 ng Bdp1 (see Material and Methods, 2.2.4.3) in 42 µL 1x 17-mer buffer (Table 27). The proteins were allowed to assemble on the template DNA for 20 min at 25°C, then a mixture (8 µL) of 50-100 ng affinity purified RNAPIII (see Material and Methods, 2.2.4.1), 0.5 mM ATP, CTP and 10 µCi [α-^{32}P] UTP (SRP-210, Hartmann Analytic) in buffer was added. Eventually, 3'-dGTP (Jena Biosciences) was added at 0.1 mM concentration to efficiently arrest all 17-mers at position +18. Forming heparin resistant ternary complexes, the production of 17/18 nt long RNAs was monitored over 0-10 min. The assays were stopped and processed as before (see Material and Methods, 2.2.7.1). 17% (v/v) PAA gels containing 7 M Urea were used to separate the produced RNAs (1000 V, 100 mA, 25 W). The gels were dried, exposed, and analyzed as above (see Material and Methods, 2.2.11.1).

Table 27: 17-mer Buffer

17-mer buffer (1x)
20 mM Tris (pH 8.0)
90 mM KCl
5 mM MgCl$_2$
0.1 mM EDTA
10% glycerol (v/v)

➔ prepared as 4x

2.2.7.3 **Initiation / reinitiation assay**

After 17-mer formation, as described in section 2.2.7.2, heparin and the missing nucleotide GTP, but without 3'-dGTP, were used to assay single round (SR) versus multiple round (MR) transcription events. Therefore, 250 µg/mL Heparin (for inhibition of reinitiation) and 0.5 mM GTP were added to the reaction after 10 min of 17-mer formation. Elongation and reinitiation

was allowed to proceed for 10 min at 25°C and products were treated as stated in section 2.2.7.1. A typical ratio for MR/SR events with all recombinant factors was ~2, as described in Ferrari et al. (2004).

2.2.8   Biochemical methods

2.2.8.1   Electrophoretic mobility shift assay (EMSA)

EMSAs were done as previously described in Kassavetis et al. (1998) with the following modifications. Briefly, protein-DNA complexes were formed in 40 mM Tris-HCl (pH 8.0), 7 mM $MgCl_2$, 3 mM DTT, 5% glycerol (v/v), 100 µg/mL BSA and 50 mM NaCl. 100 ng of ssDNA and 5 pmol of 6-FAM 5′-labeled dsDNA (See Material and Methods, 2.1.5, Table 9) was used instead of poly(dG–dC)–poly(dG–dC) and radiolabeled probes. Proteins were added as indicated. Reaction mixtures were incubated for 60 min at 25°C and separated on a 2% (w/v) agarose gel in 1x TAE at 4°C for 1h at 150 V. Gels were analyzed with a Typhoon FLA 9500 and ImageQuant TL software.

2.2.8.2   SDS polyacrylamide gel electrophoresis

Sodium dodecylsulfate polyacrylamide gel electrophoresis (SDS-PAGE) was done using a Mini Protean II system (BioRad) as described in Laemmli (1970). Samples for SDS-PAGE were mixed with SDS sample buffer (final conc. 1x) and incubated at 95°C for 3 min. After loading, the gels were run in 1x SDS-PAGE running buffer at 100–200 V until the dye front reached the bottom of the separating gel. As marker, the PageRuler[TM] Unstained Protein Ladder or PageRuler[TM] Prestained Protein Ladder (Fermentas/ Thermo Scientific) was used. Gels were disassembled and either stained in coomassie stain solution for 1 h shaking, destained with Destain solution and fixed in 10% acetic acid or applied to Western Blotting for specific protein detection. A typical 10% SDS polyacrylamide (PAA) gel contained the following mixture. (Table 28)

Table 28: SDS Polyacrylamide Gel

Component	Separation gel (10%)	Stacking gel (4.5%)
4x separating SDS-gel buffer	2.5 mL	-
4x stacking SDS-gel buffer	-	2 mL
30% Acrylamide/Bis-acrylamide (29:1)	3.33 mL	1.2 mL
ddH$_2$O	4.17 mL	4.8 mL
TEMED (100%)	10 µL	50 µL
10% APS	100 µL	50 µL
	~10 mL	~8 mL

2.2.8.3 **Western blotting**

When Western Blotting for protein detection was used, proteins were blotted in a wet-blotting tank (Biorad) from SDS-PAA gels on a nitrocellulose membrane (Porablot, Macherey & Nagel). It comprised of 3 sponges, two pieces of Whatman paper, the SDS-PAA gel, the nitrocellulose membrane, again two pieces of Whatman paper and two sponges. After assembly, proteins were transferred for 1 h and 400 mA in Wet blotting buffer. The complete transfer of proteins was verified by Ponceau S staining. The membrane was blocked in 5% BSA in 1x TBST for 1 h at mild agitation, followed by 1.5 h incubation with the primary antibody, diluted in the same buffer. After washing with 1x TBST for 3 times each 5 min, the secondary antibody coupled to horseradish peroxidase was applied and incubated for 1 h. Again, the membrane was washed 3 times for 5 min in 1x TBST. Antibody covered proteins were made visible by incubation of the blot with a CheLuminate-HRP PicoDetect ECL kit (Applichem). Light sensitive X-ray films (GE Healthcare) were exposed to the blot and developed in an Optimax TR developing machine (MS Laborgeräte) or direct pictures of the blots were taken with a ChemoCam Imager (Intas).

2.2.8.4 **Bradford assay**

Protein concentration of samples was determined by the method of Bradford with BSA as a standard (Bradford, 1976). The samples were diluted according to the calibration curve and mixed with 200 µL 1x Bradford reagent. After incubation (5-10 min) in the dark, the absorption (595 nm) was measured in a 96-well plate (VWR) in a microplate reader (Tecan Sunrise).

2.2.8.5 **GST-Pulldown**

GST fusion proteins were bound to Glutathione Sepharose and purified as described above (see Material and Methods, 2.2.4.6). Protein amounts on beads were estimated and equalized after SDS-PAGE and coomassie staining in comparison to BSA. For pulldown assays, beads with bound protein (~ 5 µg) were equilibrated with GST pulldown buffer (Table 29), blocked with BSA (10 mg/mL) for 1 h at 4°C and treated with DNase and RNase. Then, 5-10 µg of purified RNAP complexes were added and incubated 1-2 h at 4°C. After extensive washing with GST pulldown buffer for four times each 5 min at 4°C, the beads were resuspended in SDS sample buffer, boiled, and subjected to SDS-PAGE and Western Blot analysis.

Table 29: GST-Pulldown Buffer

GST-pulldown buffer
25 mM HEPES (pH 7.6)
200 mM NaCl
12.5 mM MgCl$_2$
20% glycerol
0.1% NP-40 (w/v)
1x protease inhibitors

2.2.8.6 *In vitro* interaction assay

Investigation of the direct interaction of RNAPIII and Nab2 was carried out by incubating GST-fused Nab2 (see Material and Methods, 2.2.4.6) and TEV eluate from high salt purified RNAP I or III (see Material and Methods, 2.2.4.1). Therefore, beads with bound Nab2 (30 µL) were washed with 2.5 mL PD-buffer (Table 30) followed by digestion of DNA and RNA (100 µg/mL RNase A and 25 µg/mL DNase I) for 60 min at 16°C. For this, the buffer was supplemented with 10 mM MgCl$_2$ and 10 mM CaCl$_2$. After washing, RNAPI or RNAPIII (60 µL or same amounts) was bound to beads for 1 h at 4°C followed by washing with 5 mL of PD-buffer. Treatment of the beads with 'PreScission protease' (5 µL) for up to 2 h at 16°C eluted bound complexes from the resin. Alternatively, 1x SDS sample buffer can be used for denaturating elution.

Table 30: PD-Buffer

PD-buffer
20 mM HEPES (pH 7.6)
75 mM NaCl
2 mM MgCl$_2$
1 mM DTT

2.2.8.7 Antibody generation

To investigate the potential conservation of Nab2's function in higher eukaryote cells, an antibody against the first 97 amino acids of the human Nab2 homolog Zc3h14 (isoform 1) was raised. Therefore, GST-Zc3h14 was expressed in *E. coli* and purified as described above (for purification see Material and Methods, 2.2.4.6). The beads were washed extensively with buffer NETN 1000 (see Material and Methods, 2.2.4.2) and equilibrated in buffer to elute the tagged protein natively from the beads (50 mM Tris HCl (pH 7.5) and 100 mM NaCl) with 15 mM reduced glutathione and 1x protease inhibitor. To remove the glutathione, the eluted protein fractions were applied to a PD-10 desalting column equilibrated in elution buffer without glutathione. To test the stability of the preparation, eluted

protein was incubated 24 h at 25°C, 37°C, and 42°C and possible protein degradation was monitored via SDS-PAGE. Immunization (0.5 mg per rabbit/ immunization) and antibody production was conducted by Pineda Antikörper-Service (Berlin). After each immunization, sera were received and tested for recognition of the different epitopes in comparison to pre-immune sera. Rabbits were sacrificed, when no increase in specificity between different bleeds was observed. The antibodies were aliquoted, mixed with glycerol, flash frozen and stored in -20°C or -80°C.

2.2.8.8 Fluorescence microscopy

HEK293 cells were cultivated using standard conditions and transfected with *ZC3H14* in peGFP-N3 or peGFP-N3 alone using Lipofectamine 2000 (Invitrogen). Untreated cells served as mock control. After 24-48 h of incubation, cells were fixed and prepared for staining according to Sparrer et al. (2012). Subsequently, co-localization of ZC3H14-GFP and recognition of ZC3H14 by the raised antibodies (1: 500 dilution) was investigated via Fluorescence Microscopy on a Zeiss LSM510 laser scanning microscope. Staining with DAPI was performed to visualize cell nuclei (final. conc. ~300 nM) Images were taken and analyzed with Image J (1.49v). Fluorescent images of yeast cells were taken on a Zeiss Observer Z1 microscope with a 63x oil immersion objective, after cells were mixed with potassium phosphate buffer (pH 7.0) containing 1.2 M sorbitol.

2.2.8.9 Electron microscopy

Electron micrographs of RNAPIII core complex or RNAPIII with recombinant Nab2 were obtained as negative stain micrographs using 2% uranyl acetate (Nanoprobes) in collaboration with Dr. Petra Wendler (Gene Center, LMU Munich). Usually, highly purified RNAPIII from yeast was diluted 1:40 up to 1:80 prior to application on glow-discharged (45 s at < 29.3 Pa) carbon coated electron microscopy grids (Quantifoil) (Kube et al., 2014). Single micrographs were collected using a SIS Megaview 1K CCD camera connected to a FEI Morgagni transmission electron microscope (FEI, Hillsboro, USA) at 80 keV.

3. Results

3.1 Nab2 binds to RNAPII- and RNAPIII-transcribed genes genome-wide

The poly(A) tail binding protein (PABP) Nab2 was discovered more than 20 years ago (Anderson et al., 1993). Until now, it has been described in detail how it functions to recognize poly(A) tails of nascent mRNAs and how this binding regulates poly(A) tail length, mRNA export or decay (Soucek et al. (2012) and references therein). In the nucleus, this is accomplished together with the classical factors involved in mRNA export or maturation/degradation such as Mex67-Mtr-2 or the 3'-end processing machinery (see Introduction and Soucek et al. (2012)). In a recent genome-wide analysis to unravel the function of nuclear RNA binding proteins in *S. cerevisiae*, ChIP-on-chip (Chromatin immunoprecipitation and subsequent hybridization of DNA to tiling arrays) experiments of mRNA processing and export (mRNP proteins) factors were conducted (Meinel, 2013; Meinel et al., 2013). In these studies, proteins of interest were immunoprecipitated from sheared chromatin with an average length of 200-250 bp, and purified DNA fragments were amplified before hybridizing to high density tiling arrays covering the whole yeast genome with a resolution up to four bases (David et al., 2006). These experiments also contained the generation of genome-wide occupancy data for RNAPII (represented by the subunit Rpb3) and RNAPIII (represented by the biggest subunit Rpc160), as well as for Nab2. In general, the ChIP-on chip data was generated and analyzed by Dominik M. Meinel, the Rpc160-TAP ChIP-on chip data was generated by Cornelia Burkert-Kautzsch (Meinel, 2013).

Analyzing the data for Nab2, it was found that in addition to protein coding genes, *i.e.* RNAPII transcribed genes (Meinel, 2013), high occupancies were detected for tRNA genes, transcribed by RNAPIII. Although the occupancy of Nab2 on RNAPII transcribed genes was known and expected (Gonzalez-Aguilera et al., 2011; Meinel et al., 2013), the observation that a major fraction of Nab2 is associated with RNAPIII transcribed genes genome-wide was novel. However, it was already shown that Nab2 localizes to single RNAPIII genes in *S. cerevisiae* before (Gonzalez-Aguilera et al., 2011).

The first aim in this study was to investigate the binding sites of Nab2 on the *S. cerevisiae* genome. Therefore, the occupancies of Nab2 were calculated according to the different gene classes (Fig. 10A). These were divided into protein coding genes (PCGs) (black), rRNA genes (green), sn/snoRNAs (blue), and tRNA genes (red).
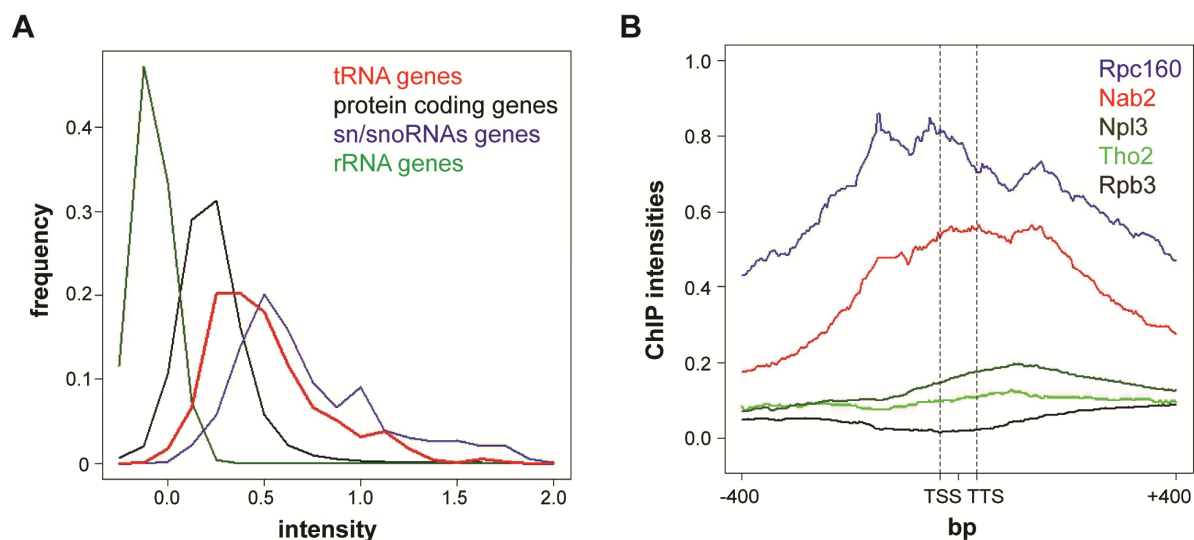
Fig. 10: Genome-wide localization of Nab2 to RNAPIII-transcribed genes. (A) Density plots for Nab2 from ChIP-on-chip experiments. Four different classes of transcripts are shown: tRNA genes (red), protein coding genes (black), sn/snoRNA genes (blue), and rRNA genes (green). Note that rRNA genes are not occupied by Nab2 and that the intensity of Nab2 on tRNA genes is even higher than on protein coding genes. **(B)** Meta-tRNA gene occupancy profiles of Nab2-TAP, TAP-Npl3, Rpb3-TAP, Rpc160-TAP, and TAP-Tho2 on intronless tRNA genes smaller than 76 bp. ChIP-chip intensities were plotted against the averaged genomic loci of non-intron containing tRNA genes. TSS: transcription start site; TTS: transcription termination site (Meinel, 2013).

The frequencies of the occupancies within a group of genes were then plotted against the signal intensities. As anticipated before, Nab2 signals were high for PCGs and sn/snoRNA genes. Remarkably, Nab2 also localized to tRNA genes (Fig. 10A, red line), whereas RNAPI transcribed genes were not occupied by Nab2. The fraction of Nab2 bound tRNA genes was even bigger than the fraction binding to protein coding genes.

To examine whether Nab2 and Rpc160, the biggest subunit of the RNA Polymerase III core complex, co-localize genome-wide on tRNA genes, we then calculated meta-tRNA gene profiles of Nab2 and Rpc160 by plotting their average nucleotide occupancy against all intronless tRNA genes < 76 bp after gene length normalization. In addition, we calculated the same for the SR-like protein Npl3, the RNAPII core subunit Rpb3, and the TREX component Tho2. As evident from Figure 10B, the meta profiles of Nab2 and Rpc160 (RNAPIII) show a strong signal at tRNA genes and are very similar in their profile shape. In contrast to that, neither Rpb3 (RNAPII) nor Tho2, or Npl3 show recruitment to tRNA genes. This indicated that Nab2 localizes to tRNA genes independent of RNAPII or other mRNP-binding proteins, which suggested a possible, RNAPII-independent recruitment of Nab2 to tRNA genes transcribed by RNAPIII.

Besides the meta-tRNA gene profile, showing that Nab2 localizes to tRNA genes, we were interested whether Nab2 also binds to other ncRNA genes transcribed by RNAPIII. Hence, we investigated the individual occupancy traces on single genes, such as the *SCR1*

gene (RNA of the signal recognition particle, Fig. 11A), the *RPR1* gene (RNA component of the nuclear RNase P, Fig. 11D) or the 5S rRNA gene (*RDN5*, Fig. 11E), which were also occupied by Nab2 and RNAPIII in the same manner (Fig. 11). As a control, the occupancy of RNAPII (Rpb3) was inspected as well. In the presented occupancy traces (Fig. 11), RNAPII only localized to the open reading frames of PCGs, which interspersed tRNA and other ncRNA genes. In contrast, Nab2 highly occupied all tested RNAPIII transcribed loci. The additional analysis of single tRNA genes also confirmed the co-occupancy of RNAPIII with Nab2, as suggested by the meta-tRNA gene profiles, while RNAPII was absent. Thus, Nab2 is present at all genes that are transcribed by RNAPIII.

To test whether the occupancy of Nab2 on RNAPIII genes is independent of RNAPII genome-wide, we calculated the peak occupancies of Nab2, RNAPII, and RNAPIII (Fig. 12).
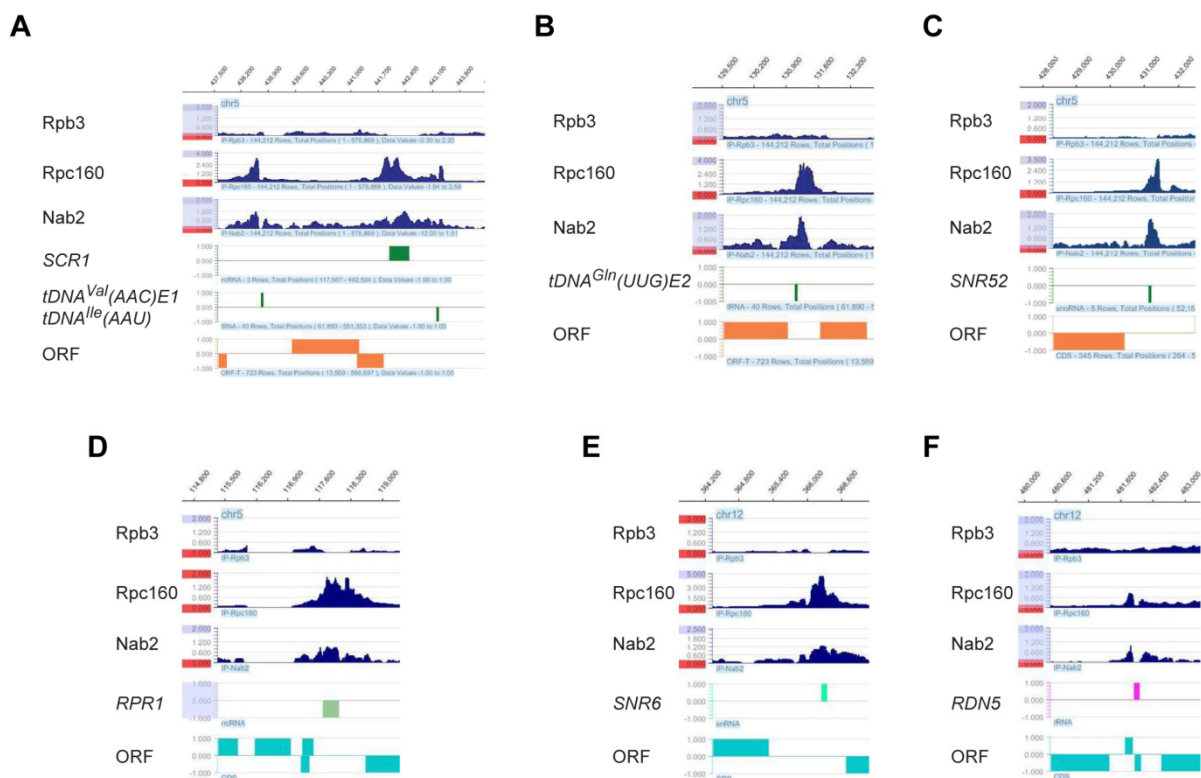
Fig. 11: Nab2 and RNAPIII co-occupy all RNAPIII transcribed genes. (*A-F*) Individual occupancy traces of Rpb3 (RNAPII), Rpc160 (RNAPIII), and Nab2 at tRNA genes as well as at the *SCR1*, *RDN5*, *SNR6*, *SNR52*, and *RPR1* gene loci show that Nab2 is recruited to all genes transcribed by RNAPIII. RNAPII (Rpb3) does not occupy these loci. "Gaps" as in **(F)** in the single traces for Nab2 and Rpc160 are due to gene duplication in the yeast genome. These duplicated genes are not represented on the used tiling arrays (personal comm. D. Meinel). Data analysis and figure preparation was done by D. Meinel.

Scatter plots of the calculated peak occupancies of Nab2 with the RNAPII subunit Rpb3 showed high correlations on protein coding genes (Fig. 12A, grey dots), whereas only poor correlations were found on tRNA genes (Fig. 12A, red dots), due to the absence of RNAPII on these genes. This is in good accordance with previous data, showing that RNAPII and

basic RNAPII transcription factors do not associate with genes transcribed by RNAPIII in *S. cerevisiae*, whereas it is a common feature in higher cells (Raha et al., 2010; Venters et al., 2011).

Likewise, calculation of the peak occupancies for Nab2 and RNAPIII (Rpc160) revealed high correlations for tRNA genes (Fig. 12B, red dots), but yielded low correlations for PCGs, which are not bound by RNAPIII (Fig. 12B, grey dots). The binding of RNAPIII at some protein coding genes in the vicinity of tRNA genes (Fig. 12B, orange dots) is most probably explained by spillover effects of the high intensity binding of RNAPIII to juxtaposed tRNA genes.

PCGs	Nab2 - Rpb3	Nab2 - Rpc160	Rpb3 - Rpc160
Correlation	0.77*	0.22*	0.02

tRNA genes	Nab2 - Rpb3	Nab2 - Rpc160	Rpb3 - Rpc160
Correlation	0.05	0.41*	0.03
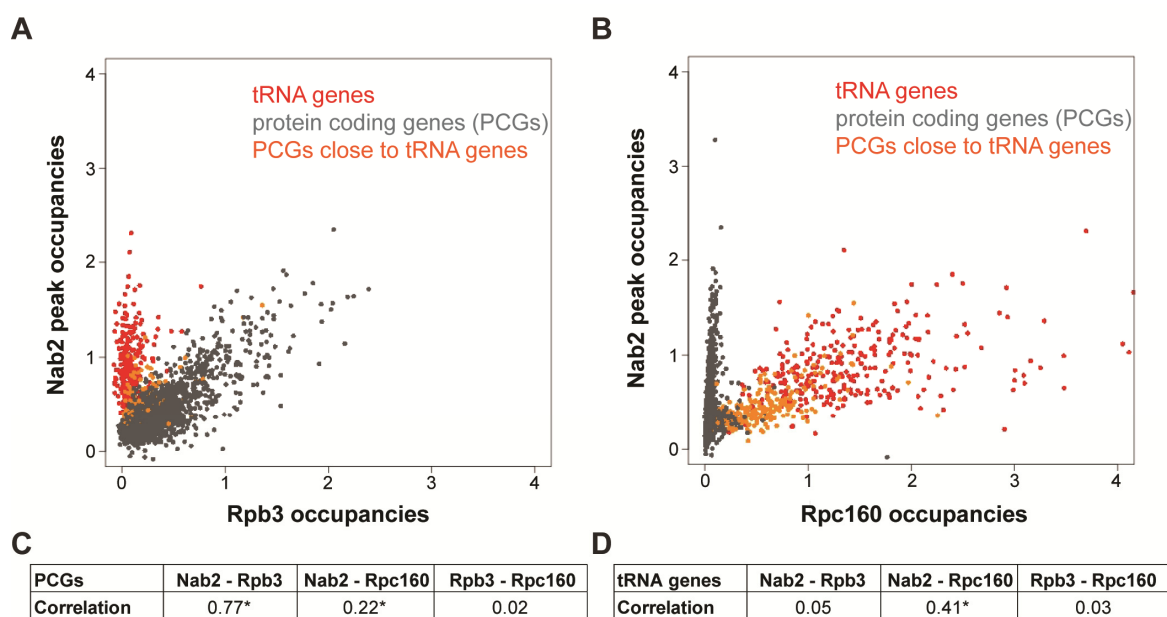
Fig. 12: Nab2 occupancy correlates highly with both RNAPII on protein coding genes and with RNAPIII on tRNA genes. (A) Scatter plot of the peak occupancies of Nab2 (y-axis) and RNAPII (Rpb3, x- axis) are depicted. Nab2 and Rpb3 correlate highly on protein coding genes (PCGs, grey dots), whereas there is poor correlation for tRNA genes (red dots). **(B)** Same as in **(A)**, but peak occupancies for Nab2 (y-axis) and Rpc160 (RNAPIII, x- axis) are shown. Nab2 and Rpc160 occupancies correlate well for tRNA genes, whereas they do not correlate for PCGs. Protein coding genes within a distance of < 250bp from RNAPIII genes are illustrated separately (orange dots) to mark potential spill-over effects of RNAPIII on PCGs. **(C)** Calculated Pearson correlation coefficients of Nab2 and Rpb3, Nab2 and Rpc160, as well as Rpb3 and Rpc160 at protein coding genes and **(D)** at tRNA genes. Interestingly, Nab2 occupancy correlates highly with Rpb3 on PCGs, but only with Rpc160 on tRNA genes. Asterisks indicate that within 100,000 permutations no similarly high Pearson correlation coefficient was obtained indicating that data sets are significantly positively correlated. The positive correlation coefficient at protein coding genes for Nab2 and Rpc160 is most likely caused by spillover effects of nearby tRNA genes (compare **(A)** and **(B)**). Data analysis and figure preparation was done by D. Meinel.

In addition, Pearson correlation coefficients were calculated for the co-occupancy of combinations of the tested proteins (Fig. 12C and D). First, no obvious correlation was present for both polymerases localizing to the same genes (Fig. 12.C and D; Rpb3-Rpc160).

Second, Nab2 had two highly specific binding preferences. It co-localized with RNAPII on protein coding genes and with RNAPIII on tRNA genes. Third, there was no fraction, where Nab2 and Rpc160 bound to PCGs, nor a fraction of Nab2 binding tRNA genes together with RNAPII.

Gonzales-Aguilera and colleagues described that Nab2 is binding to RNAPIII genes using ChIP analysis on single genes, such as the *SUP56* tRNA gene, the 5S rRNA gene, and the *SNR6* gene (Gonzalez-Aguilera et al., 2011). However, they claimed that the recruitment of Nab2 might depend on TREX or THSC/TREX-2 components, *e.g.* Hpr1, Tho1, or Thp1. They showed that these proteins are recruited to RNAPIII transcribed genes, though with very low abundance. To check this in more detail we performed ChIP analyses of Hpr1 using the same genes to evaluate the binding of the TREX subunit Hpr1 to RNAPIII target genes (see Appendix, Fig. A1). Occupancy for Hpr1 was high on *PMA1*, an intronless RNAPII transcribed gene, as expected from earlier experiments (Meinel, 2013). In contrast, the recruitment to the 5S rRNA and *SNR6* genes was neglectable, as less than 6% recruitment was observed, compared to the *PMA1* occupancy (see Appendix, Fig. A1). Furthermore, the dependency of the Nab2 recruitment on Hpr1, Tho1, or Thp1 was tested, as well as the occupancies of these proteins on exemplary RNAPIII genes (Knüppel, 2013). In summary, none of the proteins was highly enriched on the tested genes, nor was the recruitment of Nab2 reasonably decreased, contrarily to the findings of Gonzales-Aguilera and colleagues (Gonzalez-Aguilera et al., 2011; Knüppel, 2013).

From this data it can be concluded that the occupancy of Nab2 at tRNA genes is specific and independent of RNAPII or other mRNP biogenesis factors, such as Tho2. This indicates a potential second role for the poly(A)-binding protein Nab2 in addition to serving in correct mRNP biogenesis and export.

3.2 Generation of new alleles to impair Nab2 function

3.2.1 A novel temperature-sensitive allele of *NAB2*: *nab2-34*

The observation that Nab2 is specifically present at RNAPIII-transcribed genes raised the question, whether Nab2 might function in RNAPIII transcription. As Nab2 is an essential protein in *S. cerevisiae*, we aimed to use conditional alleles to study the potential role of Nab2 in RNAPIII transcription in yeast. Unfortunately, existing alleles do not have optimal properties. For example, the *nab2-1* and specially the *nab2-1-GFP* allele have an impaired growth already at permissive temperatures (compare different temperatures in Fig. 13A for

nab2-1 and *nab2-1-GFP* and Marfatia et al. (2003)). Other alleles, such as the *C437S* point mutant do not show a very pronounced temperature sensitivity (see Fig. 13A, *nab2-C437S* at different temperatures) or they require media changes for efficient depletion of Nab2 (Brockmann et al., 2012; Gonzalez-Aguilera et al., 2011). Only recently, an "anchor away" allele of Nab2 was described that localizes the nuclear fraction of Nab2 to the cytoplasm upon rapamycin treatment of the cells (Schmid et al., 2015).
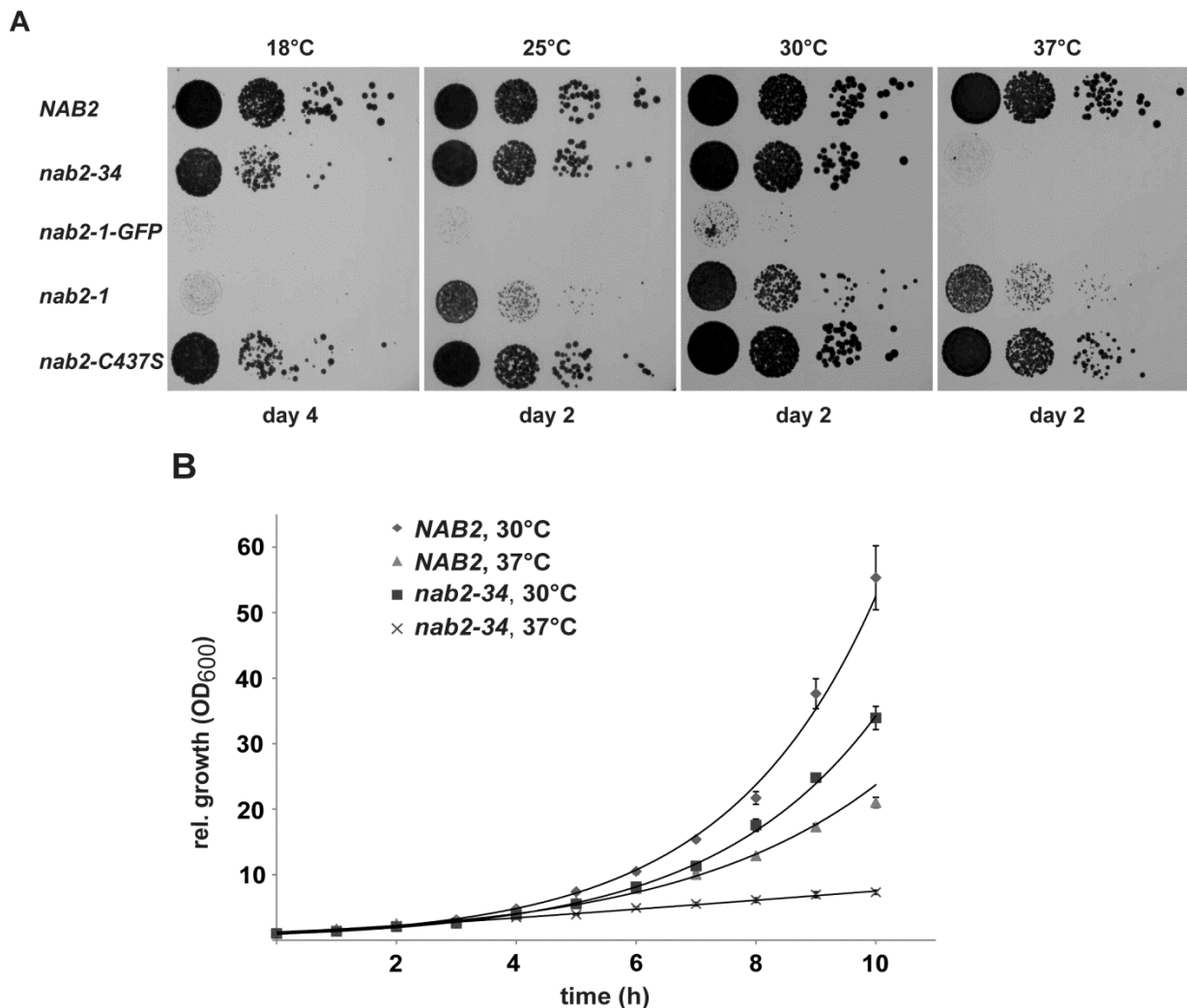
Fig. 13: Identification of *nab2-34* and comparison to existing *NAB2* ts-mutants. (A) 10-fold serial dilutions (dot spots) of strains expressing wild-type *NAB2*, the new *nab2-34* allele, the previously generated temperature sensitive *nab2-1-GFP* and *nab2-1* alleles or the *nab2-C437S* allele were spotted on YPD plates and grown for 2 or 4 days at the indicated temperatures. *nab2-34* has a severe growth defect at the non-permissive temperature. **(B)** Growth curves of *NAB2* and *nab2-34* cells at 30°C and 37°C in liquid YPD culture. The mean values and standard deviation (SD) of three replicates are shown. *nab2-34* shows the first growth defect after 4 hours of shifting to the restrictive temperature.

The system uses the fusion of an FRB-tag to Nab2 in a strain with FKBP-tagged Rpl13a. Upon addition of rapamycin, these two tags interact and Nab2 gets exported and tethered to

the cytoplasm, but not degraded. Unfortunately, this allele was not available at the time experiments were conducted.

Hence, we decided to generate our own conditional, temperature-sensitive (ts) *NAB2* allele to use it as a tool to study the new potential function of Nab2 in RNAPIII transcription. Therefore, the error prone PCR-mutated (epPCR) *NAB2* ORF was co-transformed with a linearized pRS315 yeast plasmid that had sequence homologies to the PCR fragment. After transformation, yeast cells repaired the plasmid via the homologous repair pathway. The generated transformants were subsequently screened for temperature sensitivity (see Material and Methods, 2.2.3.9).

Fig. 14: Alignment of Nab2 and Nab2-34 amino acid sequences. Sequences were aligned and single domains marked with colors. The N-terminal PWI domain (blue), the QQQP-domain (purple), the RGG domain (yellow), and the seven zinc fingers (green) are depicted. Mutations in Nab2-34 are marked in red. Identity of residues is marked by double points (highly related amino acid) or asterisks (identical amino acid). No mark indicates no sequence similarity.

The one and only allele identified this way was the *nab2-34* allele. As shown in Figure 13A, it displayed normal growth on YPD plates at 25°C and 30°C compared to wild-type (wt) cells, had a slight growth defect at 18°C, and was inviable at 37°C. Growing in liquid full medium (Fig. 13B), cells harboring the *nab2-34* mutant already showed a slight growth defect at 30°C, compared to complemented wild-type cells. Growth curves at 37°C revealed a first growth defect after four hours of growth at the restrictive temperature, although cells still

continued to grow slowly for at least nine hours (Fig. 13B). Due to its severely impaired growth at 37°C, the *nab2-34* allele was used for all subsequent experiments for which a conditional allele was needed.

Furthermore, sequencing of the mutant *NAB2* allele revealed that Nab2-34 is still produced as a full length protein containing several single amino acid exchanges due to point mutations in the coding DNA (Fig. 14, red bars).

The mutated residues were distributed throughout the whole protein-coding sequence. In most cases, ts-alleles have several changes in their amino acid sequence or truncations that complicate the prediction, which of the mutations is most important for the displayed phenotype. As most of the mutations are likely not changing the overall structure of Nab2-34 (three mutations lay within the dispensable QQQP-domain, see purple bar in Fig. 14), two positions should be emphasized. First, the histidine to proline mutation in the fourth zinc finger (Znf) and second, the arginine to cysteine mutation in zinc finger six. Both mutations could destabilize the correct complexation of the Zn^{2+} ion within the Znf fold, thereby potentially disrupting the zinc finger and its function at higher temperatures (compare to Introduction, 1.3, Fig. 4). Both mutations are in critical regions of the zinc finger and might be responsible for the potential or partial unfolding of Nab2, which could finally result in the observed ts-phenotype. Interestingly, protein levels stay constant, when cells are shifted to the non-permissive temperature, arguing against a complete unfolding and subsequent degradation of Nab2-34 (data not shown).

3.2.2 *NAB2-AID* as a second allele to deplete Nab2 from yeast cells

An alternative approach to deplete Nab2 was chosen in parallel by applying the depletion technique described by Nishimura and colleagues (Nishimura et al., 2009). This technique was named AID, which is the abbreviation for 'Auxin-inducible degron' and takes advantage of Auxin-induced degradation of polyubiquitinylated proteins. In plants, Auxins are representatives of a series of plant hormones, which control gene expression during growth and development. Within these processes, indole-3-acetic acid (IAA) is considered as the natural auxin (Nishimura et al., 2009; Teale et al., 2006). In this method, the protein of interest is fused to the AID degron, which is an auxin- or IAA-transcription repressor. Upon addition of auxin to cells, the compound binds to the F-box transport inhibitor response (Tir1) protein that is able to interact directly with the fused degron (see Fig. 15A). As the Tir1 protein can be incorporated into the SCF complex (Skp1, Cullin, and F-box), which is an E3 ubiquitin ligase complex involved in degrading proteins in yeast and other organisms, the protein of interest will be ubiquitinylated by an E2 ubiquitin conjugating enzyme leading to its rapid degradation by the proteasome. The substrate specificity of this complex is mediated

by the F-box protein – in this case Tir1 - that binds to the highly conserved Skp1 protein of the SCF complex. As Tir1 orthologues are only found in plants, the Tir1 protein of the Asian rice (*Oryza sativa*) is additionally expressed in yeast (Nishimura et al., 2009).

To generate this degron with Nab2, the genomic *NAB2* locus was tagged with the IAA17 (AID)-tag and the *osTIR1* sequence was integrated into the yeast genome, respectively.
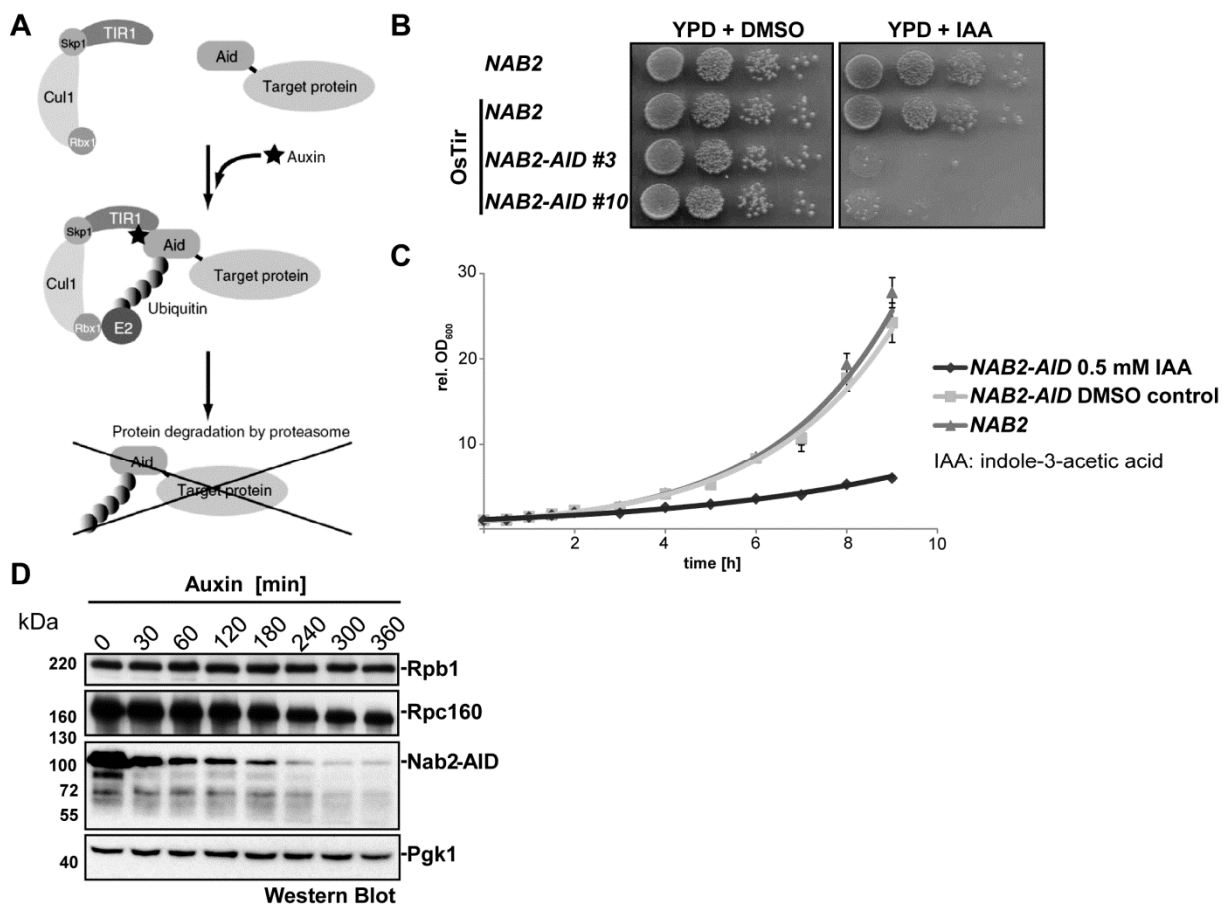
Fig. 15: The *NAB2-AID* degron can be used to mostly deplete Nab2 from cells. (A) Scheme of the AID degron system. An auxin transcription repressor is fused to a target protein. Addition of auxin (indole-3-acetic acid, IAA) to the media leads to an interaction of the fused repressor with auxin and Tir1. Tir1 in turn recruits an E2/E3-ubiquitin ligase complex (SCF) to polyubiquitinylate the fused protein and thus targets the protein to the proteasome. Image taken from Nishimura et al. (2009). **(B)** Dot spots of wild-type cells with and without integrated *OsTIR1* and two transformants with a *NAB2-AID* degron grown in full media with DMSO (control) or IAA. Depletion of Nab2 from cells resulted in severely impaired growth. **(C)** Growth curve of wild-type cells or cells harboring the *NAB2-AID* allele. Growth was only impaired when Auxin (IAA) is added to the medium. Data (n= 3) represents the mean ± standard deviation (SD). **(D)** Western blots of RNAPII (Rpb1), RNAPIII (Rpc160), Nab2-AID and Pgk1 levels upon addition of Auxin. Nab2 levels dropped massively, but could not be completely depleted by this method. Levels of RNAPIII were also slightly reduced upon Nab2 depletion. Marker sizes are in kDa.

As shown in Figure 15B, integration of *osTIR1* did not affect the growth, compared to a non-modified wild-type yeast strain, when auxin (IAA) was added.

In contrast, yeast cells harboring AID-tagged Nab2 showed a severe growth defect in the presence of auxin. To study this in more detail, growth curves were recorded for wild-type yeast cells, *NAB2-AID* cells growing in the presence of the solvent DMSO, and *NAB2-AID* cells treated additionally with IAA (Fig. 15C). Cells growing with DMSO behaved as wild-type cells, showing no delay or defect in growth, whereas auxin treated cells displayed an impaired growth after 2-3 hours of incubation. Nevertheless, the cells were able to slowly grow even after nine hours of auxin treatment. This may have resulted from insufficient depletion of the AID-tagged Nab2 from the cells. Therefore, we determined the protein levels of Nab2, Pgk1, Rpb1 (RNAPII), and Rpc160 (RNAPIII) during auxin treatment at different time points. Pgk1 served as an internal loading control of equal loading. Interestingly, Nab2 levels were reduced rapidly but not completely even after six hours of auxin treatment (Fig. 15D). Albeit very low, protein levels stayed nearly constant after treatment for four hours or longer, indicating that this degradation system is not fast enough to deplete the whole pool of Nab2. This may be due to faster neo-synthesis of Nab2 than degradation or a limiting factor in the degradation pathway, *e.g.* the availability of osTir1.

In summary, two different alleles were constructed that can be used for further analysis of Nab2 and its potential function in RNAPIII transcription. The *nab2-34* temperature-sensitive allele has the advantage of only one locus being modified and the phenotype can be easily induced by shifting the cells to 37°C in full medium. In contrast, Nab2 protein could be depleted to certain extend by the AID degron. Although Nab2 is not completely depleted from the cells using this technique, it is still advantageous over other currently existing alleles, such as *nab2-1*. No medium-shift is required, nor an addition of potential toxic compounds, such as heavy metals or drugs, as IAA is a natural derivative of phenylalanine.

3.3   The interdependency of RNAPIII and Nab2 on RNAPIII-transcribed genes

The observed genome-wide co-occupancy of Nab2 and RNAPIII (Rpc160) on RNAPIII-transcribed genes raised the question, whether the occupancy of Nab2 on RNAPIII genes is transcription dependent, pointing towards a mechanism of Nab2 in transcription of RNAPIII genes. To answer this question, single ChIP experiments were conducted to assess whether Nab2 occupancy on target genes requires RNAPIII and active transcription. We used the *rpc25-S100P* temperature-sensitive mutant that impairs transcription initiation at the restrictive temperature (Zaros and Thuriaux, 2005). To confirm the effect of this mutant on general RNA polymerase III occupancy on tRNA and other ncRNA genes, we carried out ChIP analyses with Rpc160-TAP, the biggest subunit of RNAPIII on three exemplary RNAPIII

genes: *RPR1*, *SNR6*, and *tDNA^Lys^*. After shifting to the restrictive temperature of 37°C for 6-10 h, the cells were crosslinked and analyzed. As expected, the presence of RNAPIII decreased significantly at all tested gene loci. Importantly, the occupancy of RNAPIII in shifted wild-type cells remained unchanged (Fig. 16A). In line with our hypothesis that Nab2 might have a role in RNAPIII transcription or processing, occupancy of Nab2 also decreased significantly in mutant cells, whereas it stayed the same in *RPC25* cells (Fig. 16B). This finding suggested that efficient Nab2 recruitment to RNAPIII target genes is dependent either on active transcription by the polymerase or the sole presence of RNAPIII on its genes.

Next, we investigated whether Nab2 is also required for full occupancy of RNAPIII on its genes. This would be another hint for a role of Nab2 in RNAPIII transcription. Hence, the novel *nab2-34* mutant was used and cells were shifted for three hours to 37°C prior to ChIP analysis. Rpc160-TAP occupancy in *NAB2* and *nab2-34* cells at 30°C was normalized to 100% (Fig. 16C).
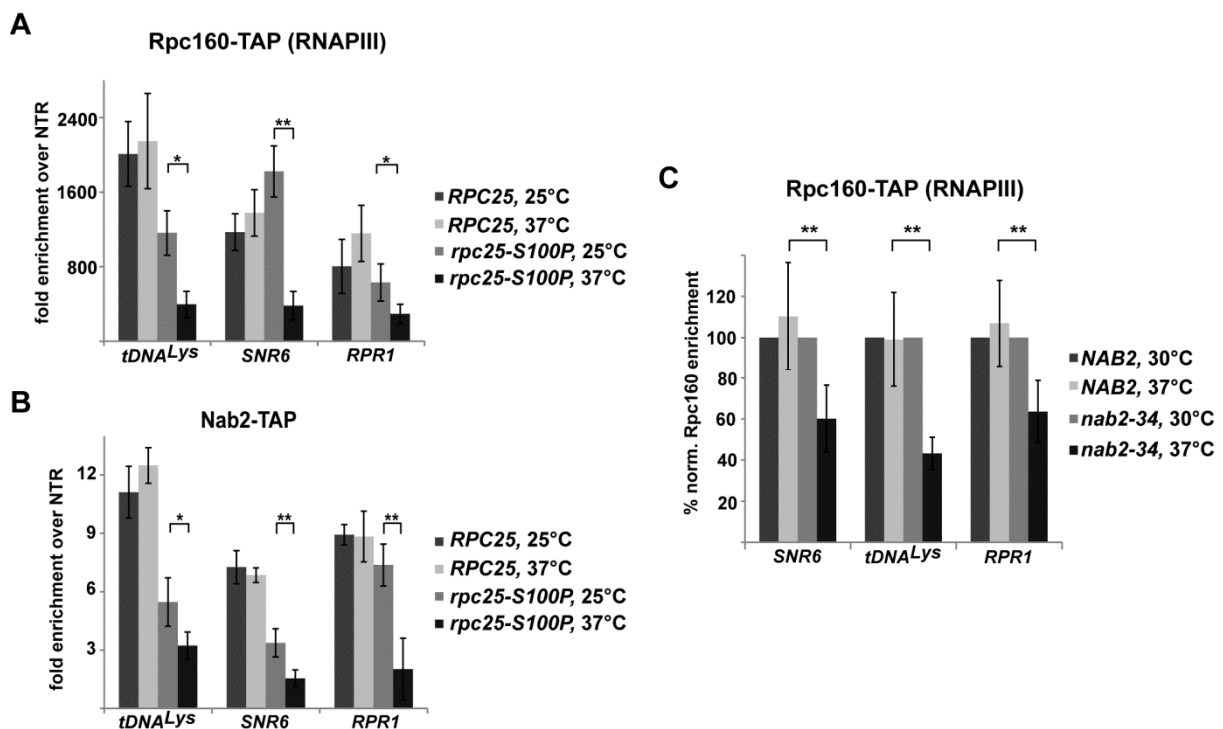
Fig. 16: Nab2 and RNAPIII occupancies on RNAPIII-transcribed genes are interdependent. Occupancy of Nab2 in RNAPIII-transcribed genes is transcription-dependent. ChIP analysis of Rpc160-TAP **(A)** and Nab2-TAP **(B)** in *RPC25* and *rpc25-S100P* cells (Zaros and Thuriaux, 2005) at selected genes at the indicated temperatures. Occupancies of Rpc160 and Nab2 are reduced in the mutant at the restrictive temperature. Data (n ≥ 3) represent the mean ± SD; *: $p < 0.05$; **: $p < 0.01$. **(C)** Nab2 is needed for full RNAPIII occupancy on its target genes. ChIP analysis of Rpc160-TAP in *NAB2* and *nab2-34* cells at indicated temperatures. Data (n ≥ 3) represent the mean ± SD; **: $p < 0.01$.

The occupancy of RNAPIII did not change in the complemented wild-type cells, whereas shifting the Nab2 mutant to the restrictive temperature, resulted in a ~50% decrease of

RNAPIII occupancy on tested genes (Fig. 16C, black columns). Interestingly, this effect was observed even before the cells showed a growth defect, indicating that the diminished presence of RNAPIII on target genes is a direct effect of Nab2.

Taken together, the transcription-dependent and the genome-wide association of Nab2 with RNAPIII at RNAPIII-transcribed genes, as well as the requirement of functional Nab2 for full occupancy of RNAPIII on its genes suggest a function for Nab2 in RNAPIII transcription.

3.4   RNAPIII and Nab2 interact directly

Since it was observed that Nab2 and RNAPIII co-occupy tRNA and other ncRNA genes and that they are interdependent on each other, they most probably should interact, if Nab2 has a function in RNAPIII transcription. Therefore, we investigated the physical interaction of Nab2 with the RNA polymerase. A *NAB2-TAP* tagged strain containing an HA-tagged RNAPIII (on Rpc160) was subjected to tandem affinity purification (TAP) from 2 L yeast culture. The purification was successful, as the Nab2 importing karyopherin Kap104 was co-purifying (see Fig. 17, the second most intense band in the Nab2-TAP purification) Subsequent Western blot analysis was applied to reveal a potential co-purification. Indeed, Rpc160-HA and thus likely the whole RNAPIII complex co-purified with Nab2 (Fig. 17A, lane 5). A *RPC160-HA* strain without a TAP-tag served as negative control and as evident from Figure 17A, lane 4, no protein purification was visible on the Coomassie blue stained SDS-PAA gel. More importantly, no HA signal could be detected in the Western blot, indicating that the binding of RNAPIII is specifically dependent on Nab2.

We additionally purified the RNAPIII core enzyme via an *RPC160-TAP* tagged strain under the same conditions and tested for co-purification of Nab2 (Fig. 17A, lane 6). As expected from the results of the Nab2 purification, Nab2 co-purified in the RNAPIII purification. Pgk1, the cytoplasmic phosphoglycerate kinase 1, served as a negative control for unspecific co-purification.

Due to the fact that the whole cell extracts were treated with DNase I and RNase A, we concluded that the observed physical interaction of Nab2 and RNAPIII is most likely DNA- and RNA-independent.

Since it could not be concluded from this experiment, whether the observed interaction of Nab2 with RNAPIII is direct or mediated by auxiliary factors, we performed *in vitro* pulldown experiments (Fig. 17B). To do so, RNAPIII was highly purified from *S. cerevisiae* under stringent conditions (800 mM NaCl) that yield the core components of the RNAPIII complex.
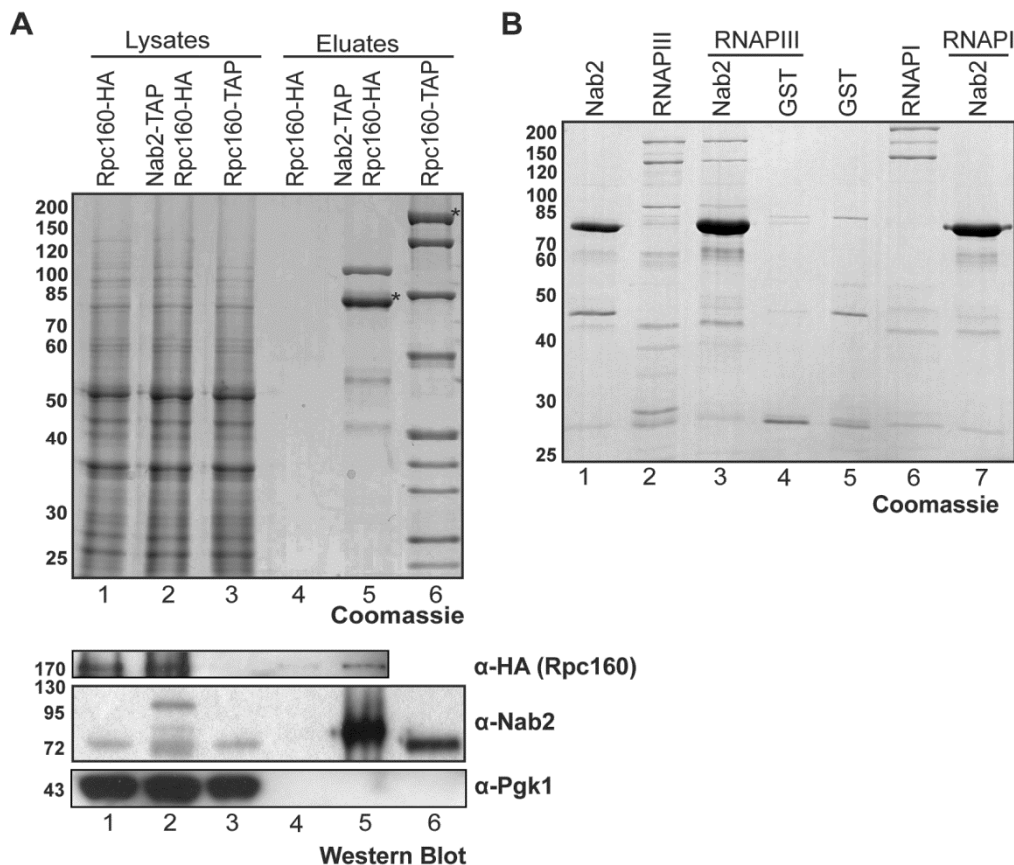
Fig. 17: Nab2 interacts with RNAPIII *in vivo* and *in vitro*. (A) Tandem affinity purification (TAP) of Nab2-TAP, Rpc160-HA and Rpc160-TAP (upper panel) was performed under standard conditions, using 100 mM NaCl, DNase I and RNase A. A representative 10% SDS-PAA gel stained with Coomassie brilliant blue is shown. Asterisks denote the tagged subunits that were purified. Co-purification of RNAPIII and Nab2 was assessed by Western Blot (lower panel) against HA or Nab2. Pgk1 and a non-TAP-tagged Rpc160-HA tagged strain served as internal controls. Nab2 and Rpc160 can be natively purified and interact *in vivo*. The different signals for Nab2 in the Western Blots (lanes 2 and 5) can be explained as different degradation products. In lane 2, whole lysate is blotted before incubation with IgG Sepharose. As the TAP tag is a tripartite tag, the upper band corresponds to the full tag (Protein A-TEV-CBP), the middle one to the CBP part of the tag and the lowest band might represent Nab2 that completely lost the tag. The CBP part of the tag is also responsible for the molecular weight increase observed in lane 5 compared to lane 6. **(B)** Nab2 interacts directly with RNAPIII *in vitro*. Pulldown assays were performed with GST-Nab2 immobilized to glutathione coupled resin and incubation with RNAPIII purified from yeast. Purified GST from *E. coli* and *S. cerevisiae* RNAPI served as negative controls. A representative Coomassie blue-stained SDS-PAA gel (10%) is shown. Nab2 interacts with RNAPIII directly and specifically. Marker sizes are in kDa.

Nab2 was N-terminally GST-tagged (the tag also contained a cleavage site for 'PreScission' protease) and purified to near homogeneity from *E. coli* and bound to GST beads. Furthermore, negative controls were included. On the one hand, GST (Glutathione-S-transferase) only bound to beads served as negative control for unspecific binding of the polymerase (Fig. 17B, lane 5). On the other hand, RNAPI, which was purified as RNAPIII and was TAP-tagged on the biggest subunit Rpa190, served as control (Fig. 17B, lane 6).

Before incubation with RNAPIII, GST-Nab2 did not show a high-molecular weight bands on Coomassie gels (Fig. 17B, lane 1). After incubation with RNAPIII from yeast (Fig. 17B, lane 2) and 'elution' with 'PreScission' protease, proteins were subjected to SDS-

PAGE on a 10% SDS-PAA gel. Intriguingly, RNAPIII bound to recombinant GST-Nab2 directly (Fig. 17B, lane 3). We could further argue that this interaction is specific for Nab2, as GST alone did not bind to RNAPIII (Fig. 17B, lane 4), and GST-Nab2 could not pulldown RNAPI under the same conditions (Fig. 17B, lane 7).

The presented experiments showed that Nab2 and RNAPIII interact *in vivo* and that this interaction is direct and specific. To map the Nab2 region that is required to bind to RNAPIII, GST-fusions of Nab2 deletion constructs were produced (Fig. 18B) and subsequently incubated with RNAPIII purified as described above. An overview of the tested constructs is given in Figure 18A. All constructs were purified to homogeneity, coupled to GST-beads, and amounts were adjusted on SDS-gels. The co-purification of RNAPIII with these constructs was eventually assessed by Western blotting against the CBP-tag of the polymerase. These experiments revealed that RNAPIII binds to the first four zinc fingers of Nab2 alone or in combination with the RGG domain (Fig. 18C). In one set of experiments, the RGG domain alone was also able to interact with the polymerase (Fig. 18C, (2)).
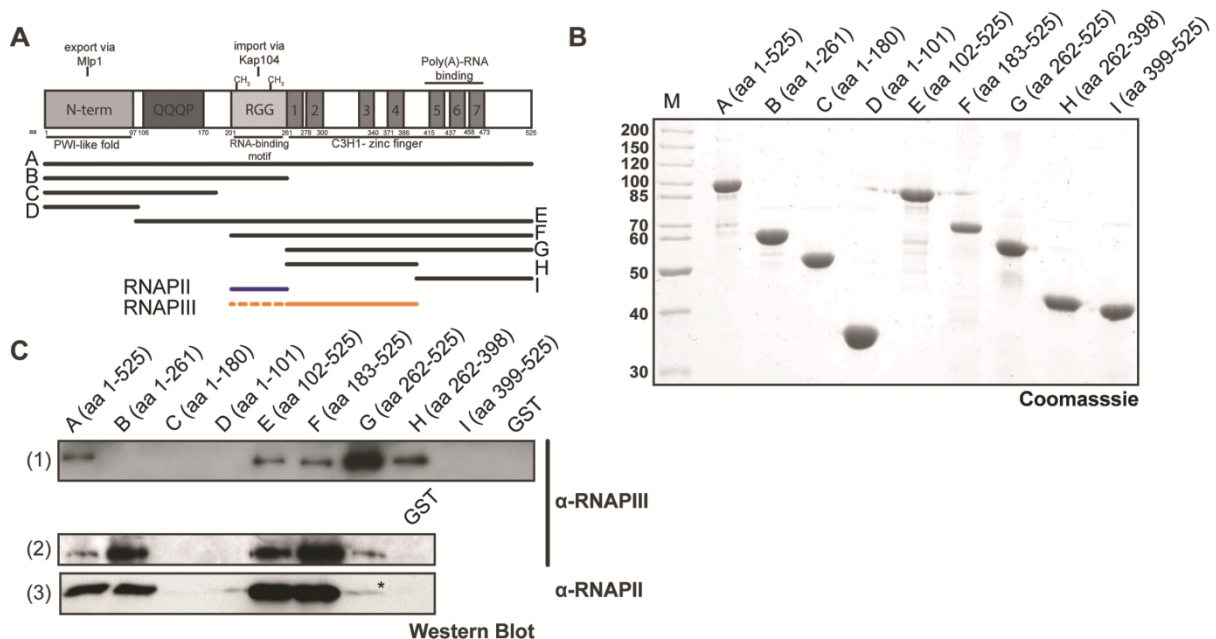
Fig. 18: The zinc finger and the RGG domain of Nab2 are crucial for RNAPIII interaction. (A) Schematic overview of the Nab2 truncation constructs used in the GST-Pulldowns. Interaction domains of RNAPII (orange) and III (blue) are highlighted. **(B)** A representative, Coomassie-blue stained 10% SDS-PAA gel with purified GST-Nab2 truncations is shown. **(C)** Representative Western blots of the *in vitro* GST-Nab2-pulldowns are shown. For Western Blot detection, an antibody detecting the Calmodulin binding peptide was used. The asterisk in **(C)** marks spill over from the neighboring well. The Western Blot (1) was taken from (Damayanova, 2012). Nab2 interacts with RNAPII via the RGG domain, whereas the interaction with RNAPIII can also be mediated by the first four zinc fingers. Marker sizes are in kDa.

In addition to RNAPIII, the binding of Nab2 to RNAPII (Rpb3-TAP) was also tested in this assay. The reason for this was the genome-wide binding of Nab2 on RNAPII genes with

RNAPII in the earlier mentioned ChIP-on-chip (Fig. 12 and Meinel et al. (2013)). Surprisingly, RNAPII also bound to full length Nab2 *in vitro* and to a region closely to the mapped binding domain of RNAPIII. In this case, the presence of the RGG domain within the Nab2 deletion construct was required for RNAPII interaction, as no construct without this domain could pull-down RNAPII (Fig. 18C).

The results gained from the *in vitro* pulldowns are summarized in the lower part of Figure 18A.

In summary, the interaction assays revealed that Nab2 interacts with RNAPIII *in vivo* and *in vitro* via the first four zinc fingers and potentially with the RGG domain. Interestingly, RNAPII also showed physical interaction with Nab2. In this case, the interaction is also direct, as affinity purified components were used in pulldown assay and Nab2 most probably requires the presence of the RGG domain alone to bind to RNAPII. As it was previously not known, whether Nab2 binds to RNAPII, this is the first evidence of a direct interaction.

3.5   Transcriptome-wide binding of Nab2 to tRNAs and other ncRNAs

As Nab2 was identified in an early study investigating proteins that bind to poly(A) tails in yeast, it is a founding member of the poly(A) binding protein family (Anderson et al., 1993). Since then, the properties of how Nab2 binds to poly(A) tails and other RNA sequences have been examined in detail (Green et al., 2002; Kelly et al., 2007; Marfatia et al., 2003). Nab2 can bind highly specific to poly(A) RNA, however binding to poly(G), poly(U), and unspecific RNA sequences have been described additionally (Anderson et al., 1993; Tuck and Tollervey, 2013). As Nab2 associates with RNAPIII on its target genes and interacts directly with this polymerase, we were interested whether Nab2 is also able to bind to tRNAs and other ncRNAs. Therefore, we analyzed the CRAC data (crosslinking and analysis of cDNA) that was generated recently by Tuck and Tollervey to determine the transcriptome-wide RNA binding of several RBPs in yeast (Tuck and Tollervey, 2013). In detail, they identified all transcripts bound by 13 mRNA processing, export, and turnover proteins in *S. cerevisiae in vivo*. Nab2 was among these proteins.

Analysis of the published data was conducted together with Dominik Meinel (Bayerisches Landesamt für Gesundheit und Lebensmittelsicherheit, Oberschleissheim, Meinel (2013)) to investigate the potential binding of Nab2 to RNAPIII transcripts *in vivo*. We first calculated a meta profile of all non-intron containing tRNAs with a length of ≤ 76 nt by alignment of all tRNA reads to their transcription start sites on the yeast genome

('0' represents the TSS; Fig. 19A). Importantly, this data revealed a binding of Nab2 to the bodies of intronless tRNAs (Fig. 19A).
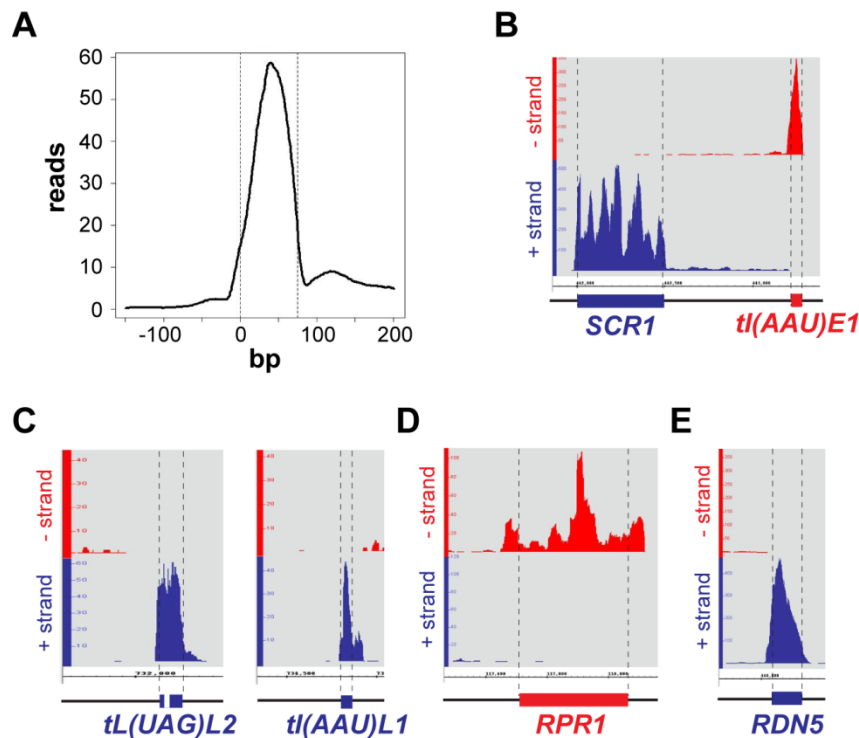
Fig. 19: Nab2 binds to tRNAs and other ncRNAs transcribed by RNAPIII *in vivo*. Analysis of the genome-wide CRAC data set (Tuck and Tollervey, 2013) revealed Nab2 binding to premature tRNA and other ncRNA transcripts. **(A)** Meta profile of Nab2 binding to intronless tRNAs ≤ 76 nt. '0' indicates the corresponding transcription start site on the yeast genome. **(B-E)** Hit distribution of Nab2 along selected tRNA and ncRNA genes. Retrieved signals were annotated to the respective genes from SGD (www.yeastgenome.org). The gene orientation was considered, as the plus strand is shown in blue, the minus strand in red. The mature 5'- and 3'-ends of the newly synthesized transcripts are indicated by the dashed lines and the colored bars below each panel. Hence, the *SCR1* transcript **(B)** and the 5S rRNA **(E)** have no or no pronounced precursor molecules in the cell or Nab2 does not bind them. **(C)** The gap in the *tRNA^{Leu}* gene represents an intronic sequence that is later removed. **(D)** Extensive precursors are known for the *RPR1* gene. The analysis was done together with Dominik Meinel Bayerisches Landesamt für Gesundheit und Lebensmittelsicherheit, Oberschleissheim, Meinel (2013)).

Furthermore, the results from this meta profile can be generalized to all tRNAs, as Nab2 also bound to the bodies of intron-containing tRNAs, including intronic sequences (Fig. 19B and C).

Interestingly, an additional but lower binding was detected downstream of the mature tRNA sequences indicating that Nab2 binds to pre-tRNAs already during or shortly after transcription (Fig. 19A and C). The binding of Nab2 to pre-tRNA introns, which is depicted for *tL(UAG)L2* (Fig. 19C) is in line with this observation.

A closer inspection of the CRAC data additionally revealed that Nab2 also bound to other ncRNAs, such as *RDN5*, *RPR1*, or *SCR1* (Fig. 19B-E), which are important structural

and functional RNAs in translation, tRNA processing, and guiding the translating ribosome to the endoplasmic reticulum (ER). Again, binding of Nab2 to precursor ncRNA was observed, *e.g.* for *RPR1*, the RNA component of RNase P. This RNA possesses a ~84 nt 5'-leader sequence and a 3'-trailer. Both precursor sequences, as well as the whole body of this ncRNA showed binding by Nab2. Shortly after transcription, the leader sequence is processed (Lee et al., 1991), again pointing towards a co-transcriptional binding of Nab2 to RNAPIII transcribed precursor RNA.

In summary, Nab2 was found to bind to all tRNAs and ncRNAs transcripts investigated. This binding was not only observed to mature, but also to non-processed RNAPIII transcripts, suggesting an interaction with Nab2 as these transcripts are being synthesized.

3.6   Nab2 is required for efficient RNAPIII transcription *in vitro* and *in vivo*

3.6.1   The *nab2-34* mutant causes an *in vivo* RNAPIII transcription defect

Having found that Nab2 interacts with RNAPIII and its transcripts, as well as the fact that full RNAPIII occupancy on its target genes depends on functional Nab2, we wanted to determine whether Nab2 is also required for maintenance of RNAPIII transcript levels *in vivo*. For this purpose Northern blot analyses of tRNA and other ncRNAs were conducted. The steady-state levels, as well as the *de novo* synthesis of RNAPIII transcripts were investigated by blotting total RNA extracted from wild-type cells or *nab2-34* mutant cells shifted to the restrictive temperature (37°C) for up to six hours (Fig. 20A). Northern blots of the *rpc25-S100P* mutant and the respective *RPC25* strain, prepared in parallel, served as a positive control (Fig. 20B). Three exemplary RNA levels, $tRNA^{Ile}(UAU)L$, *RPR1*, and *SNR6*, were measured and normalized to the amounts of the respective RNA in wild-type cells. For *RPR1* and the tRNA, levels of the precursor were analyzed (upper bands in Fig. 20A and B). However, no precursor molecules are known for *SNR6* RNA. The RNAPII-synthesized *SNR14* RNA was included as control (lowest panel in Fig. 20A and B). In addition, RNA of each sample was analyzed by agarose gel electrophoresis to control RNA quality and to verify equal loading by quantification of 25S and 18S rRNA levels (see Appendix, Fig. A2).

After shifting the cells for six hours to the restrictive temperature, the levels of all three transcripts decreased significantly in the *nab2-34* and *rpc25-S100P* mutant cells, when compared to RNA isolated from wt cells (Fig. 20C-E). Importantly, a reduction of 30-50% was observed in the *nab2-34* mutant. The effect of the polymerase mutant was even more

pronounced with levels reduced from 50% without shifting the cells, to less than 10% after shifting the mutant to 37°C for the pre-tRNA signals.
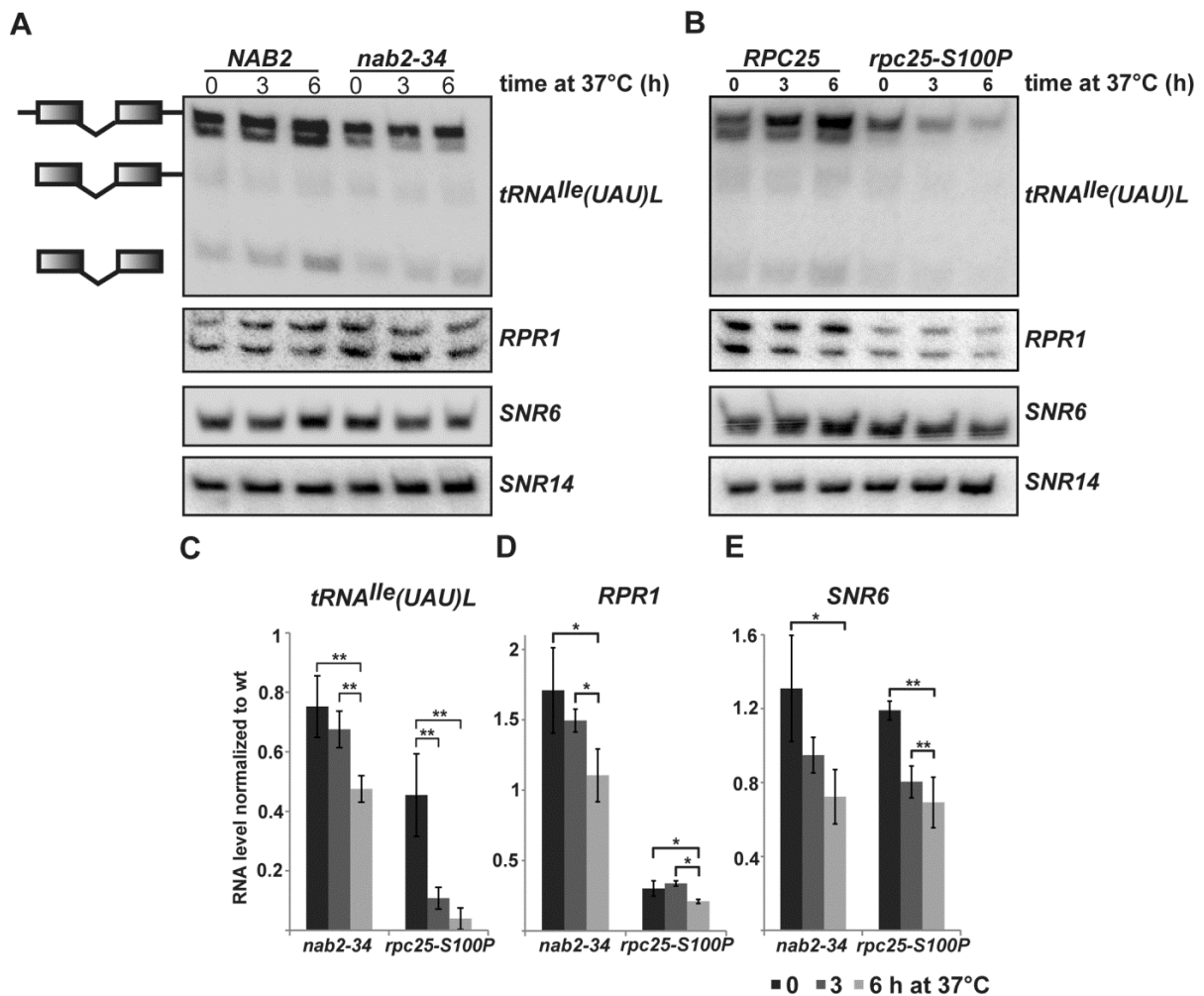

Fig. 20: Nab2 is important for normal tRNA and ncRNA neo-synthesis *in vivo*. Northern Blot analyses of *tRNA[Ile]*, *RPR1*, *SNR6*, and *SNR14* levels, a RNAPII control, in *NAB2* and *nab2-34* **(A)** or *RPC25* and *rpc25-S100P* **(B)** harboring cells shifted to the indicated temperatures for 0-6 hours. Representative blots of total RNA are shown. **(C-E)** Quantification of Northern Blot levels for *tRNA[Ile](UAU)L* (two highest bands) **(C)**, *RPR1* (upper band) **(D)**, and *SNR6* **(E)**. Levels were normalized to the corresponding wild-type strains (set to 1 at 30°C). Data (n ≥ 3) represent the mean ± SD; *: $p < 0.05$. Equal loading was verified by agarose gel electrophoresis and quantification of 25S and 18S rRNA levels (see Appendix, Fig. A2).

Since the probe for *tRNA[Ile](UAU)L* localized to the intron and *RPR1* has extended 5'- and 3'-extensions, precursor level were detected and quantified (Fig. 20C-E). Therefore, it is likely that the *de novo* synthesis of RNAPIII transcripts is impaired in the *nab2-34* cells. The same effect was also shown for the *rpc25-S100P* mutant, which is known to affect transcription initiation in *S. cerevisiae*. Thus, Nab2 is most likely involved in the transcription of RNAPIII and could be necessary for full transcriptional activity of RNAPIII *in vivo*.

### 3.6.2 Full transcriptional activity of RNAPIII depends on functional Nab2 *in vitro*

To corroborate a role of Nab2 in RNAPIII transcription, RNAPIII transcription assays were set up. The protocol described in Schultz et al. (1991) and Schultz et al. (1992) was modified as stated in the Material and Methods section (see Material and Methods, 2.2.6). Transcription active extracts of wild-type and *nab2-34* cells grown at 30°C were prepared and treated with α-amanitin to inhibit RNAPII transcription. RNAPIII transcriptional activity of these extracts was tested using two different templates: (i) the *tRNA^{Ala}(UGC)E* gene (Fig. 21A) and (ii) the *SNR6* gene (Fig. 21B). Using this assay, the *de novo* synthesis of RNAPIII transcripts could be determined (Fig. 21A and B). For both templates, a severely reduced synthesis was observed in the extracts prepared from the *nab2-34* mutant when incubated at 37°C instead of 25°C.
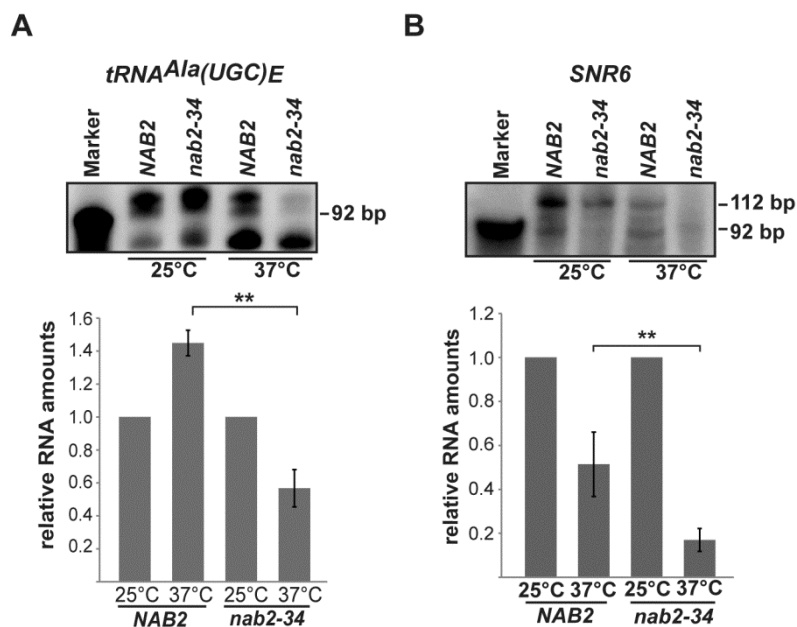
Fig. 21: Functional Nab2 is required for wild-type RNAPIII transcription levels *in vitro*. Transcription assay were carried out using whole transcription active extracts of *NAB2* or *nab2-34* cells and the reporter genes *tRNA^{Ala}(UGC)E* **(A)** or *SNR6* **(B)** on plasmids. Graphs below present quantifications normalized to the synthesized RNA amount in wild-type extracts at 25°C and 37°C. Data (n > 3) represent the mean ± SD; **: p <0.01 and representative gels are shown.

However, the temperature shift resulted in different outcome for the wild-type extract. When using the tRNA gene as a template, a slight increase of transcriptional activity was observed (Fig. 21A, compare first two columns). In contrast, the use of the *SNR6* template resulted in a reduction to approximately 50% of RNA synthesis (Fig. 21B, compare first two columns) compared to transcription in the respective non-shifted extracts. The increase in signal resulted from increased transcription and enhanced processing of tRNAs, as the lower bands represent processed tRNAs (Fig. 21A, upper panel, compare first and last two lanes).

Interestingly, it can be suggested from this data that transcription of the $tRNA^{Ala}$ gene rather than processing was impaired, as the overall amount of transcripts was lower, but still underwent cleavage (Fig. 21A, compare ratios of lower and higher bands for *NAB2* and *nab2-34* cells at 25°C and 37°C). Thus, the shift seemed to have no major effects on processing in the prepared extracts. As for *SNR6*, no precursors are described, the additional faint bands probably resulted from aberrant start site selection or degradation of the product.
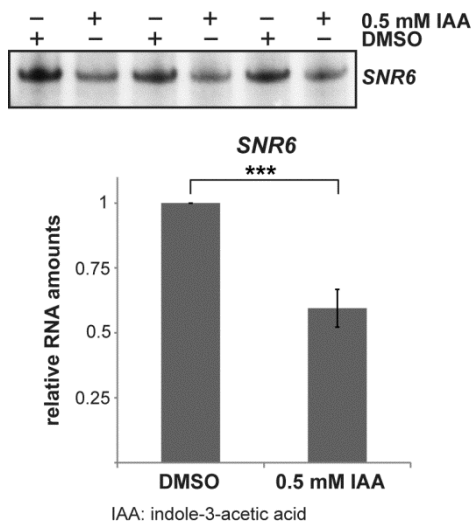
Fig. 22: Depletion of Nab2-AID leads to reduced ncRNA transcription *in vitro*. Transcription assays were carried out using whole cell transcription active extracts of *NAB2-AID* harboring cells. Upon depletion for 2.5 hours using Auxin or DMSO only, transcription activity of the extract on the *SNR6* reporter gene was reduced. Data (n=1, three tech. replicates) represent the mean ± SD; ***: p < 0.001.

In another set of experiments, *NAB2-AID* degron harboring cells were used to generate the *in vitro* transcription cell extracts. Prior to cell harvesting and extract generation, cells were treated for 2.5 hours with 0.5 mM IAA (auxin) solved in DMSO or with DMSO only. The auxin treatment showed reduced Nab2 levels in Western Blots, but no growth defect of the cells yet (compare to Fig. 15C and D). Standard *in vitro* transcription assays were then carried out as before, with the exception that no temperature shift was required (Fig. 22). Signals were normalized to the amount of RNA synthesized by the DMSO treated cells. Remarkably, the depletion of Nab2 decreased the *de novo* synthesis of *SNR6* around 50%.

This result, together with the transcription defect in the *nab2-34* mutant, pointed towards a direct function of Nab2 in the RNAPIII transcription.

3.6.3 Nab2 stimulates RNAPIII transcription *in vitro*

To show that Nab2 has a direct function in RNAPIII transcription, it should affect transcriptional outputs in this assay. Hence, when Nab2 would be added back or provided in excess, a stimulatory effect on the *in vitro* RNAPIII transcription could be expected. Accordingly, add-back transcription assays using *NAB2* and *nab2-34* transcription active extracts were conducted at 25°C and 37°C on the *SNR6* template.

Recombinantly produced and purified Nab2 (Fig. 25) was added in increasing amounts to the extracts incubated at 37°C and the amount of newly synthesized RNA was quantified (Fig. 23). Nab2 stimulated the reduced transcriptional activity in the *nab2-34* extracts that were shifted to 37°C in a dose dependent manner (Fig. 23). Interestingly, recombinant Nab2 also slightly stimulated the transcriptional activity of wild-type extracts, but only at higher concentrations. The additional bands on the gels are most likely due to degradation of the newly synthesized RNA or arise from alternative start site selection on the corresponding gene.

The observation that extracts of *nab2-34* yielded lower RNAPIII transcription suggested that Nab2 is involved in the transcriptional processes of RNAPIII. Furthermore, the add-back of recombinant Nab2 protein showed that the function of Nab2 on RNAPIII transcription is direct.
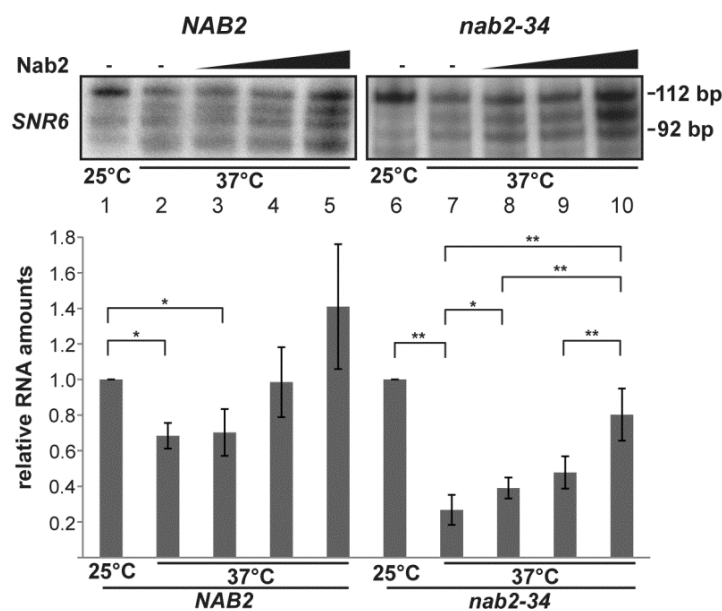

Fig. 23: Recombinant Nab2 rescues deficient transcription in *nab2-34* cell extracts. Standard *in vitro* transcription assays were performed as before in extracts from *NAB2* (lanes 1-5) or *nab2-34* cells (lanes 6-10) at the permissive (25°C, lanes 1 and 6) or restrictive temperature (37°C, lanes 2-5 & 7-10) on the *SNR6* reporter gene. Recombinant Nab2 was purified from *E. coli* and titrated in (lanes 3-5 and 8-10 with 100, 200, 300, and 400 ng Nab2). The amount of *SNR6* RNA was quantified and the RNA amount at 25°C was set to 1 (mean of $n > 3 \pm SD$; *: $p < 0.05$; **: $p < 0.01$). Nab2 stimulates RNAPIII transcription in a dose dependent manner.

### 3.6.4 Nab2 functions directly in RNAPIII transcription

In order to proof the direct influence of Nab2 on the transcriptional activity of RNAPIII, we performed fully reconstituted *in vitro* transcription assays. The advantage of such an assay is that nearly all indirect effects can be excluded, as only the most basic transcription

machinery is present in these experiments. Thus, a fully reconstituted *in vitro* transcription system was set up accordingly to Huet et al. (1996), Ducrot et al. (2006), and Ferrari et al. (2004). But instead of using the 'B" fraction', which is a whole cell extract derived fraction eluted from a cation exchange column (Bio-Rex 70, Bio-Rad), TFIIIB should be isolated from yeast. Unfortunately, the purification with either TAP-tagged Bdp1 or Brf1 did not yield the trimeric, pure TFIIIB complex (Fig. 24, middle lane). Only a single band was visible on the SDS-gels corresponding to the tagged protein (Fig. 24, TFIIIB (Bdp1-TAP)). Therefore, TFIIIB was recombinantly purified from *E. coli* (Fig. 25) and reassembled before it was used in the transcription assays. Tbp and Bdp1 purified well under the described conditions (see Material and Methods, 2.2.4.3-5 and Kassavetis et al. (1998); Kumar et al. (1997)). Brf1 though had to be purified under denaturing conditions, refolded over night by dialysis, and stored in high salt buffer. This may explain the fair gel quality in Figure 25 for Brf1.
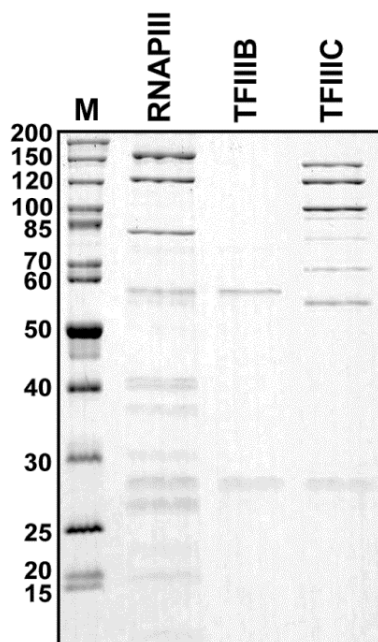

Fig. 24: Purification of RNAPIII, TFIIIB and TFIIIC from *S. cerevisiae* using TAP. A Coomassie-blue stained 10% SDS-PAA gel was used to separate the purified RNAPIII, TFIIIB and TFIIIC samples. RNAPIII was purified as the core complex with up to 12 separately distinguishable bands. TFIIIB (Bdp1-TAP) purification failed under the given conditions due to an unknown reason. Only a single band was detected with an approximate weight of 55 kDa. TFIIIC (Tfc1-TAP) was successfully purified and all six subunits are visible on the gel. The low molecular weight band (~27 kDa) in the TFIIIB and TFIIIC purifications corresponds to the TEV protease, which was used to elute the protein complexes from the beads. Marker sizes are in kDa.

Additionally, RNAPIII and TFIIIC were not purified via classical chromatography as described in Huet et al. (1996). Instead, RNAPIII was purified as before using TAP and high salt washing to yield the pure but functional polymerase (see Material and Methods, 2.2.4.1). TFIIIC was also TAP-tagged on the Tfc1 subunit and purified under the same conditions as RNAPIII.
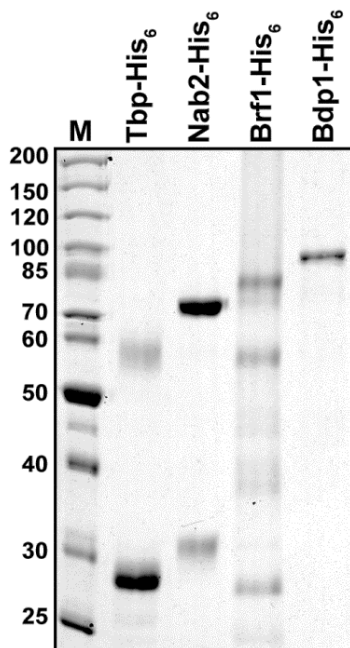
Fig. 25: Purification of recombinant TFIIIB subunits and Nab2. A Coomassie-blue stained 10% SDS-PAA gel was used to separate the purified and recombinant TFIIIB subunit and Nab2 samples. Tbp has a molecular weight of 27 kDa, Nab2 an aberrant running behavior, as its calculated weight is 58 kDa but is detected at around 70 kDa. The purification of Brf1 showed some contaminations, although the main band corresponds to Brf1 (70 kDa, but running slightly higher). Bdp1 has a molecular weight of 90 kDa and was also purified successfully. Marker sizes are in kDa.

In contrast to TFIIIB, RNAPIII and TFIIIC isolated from *S. cerevisiae* purified well and presented as the full complexes, as far as could be judged by SDS-gel electrophoresis (Fig. 24). In addition, Figure 25 shows a typical purification of Nab2. One additional band was often detected, migrating at low molecular weight. This is most likely a degradation product of Nab2 that still contained the His-Tag.
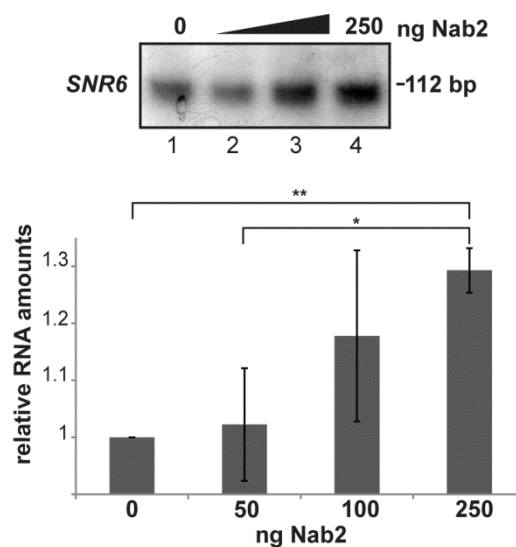
Fig. 26: Nab2 directly stimulates RNAPIII transcription *in vitro*. A fully reconstituted *in vitro* transcription assay was set up. After pre-incubation of the SNR6 reporter gene with recombinant TFIIIB, varying amounts (0, 50, 100 and 250 ng) of Nab2 and highly purified TFIIIC, purified RNAPIII from yeast was added and transcription was started. The newly synthesized amount of *SNR6* RNA was quantified and levels without Nab2 were set to 1. Data (n= 3) represent the mean ± SD, *: $p < 0.05$ and **: $p < 0.01$. A representative gel is shown.

Having purified all necessary proteins to reconstitute a minimal RNAPIII transcription system *in vitro*, transcription assays were carried out and increasing amounts Nab2 were titrated in

(Fig. 26). Overall, the transcription activity of this basic apparatus was low, as described in Ducrot et al. (2006) and Ferrari et al. (2004). Importantly, Nab2 again stimulated RNAPIII transcription in this minimal system in a dose dependent manner, even though less Nab2 was used than in previous experiments (Fig. 26).

Taken together, the *in vitro* transcription experiments with whole cell extracts, the add-back experiments, and - most importantly - the fully *in vitro* reconstituted transcription assays showed that Nab2 has a direct function in RNAPIII transcription.

3.7   Towards a molecular function of Nab2 in RNAPIII transcription

3.7.1   ChIP profiles of the RNAPIII transcription apparatus on *SCR1*

Knowing that Nab2 has a direct function in transcription of RNAPIII *in vitro*, we wanted to unravel its molecular function. As a first step towards this, we performed ChIP assays on the longest gene transcribed by RNAPIII in yeast, *SCR1*. *SCR1* codes for the 522 nt RNA subunit of the signal recognition particle (SRP), which is an abundant and evolutionary conserved ribonucleoprotein complex crucial for targeting translating ribosomes and hence synthesized proteins to the endoplasmic reticulum. It is the only RNAPIII-transcribed gene long enough to allow analysis of the spatial distribution of the proteins of interest. The distribution of Nab2 and comparison to the RNAPIII transcription apparatus could yield a first hint for the molecular mechanism of Nab2 in RNAPIII transcription.

ChIP profiles over the whole gene locus, including up- and downstream regions, were generated for RNAPIII (Rpc160-TAP), TFIIIC (Tfc1-TAP), TFIIIB (Bdp1-TAP), and Nab2 (Nab2-TAP) according to Tavenet et al. (2009) (see Fig. 27). A schematic overview of the gene and the amplified regions is given in Figure 27A. RNAPIII and the two transcription factors showed profiles similar as described before (Tavenet et al., 2009). RNAPIII (Fig. 27B) has the highest occupancy 5'-end of the gene body, where it is assembled on the DNA and initiation occurs. As this process is considered to be the rate-limiting step in transcription, the presence of RNAPIII is highest at this DNA fragment. Furthermore, a gradual decrease of RNAPIII over the gene body and downstream of the gene was observed. TFIIIC also preferentially bound to a region within 200 bp around the transcription start site (Fig. 27C). In this region, mostly 60-80 bp downstream of the transcription start, the A- and B-box elements are located, which are the main recruitment site for TFIIIC. The third basic component, TFIIIB, located primarily over the TATA box and the transcription start site, as expected (Fig. 27D, see Introduction, 1.4.4). Interestingly, TFIIIB did not show major recruitment but for the very 5'-end of *SCR1*.
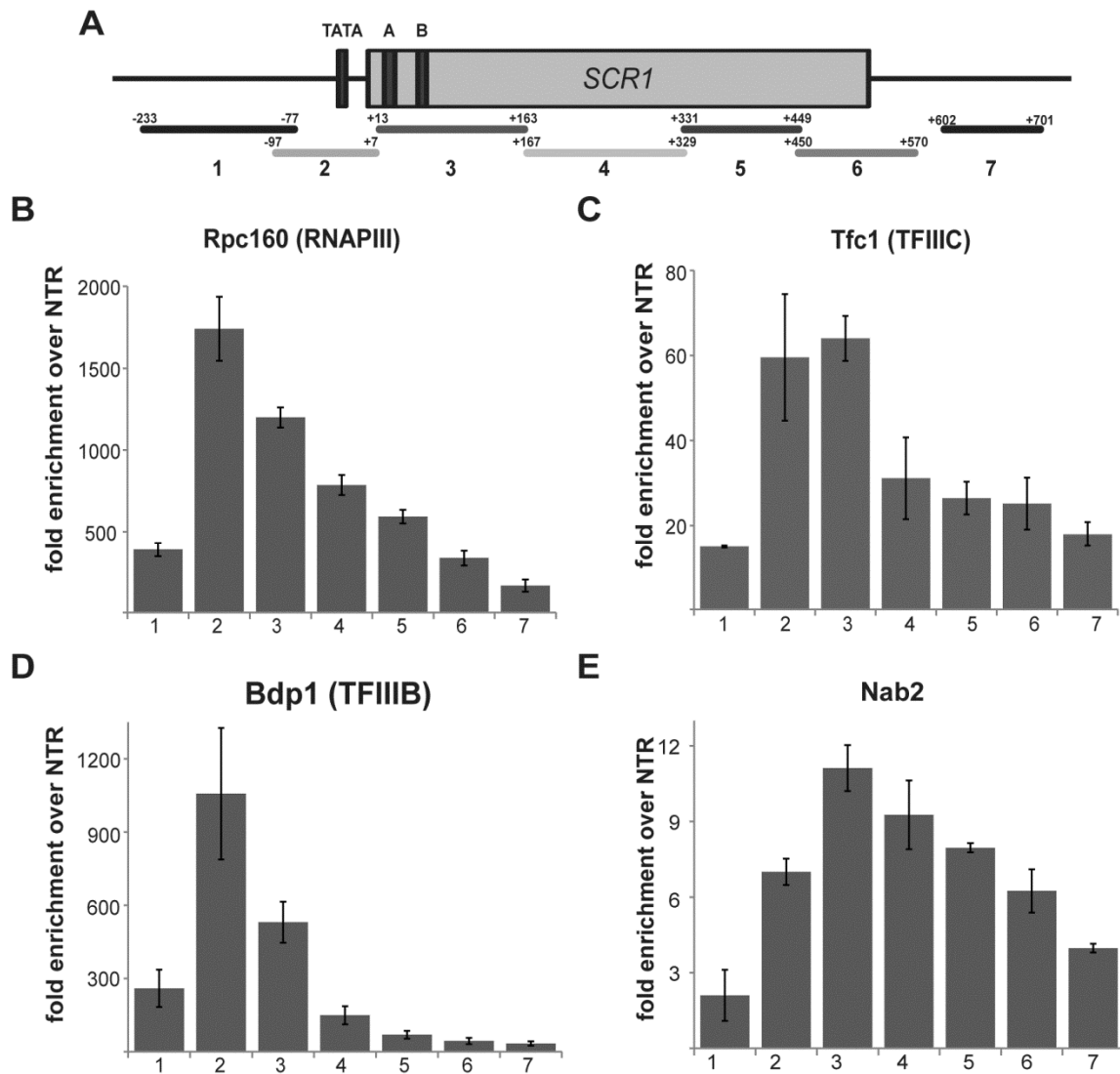
Fig. 27: ChIP profiles of RNAPIII, TFIIIB, TFIIIC and Nab2 on the longest RNAPIII-transcribed gene, *SCR1*. (A) A scheme of *SCR1*, the longest RNAPIII transcribed gene, and amplified sequences are depicted. ChIP occupancy profiles of **(B)** Rpc160-TAP (RNAPIII), **(C)** Tfc1-TAP (TFIIIC), **(D)** Bdp1-TAP (TFIIIB) and **(E)** Nab2-TAP are shown. Data (n > 3) represent the mean ± SD.

As *SCR1* contains a TATA-box, the combination of the TFIIIC-dependent TFIIIB recruitment and the binding of the TFIIIB subunit Tbp to the TATA-box efficiently recruits TFIIIB to the observed DNA site.

As expected from earlier experiments, Nab2 bound to the whole gene body. The 5'- and 3'- surrounding sequences were less occupied, arguing for a precise recruitment to the *SCR1* gene (Fig. 27E, 1 and 7). Furthermore, Nab2 showed a preference to bind to the 5'-end of *SCR1* with decreasing occupancies towards the 3'-end of the gene. In comparison to RNAPIII, Nab2 peak recruitment was located more to the 3' and the decrease was less across the whole gene. Based on this experiment, it was suggested that Nab2 primarily binds to a region around the transcription start site that is also occupied by the transcription factors,

as well as the RNA polymerase III. This in turn implies a potential function of Nab2 in transcription initiation.

3.7.2 ChIP profiles of the RNAPIII transcription apparatus in *nab2-34* cells

Earlier findings in the course of this study showed that full occupancy of RNAPIII was dependent on functional Nab2 (see Fig. 16). Due to the major recruitment of Nab2 to the 5'-region of *SCR1*, we hypothesized that it could function in transcription initiation (Fig. 27). Thus, we were interested whether Nab2 is also needed for full occupancy of the RNAPIII transcription initiation factors TFIIIB and TFIIIC. To test for this, ChIP profile analyses were performed as before with TAP-tagged TFIIIB and TFIIIC subunits in *NAB2* and *nab2-34* cells shifted to the restrictive temperature (37°C) for three hours (see Fig. 28 and Results, 3.3, Fig.16). Profiles of RNAPIII were generated in addition as control.

As anticipated, RNAPIII occupancies were decreased over the whole gene body, when Nab2 function was compromised (Fig. 28A). Remarkably, the TFIIIB occupancies were also reduced over the complete gene locus in the *nab2-34* cells shifted to 37°C, with the biggest loss observed over the gene section containing the TATA-box (Fig. 28B). This reduction of occupancy seemed to be independent of TFIIIC, as TFIIIC occupancies were also tested in this assay and showed no significant change in the shifted mutant compared to wild-type cells (Fig. 28C).

To confirm whether the observed decrease in TFIIIB is a general feature of the *nab2-34* mutant cells we tested more genes by inspection of the three exemplary genes *SNR6*, *tDNA^{Lys}*, and *RPR1*, which were used before (Fig. 29). Again, impairing Nab2 function resulted in a significant loss of TFIIIB (Fig. 29A) but not TFIIIC (Fig. 29B) occupancy on all tested genes. As TFIIIB is a key component in recruiting RNAPIII to the promoter region of the gene to be transcribed and is known to be involved in DNA melting, as well as PIC formation, the reduced TFIIIB occupancy in the *nab2-34* cells is most likely the reason for the lower RNAPIII occupancy. This could furthermore explain the reduced transcriptional activity in the different *in vitro* transcription assays.

Taken together with the previous ChIP observations, these results showed that Nab2 is specifically required for full TFIIIB and RNAPIII occupancy *in vivo*.
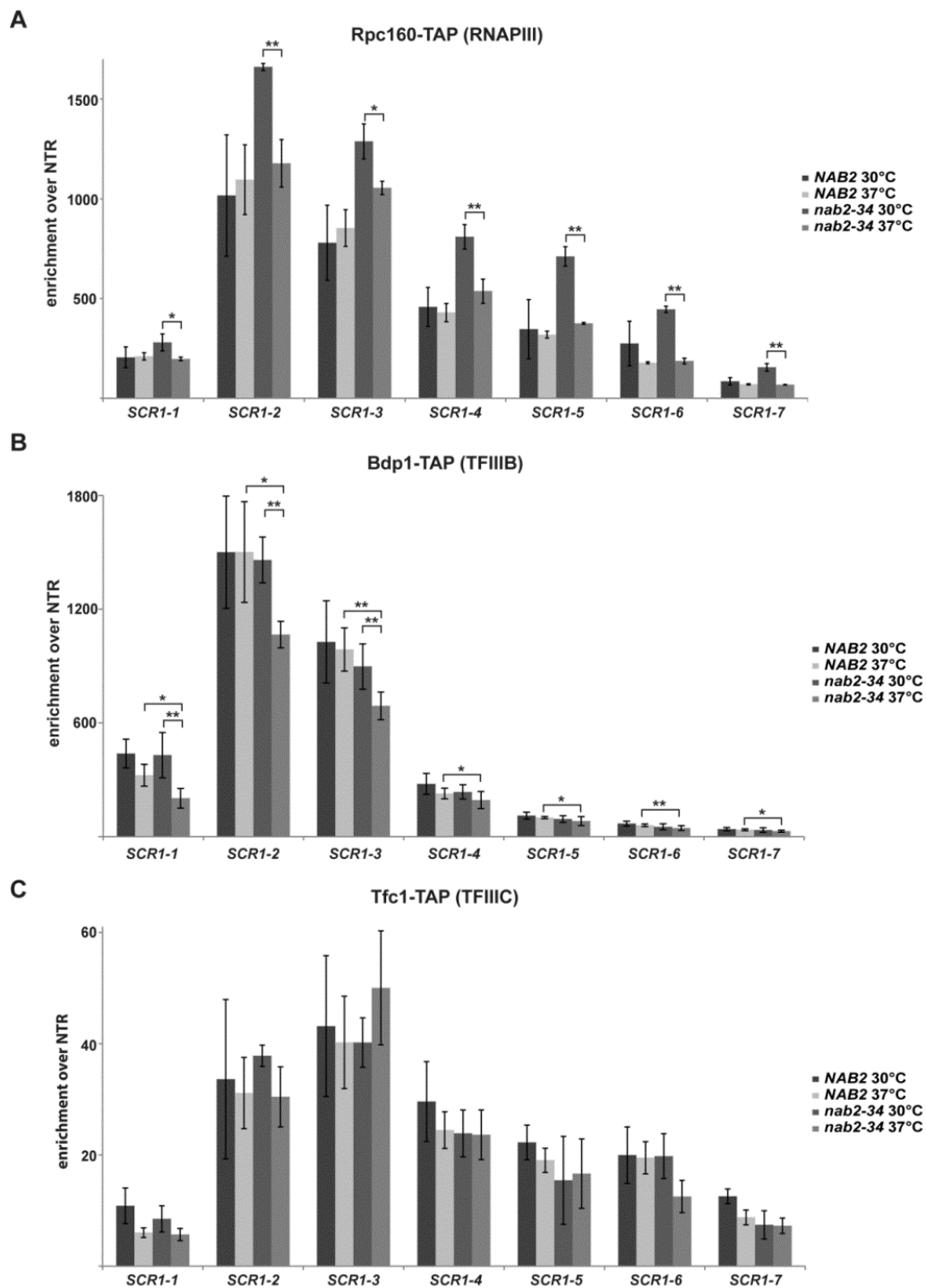
Fig. 28: Nab2 is required for full occupancy of RNAPIII and TFIIIB but not of TFIIIC on *SCR1*. ChIP occupancy profiles of **(A)** Rpc160-TAP (RNAPIII), **(B)** Bdp1-TAP (TFIIIB), and **(C)** Tfc1-TAP (TFIIIC) were assessed in *NAB2* or *nab2-34* harboring cells after shift to the restrictive temperature (37°C) for three hours. *SCR1-1* to *SCR1-7* are according to Figure 27A. Data represent the mean ± SD of at least three independent replicates, *: $p < 0.05$ and **: $p < 0.01$.
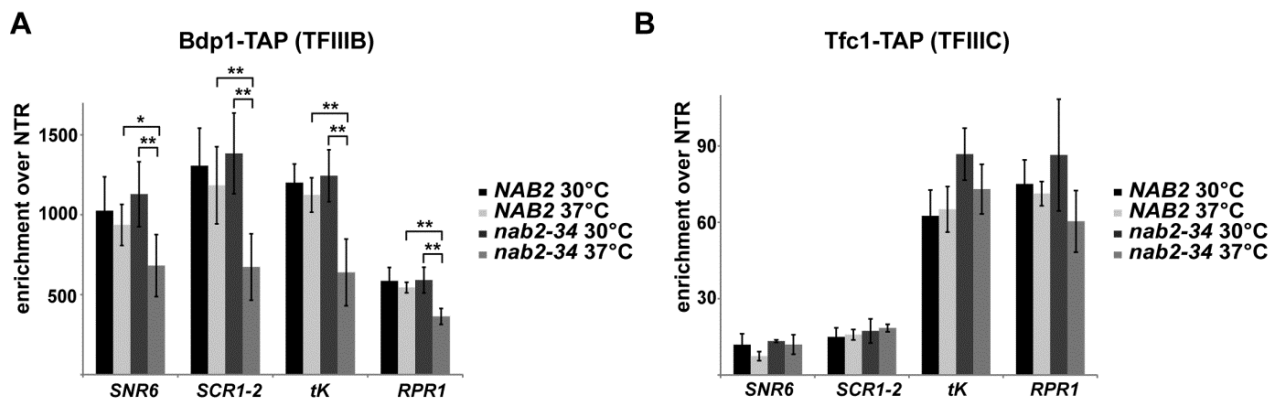
Fig. 29: TFIIIB occupancy is reduced on several genes in *nab2-34*. ChIP-qPCR experiments as in Figure 27 in *NAB2* and *nab2-34* cells. **(A)** Bdp1-TAP (TFIIIB), but not **(B)** Tfc1-TAP (TFIIIC) occupancies on *RPR1*, *SNR6* and *tK* (lysine tRNA locus) were reduced in the mutant at the restrictive temperature. Data (n ≥3) represent the mean ± SD; *: $p < 0.05$; **: $p < 0.01$.

3.7.3 TFIIIB interacts with Nab2 *in vivo*

Based on the results that functional Nab2 is needed to fully recruit to or stabilize TFIIIB at tRNA and other ncRNA gene promoters (Fig. 28 + 29), it seemed likely that they also should interact with each other *in vivo*.
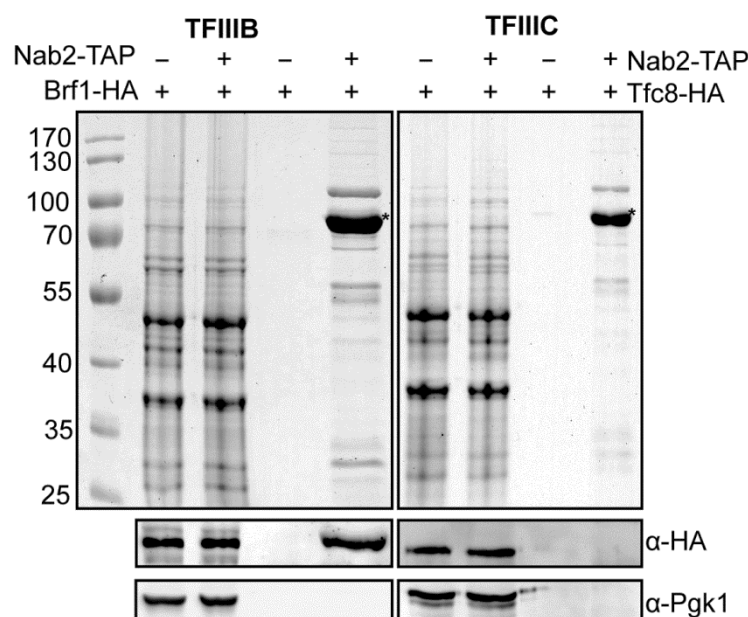
Fig. 30: Nab2 interacts with TFIIIB, but not TFIIIC *in vivo*. Strains expressing *NAB2-TAP* were additionally tagged with a C-terminal HA-tag on either Brf1 (TFIIIB, left panels) or Tfc8 (TFIIIC, right panels). Strains without TAP-tag served as negative control. Copurification of Brf1 and Tfc8 with Nab2 was assessed by Western blotting against the HA epitope. Tagged Nab2 is marked with an asterisk and Pgk1 served as negative control. Representative 10% Coomassie-blue stained SDS-PAA gels and Western blot are shown. Marker sizes are in kDa.

To test for a potential interaction, Nab2-TAP was purified from *S. cerevisiae* by TAP and co-purification of either TFIIIB (Brf1-HA) or TFIIIC (Tfc8-HA) was assessed using Western blotting (Fig. 31). Strains carrying no TAP-tag on Nab2 but either Brf1-HA or Tfc8-HA served as negative controls. The purification quality was further monitored by analyzing the non-specific co-purification of Pgk1. The native purification of Nab2-TAP was successful, as it yielded the typical co-purifying proteins, as described above.

Indeed, Nab2 purifications revealed the presence of Brf1, a subunit of TFIIIB, and thus most likely the whole TFIIIB complex interacts with Nab2 *in vivo* (Fig. 30, left panel). In contrast, Tfc8 (TFIIIC) did not show co-purification with Nab2 (Fig. 30, right panel), in line with the fact that occupancy of TFIIIC is not affected by the *nab2-34* mutant (Fig. 28 and 29). In summary, this demonstrated that Nab2 is able to interact with the TFIIIB subunit Brf1 *in vivo.*

3.7.4 Nab2 stabilizes TFIIIB and increases its affinity to promoter DNA

TFIIIB, the trimeric transcription initiation factor comprised of Bdp1, Brf1, and Tbp, has a key role in RNAPIII transcription, as its presence is mandatory at all three kinds of promoters, and RNAPIII is recruited mainly via the subunit Bdp1 (Kassavetis et al. (1990) and reviewed in Acker et al. (2013); Geiduschek and Kassavetis (2001)).

Nab2 interacts with TFIIIB and is required for full TFIIIB occupancy. This prompted us to investigate whether and how Nab2 influences the binding of TFIIIB to the promoter DNA of tRNA and other ncRNA genes. Therefore, electrophoretic mobility shift assays (EMSAs) were performed with recombinant TFIIIB and Nab2 to test whether Nab2 could increase the fraction of TFIIIB bound to a cognate promoter DNA. The used template, TA-30-B6, is a 76 bp long, double stranded DNA (dsDNA) derived from the 5'-end of the yeast *SUP4* tRNA gene tY(GUA)J2 encoding a tyrosine tRNA, as described in Kassavetis et al. (1998). Its molecular characteristics are a 6 bp long TATA box (TATAAA) with 2 nt mismatches flanking each site (see Fig. 31A). This combination should favor an *in vitro* Tbp binding to the dsDNA independent of TFIIIC, which is naturally required to efficiently recruit TFIIIB to tRNA promoters. More importantly, this particular tRNA derived sequence only allows a specific and sequential binding of TFIIIB to the DNA (Grove et al., 1999; Kassavetis et al., 1998). Hence, the first component being able to bind to the DNA is Tbp, followed by binding of Brf1. The Tbp-Brf1 subcomplex is also often referred to as B'-complex.
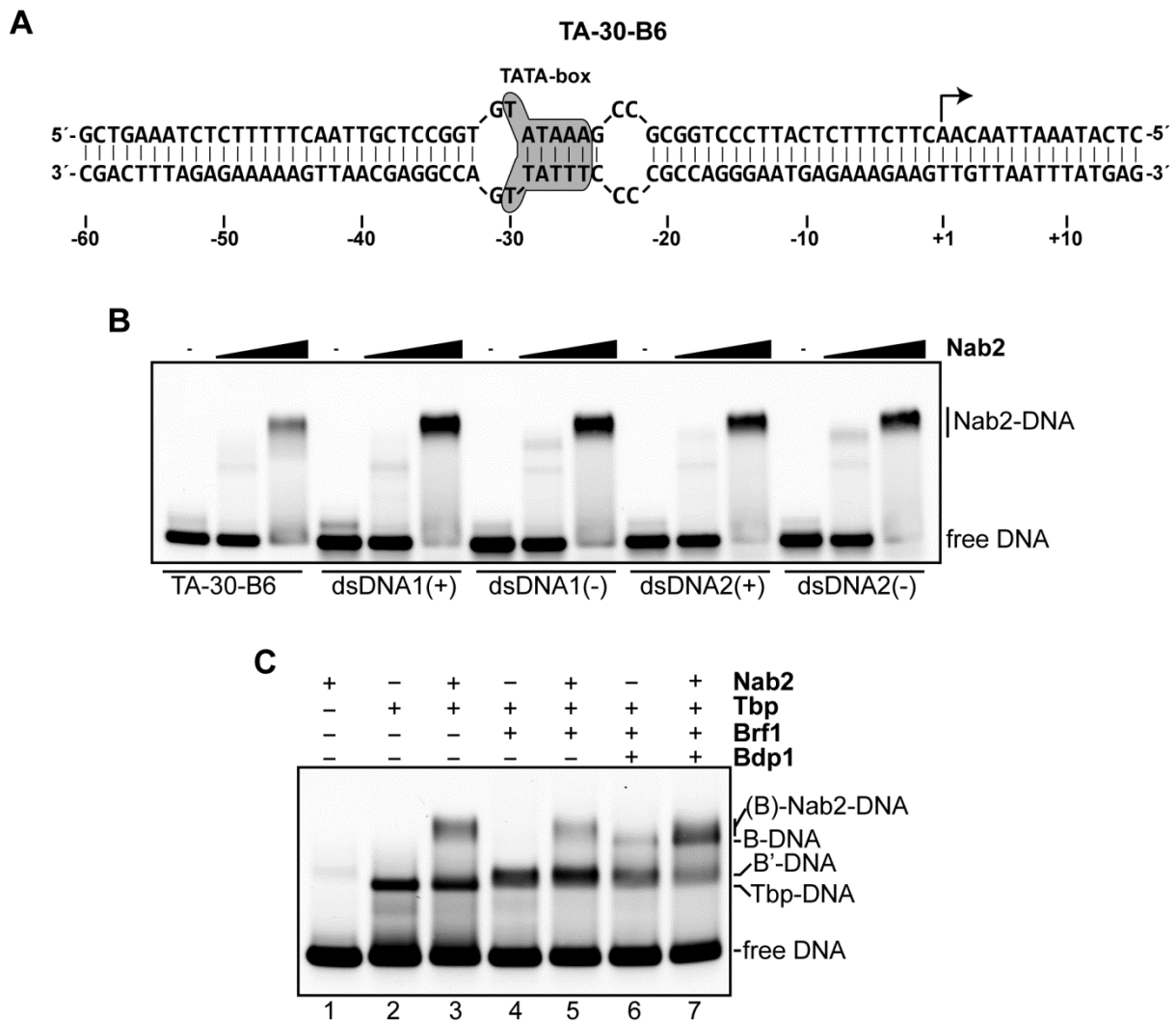
Fig. 31: Nab2 increases the affinity of TFIIIB to promoter DNA *in vitro*. Electrophoretic mobility shift assays (EMSA) of Nab2 and different dsDNA probes. (A) Schematic view of the TA-30-B6 dsDNA used in this assay. (B) Increasing amounts of Nab2-His$_6$ (0, 0.5, and 1 μg) were incubated with the specific RNAPIII promoter dsDNA (TA-30-B6 Kassavetis et al. (1998)) and four scrambled probes with (dsDNA1(+) and dsDNA2(+)) and without (dsDNA1(-) and dsDNA2(-)) two 2-nucleotide mismatches. (C) EMSA of Nab2 and TFIIIB binding to TA-30-B6 DNA. Formed DNA-protein complexes are indicated at the right side. TFIIIB assembles in the absence of Nab2, but more complex is assembled when Nab2 is present. Furthermore, a supershift is induced by Nab2, as soon as Tbp has initially bound to the DNA.

Both proteins form a very stable interaction that is even preserved during chromatography. In contrast, associated Bdp1, the last component to form the complete TFIIIB complex, is easily lost (Kassavetis et al., 2006).

Being characterized as a poly(A)-binding protein that can also bind other RNA sequences and displays unspecific binding to RNA (Kelly et al., 2007; Tuck and Tollervey, 2013), a potential unspecific binding of Nab2 to TA-30-B6 should be ruled out. Thus, we tested Nab2 binding to four dsDNAs in addition to TA-30-B6 and also evaluated binding of different amounts of Nab2 to the mentioned dsDNAs. The additional dsDNAs were derived from the

TA-30-B6 probe by scrambling the given sequence (see Material and Methods, 2.1.5, Table 9). Two dsDNAs (dsDNA1$^+$ and dsDNA2$^+$) contained the two two-nucleotide mismatches, whereas the mismatches were absent in the other two dsDNAs (dsDNA1$^-$ and dsDNA2$^-$). In addition, dsDNA1$^{+/-}$ did not contain repeating nucleotides (*e.g.* AA or UU), though in the sequences of dsDNA2$^{+/-}$ double nucleotides were allowed.

Nab2 bound to these DNAs only at high amounts (1 µg) and the least to the original TFIIIB probe TA-30-B6 (Fig. 31B). This indicated that signals derived from Nab2 binding in the TFIIIB dependent EMSA should not derive from unspecific background binding of Nab2, as also lower concentrations of Nab2 were used.

The advantage of the sequential binding of TFIIIB to the TA-30-B6 dsDNA was exploited when testing the potential effect of Nab2 on this binding (Fig. 31C), by incubating different TFIIIB subunit combinations with or without Nab2 on the target DNA.

Within these experiments and as expected, the stepwise association of TFIIIB could be reproduced (Fig. 31C, lanes 2, 4, and 6 and Kassavetis et al. (1998)). Tbp, although being the smallest protein, had the biggest impact on shifting its bound DNA (Fig. 31C, lane 2). This is due to the massive kink that is introduced to the DNA upon binding of Tbp (Braun et al., 1992; Grove et al., 1999; Leveillard et al., 1991). An only slight increase of this shift was detectable upon binding of Brf1 and formation of B' (Fig. 31C, lane 4). When the last component Bdp1 was added, a moderate shift was observed (Fig. 31C, lane 6).

Having set up and tested the EMSA with TFIIIB only, the effect of Nab2 on this stepwise association was tested. When Tbp was bound to the TA-30-B6 probe, Nab2 could also bind to the DNA and induce a supershift (Fig. 31C, lane 3 and compare to lanes 1-3). This supershift was also detected, when Nab2 was added either in combination with the B' subcomplex (Fig. 31C, lane 5) or the whole TFIIIB complex (Fig. 31C, lane 7). Nab2 additionally increased the amount of total protein associated to the DNA.

In conclusion, we showed that Nab2 is needed to efficiently assemble the RNAPIII initiation complex by increasing the overall binding of TFIIIB to the promoter DNA *in vitro*. This could be accomplished by either physically recruiting Brf1 or Bdp1 to Tbp-DNA or by stabilizing TFIIIB once the complex bound initially to the DNA.

### 3.7.5 Nab2 stabilizes TFIIIB in *in vitro* transcription assays

To characterize the stabilization / recruitment of TFIIIB by Nab2 on target genes in more detail, we used a modified version of the '17-mer assay' (Dieci and Sentenac, 1996). In this assay a unique property of the *SUP4* tRNA gene is exploited. Figure 32A displays the transcription start site region of *SUP4* on the coding strand. As the first guanosine is

incorporated at position +18 only, leaving out GTP from the reaction results in pausing of the polymerase as it tries to incorporate the missing guanosine at this position (Dieci and Sentenac, 1996). This pausing can be resolved in three different ways: (1) the polymerase is stalled and waiting until GTP is available, (2) the polymerase switches from elongating to backtracking and cleavage of 2-3 nt of the RNA, followed by new synthesis (Bobkova and Hall, 1997; Chedin et al., 1998), or (3) the transcription bubble collapses thereby releasing the polymerase and the 17-mer transcript. As the transcription apparatus with DNA and RNA can be purified, it is considered stable favoring the first mentioned possibility (Dieci and Sentenac, 1996; Kassavetis et al., 1989).

Importantly, the DNA mimicking property of heparin is employed in this assay to sequester non DNA-bound polymerases that are either not assembled on DNA or were released from the gene after completing an entire round of transcription.

With this set up, we were able to distinguish three different phases of tRNA gene transcription: (1) Initiation, which is characterized by the 17-mer formation, (2) elongation, as GTP will be added to the stalled 17-mers and production of full length RNA can be monitored, yet released polymerases are sequestered by heparin or (3) reinitiation, where multiple rounds of transcription are allowed after initial 17-mer formation. To set up a reinitiation assay from the single round 17-mer assay, GTP is added after 17-mer formation and half of the samples were eventually treated with heparin.
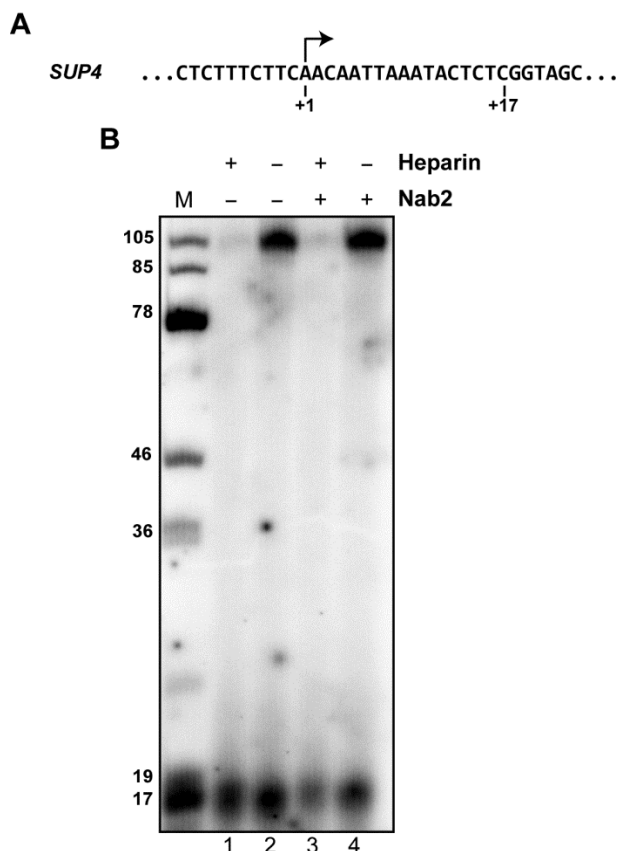
Fig. 32: Nab2 might stabilize the PIC on transcription templates *in vitro*. A scanned phosphorimage of a typical initiation / reinitiation assay is presented. Fully *in vitro* reconstituted transcription assays were set up under 17-mer formation conditions. These were incubated with or without recombinant Nab2 and subsequently allowed to form 17-mers. After synthesis of this product, half of the samples were supplemented with Heparin (0.25 mg/mL) and elongation/ reinitiation was allowed. The reactions were stopped and products were separated on 17% (v/v) PAA-Urea gels after RNA precipitation. DpnI digested pcDNA3.1 radiolabeled with [γ-32P] ATP served as an internal length standard (M: Marker in bases).

Comparing the transcriptional output of reactions complemented with or without Nab2 would allow identification, whether Nab2 is involved in transcription initiation, elongation or reinitiation.

Interestingly, first results point towards a stabilizing role of Nab2 as suggested by the *in vitro* DNA binding experiments from above (Fig. 31C). In general when heparin was present, 17-mer transcripts are produced, but only low amounts of full length transcript (Fig. 32, lane 1). This was expected as only one round of transcription is allowed, due to the excess of heparin that captures RNAPIII. Lane two of Figure 32 shows the result from reactions treated the same, but no heparin was added. This resulted in production of full length tRNA transcripts; still, 17-mers could be detected. Addition of Nab2 and heparin resulted in lower amounts of 17-mers in general (Fig. 32, compare lanes 1 and 3), but yielded the same or even more full length transcripts, when heparin was omitted from this assay (Fig. 32, compare lanes 2 and 4).

This presents Nab2 as a factor necessary for stabilization of TFIIIB and the initial PIC. Lower transcript amounts (17-mers) in the single round transcription assay with heparin and Nab2 (Fig. 32, lane 3) argued for less abortive transcription in the presence of Nab2. In line with that, increased amount of abortive was observed when Nab2 was absent (Fig. 32, lane 1). Hence, a more stable initiating RNA polymerase III that is still in the vicinity of the promoter together with TFIIIB and Nab2 could result in an increase in full length transcript production (Fig. 32, lane 4). Alternatively, lower 17-mer signals could have resulted from more efficient elongation when Nab2 was present. Furthermore, presence of Nab2 and stabilization of TFIIIB might not only enhance initial transcription initiation but also ease facilitated reinitiation/ recycling. Whether this is true, still remains to be shown by *e.g.* 17-mer assays under single round transcription conditions.

3.8   Generation of an anti-ZC3H14 antibody

As Nab2 is highly conserved from yeast to humans (see Introduction, 1.3 and Fig. 3), we raised the question, whether the newly identified function of Nab2 in RNAPIII transcription might be also conserved in higher organisms. To study this potential role in higher cells, such as human cell culture, interaction assays and ChIP would be of great interest. A versatile tool, which could be used for many experiments, is an antibody that recognizes the human Nab2 orthologue ZC3H14. Therefore, we decided to raise an antibody against this protein. A region of the proteins that proved well for this, are the first 97 amino acids of isoform 1 of ZC3H14 (Leung et al., 2009).

The N-terminus of ZC3H14 was hence GST-tagged, produced in *E. coli* and purified to near homogeneity (Fig. 33A). Two rabbits were then initially immunized with 500 µg of protein each for 40 days with three boosts (Pineda, Berlin). After this initial immunization, samples were tested for recognition of purified GST-ZC3H14. This was repeated monthly until the immune response of the animals peaked and antibodies showed specific reactivity (Fig. 33B). In our case, serum of day 240 post immunization was chosen. The serum was then tested for recognition of endogenous ZC3H14 isoforms and ectopically expressed ZC3H14-GFP, using whole cell extracts from HeLa cells (Fig. 33B).
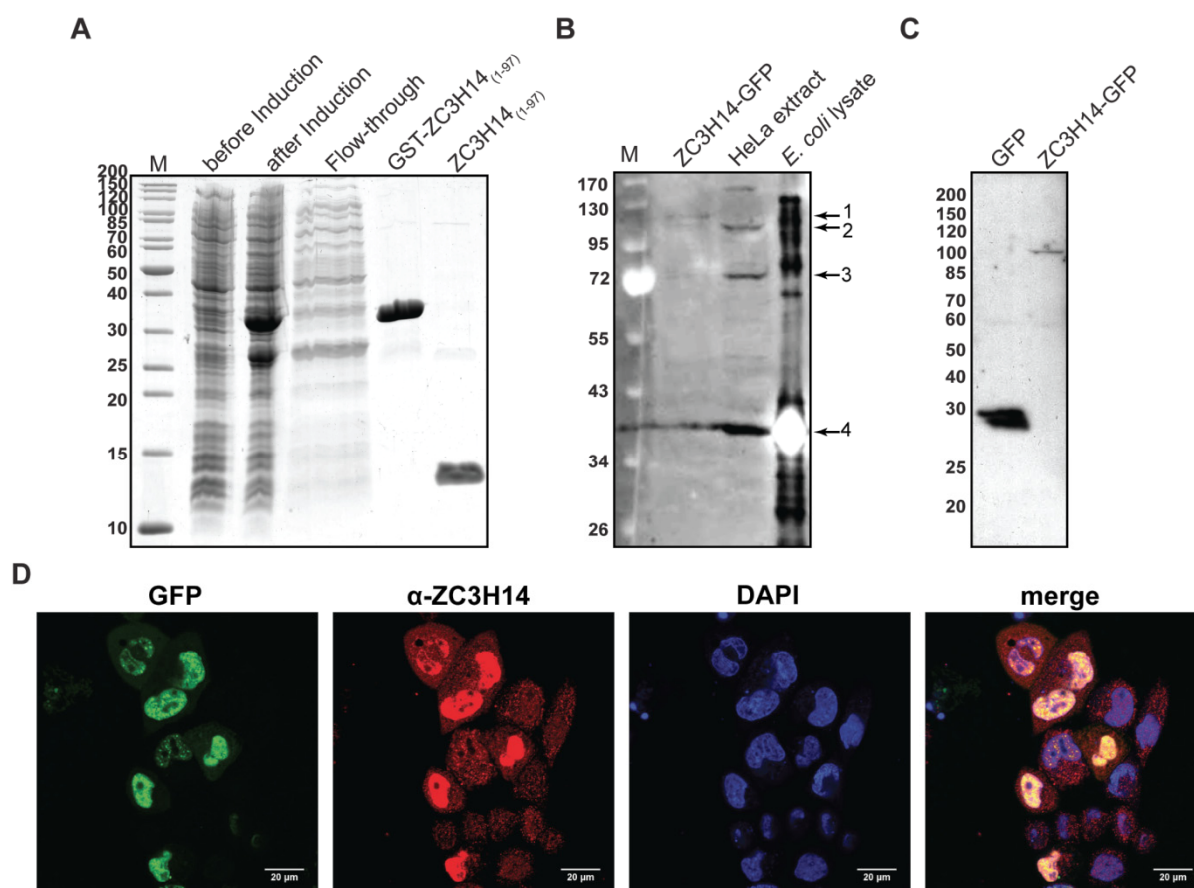
Fig. 33 Generation of an human anti-ZC3H14 antibody. (A) Purification of GST-fused ZC3H14$_{(1-97)}$ (first97 amino acids) from *E. coli*. The last lane shows the purified ZC3H14 fragment, which has been cut by 'PreScission protease' to remove the GST-tag. A 12% Coomassie-blue stained SDS-PAA gel is shown. Marker sizes are in kDa. **(B)** Western blot analysis of the ZC3H14 epitope recognition by the anti-ZC3H14 antibody from immunized rabbit #2 after 240 days of immunization (1: 1000 dilution). (1) ZC3H14-GFP, (2) ZC3H14 isoform 1, (3) ZC3H14 isoform 2 /3 and (4) GST-ZC3H14$_{(1-97)}$ from *E. coli* lysate. Marker sizes are in kDa. **(C)** ZC3H14-GFP is barely expressed in HeLa cells. Western blot of HeLa cells transfected with ZC3H14-GFP or GFP alone and detection of GFP (1:2000, mouse). Marker sizes are in kDa. **(D)** Fluorescence microscopy of transfected HEK293 cells. ZC3H14-GFP was transfected 24-48 h before cells were fixed and stained. The anti-ZC3H14 antibody (animal #2, day 240) was diluted to 1:1000 and DNA was stained using DAPI. The overlay of all images is depicted on the very right.

The anti-ZC3H14 antibody (animal #2) recognized two bands, corresponding to isoform 1, 2, and 3 that harbor the respective N-terminal domain or parts of it (see Fig. 33B and Introduction 1.3, Figure 3). It then should be tested, whether this antibody can also be used in immunofluorescence microscopy. Therefore, HEK293 cells were transfected with ZC3H14-GFP and subjected to Western blotting to control the production of the tagged ZC3H14 (Fig. 33C); GFP only transfected cells served as positive control. ZC3H14-GFP was observed at the expected molecular weight (Fig. 33C), and fluorescence microcopy was performed with these cells and antibodies from both immunized animals. The anti-ZC3H14 antibody (animal #2) showed co-localization with the GFP signal in cell nuclei (Fig. 33D, merge), whereas this was not the case for the antibody from animal #1 (data not shown). Therefrom, it was concluded that the anti-ZC3H14 antibody collected from animal #2 recognizes ZC3H14 in Western blot (denatured protein) and most likely the native conformation in HEK293 cells.

In summary, the new antibody recognizing ZC3H14 is a versatile tool that will enable us to investigate the potential conservation of Nab2's function in higher cells.

3.9   Electron microscopy of RNAPIII

After having identified that Nab2 and RNAPIII can interact directly *in vitro*, an additional aim was to reconstitute this binding and to subsequently locate Nab2 on RNAPIII using Electron microscopy (EM). Sample processing, image acquisition and data analysis was done in collaboration with Dr. Petra Wendler (Gene Center, LMU Munich). For this, stringently purified RNAPIII from *S. cerevisiae* and Nab2 purified from *E. coli* were mixed, incubated and processed as for the *in vitro* interaction assays (see Results 3.4, Fig. 17). The same procedure was done for RNAPIII only. Samples were then prepared for negative stain electron microscopy (EM) according to Kube et al. (2014) (see Material & Methods, 2.2.8.9) and images were taken on a FEI Morgagni transmission electron microscope. A typical grid image for RNAPIII preparations is shown in Figure 34A.

With an approximate diameter of 20 nm, the bright triangular or square shaped objects represented differently oriented polymerases on the grid. This size and shape corresponded well to what was described earlier (Fernandez-Tornero et al., 2011; Fernandez-Tornero et al., 2007). Initial class building was performed for the acquired data sets with 2751 particles for the RNAPIII alone and 1305 particles for the reconstituted RNAPIII-Nab2 interaction (Fig. 34B, RNAPIII samples). Again, these classes can be considered as different orientations of the RNA polymerase on the grid. The class averages were used for multi-variate analysis

and 2D multi reference alignments to create EM maps. Final visualization of the EM maps was done using Pymol (Fig. 34C, RNAPIII samples).
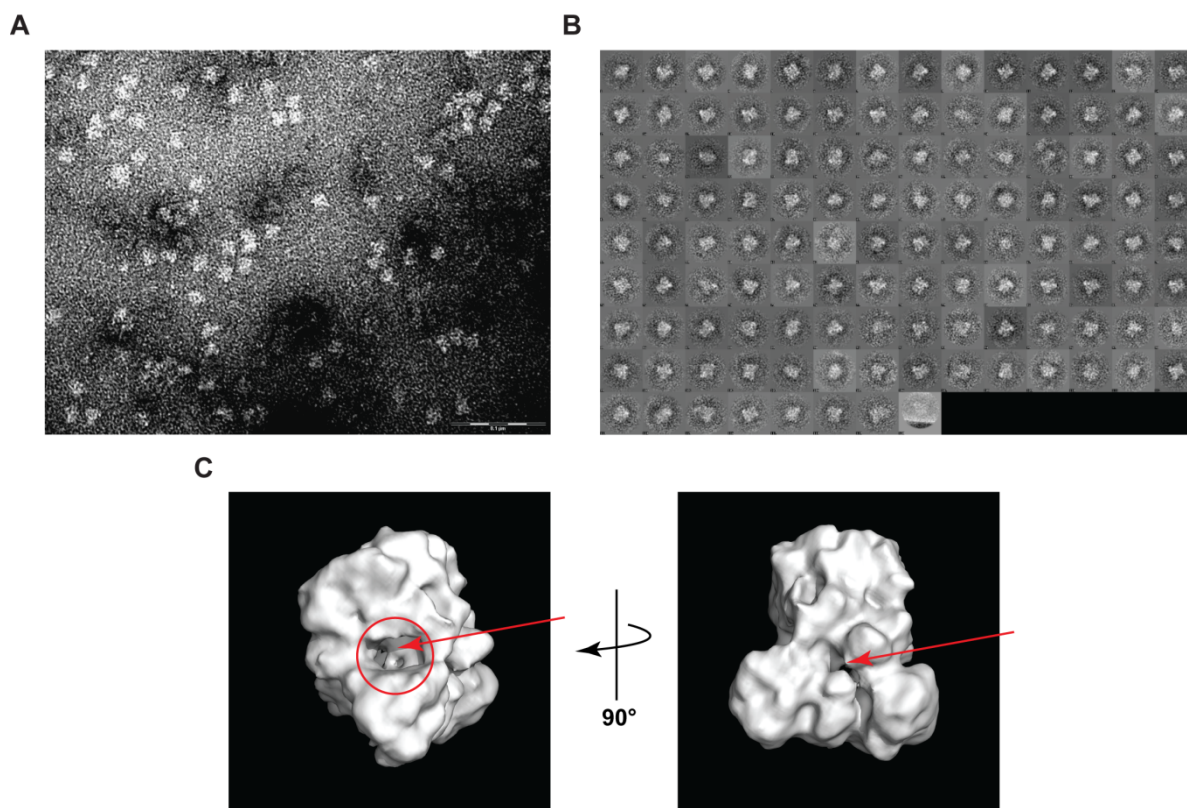
Fig. 34: Reconstruction of an initial 3D RNAPIII model from electron microscopy micrographs. (A) A representative electron micrograph showing negatively stained RNAPIII complexes from *S. cerevisiae* spotted on a carbon coated electron microscopy grid. The single, bright polymerases were distributed evenly all over the grid and could be picked for analysis. Note that differences in size and shape are due to the orientation of RNAPIII on the grid. **(B)** Class averages of the RNAPIII are shown. These represent different orientations of the polymerase complex on the grid. **(C)** Initial reconstruction of the core RNAPIII enzyme. The previously compiled class averages were used to generate this 3D reconstruction of the polymerase. The circle in the left panel most probably displays the DNA entry / exit site. The arrow points to a density potentially involved in DNA strand separation. The arrow in the right image points toward the likely RNA exit site of the polymerase (compare to Fernandez-Tornero et al. (2011); Fernandez-Tornero et al. (2010)). The 3D model was generated using Pymol software (v.1.3)

Comparison of the initial maps of RNAPIII alone and RNAPIII with Nab2 unfortunately did not reveal any additional and reliable densities that could be attributed to Nab2 (data not shown and see Appendix, Fig. A3). This might be due to the fact that the initial datasets were not accurate enough on the outer surface of the polymerase. On the other hand Nab2 most probably has several unstructured regions, which impede a three-dimensional prediction of Nab2. This might be the reason why it has not been crystalized yet and was not detected as a compact density in the EM maps. To circumvent this problem gold labeling of Nab2-His$_6$ was tested. However, as the Ni-NTA-gold particles bound non-specifically to RNAPIII itself, this approach could not be followed up further.

Irrespectively of the not yet solved RNAPIII-Nab2 structure, it was possible to generate an initial 3D map of RNAPIII that showed some major features as described by Fernandez-Tornero et al. (2010) and Fernandez-Tornero et al. (2007). For example, the DNA entry / exit site, as well as the RNA exit site of the RNA polymerase III could be assigned (Fig. 34C, red circle and arrows).

The initial 3D reconstruction of RNAPIII provides proof that TAP purification yields complexes in native shape, which can be used for structure determination in general. Unfortunately, Nab2 could not be localized yet. To potentially show the binding site of Nab2 to the core RNAPIII enzyme, this system needs improvement. One the one hand, a bigger dataset could be generated, on the other hand, alternative approaches, such as cryo-EM should be tested.

4. Discussion

The aim of this PhD project was to identify the role of the poly(A)-binding protein Nab2 in RNA Polymerase III transcription. Initially proposed by a genome-wide association of Nab2 with RNAPIII, the recruitment of Nab2 and RNAPIII on RNAPIII-transcribed genes was further investigated. In addition, the molecular interaction of Nab2 and the RNAPIII enzyme was shown *in vivo* and *in vitro*. Finally, a direct participation in RNAPIII transcription was demonstrated and the molecular function of Nab2 was unveiled. Nab2 is important for stabilizing the RNAPIII transcription factor TFIIIB on promoter DNA and, hence, transcription initiation.

4.1 The generation of new *NAB2* alleles

4.1.1 *nab2-34*: A novel temperature sensitive allele of *NAB2*

The poly(A)-binding protein Nab2 is one of the founding members of the poly(A)-binding protein family and binds to the poly(A) tail of mRNAs with its zinc finger modules. Importantly, the well described RGG (Arginine-arginine-glycine) domain that is located N-terminally of the ZnF modules in Nab2, does not bind to RNA (Anderson et al., 1993; Marfatia et al., 2003). This domain is often found in hnRNPs that were identified to bind poly(A)-containing mRNAs, such as Npl3 or Hrp1, and was described to mediate nucleic acid binding, as well as export by methylation of its arginine residues by PRMTs (protein arginine methyltransferases) (Bossie et al., 1992; Valentini et al., 1999; Xu and Henry, 2004).

In addition to binding to poly(A) tails, Nab2 has been intensively studied and its roles in mRNA export, poly(A) tail length control, as well as mRNA stability have been established (Batisse et al., 2009; Gallardo et al., 2003; Grenier St-Sauveur et al., 2013; Hector et al., 2002; Kelly et al., 2007; Schmid et al., 2015; Schmid et al., 2012).

A previous genome-wide study of the localization of several mRNA-binding proteins from our research group identified that Nab2 occupies all RNAPIII-transcribed genes (see Results, 3.1, Fig. 10, 11 and 12 and Meinel et al. (2013)). This is in good correlation with the recent observation by Gonzalez-Aguilera and colleagues that Nab2 localizes to five different RNAPIII-transcribed genes (Gonzalez-Aguilera et al., 2011). They showed that Nab2 associates with genes transcribed by RNAPII and RNAPIII in a TREX and TREX-2-dependent manner. Furthermore, they speculated that Nab2 might play a role in the metabolism of RNAPI and RNAPIII transcripts, as suggested by *e.g.* a microarray analysis of the *nab2-1-GFP* allele. In contrast to the study presented here, Gonzalez-Aguilera and

colleagues excluded a role for Nab2 in RNAPIII transcription (Gonzalez-Aguilera et al., 2011). The reason for this might be that the used *nab2-1-GFP* mutant most likely shows secondary effects, due to the extremely slow growth even under optimal growth conditions, and that the function of Nab2 in RNAPIII transcription was missed.

To avoid using the *nab2-1* mutant or other available alleles of the essential *NAB2* gene, we generated our own temperature-sensitive *NAB2* allele, *nab2-34*. The Nab2-34 protein is fully produced and contains several mutations (see Results, 3.2.1, Fig. 14). Hence, it is interesting to argue which of the acquired missense mutations may be responsible for causing the growth retardation on the one hand and the observed effects on RNAPIII transcription on the other hand or both at once.

Three of the mutated residues localized to the QQQP domain of Nab2 (see Results, 3.2.1, Fig. 14). Although they may change the local protein folding, an influence of these mutations on the overall structure of Nab2 seems unlikely, as this domain can be omitted from the protein without any consequences for cell fitness (Marfatia et al., 2003). All other residue changes could result in the mutant phenotype. In particular, we discuss two amino acid exchanges in the zinc finger domains in the following paragraphs, which could play an important role in the function of Nab2 and its role in RNAPIII transcription.

The zinc finger domain of Nab2 is highly conserved in evolution and each Nab2 orthologue contains at least 3-5 of these CCCH-type zinc fingers (ZnF, see below Fig. 36 and Leung et al. (2009)). The zinc fingers display high homology to each other and are thought to coordinate one Zn^{2+}-ion by three cysteine residues and one histidine (Brockmann et al., 2012). In Nab2, the last three zinc fingers have been extensively studied and their role in poly(A)-binding is well established (Brockmann et al., 2012; Kelly et al., 2010; Kelly et al., 2007). In contrast, the first four zinc fingers are only weakly binding to poly(A) RNA and are most probably not the primary domain required to fulfill Nab2's functions in poly(A) tail length control and mRNA export - though they are essential (Marfatia et al., 2003).

Recognition of RNA by CCCH-type ZnFs is most likely similar as described for the human Tis11d (Hudson et al., 2004). This factor is an ARE-binding (AU-rich element) protein involved in regulating mRNA turnover and specifically binds to RNA with a tandem CCCH-type zinc finger domain (Brockmann et al., 2012; Hudson et al., 2004). The binding to RNA is mediated via a combination of electrostatic and hydrogen-bonding interactions with additional stacking of RNA bases between conserved aromatic amino acid side chains in an intercalative manner (Hudson et al., 2004). Interestingly, an overlay of a zinc finger of Tis11d and ZnF 5 of Nab2 showed very high similarity in the three-dimensional structure, suggesting a similar recognition mode of RNA by Nab2 (Brockmann et al., 2012). Also, an analogous RNA recognition mode was found for the orthologue of Nab2 in *Chaetomium thermophilum*

(Kuhlmann et al., 2013). The purine ring of adenosine stacks against an aromatic side chain and overall the RNA seems to be buried in a positively charged grove built up by Znf 3-5 (Kuhlmann et al., 2013).

Other proteins involved in RNAPII and RNAPIII transcription contain single or arrays of zinc finger modules that mediate DNA, RNA, or even protein-protein interactions. For example TFIIB has an N-terminal zinc finger that is necessary for binding to Tbp and efficient recruitment of RNAPII-TFIIF to the promoter (Buratowski and Zhou, 1993). On the other hand, TFIIIA contains an array of nine zinc fingers in most organisms that are necessary to bind to the 5S rDNA, more specifically to the ICR, and the 5S rRNA itself (Rothfels et al. (2007) and reviewed in Layat et al. (2013)). As the first four zinc fingers in Nab2 only contain a moderate affinity to poly(A) RNA (Marfatia et al., 2003), they could either be necessary to bind to nascent RNAPIII transcripts in a specific or non-specific manner, RNAPIII itself, or mediate the TFIIIB stabilization on promoter DNA by interaction with TBP and Brf1, which also has a zinc finger domain in its very N-terminus (Buratowski and Zhou, 1992). This is in accordance with our finding of the *in vitro* interaction between the first four zinc fingers of Nab2, potentially together with the RGG domain, and RNAPIII (see Results, 3.4, Fig. 18). Furthermore, it is crucial to investigate whether TFIIIB subunits can interact with this or another domain of Nab2 *in vitro*, as full length Nab2 interacts with the TFIIIB subunit Brf1 *in vivo* and with Tbp *in vitro* (see Results, 3.7.3, Fig. 30 and 3.7.4, Fig. 31). More detailed experiments regarding the interacting domains of Nab2 with TFIIIB and RNAPIII could lead to a better understanding of the molecular interplay of Nab2 with the RNAPIII transcription apparatus in *S. cerevisiae*.

Considering the importance of the zinc fingers for Nab2 function in the cell, it was interesting that one mutation in *nab2-34* leads to a histidine to proline mutation in the fourth zinc finger. As the zinc ion is important for the overall structure and function of the CCCH-type ZnF module (Hudson et al., 2004), this mutation may lead to the disruption of the ZnF domain in general and could cause the *nab2-34* phenotype when shifted to the restrictive temperature. Another mutation in the sixth zinc finger module of Nab2 could lead to a similar defect (R438C mutation, see Results, 3.2.1, Fig. 14). Although all conserved residues of the ZnF are present, the additional cysteine residue neighboring the first cysteine of ZnF six may disturb the correct complexation of the central zinc ion and hence destabilize the ZnF module at higher temperatures. The ability of the mutant Nab2 to bind zinc atoms could be tested and compared to wild-type Nab2 using different techniques, such as ICP-OES (inductively coupled plasma optical emission spectrometry, Jobst et al. (2010)) or UV-VIS spectroscopy (Lottspeich and Engels, 2012). Furthermore, CD spectroscopy (circular dichroism) of Nab2-34 and Nab2 could provide initial insight in the structural changes of the mutant at the

permissive/ restrictive temperature (Lottspeich and Engels, 2012).

To identify the residue changes that are responsible for the mutant phenotype, individual or combinations of mutations in Nab2-34 should be introduced into the wild-type protein and subsequently tested for a phenotype.

4.1.2 *NAB2-AID*: Depletion with a plant hormone

As an alternative approach to impair the function of Nab2 without applying drugs or toxic compounds, we used the AID-degron system. This system employs the natural, phenylalanine derived compound auxin to deplete Nab2 from cells (see Results, 3.2.2, Fig. 15). Indeed, Nab2 could be depleted and the mutant showed comparable phenotypes as the *nab2-34* mutant in growth and an *in vitro* transcription assay. Unfortunately, ChIP experiments were not reproducible using this system (data not shown). The difference to regular ChIP assays conducted in the lab was that the auxin was solved in DMSO and cells were treated with this solution. An effect of the DMSO on cross-linking would not be expected, as it does not seem to have any influence on the assay in *e.g. S. pombe* (Kanke et al., 2011) and the negative control in our assay varied as well. One potential explanation would be that in some cases, residual Nab2, which was not degraded upon degron activation (see Results, 3.2,2, Fig. 15D), could still function on RNAPIII genes and, thus, the ChIP assay could have revealed varying results. To address this problem, future studies should put an emphasis on the complete and rapid degradation of the target protein. Therefore, one could use the improved toolkit for the AID degron (Morawska and Ulrich, 2013), which offers an optimized AID-tag along with new tagging strategies (N-terminal tagging and new selection markers). Other options would be the use of alternative auxin-responsive (IAA) proteins with shorter half-lives that promote enhanced degradation or the fusion of multiple tandem AID sequences to the protein of interest (Havens et al., 2012; Kubota et al., 2013).

Nevertheless, having generated the temperature-sensitive *nab2-34* mutant, we were able to investigate the potential function of Nab2 in RNAPIII transcription.

4.2   Nab2 functions in RNAPIII transcription

4.2.1   Nab2 and RNAPIII transcription initiation

Using the novel allele, we substantiated our genome-wide findings, as we were able to demonstrate that full occupancies of Nab2 and RNAPIII on RNAPIII-transcribed genes depend on each other. Furthermore, a direct interaction of Nab2 with the polymerase was observed, pointing towards a direct function in RNAPIII transcription. In addition, we showed

that Nab2 is necessary for wild-type levels of tRNAs and other ncRNAs and indeed functions directly in RNAPIII transcription. Studying the molecular function of Nab2 in this process, we found that Nab2 stabilizes the transcription initiation factor TFIIIB on DNA and is therefore needed for transcription initiation of RNAPIII (see Fig. 35, upper part). Importantly, this can also explain the effects observed for RNAPIII in the *nab2-34* mutant, as TFIIIB has key functions in recruiting RNAPIII to the respective gene and is necessary for transcription at all three types of RNAPIII promoters (Kassavetis et al. (1990) and Dieci et al. (2007); Geiduschek and Kassavetis (2001) and references therein).

The initial results of the reinitiation assay can be explained when considering the proposed stabilization function of Nab2 on TFIIIB *in vitro*, as well as the physical interaction of Nab2 with the polymerase. Once Tbp is recruited to the target gene via a TATA box or the interaction with Brf1 / TFIIIC (Dumay-Odelot et al., 2002; Male et al., 2015), Nab2 could form a much tighter pre-initiation complex (PIC) together with TFIIIB and RNAPIII that subsequently allows the synthesis of the 17-mer transcript. Hypothetically, this DNA-RNA-protein complex might be more stable in the presence of Nab2 and, hence, less RNAPIII might dissociate from the gene after 17-mer synthesis and thus less signal would be expected in contrast to a repetitive reinitiating and aborting polymerase. This theory is supported by the observation that only a few 17-mer transcripts were elongated in the absence of Nab2 and presence of heparin. This illustrates that a big proportion of 17-mers was released before elongation occurred and that the polymerase was eventually sequestered by heparin.

A second, simpler explanation for less 17-mers in this assay is enhanced elongation of the transcripts in the presence of Nab2. As the generated products may be distributed everywhere between the 17-mer and full length transcript, quantification of these intermediate products is difficult in this setup.

Nonetheless, it is necessary to show that initial 17-mer formation is more efficient in the presence of Nab2 and that switching to productive elongation is more effective.

4.2.2 **Nab2 may have a role in 'facilitated recycling'**

The stabilization of TFIIIB on its promoter DNA and the interaction with Nab2 also suggests a second role of Nab2 in RNAPIII transcription. As tRNAs and other ncRNAs are required in high amounts in growing cells and the fact that initiation and PIC formation is the rate limiting step in RNAPIII transcription, a mechanism called facilitated recycling was proposed (see Introduction, 1.4.6, Fig. 8, and Dieci and Sentenac (1996)). Such a process in which the polymerase is reloaded quickly on the same gene locus (gene commitment) is a prerequisite to achieve the observed high synthesis rates especially for longer genes, such as the *SCR1*

and *SNR6* loci, as well as for tRNA genes (Dieci et al., 2002; Dieci and Sentenac, 1996; Ferrari et al., 2004). Recycling of the RNAPIII enzyme seems to be a conserved mechanism, as it was also observed in humans to protect RNAPIII from repression by Maf1 (Cabart et al., 2008).

Nab2 could positively influence the facilitated recycling by fixing TFIIIB to the promoter of the gene being transcribed by RNAPIII. When transcription is terminated, Nab2 could interact with the polymerase and together with TFIIIB recruit it to the same gene to directly undergo another round of transcription (Fig. 35; an artistic view of the initiation/reinitiation mechanism of RNAPIII is presented in Sentenac and Riva (2013)). Similarly, hnRNP R interacts with scaffold components of the RNAPII transcription machinery (Mediator, Tbp and TFIIH) and facilitates RNAPII reinitiation on the c-Fos gene in higher cells (Fukuda et al., 2013). To reload RNAPIII on the target gene, TFIIIB and Nab2 would not need to establish long distance interactions with RNAPIII. It has been described that transcription initiation factors and other auxiliary proteins introduce kinks into the DNA to be transcribed and thus a loop may be formed (Braun et al., 1992; Grove et al., 1999; Leveillard et al., 1991). This would greatly reduce the spatial distance of the terminator and the promoter, facilitating a directed DNA 'hopping' to the promoter by the transcription apparatus. More general, it would be interesting whether the proposed loop formation is a feature required for facilitated recycling. Therefore, a physically immobilized and linear template could be used for transcription assay under single and multiple round transcription conditions. If a sterical rearrangement is crucial for the facilitated recycling, one should observe a lower reinitiation rate as compared to a non-immobilized template.

'Gene looping' was observed in yeast and mammalian cells and is a common mechanism for transcriptional activation of genes, high level RNAPII transcription and efficient recycling. The formation of a loop thereby juxtaposes promoter and terminator regions spatially, which is especially important for long genes. (Ansari and Hampsey, 2005; O'Reilly and Greaves, 2007; O'Sullivan et al., 2004; Tan-Wong et al., 2008; Yudkovsky et al., 2000). This mechanism involves the mediator complex, TFIIB, TFIIH and other basic transcription initiation factors, as well as parts of the 3'-end processing machinery (*e.g.* the cleavage and polyadenylation factor) (Calvo and Manley, 2003; He et al., 2003; Singh and Hampsey, 2007; Yudkovsky et al., 2000). For example, TFIIB and the co-activator PC4 / Sub1 interact with the 3'-end processing machinery, thereby creating a scaffold for gene looping (Calvo and Manley, 2005).

Analogous, Nab2 could promote gene looping on RNAPIII-transcribed genes by stabilizing TFIIIB and the pre-initiation complex. This could either favor gene activation or facilitated recycling on target genes (Fig. 35, bent not shown).

In addition, the stability of TFIIIB on the DNA in the presence of Nab2 should be

tested in further detail. To this end, magnetic traps could be used, in which a TFIIIB-Nab2 complex would be assembled on a fixed DNA and stability could be tested by twisting or stretching the DNA (Lionnet et al., 2012). As TFIIIB induces a strong kink in the bound DNA, one could then test whether Nab2 makes the complex more resistant against exogenously applied force, additionally arguing for a stabilization function of Nab2 on TFIIIB.

4.2.3 Nab2 and its potential RNAPIII binding site

Using tandem affinity purification, we identified an interaction of Nab2 and the RNAPIII enzyme. This was confirmed by *in vitro* pull-down assays and we could show that this interaction is direct and involves the first four zinc fingers of Nab2. Interestingly, Nab2 was also found to bind to RNAPII *in vitro* but needed the RGG domain in addition. In contrast, no RNAPI interaction was observed. This raised the question, which RNAPIII subunit can interact with Nab2 and whether Nab2 binds to the same protein in RNAPII and RNAPIII. Table 31 displays all RNA polymerase subunits, their homologies, as well as the basic transcription factors from *S. cerevisiae*.

Inspection of this table revealed that there is no subunit that is only shared by RNAPII and RNAPIII. Either a subunit is shared by all polymerases or at least by RNAPI and RNAPIII (*e.g.* Rpb6 for all polymerases or AC40 for RNAPI and RNAPIII). Hence, the interaction of Nab2 with RNAPII and RNAPIII could be mediated via completely different proteins on one side or by proteins that show a high degree of homology on the other side. A candidate for the first hypothesis would be Rpc31, which shows neither a paralogue nor a homologue among the different polymerases. Candidates for the second possibility are all RNAPIII subunits marked with an asterisk in Table 31. Some of them also show homology to RNAPI subunits, making them rather unlikely candidates, such as Rpa49 that is functionally and structurally related to the Rpc37/Rpc53 subcomplex (Beckouet et al., 2008; Landrieux et al., 2006). Another candidate is Rpc82, which shows homology to TFIIEα, but no direct homologue for RNAPI is known.

As we could also show that Nab2 binds to TFIIIB, one could argue that Nab2 may interact similarly with the RNAPII pre-initiation complex or general transcription factors to facilitate RNAPII recruitment (reviewed in Naar et al. (2001)).

To finally be able to draw a conclusion, the GST-pulldowns of Nab2 and RNAPIII should be repeated to define the minimal RNAPIII-binding domain of Nab2. Here, particular emphasis should be put on the first four zinc fingers of Nab2 and deletion constructs of those. Furthermore, co-purification of RNAPIII / TFIIIB with an additional, but truncated copies of Nab2 (Nab2-TAP) will reveal the minimum binding domain *in vivo*.

Table 31: Yeast RNA Polymerase Subunits, Homology and Transcription Factors in *S. cerevisiae*

RNAPI	RNAPII	RNAPIII	Function
Core			
Rpa190	Rpb1	Rpc160	Active center
Rpa135	Rpb2	Rpc128	
AC40	Rpb3	Rpc40 (AC40)	[1]
AC19	Rpb11	Rpc19 (AC19)	
Rpb6	Rpb6	Rpb6 (ABC23)	
Rpb5	Rpb5	Rpb5 (ABC27)	
Rpb8	Rpb8	Rpb8 (ABC14.5)	[2]
Rpb10	Rpb10	Rpb10 (ABC10β)	
Rpb12	Rpb12	Rpb12 (ABC10α)	
Rpa12.2	Rpb9 and TFIIS	Rpc11*	RNA cleavage
Rpa14	Rpb4	Rpc17*	Initiation complex formation
Rpa43	Rpb7	Rpc25*	
General transcription factors			
Rpa49	TFIIFα	Rpc37*	Initiation/Termination[3]
Rpa34.5	TFIIFβ	Rpc53*	Initiation/Termination[3]
	TFIIEα	Rpc82*	Open complex formation and stabilization
Rpa49	TFIIEβ	Rpc34*	
		Rpc31*	
TBP	TBP	TBP	DNA binding
	TBP-assoc. factors		
Rrn7	TFIIB (Sua7)	Brf1	TBP/polymerase binding
		Bdp1	
	Mediator		Transcriptional coactivator
	TFIIH		PIC formation
		TFIIIC	A/B box binding

[1]: Core subunits of RNAPIII. [2]: subunits shared by all polymerases (ABC). The number at ABC represents the molecular weight in kDa. [3]: Termination was shown for RNAPIII (Arimbasseri and Maraia, 2015). *: These subunits are RNAPIII specific. However, some show homologies to general RNAPII transcription factors. This table was generated using data from Geiduschek and Kassavetis (2001); Vannini and Cramer (2012) and SGD (www.yeastgenome.org).

### 4.2.4 Nab2 may serve in transcription elongation of RNAPIII

Poly(A) RNA-binding is the best investigated property of Nab2, since its discovery more than two decades ago (Anderson et al., 1993). In the course of this study we additionally identified that Nab2 binds to newly synthesized but yet not processed RNAPIII transcripts *in vivo* (see Results, 3.5, Fig. 19). Therefore, it is very likely that binding occurs already during or shortly after transcription of the corresponding gene. Furthermore, Nab2 localizes to the whole gene body of *SCR1* in the ChIP profiles (see Results, 3.7.1, Fig. 27). Thus, Nab2 may be needed

for transcription elongation of RNAPIII, comparable to the earlier mentioned THO complex (Chavez et al., 2000) or Npl3 (Bucheli and Buratowski, 2005; Deka et al., 2008) in RNAPII transcription. Alternatively, Nab2 could function in preventing R-loops, similar to what was found for the TREX and THSC complex in RNAPII transcription (Gonzalez-Aguilera et al., 2008; Huertas and Aguilera, 2003). These R-loops (RNA-DNA hybrids with an additional displaced DNA strand) occur during *e.g.* transcription elongation and can cause genome instability and even chromosome fragility (reviewed in Aguilera and Garcia-Muse (2012)). To prevent such an event, Nab2 could bind to the nascent transcripts at the transiently opened DNA double strand (Fig. 35, lower part).

The co-transcriptional binding of Nab2 to RNAPIII transcripts could also be necessary for guiding newly synthesized RNAs to processing or degradation enzymes. For example, Nab2 could bind to oligo(dA)-tRNAs (which is a signal for tRNA degradation), similarly as to poly(A) RNA and interact with Rrp6, as described for the decay of mRNAs (Kadaba et al., 2006; Parker, 2012; Schmid et al., 2012). To investigate such a hypothetical role, RNA immunoprecipitation and subsequent sequencing of the products (RIP-Seq) could be performed with Nab2 in a RNA exosome mutant, such as the described *Δrrp6* mutant (Roth et al., 2009; Schmid et al., 2012). This mutant would be deficient in the nuclear decay of RNAs and hence cleaved products still bound by Nab2 could be identified. If cleaved 5'-leaders or intronic RNA molecules will be bound by Nab2, it would argue that Nab2 might be involved in directing the newly synthesized products from the RNA polymerase to its processing enzymes, thereby linking transcription and maturation of tRNAs and ncRNAs. A similar mechanism was described for the Nab2 Mex67-Mtr2 interaction. Here, Nab2 binds to the polyadenylated mRNA and is involved in recruiting the conserved exporter Mex67-Mtr2 (Iglesias et al., 2010). Additionally, Nab2 was described in the regulation of pre-mRNA abundance. In more detail, it was found that Nab2 can be displaced from poly(A) tails by Rrp6, which possibly leads to the degradation of the mRNA (Roth et al., 2005; Schmid et al., 2012). Therefrom, it would be interesting to investigate a potential role of Nab2 in tRNA metabolism.

Regardless of the co-transcriptional binding of Nab2, it does not seem to influence processing of pre-tRNAs itself (removal of 5'-leaders, 3'-trailers, or splicing), as these or partially processed precursors did not accumulate in the *nab2-34* mutant grown at the restrictive temperatures (see Results, 3.6.1, Fig. 20). Although tRNAs are spliced in the cytoplasm (Hopper and Huang, 2015), no export defect was obvious and no precursor RNAs were accumulating over time, further opposing a role of Nab2 in the processing of tRNAs (data not shown, Lüling (2014) and pers. commun. Anita Hopper, Ohio State University,

Columbus). However, potential defects in base modification of tRNAs were not investigated in the *nab2-34* mutant and, hence, could be tested.
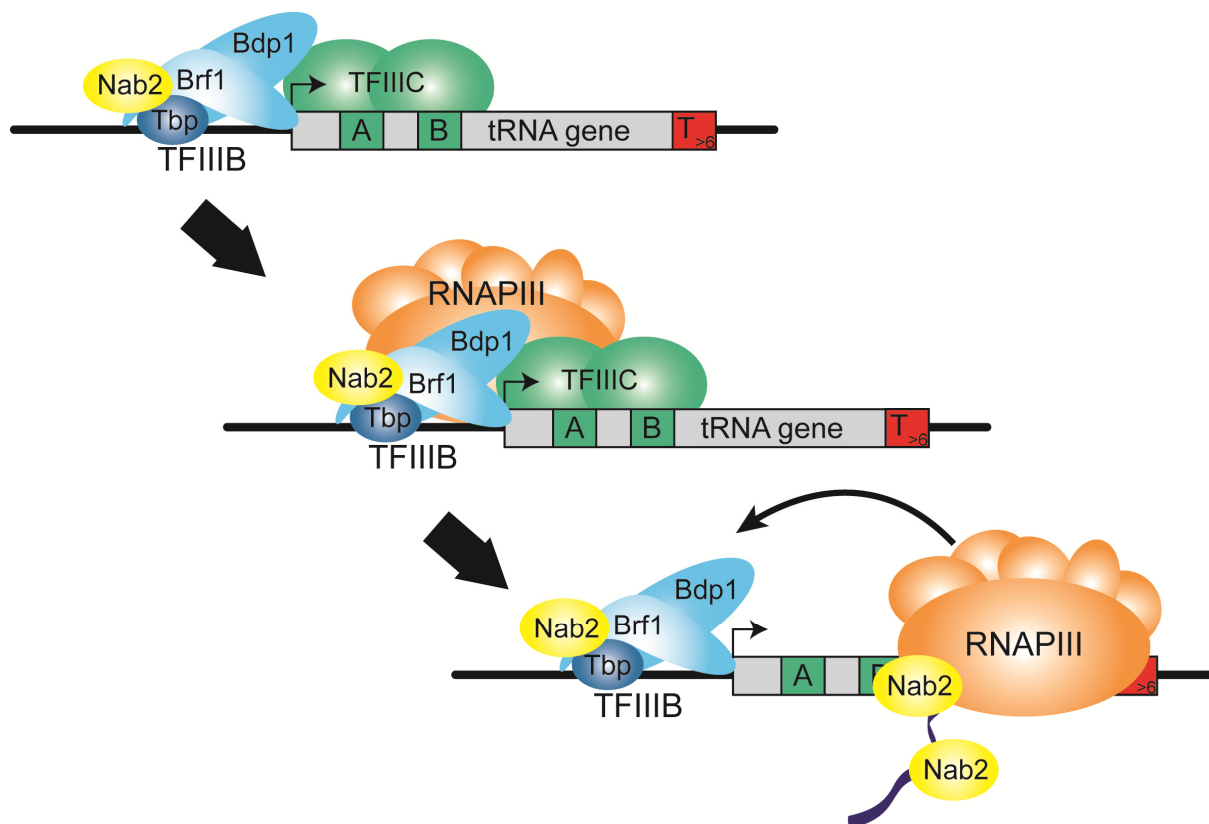
Fig. 35: Model of Nab2 functioning in RNAPIII transcription. A three-step working model of how Nab2 could function in RNAPIII-mediated transcription. In upper part, Nab2 helps to stabilize TFIIIB on its promoter DNA to assemble wild-type levels of TFIIIB. Then Nab2 might help to recruit RNAPIII to the transcription initiation site together with TFIIIB and TFIIIC (middle part). Finally, Nab2 binds to newly, non-processed tRNA and other ncRNA transcripts and may travel with the polymerase through the gene (lower part). On the other hand, Nab2 could play a role in reinitiation of transcription, by stabilizing TFIIIB on the DNA and thereby favoring facilitated recycling of RNAPIII.

4.3 'Gene gating' by tethering Nab2 to nuclear pores?

During the last decades, a working model was developed in which actively transcribed genes are relocated to the nuclear pore to efficiently link transcription to mRNA export (see Introduction, 1.2.2 and Blobel (1985); Burns and Wente (2014)). This model was termed 'gene gating' and was not only described in yeast, but examples have been identified in many higher cells (Burns and Wente (2014) and references therein). Interestingly, the nuclear periphery marks a mostly repressive environment for gene expression. Contrary, the NPCs (nuclear pore complexes) represent active zones of transcription (Dilworth et al., 2005; Ishii et al., 2002). As an example, the inducible genes *GAL1* or *HSP104* are relocated to the

NPC for maximal transcriptional output in *S. cerevisiae* upon activation and require special nucleoporins at the nuclear periphery (detailed in Burns and Wente (2014) and Steglich et al. (2013)). Of course, this relocalization is also dependent on other factors, such as the chromatin or transcriptional status of the surrounding genome (Brickner and Walter, 2004; Casolari et al., 2004). In addition, genome-wide data from *S. cerevisiae* showed that a variety of Nups associate with many active RNAPII genes (Casolari et al., 2004; Schmid et al., 2006).

Besides the fact that overall knowledge of genome organization is still poor, even less is known about 'gene gating' in RNAPIII gene expression. One study conducted in *C. elegans* revealed that knock-down of NPP-13 (the homologue of the vertebrate Nup93) leads to a maturation defect of nearly all snoRNAs transcribed by RNAPIII (Ikegami and Lieb, 2013). Although being no proof for a direct gene gating mechanism in RNAPIII transcription, it could demonstrate the involvement of Nups in RNAPIII transcription.

Another very recent study by Iwasaki and colleagues identified an interaction of the kleisin subunit of condensin with Tbp in fission yeast (Iwasaki et al., 2015). When Tbp was associated with condensin, actively transcribed RNAPIII genes were relocated to the centromeres of chromosomes at the nuclear membrane. Whether this is in spatial proximity to NPCs was not investigated.

Interestingly, it was shown recently that tDNAs are relocated to the NPCs during their peak expression in M phase of *S. cerevisiae* in a Los1 (a major tRNA exportin, see Introduction, 1.5.2) dependent manner (Chen and Gartenberg, 2014). Furthermore, it was shown that this relocation connects RNAPIII transcription with pre-tRNA export, but did not affect RNAPIII association with its genes or the transcriptional output in general. Moreover, it was hypothesized that relocation by the transcribing RNAPIII machinery to NPCs could be a mechanism to prevent collisions of DNA replication forks (Chen and Gartenberg, 2014).

It is known that Nab2 interacts with the nuclear pore associated protein Mlp1 via physical contacting the N-terminal domain of Nab2 (see Introduction, 1.2.2, Fig. 2; 1.3 and Fasken et al. (2008); Grant et al. (2008)). Thus, Nab2 is thought to be important for linking mRNA processing to nuclear export. Having in mind that Nab2 is interacting with TFIIIB and RNA polymerase III directly and is involved in stabilizing TFIIIB to promoter DNA, one might hypothesize whether Nab2 can also interact with Mlp1 when bound to TFIIIB. Thus, Nab2 could hypothetically function in linking active transcription of RNAPIII to export of tRNAs and other ncRNAs, such as the *SCR1* RNA, by relocating actively transcribed genes to the NPC.

4.4   Coupling of RNAPII and RNAPIII transcription systems

In contrast to higher organisms, it was shown that RNAPII and classical RNAPII transcription factors do not occupy RNAPIII genes nor their promoter areas in the budding yeast *S. cerevisiae* (Barski et al., 2010; Raha et al., 2010; Venters et al., 2011). Therefore, the transcription systems are considered to be independent of each other, despite the presence of some RNAPII regulators on RNAPIII genes, *e.g.* Yap6 or Reb1 (Venters et al., 2011). In our genome-wide analysis, we observed that Nab2 occupied genes transcribed by both transcription systems (RNAPII and RNAPIII), but only with the corresponding RNA polymerase.

As Nab2 is the first mRNP biogenesis factor identified to play a role in RNAPIII transcription, it will be of great interest to investigate whether more proteins involved in RNAPII transcription or metabolism are having a second function in RNAPIII transcription. Some examples have been described already, such as Dst1 or Sub1 in yeast (Ghavi-Helm et al., 2008; Tavenet et al., 2009). Sub1, for example, is involved in transcription elongation of RNAPII and 3'-end processing of mRNA (Conesa and Acker (2010) and references therein) and was also shown to function in RNAPIII transcription (Tavenet et al., 2009; Wang and Roeder, 1998). Dst1 / TFIIS, as a second example, is an important protein in RNAPII transcription, as it is required for stimulation of the intrinsic transcript cleavage activity of RNAPII (Qian et al., 1993). As Rpc11 mediates this cleavage activity for the RNAPIII enzyme (Chedin et al., 1998), it was surprising that Dst1 also occupies RNAPIII-transcribed genes (Carriere et al., 2012; Ghavi-Helm et al., 2008; Venters et al., 2011). However, Ghavi-Helm and colleagues showed that Δ*dst1* mutant cells showed reduced tRNA synthesis *in vivo* and that Dst1 may influence start site selection of RNAPIII transcription (Ghavi-Helm et al., 2008).

We observed that Nab2 and Rpc160 together show occupancies on PCGs that are close to tRNA genes. Here, Nab2 and RNAPIII could be necessary for barrier formation against heterochromatin spreading during RNAPII transcription and co-transcriptional RNA processing. The general ability of RNAPIII and TFIIIC in barrier formation is described for single loci and genome-wide (see Introduction, 1.4.5; Noma et al. (2006); Scott et al. (2007)). Moreover, transcription activity could be regulated by the presence of RNAPIII and Nab2, similar to what was described for TFIIIC (Kleinschmidt et al., 2011).

Hence, proteins involved in RNAPII and RNAPIII transcription and metabolism could coordinate both transcription systems. They could act synergistically, thereby generating important junction points between the two transcription systems.

4.5   Conservation of Nab2 in higher eukaryotes

As outlined in the introduction, Nab2 is highly conserved from yeast to humans (see Introduction 1.3.3). An alignment of the Nab2 orthologues from different organisms is presented in Figure 36. Although all proteins differ in size and also in domain composition, some basic features are the same in all analyzed organisms. For example, many orthologues share a nuclear localization sequence (NLS). It is needed for the repetitive import of Nab2 after each round of mRNA export to the cytoplasm (Kelly et al., 2012). Besides the NLS, all Nab2 orthologues and splice variants contain an array of zinc fingers, varying from three zinc fingers in *S. pombe* to seven zinc fingers in *S. cerevisiae* (see Discussion, 4.5, Fig. 36 and Grenier St-Sauveur et al. (2013); Guthrie et al. (2009); Kelly et al. (2014); Leung et al. (2009)). When these zinc fingers are aligned (Fig. 36) they show high conservation. This is due to two characteristics: (i) all zinc fingers are CCCH-type complexing one zinc atom and (ii) neighboring amino acids are fairly conserved.

Interestingly, the first and the last two zinc fingers of the budding yeast Nab2 are very well conserved, whereas the fourth and fifth zinc fingers are not conserved in higher eukaryotes and modestly in other fungi species (Fig. 36 and Fig. A4). The conservation of the last zinc finger module is not surprising, as it is important for the poly(A) tail recognition in yeast and higher organisms (Kelly et al., 2014; Kelly et al., 2007; Pak et al., 2011). For example, poly(A) RNA binding was shown for the *Drosophila* orthologue (dNab2), as well as for the human and rat orthologue of Nab2 (ZC3H14) (Kelly et al., 2007; Pak et al., 2011). In addition, Nab2 is required for correct poly(A) tail length in *D. melanogaster* and most probably also in humans, showing that the most well described functions of Nab2 in gene expression of mRNAs are conserved throughout evolution (Kelly et al., 2014; Pak et al., 2011).

As we have identified a novel function for Nab2 in RNAPIII transcription, it would be of great interest to know, whether this function is conserved in a similar way across different organisms. An argument supporting this is the good conservation of the first zinc finger array, which we found to interact with the RNAPIII *in vitro*. The fourth and fifth zinc finger may be repetitive and not needed in other cells, as yeast has the longest array of zinc fingers within all orthologues (see Fig. 36, Introduction, 1.3, Fig. 3, and Grenier St-Sauveur et al. (2013)).

To investigate the potential conservation of Nab2's role in RNAPIII transcription, experiments in higher cells are required. As a starting point ChIP-Seq and single ChIP experiments of Nab2 and RNAPIII in Drosophila or human cell lines will generate genome-wide data that could be used to judge, whether Nab2 occupies RNAPIII-transcribed genes.
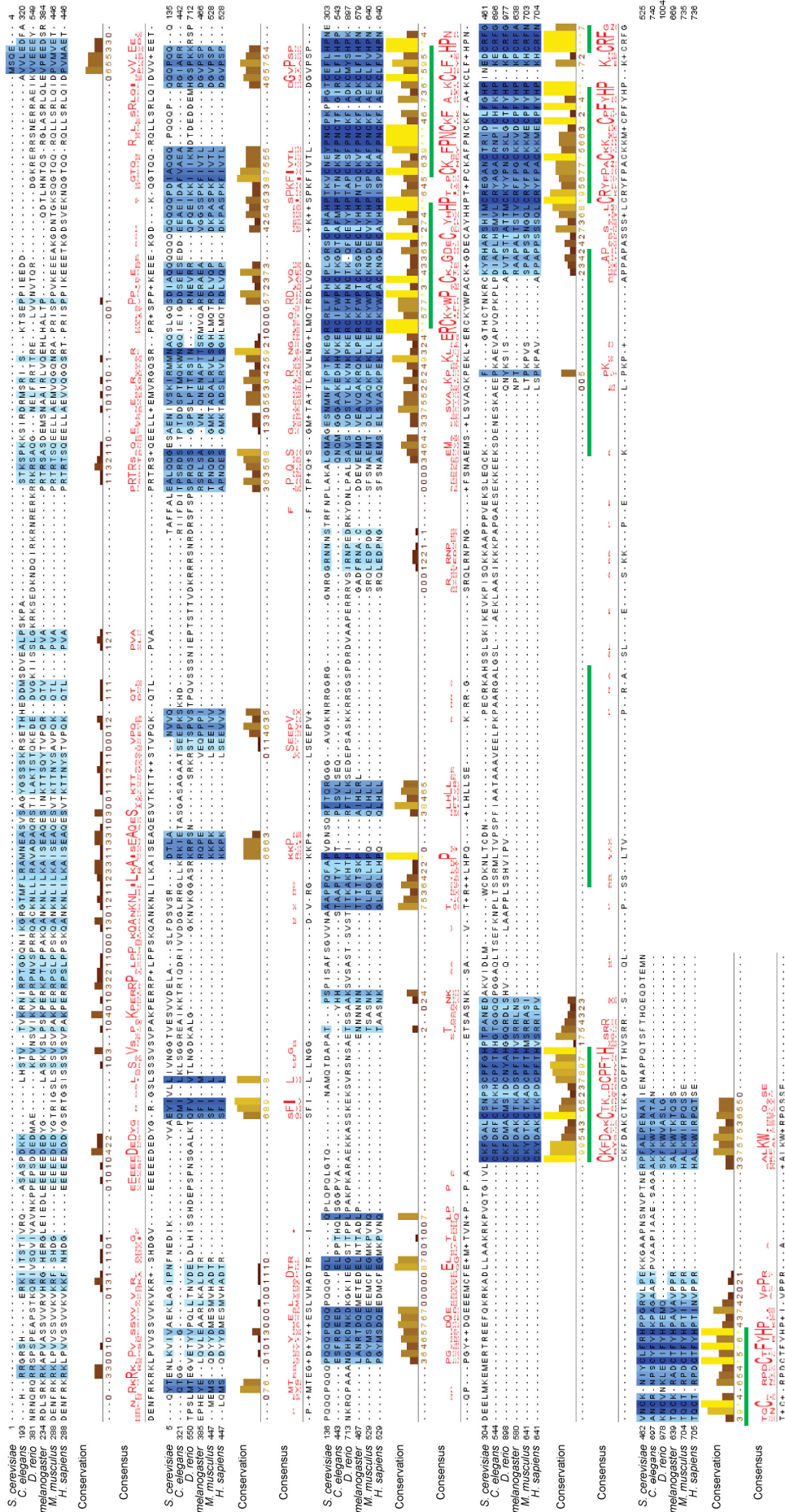
Fig. 36: Alignment of Nab2 and its orthologues in different species. An alignment of Nab2 and its orthologues from *Caenorhabditis elegans* (sut-2), *Danio rerio* (ZC3H14), *Drosophila melanogaster* (dNab2), *Mus musculus* (Msut-2) and *Homo sapiens* (ZC3H14) is shown. Different shades of blue indicate the degree of conservation between the different organisms. The degree of conservation (in yellow and brown), as well as the consensus sequences (red letters) are indicated below the alignments. Remarkably, the C-terminal zinc fingers are highly conserved throughout species. Green bars mark the seven zinc finger in *S. cerevisiae* Nab2. Note that, the very N-termini of the Nab2 orthologues

are not shown, as they have no homology to the *S. cerevisiae* Nab2. The alignment file was generated with Clustal Omega multiple sequence alignment software (Sievers et al., 2011) and modified using Jalview2 software (Waterhouse et al., 2009).

Furthermore, immunoprecipitation of RNAPIII or the Nab2 orthologue would be useful to study their potential physical interaction. For this, the generated ZC3H14 antibody will be of great use, as it detects native as well as denatured ZC3H14.

4.6 Proteome-wide studies failed to purify Nab2 with RNAPIII so far

In a recent study, Nguyen and colleagues performed purifications of RNAPIII after *in vivo* crosslinking to identify the proteins associated with RNAPIII in yeast (Nguyen et al., 2015). Although identifying more proteins than earlier studies (Collins et al., 2007; Gavin et al., 2006), still several RNAPIII transcription effectors could not be retrieved, such as Nhp6, Yox1, Fkh1, Reb1, Yap6, or most of TFIIIC (Kruppa et al., 2001; Venters et al., 2011).

This was also the case for Nab2. Other proteins were only hardly detected in one replicate of the purifications, *e.g.* Dst1 or Sub1 (Ghavi-Helm et al., 2008; Tavenet et al., 2009). This may be due to inefficient cross-linking as described earlier (Kurdistani et al., 2002), which could result in the dissociation of less tightly bound proteins as compared to Maf1. Using a whole cell or nuclear lysate instead of a chromatin preparation (more protein), a different cross-linker (more cross-links), or different purification buffers could increase the fraction of cross-linked proteins involved in RNAPIII transcription. Especially the extraction buffer after cross-linking seemed to have a big influence on the outcome of the purification quality (see Fig. 1A of Nguyen et al. (2015)). Optimizing these steps should increase the number or specificity of identified proteins.

4.7 Conclusions

The correct and regulated expression of genes is a crucial process in living organisms. Extensive research was conducted to unravel the basic mechanisms of how RNA polymerases function in many different organisms. Starting from the identification of the sigma factors in bacteria up to genome- and transcriptome-wide sequencing data for RNA polymerases, their transcription factors or mRNP biogenesis protein, many fascinating details were discovered (Baejen et al., 2014; Burgess et al., 1969; Mayer et al., 2010; Meinel et al., 2013). Beside the well investigated RNAPII, RNAPI and RNAPIII were neglected over years,

as they only have small sets of genes to be transcribed and only few mandatory and basic regulating factors. Hence, details of these transcription systems, including a high-resolution three-dimensional structure of RNAPIII, are still lacking.

Applying genome-wide analysis of the Nab2 binding to the yeast genome, we identified the very first mRNP biogenesis factor involved in RNAPIII transcription in the present study. Furthermore, analysis of the published CRAC data set of Tuck and colleagues revealed transcriptome-wide binding of Nab2 to precursors of tRNAs and other RNAPIII transcripts (Tuck and Tollervey, 2013). To unravel the need of Nab2 binding to newly synthesized RNAs, as a potential elongation factor, to monitor correct RNA modifications, or to prevent the already mentioned R-loops will contribute to the understanding of RNA-binding proteins in transcription.

Additionally, we aimed to dissect the molecular mechanism of how Nab2 can function in the transcription of RNAPIII genes. Our study revealed Nab2 as a novel factor required for the initiation and potentially also reinitiation of RNAPIII transcription in the budding yeast *S. cerevisiae.* Hence, it will essential to test whether this function is also conserved in other organisms, for example *D. melanogaster* or *H. sapiens*, in which Nab2 was shown to be important for poly(A) RNA-binding.

Moreover, it will be interesting to study whether other factors of the RNAPII gene expression machinery or mRNP related proteins might also have a second role in the transcription, processing, or export of RNAPIII transcripts.

Finally, the new role for Nab2 in RNAPIII transcription may also point towards intertwined RNAPII / RNAPIII transcription systems. Therefore, proteins such as Nab2, Dst1, or Sub1 could coordinate the two transcription systems. Furthermore, downstream processes (processing, export of RNA) might be linked to efficiently regulate and coordinate overall gene expression. Investigating the potential coordination of these important cellular pathways could lead to a better understanding of global gene expression in eukaryotic cells.

5. References

Acker, J., C. Conesa and O. Lefebvre (2013). 'Yeast RNA polymerase III transcription factors and effectors.' *Biochim Biophys Acta* **1829**(3-4): 283-295.

Aebi, M., G. Kirchner, J.-Y. Chen, U. Vijayraghavan, A. Jacobson, N. C. Martin and J. Abelson (1990). 'Isolation of a Temperature-sensitive Mutant with an Altered tRNA Nucleotidyltransferase and Cloning of the Gene Encoding tRNA Nucleotidlytransferase in the Yeast *Saccharomyces cerevisiae*.' *J Biol Chem* **265**(27): 16216-16220.

Aguilera, A. and T. Garcia-Muse (2012). 'R loops: from transcription byproducts to threats to genome stability.' *Mol Cell* **46**(2): 115-124.

Aitchison, J. D., G. Blobel and M. P. Rout (1996). 'Kap104p: A Karyopherin Involved in the Nuclear Transport of Messenger RNA Binding Proteins.' *Science* **274**(5287): 624-627.

Aitchison, J. D. and M. P. Rout (2012). 'The yeast nuclear pore complex and transport through it.' *Genetics* **190**(3): 855-883.

Amrani, N., M. Minet, M. Le Gouar, F. Lacroute and F. Wyers (1997). 'Yeast Pab1 interacts with Rna15 and participates in the control of the poly(A) tail length in vitro.' *Mol Cell Biol* **17**(7): 3694-3701.

Anderson, J. T., S. M. Wilson, K. V. Datar and M. S. Swanson (1993). 'NAB2: a yeast nuclear polyadenylated RNA-binding protein essential for cell viability.' *Mol Cell Biol* **13**(5).

Anderson, P. and P. Ivanov (2014). 'tRNA fragments in human health and disease.' *FEBS Lett* **588**(23): 4297-4304.

Ansari, A. and M. Hampsey (2005). 'A role for the CPF 3'-end processing machinery in RNAP II-dependent gene looping.' *Genes Dev* **19**(24): 2969-2978.

Apponi, L. H., S. M. Kelly, M. T. Harreman, A. N. Lehner, A. H. Corbett and S. R. Valentini (2007). 'An interaction between two RNA binding proteins, Nab2 and Pub1, links mRNA processing/export and mRNA stability.' *Mol Cell Biol* **27**(18): 6569-6579.

Arimbasseri, A. G., G. A. Kassavetis and R. J. Maraia (2014). 'Transcription. Comment on "Mechanism of eukaryotic RNA polymerase III transcription termination".' *Science* **345**(6196): 524.

Arimbasseri, A. G. and R. J. Maraia (2013). 'Distinguishing core and holoenzyme mechanisms of transcription termination by RNA polymerase III.' *Mol Cell Biol* **33**(8): 1571-1581.

Arimbasseri, A. G. and R. J. Maraia (2015). 'Mechanism of Transcription Termination by RNA Polymerase III Utilizes a Non-template Strand Sequence-Specific Signal Element.' *Mol Cell* **58**(6): 1124-1132.

Arimbasseri, A. G., K. Rijal and R. J. Maraia (2013). 'Transcription termination by the eukaryotic RNA polymerase III.' *Biochim Biophys Acta* **1829**(3-4): 318-330.

Baejen, C., P. Torkler, S. Gressel, K. Essig, J. Soding and P. Cramer (2014). 'Transcriptome maps of mRNP biogenesis factors define pre-mRNA recognition.' *Mol Cell* **55**(5): 745-757.

Baltz, A. G., M. Munschauer, B. Schwanhausser, A. Vasile, Y. Murakawa, M. Schueler, N. Youngs, D. Penfold-Brown, K. Drew, M. Milek, E. Wyler, R. Bonneau, M. Selbach, C. Dieterich and M. Landthaler (2012). 'The mRNA-bound proteome and its global occupancy profile on protein-coding transcripts.' *Mol Cell* **46**(5): 674-690.

Barski, A., I. Chepelev, D. Liko, S. Cuddapah, A. B. Fleming, J. Birch, K. Cui, R. J. White and K. Zhao (2010). 'Pol II and its associated epigenetic marks are present at Pol III-transcribed noncoding RNA genes.' *Nat Struct Mol Biol* **17**(5): 629-634.

Batisse, J., C. Batisse, A. Budd, B. Bottcher and E. Hurt (2009). 'Purification of nuclear poly(A)-binding protein Nab2 reveals association with the yeast transcriptome and a messenger ribonucleoprotein core structure.' *J Biol Chem* **284**(50): 34911-34917.

Beckouet, F., S. Labarre-Mariotte, B. Albert, Y. Imazawa, M. Werner, O. Gadal, Y. Nogi and P. Thuriaux (2008). 'Two RNA polymerase I subunits control the binding and release of Rrn3 during transcription.' *Mol Cell Biol* **28**(5): 1596-1605.

Bhargava, P. (2013). 'Epigenetic regulation of transcription by RNA polymerase III.' *Biochim Biophys Acta* **1829**(10): 1015-1025.

Bhargava, P. and G. A. Kassavetis (1999). 'Abortive initiation by Saccharomyces cerevisiae RNA polymerase III.' *J Biol Chem* **274**(37): 26550-26556.

Birney, E., S. Kumar and A. R. Krainer (1993). 'Analysis of the RNA-recognition motif and RS and RGG domains: conservation in metazoan pre-mRNA splicing factors.' *Nucleic Acids Res* **21**(25): 5803-5816.

Bjork, P. and L. Wieslander (2014). 'Mechanisms of mRNA export.' *Semin Cell Dev Biol* **32**: 47-54.

Blobel, G. (1985). 'Gene gating: a hypothesis.' *Proc Natl Acad Sci U S A* **82**(24): 8527-8529.

Bobkova, E. V. and B. D. Hall (1997). 'Substrate specificity of the RNase activity of yeast RNA polymerase III.' *J Biol Chem* **272**(36): 22832-22839.

Bossie, M. A., C. DeHoratius, G. Barcelo and P. Silver (1992). 'A mutant nuclear protein with similarity to RNA binding proteins interferes with nuclear import in yeast.' *Mol Biol Cell* **3**(8): 875-893.

Bradford, M. M. (1976). 'A rapid and sensitive method for the quantitation of microgram quantities of protein utilizing the principle of protein-dye binding.' *Anal Biochem* **72**: 248-254.

Braglia, P., S. L. Dugas, D. Donze and G. Dieci (2007). 'Requirement of Nhp6 proteins for transcription of a subset of tRNA genes and heterochromatin barrier function in Saccharomyces cerevisiae.' *Mol Cell Biol* **27**(5): 1545-1557.

Braun, B. R., G. A. Kassavetis and E. P. Geiduschek (1992). 'Bending of the Saccharomyces cerevisiae 5S rRNA Gene in Transcription Factor Complexes.' *J Biol Chem* **267**(31): 22562-22569.

Breslow, D. K., D. M. Cameron, S. R. Collins, M. Schuldiner, J. Stewart-Ornstein, H. W. Newman, S. Braun, H. D. Madhani, N. J. Krogan and J. S. Weissman (2008). 'A comprehensive strategy enabling high-resolution functional analysis of the yeast genome.' *Nat Methods* **5**(8): 711-718.

Bretes, H., J. O. Rouviere, T. Leger, M. Oeffinger, F. Devaux, V. Doye and B. Palancade (2014). 'Sumoylation of the THO complex regulates the biogenesis of a subset of mRNPs.' *Nucleic Acids Res* **42**(8): 5043-5058.

Brickner, J. H. and P. Walter (2004). 'Gene Recruitment of the Activated INO1 Locus to the Nuclear Membrane.' *PLoS Biol* **2**(11): e342.

Brockmann, C., S. Soucek, S. I. Kuhlmann, K. Mills-Lujan, S. M. Kelly, J. C. Yang, N. Iglesias, F. Stutz, A. H. Corbett, D. Neuhaus and M. Stewart (2012). 'Structural basis for polyadenosine-RNA binding by Nab2 Zn fingers and its function in mRNA nuclear export.' *Structure* **20**(6): 1007-1018.

Brow, D. A. and C. Guthrie (1990). 'Transcription of a yeast U6 snRNA gene requires a polymerase III promoter element in a novel position.' *Genes & Development* **4**(8): 1345-1356.

Brun, I., A. Sentenac and M. Werner (1997). 'Dual role of the C34 subunit of RNA polymerase III in transcription initiation.' *EMBO J* **16**(18): 5730-5741.

Bucheli, M. E. and S. Buratowski (2005). 'Npl3 is an antagonist of mRNA 3' end formation by RNA polymerase II.' *EMBO J* **24**(12): 2150-2160.

Buratowski, S. (2009). 'Progression through the RNA polymerase II CTD cycle.' *Mol Cell* **36**(4): 541-546.

Buratowski, S. and H. Zhou (1992). 'A suppressor of TBP mutations encodes an RNA polymerase III transcription factor with homology to TFIIB.' *Cell* **71**(2): 221-230.

Buratowski, S. and H. Zhou (1993). 'Functional domains of transcription factor TFIIB.' *Proc Natl Acad Sci U S A* **90**(12): 5633-5637.

Burgess, R. R., A. A. Travers, J. J. Dunn and E. K. Bautz (1969). 'Factor stimulating transcription by RNA polymerase.' *Nature* **221**(5175): 43-46.

Burns, L. T. and S. R. Wente (2014). 'From hypothesis to mechanism: uncovering nuclear pore complex links to gene expression.' *Mol Cell Biol* **34**(12): 2114-2120.

Cabart, P., J. Lee and I. M. Willis (2008). 'Facilitated recycling protects human RNA polymerase III from repression by Maf1 in vitro.' *J Biol Chem* **283**(52): 36108-36117.

Calvo, O. and J. L. Manley (2003). 'Strange bedfellows: polyadenylation factors at the promoter.' *Genes Dev* **17**(11): 1321-1327.

Calvo, O. and J. L. Manley (2005). 'The transcriptional coactivator PC4/Sub1 has multiple functions in RNA polymerase II transcription.' *EMBO J* **24**(5): 1009-1020.

Carballo, E., W. S. Lai and P. J. Blackshear (1998). 'Feedback inhibition of macrophage tumor necrosis factor-alpha production by tristetraprolin.' *Science* **281**(5379): 1001-1005.

Carriere, L., S. Graziani, O. Alibert, Y. Ghavi-Helm, F. Boussouar, H. Humbertclaude, S. Jounier, J. C. Aude, C. Keime, J. Murvai, M. Foglio, M. Gut, I. Gut, M. Lathrop, J. Soutourina, M. Gerard and M. Werner (2012). 'Genomic binding of Pol III transcription machinery and relationship with TFIIS transcription factor distribution in mouse embryonic stem cells.' *Nucleic Acids Res* **40**(1): 270-283.

Carter, R. and G. Drouin (2010). 'The Increase in the Number of Subunits in Eukaryotic RNA Polymerase III Relative to RNA Polymerase II Is due to the Permanent Recruitment of General Transcription Factors.' *Molecular Biology and Evolution* **27**(5): 1035-1043.

Castello, A., B. Fischer, K. Eichelbaum, R. Horos, B. M. Beckmann, C. Strein, N. E. Davey, D. T. Humphreys, T. Preiss, L. M. Steinmetz, J. Krijgsveld and M. W. Hentze (2012). 'Insights into RNA biology from an atlas of mammalian mRNA-binding proteins.' *Cell* **149**(6): 1393-1406.

Chanarat, S., C. Burkert-Kautzsch, D. M. Meinel and K. Strasser (2012). 'Prp19C and TREX: interacting to promote transcription elongationand mRNA export.' *Transcription* **3**(1): 8-12.

Chanarat, S., M. Seizl and K. Strasser (2011). 'The Prp19 complex is a novel transcription elongation factor required for TREX occupancy at transcribed genes.' *Genes Dev* **25**(11): 1147-1158.

Chaussivert, N., C. Conesa, S. Shaaban and A. Sentenac (1995). 'Complex interactions between yeast TFIIIB and TFIIIC.' *J Biol Chem* **270**(25): 15353-15358.

Chavez, S., T. Beilharz, A. G. Rondon, H. Erdjument-Bromage, P. Tempst, J. Q. Svejstrup, T. Lithgow and A. Aguilera (2000). 'A protein complex containing Tho2, Hpr1, Mft1 and a novel protein, Thp2, connects transcription elongation with mitotic recombination in Saccharomyces cerevisiae.' *EMBO J* **19**(21): 5824-5834.

Chedin, S., M. Riva, P. Schultz, A. Sentenac and C. Carles (1998). 'The RNA cleavage activity of RNA polymerase III is mediated by an essential TFIIS-like subunit and is important for transcription termination.' *Genes & Development* **12**(24): 3857-3871.

Chekanova, J. A. (2003). 'Evidence that poly(A) binding protein has an evolutionarily conserved function in facilitating mRNA biogenesis and export.' *RNA* **9**(12): 1476-1490.

Chen, M. and M. R. Gartenberg (2014). 'Coordination of tRNA transcription with export at nuclear pore complexes in budding yeast.' *Genes Dev* **28**(9): 959-970.

Chernyakov, I., J. M. Whipple, L. Kotelawala, E. J. Grayhack and E. M. Phizicky (2008). 'Degradation of several hypomodified mature tRNA species in Saccharomyces cerevisiae is mediated by Met22 and the 5'-3' exonucleases Rat1 and Xrn1.' *Genes Dev* **22**(10): 1369-1380.

Ciganda, M. and N. Williams (2011). 'Eukaryotic 5S rRNA biogenesis.' *Wiley Interdiscip Rev RNA* **2**(4): 523-533.

Collins, S. R., K. M. Miller, N. L. Maas, A. Roguev, J. Fillingham, C. S. Chu, M. Schuldiner, M. Gebbia, J. Recht, M. Shales, H. Ding, H. Xu, J. Han, K. Ingvarsdottir, B. Cheng, B. Andrews, C. Boone, S. L. Berger, P. Hieter, Z. Zhang, G. W. Brown, C. J. Ingles, A. Emili, C. D. Allis, D. P. Toczyski, J. S. Weissman, J. F. Greenblatt and N. J. Krogan (2007). 'Functional dissection of protein complexes involved in yeast chromosome biology using a genetic interaction map.' *Nature* **446**(7137): 806-810.

Conesa, C. and J. Acker (2010). 'Sub1/PC4 a chromatin associated protein with multiple functions in transcription.' *RNA Biol* **7**(3): 287-290.

Damayanova, A. (2012). *In Vitro Analysis of the RNA Polymerase Interaction Domain in Nab2*, LMU Munich. **Master thesis**.

David, L., W. Huber, M. Granovskaia, J. Toedling, C. J. Palm, L. Bofkin, T. Jones, R. W. Davis and L. M. Steinmetz (2006). 'A high-resolution map of transcription in the yeast genome.' *Proc Natl Acad Sci U S A* **103**(14): 5320-5325.

Deka, P., M. E. Bucheli, C. Moore, S. Buratowski and G. Varani (2008). 'Structure of the yeast SR protein Npl3 and Interaction with mRNA 3'-end processing signals.' *J Mol Biol* **375**(1): 136-150.

Deng, J., R. N. Ptashkin, Y. Chen, Z. Cheng, G. Liu, T. Phan, X. Deng, J. Zhou, I. Lee, Y. S. Lee and X. Bao (2015). 'Respiratory syncytial virus utilizes a tRNA fragment to suppress antiviral responses through a novel targeting mechanism.' *Mol Ther*.

Deprez, E., R. Arrebola, C. Conesa and A. Sentenac (1999). 'A subunit of yeast TFIIIC participates in the recruitment of TATA-binding protein.' *Mol Cell Biol* **19**(12): 8042-8051.

Dheur, S., K. R. Nykamp, N. Viphakone, M. S. Swanson and L. Minvielle-Sebastia (2005). 'Yeast mRNA Poly(A) tail length control can be reconstituted in vitro in the absence of Pab1p-dependent Poly(A) nuclease activity.' *J Biol Chem* **280**(26): 24532-24538.

Dieci, G., M. C. Bosio, B. Fermi and R. Ferrari (2013). 'Transcription reinitiation by RNA polymerase III.' *Biochim Biophys Acta* **1829**(3-4): 331-341.

Dieci, G., G. Fiorino, M. Castelnuovo, M. Teichmann and A. Pagano (2007). 'The expanding RNA polymerase III transcriptome.' *Trends Genet* **23**(12): 614-622.

Dieci, G., S. Giuliodori, M. Catellani, R. Percudani and S. Ottonello (2002). 'Intragenic promoter adaptation and facilitated RNA polymerase III recycling in the transcription of SCR1, the 7SL RNA gene of Saccharomyces cerevisiae.' *J Biol Chem* **277**(9): 6903-6914.

Dieci, G. and A. Sentenac (1996). 'Facilitated recycling Pathway for RNA Polymerase III.' *Cell* **84**(2): 245-252.

Dilworth, D. J., A. Suprapto, J. C. Padovan, B. T. Chait, R. W. Wozniak, M. P. Rout and J. D. Aitchison (2001). 'Nup2p dynamically associates with the distal regions of the yeast nuclear pore complex.' *J Cell Biol* **153**(7): 1465-1478.

Dilworth, D. J., A. J. Tackett, R. S. Rogers, E. C. Yi, R. H. Christmas, J. J. Smith, A. F. Siegel, B. T. Chait, R. W. Wozniak and J. D. Aitchison (2005). 'The mobile nucleoporin Nup2p and chromatin-bound Prp20p function in endogenous NPC-mediated transcriptional control.' *The Journal of Cell Biology* **171**(6): 955-965.

Donze, D. (2012). 'Extra-transcriptional functions of RNA Polymerase III complexes: TFIIIC as a potential global chromatin bookmark.' *Gene* **493**(2): 169-175.

Ducrot, C., O. Lefebvre, E. Landrieux, J. Guirouilh-Barbat, A. Sentenac and J. Acker (2006). 'Reconstitution of the yeast RNA polymerase III transcription system with all recombinant factors.' *J Biol Chem* **281**(17): 11685-11692.

Dumay-Odelot, H., J. Acker, R. Arrebola, A. Sentenac and C. Marck (2002). 'Multiple roles of the tau131 subunit of yeast transcription factor IIIC (TFIIIC) in TFIIIB assembly.' *Mol Cell Biol* **22**(1): 298-308.

Dumay-Odelot, H., S. Durrieu-Gaillard, D. Da Silva, R. G. Roeder and M. Teichmann (2010). 'Cell growth- and differentiation-dependent regulation of RNA polymerase III transcription.' *Cell Cycle* **9**(18): 3687-3699.

Eckmann, C. R., C. Rammelt and E. Wahle (2011). 'Control of poly(A) tail length.' *Wiley Interdiscip Rev RNA* **2**(3): 348-361.

Edery, I. and N. Sonenberg (1985). 'Cap-dependent RNA splicing in a HeLa nuclear extract.' *Proc Natl Acad Sci U S A* **82**(22): 7590-7594.

El Yacoubi, B., M. Bailly and V. de Crecy-Lagard (2012). 'Biosynthesis and function of posttranscriptional modifications of transfer RNAs.' *Annu Rev Genet* **46**: 69-95.

Ellisdon, A. M., L. Dimitrova, E. Hurt and M. Stewart (2012). 'Structural basis for the assembly and nucleic acid binding of the TREX-2 transcription-export complex.' *Nat Struct Mol Biol* **19**(328-336).

Eschenlauer, J. B., M. W. Kaiser, V. L. Gerlach and D. A. Brow (1993). 'Architecture of a Yeast U6 RNA Gene Promoter.' *Mol Cell Biol* **13**(5): 3015-3026.

Faghihi, M. A., F. Modarresi, A. M. Khalil, D. E. Wood, B. G. Sahagan, T. E. Morgan, C. E. Finch, G. St Laurent, 3rd, P. J. Kenny and C. Wahlestedt (2008). 'Expression of a noncoding RNA is elevated in Alzheimer's disease and drives rapid feed-forward regulation of beta-secretase.' *Nat Med* **14**(7): 723-730.

Fasken, M. B., M. Stewart and A. H. Corbett (2008). 'Functional significance of the interaction between the mRNA-binding protein, Nab2, and the nuclear pore-associated protein, Mlp1, in mRNA export.' *J Biol Chem* **283**(40): 27130-27143.

Fernandez-Tornero, C., B. Bottcher, U. J. Rashid and C. W. Muller (2011). 'Analyzing RNA polymerase III by electron cryomicroscopy.' *RNA Biol* **8**(5): 760-765.

Fernandez-Tornero, C., B. Bottcher, U. J. Rashid, U. Steuerwald, B. Florchinger, D. P. Devos, D. Lindner and C. W. Muller (2010). 'Conformational flexibility of RNA polymerase III during transcriptional elongation.' *EMBO J* **29**(22): 3762-3772.

Fernandez-Tornero, C., B. Bottcher, M. Riva, C. Carles, U. Steuerwald, R. W. Ruigrok, A. Sentenac, C. W. Muller and G. Schoehn (2007). 'Insights into transcription initiation and termination from the electron microscopy structure of yeast RNA polymerase III.' *Mol Cell* **25**(6): 813-823.

Ferrari, R. and G. Dieci (2008). 'The transcription reinitiation properties of RNA polymerase III in the absence of transcription factors.' *Cell Mol Biol Lett* **13**(1): 112-118.

Ferrari, R., C. Rivetti, J. Acker and G. Dieci (2004). 'Distinct roles of transcription factors TFIIIB and TFIIIC in RNA polymerase III transcription reinitiation.' *Proc Natl Acad Sci U S A* **101**(37): 13442-13447.

Fischer, T., K. Strasser, A. Racz, S. Rodriguez-Navarro, M. Oppizzi, P. Ihrig, J. Lechner and E. Hurt (2002). 'The mRNA export machinery requires the novel Sac3p-Thp1p complex to dock at the nucleoplasmic entrance of the nuclear pores.' *EMBO J* **21**(21): 5843-5852.

Floer, M. and G. Blobel (1996). 'The nuclear transport factor karyopherin beta binds stoichiometrically to Ran-GTP and inhibits the Ran GTPase activating protein.' *J Biol Chem* **271**(10): 5313-5316.

French, S. L., Y. N. Osheim, D. A. Schneider, M. L. Sikes, C. F. Fernandez, L. A. Copela, V. A. Misra, M. Nomura, S. L. Wolin and A. L. Beyer (2008). 'Visual analysis of the yeast 5S rRNA gene transcriptome: regulation and role of La protein.' *Mol Cell Biol* **28**(14): 4576-4587.

Fukuda, A., M. Shimada, T. Nakadai, K. Nishimura and K. Hisatake (2013). 'Heterogeneous nuclear ribonucleoprotein R cooperates with mediator to facilitate transcription reinitiation on the c-Fos gene.' *PLoS One* **8**(8): e72496.

Gabrielsen, O. S., N. Marzouki, A. Ruet, A. Sentenac and P. Fromageot (1989). 'Two polypeptide chains in yeast transcription factor tau interact with DNA.' *J Biol Chem* **264**(13): 7505-7511.

Gabrielsen, O. S. and A. Sentenac (1991). 'RNA polymerase III (C) and its transcription factors.' *Trends Biochem Sci* **16**(11): 412-416.

Gallardo, M., R. Luna, H. Erdjument-Bromage, P. Tempst and A. Aguilera (2003). 'Nab2p and the Thp1p-Sac3p complex functionally interact at the interface between transcription and mRNA metabolism.' *J Biol Chem* **278**(26): 24225-24232.

Gary, J. D., W. J. Lin, M. C. Yang, H. R. Herschman and S. Clarke (1996). 'The Predominant Protein-arginine Methyltransferase frome Saccharomyces cerevisiae.' *J Biol Chem* **271**(21): 12585-12594.

Gavin, A. C., P. Aloy, P. Grandi, R. Krause, M. Boesche, M. Marzioch, C. Rau, L. J. Jensen, S. Bastuck, B. Dumpelfeld, A. Edelmann, M. A. Heurtier, V. Hoffman, C. Hoefert, K. Klein, M. Hudak, A. M. Michon, M. Schelder, M. Schirle, M. Remor, T. Rudi, S. Hooper, A. Bauer, T. Bouwmeester, G. Casari, G. Drewes, G. Neubauer, J. M. Rick, B. Kuster, P. Bork, R. B. Russell and G. Superti-Furga (2006). 'Proteome survey reveals modularity of the yeast cell machinery.' *Nature* **440**(7084): 631-636.

Geiduschek, E. P. and G. A. Kassavetis (2001). 'The RNA Polymerase III Transcription Apparatus.' *J Mol Biol* **310**: 1-26.

Ghavi-Helm, Y., M. Michaut, J. Acker, J. C. Aude, P. Thuriaux, M. Werner and J. Soutourina (2008). 'Genome-wide location analysis reveals a role of TFIIS in RNA polymerase III transcription.' *Genes Dev* **22**(14): 1934-1947.

Gilbert, W. and C. Guthrie (2004). 'The Glc7p nuclear phosphatase promotes mRNA export by facilitating association of Mex67p with mRNA.' *Mol Cell* **13**(2): 201-212.

Gonzalez-Aguilera, C., C. Tous, R. Babiano, J. de la Cruz, R. Luna and A. Aguilera (2011). 'Nab2 functions in the metabolism of RNA driven by polymerases II and III.' *Mol Biol Cell* **22**(15): 2729-2740.

Gonzalez-Aguilera, C., C. Tous, B. Gomez-Gonzalez, P. Huertas, R. Luna and A. Aguilera (2008). 'The THP1-SAC3-SUS1-CDC31 complex works in transcription elongation-mRNA export preventing RNA-mediated genome instability.' *Mol Biol Cell* **19**(10): 4310-4318.

Grant, R. P., N. J. Marshall, J. C. Yang, M. B. Fasken, S. M. Kelly, M. T. Harreman, D. Neuhaus, A. H. Corbett and M. Stewart (2008). 'Structure of the N-Terminal Mlp1-Binding Domain of the Saccharomyces cerevisiae mRNA-Binding Protein Nab2.' *J Mol Biol* **376**(4): 1048-1059.

Green, D. M., C. P. Johnson, H. Hagan and A. H. Corbett (2003). 'The C-terminal domain of myosin-like protein 1 (Mlp1p) is a docking site for heterogeneous nuclear ribonucleoproteins that are required for mRNA export.' *Proc Natl Acad Sci U S A* **100**(3): 1010-1015.

Green, D. M., K. A. Marfatia, E. B. Crafton, X. Zhang, X. Cheng and A. H. Corbett (2002). 'Nab2p is required for poly(A) RNA export in Saccharomyces cerevisiae and is regulated by arginine methylation via Hmt1p.' *J Biol Chem* **277**(10): 7752-7760.

Grenier St-Sauveur, G., S. Soucek, A. H. Corbett and F. Bachand (2013). 'Poly(A) tail-mediated gene regulation by opposing roles of Nab2 and Pab2 nuclear poly(A)-binding proteins in pre-mRNA decay.' *Mol Cell Biol* **33**(23): 4718-4731.

Grove, A., G. A. Kassavetis, T. E. Johnson and E. P. Geiduschek (1999). 'The RNA polymerase III-recruiting factor TFIIIB induces a DNA bend between the TATA box and the transcriptional start site.' *J Mol Biol* **285**(4): 1429-1440.

Grummt, F., I. Grummt, H. J. Gross, M. Sprinzl, D. Richter and V. A. Erdmann (1974). 'Effects of TψCG on the enzymatic binding of eukaryotic and prokaryotic initiator tRNAs to rat liver ribosomes.' *FEBS Lett* **42**(1): 15-17.

Guffanti, E., R. Ferrari, M. Preti, M. Forloni, O. Harismendy, O. Lefebvre and G. Dieci (2006). 'A minimal promoter for TFIIIC-dependent in vitro transcription of snoRNA and tRNA genes by RNA polymerase III.' *J Biol Chem* **281**(33): 23945-23957.

Guthrie, C. R., L. Greenup, J. B. Leverenz and B. C. Kraemer (2011). 'MSUT2 is a determinant of susceptibility to tau neurotoxicity.' *Hum Mol Genet* **20**(10): 1989-1999.

Guthrie, C. R., G. D. Schellenberg and B. C. Kraemer (2009). 'SUT-2 potentiates tau-induced neurotoxicity in Caenorhabditis elegans.' *Hum Mol Genet* **18**(10): 1825-1838.

Gwizdek, C., N. Iglesias, M. S. Rodriguez, B. Ossareh-Nazari, M. Hobeika, G. Divita, F. Stutz and C. Dargemont (2006). 'Ubiquitin-associated domain of Mex67 synchronizes recruitment of the mRNA export machinery with transcription.' *Proc Natl Acad Sci U S A* **103**(44): 16376-16381.

Hall, T. M. (2005). 'Multiple modes of RNA recognition by zinc finger proteins.' *Curr Opin Struct Biol* **15**(3): 367-373.

Hani, J. and H. Feldmann (1998). 'tRNA genes and retroelements in the yeast genome.' *Nucleic Acids Res* **26**(3): 689-696.

Haussecker, D., Y. Huang, A. Lau, P. Parameswaran, A. Z. Fire and M. A. Kay (2010). 'Human tRNA-derived small RNAs in the global regulation of RNA silencing.' *RNA* **16**(4): 673-695.

Havens, K. A., J. M. Guseman, S. S. Jang, E. Pierre-Jerome, N. Bolten, E. Klavins and J. L. Nemhauser (2012). 'A synthetic approach reveals extensive tunability of auxin signaling.' *Plant Physiol* **160**(1): 135-142.

He, X., A. U. Khan, H. Cheng, D. L. Pappas, Jr., M. Hampsey and C. L. Moore (2003). 'Functional interactions between the transcription and mRNA 3' end processing machineries mediated by Ssu72 and Sub1.' *Genes Dev* **17**(8): 1030-1042.

Hector, R. E., K. R. Nykamp, S. Dheur, J. T. Anderson, P. J. Non, C. R. Urbinati, S. M. Wilson, L. Minvielle-Sebastia and M. S. Swanson (2002). 'Dual requirement for yeast hnRNP Nab2p in mRNA poly(A) tail length control and nuclear export.' *EMBO J* **21**(7): 1800-1810.

Hobeika, M., C. Brockmann, F. Gruessing, D. Neuhaus, G. Divita, M. Stewart and C. Dargemont (2009). 'Structural requirements for the ubiquitin-associated domain of the mRNA export factor Mex67 to bind its specific targets, the transcription elongation THO complex component Hpr1 and nucleoporin FXFG repeats.' *J Biol Chem* **284**(26): 17575-17583.

Hodge, C. A., H. V. Colot, P. Stafford and C. N. Cole (1999). 'Rat8p/Dbp5p is a shuttling transport factor that interacts with Rat7p/Nup159p and Gle1p and suppresses the mRNA export defect of xpo1-1 cells.' *EMBO J* **18**(20): 5778-5788.

Hollingworth, D., C. G. Noble, I. A. Taylor and A. Ramos (2006). 'RNA polymerase II CTD phosphopeptides compete with RNA for the interaction with Pcf11.' *RNA* **12**(4): 555-560.

Hopper, A. K. (2013). 'Transfer RNA post-transcriptional processing, turnover, and subcellular dynamics in the yeast Saccharomyces cerevisiae.' *Genetics* **194**(1): 43-67.

Hopper, A. K. and H. Y. Huang (2015). 'Quality Control Pathways for Nucleus-Encoded Eukaryotic tRNA Biosynthesis and Subcellular Trafficking.' *Mol Cell Biol* **35**(12): 2052-2058.

Horak, C. E., N. M. Luscombe, J. Qian, P. Bertone, S. Piccirrillo, M. Gerstein and M. Snyder (2002). 'Complex transcriptional circuitry at the G1/S transition in Saccharomyces cerevisiae.' *Genes Dev* **16**(23): 3017-3033.

Hossain, M. A., C. Chung, S. K. Pradhan and T. L. Johnson (2013). 'The Yeast Cap Binding Complex Modulates Transcription Factor Recruitment and Establishes Proper Histone H3K36 Trimethylation during Active Transcription.' *Mol Cell Biol* **33**(4): 785-799.

Hudson, B. P., M. A. Martinez-Yamout, H. J. Dyson and P. E. Wright (2004). 'Recognition of the mRNA AU-rich element by the zinc finger domain of TIS11d.' *Nat Struct Mol Biol* **11**(3): 257-264.

Huertas, P. and A. Aguilera (2003). 'Cotranscriptionally formed DNA:RNA hybrids mediate transcription elongation impairment and transcription-associated recombination.' *Mol Cell* **12**(3): 711-721.

Huet, J., N. Manaud, G. Dieci, G. Peyroche, C. Conesa, O. Lefebvre, A. Ruet, M. Riva and A. Sentenac (1996). 'RNA Polymerase III and Class III Transcription Factors from Saccharomyces cerevisiae.' *Methods Enzymol* **273**: 249-267.

Hurt, E. and M. Beck (2015). 'Towards understanding nuclear pore complex architecture and dynamics in the age of integrative structural analysis.' *Curr Opin Cell Biol* **34**: 31-38.

Iglesias, N., E. Tutucci, C. Gwizdek, P. Vinciguerra, E. Von Dach, A. H. Corbett, C. Dargemont and F. Stutz (2010). 'Ubiquitin-mediated mRNP dynamics and surveillance prior to budding yeast mRNA export.' *Genes Dev* **24**(17): 1927-1938.

Ikegami, K. and J. D. Lieb (2013). 'Integral nuclear pore proteins bind to Pol III-transcribed genes and are required for Pol III transcript processing in C. elegans.' *Mol Cell* **51**(6): 840-849.

Ishii, K., G. Arib, C. Lin, G. Van Houwe and U. K. Laemmli (2002). 'Chromatin Boundaries in Budding Yeast: The Nuclear Pore Connection.' *Cell* **109**(5): 551-562.

Iwasaki, O., H. Tanizawa, K. D. Kim, Y. Yokoyama, C. J. Corcoran, A. Tanaka, E. Skordalakes, L. C. Showe and K. I. Noma (2015). 'Interaction between TBP and Condensin Drives the Organization and Faithful Segregation of Mitotic Chromosomes.' *Mol Cell*.

Jani, D., S. Lutz, N. J. Marshall, T. Fischer, A. Kohler, A. M. Ellisdon, E. Hurt and M. Stewart (2009). 'Sus1, Cdc31, and the Sac3 CID region form a conserved interaction platform that promotes nuclear pore association and mRNA export.' *Mol Cell* **33**(6): 727-737.

Jani, D., E. Valkov and M. Stewart (2014). 'Structural basis for binding the TREX-2 complex to nuclear pores, GAL1 localisation and mRNA export.' *Nucleic Acids Res* **42**(10): 6686-6697.

Janke, C., M. M. Magiera, N. Rathfelder, C. Taxis, S. Reber, H. Maekawa, A. Moreno-Borchart, G. Doenges, E. Schwob, E. Schiebel and M. Knop (2004). 'A versatile toolbox for PCR-based tagging of yeast genes: new fluorescent proteins, more markers and promoter substitution cassettes.' *Yeast* **21**(11): 947-962.

Joazeiro, C. A., G. A. Kassavetis and E. P. Geiduschek (1994). 'Identical components of yeast transcription factor IIIB are required and sufficient for transcription of TATA box-containing and TATA-less genes.' *Mol Cell Biol* **14**(4): 2798-2808.

Jobst, B., K. Schuhle, U. Linne and J. Heider (2010). 'ATP-dependent carboxylation of acetophenone by a novel type of carboxylase.' *J Bacteriol* **192**(5): 1387-1394.

Johnson, S. A., G. Cubberley and D. L. Bentley (2009). 'Cotranscriptional recruitment of the mRNA export factor Yra1 by direct interaction with the 3' end processing factor Pcf11.' *Mol Cell* **33**(2): 215-226.

Juo, Z. S., G. A. Kassavetis, J. Wang, E. P. Geiduschek and P. B. Sigler (2003). 'Crystal structure of a transcription factor IIIB core interface ternary complex.' *Nature* **422**(6931): 534-539.

Kadaba, S., X. Wang and J. T. Anderson (2006). 'Nuclear RNA surveillance in Saccharomyces cerevisiae: Trf4p-dependent polyadenylation of nascent hypomethylated tRNA and an aberrant form of 5S rRNA.' *RNA* **12**(3): 508-521.

Kanke, M., K. Nishimura, M. Kanemaki, T. Kakimoto, T. S. Takahashi, T. Nakagawa and H. Masukata (2011). 'Auxin-inducible protein depletion system in fission yeast.' *BMC Cell Biol* **12**: 8.

Karkusiewicz, I., T. W. Turowski, D. Graczyk, J. Towpik, N. Dhungel, A. K. Hopper and M. Boguta (2011). 'Maf1 protein, repressor of RNA polymerase III, indirectly affects tRNA processing.' *J Biol Chem* **286**(45): 39478-39488.

Kassavetis, G. A., B. R. Braun, L. H. Nguyen and E. P. Geiduschek (1990). 'S. cerevisiae TFIIIB is the transcription initiation factor proper of RNA polymerase III, while TFIIIA and TFIIIC are assembly factors.' *Cell* **60**(2): 235-245.

Kassavetis, G. A., R. Driscoll and E. P. Geiduschek (2006). 'Mapping the principal interaction site of the Brf1 and Bdp1 subunits of Saccharomyces cerevisiae TFIIIB.' *J Biol Chem* **281**(20): 14321-14329.

Kassavetis, G. A., A. Kumar, E. Ramirez and E. P. Geiduschek (1998). 'Functional and Structural Oragnization of Brf, the TFIIB-Related Component of the RNA polymerase III Transcription Initiation Complex.' *Mol Cell Biol* **18**(9): 5587-5599.

Kassavetis, G. A., G. A. Letts and E. P. Geiduschek (2001). 'The RNA polymerase III transcription initiation factor TFIIIB participates in two steps of promoter opening.' *EMBO J* **20**(11): 2823-2834.

Kassavetis, G. A., D. L. Riggs, R. Negri, L. H. Nguyen and E. P. Geiduschek (1989). 'Transcription factor IIIB generates extended DNA interactions in RNA polymerase III transcription complexes on tRNA genes.' *Mol Cell Biol* **9**(6): 2551-2566.

Kassavetis, G. A., E. Soragni, R. Driscoll and E. P. Geiduschek (2005). 'Reconfiguring the connectivity of a multiprotein complex: fusions of yeast TATA-binding protein with Brf1, and the function of transcription factor IIIB.' *Proc Natl Acad Sci U S A* **102**(43): 15406-15411.

Kassavetis, G. A. and D. F. Steiner (2006). 'Nhp6 is a transcriptional initiation fidelity factor for RNA polymerase III transcription in vitro and in vivo.' *J Biol Chem* **281**(11): 7445-7451.

Kaufmann, E. (1993). 'In vitro binding to the leucine tRNA gene identifies a novel yeast homeobox gene.' *Chromosoma* **102**(3): 174-179.

Kelly, S. M., R. Bienkowski, A. Banerjee, D. J. Melicharek, Z. A. Brewer, D. R. Marenda, A. H. Corbett and K. H. Moberg (2015). 'The Drosophila ortholog of the Zc3h14 RNA binding protein acts within neurons to pattern axon projection in the developing brain.' *Dev Neurobiol*.

Kelly, S. M., S. W. Leung, L. H. Apponi, A. M. Bramley, E. J. Tran, J. A. Chekanova, S. R. Wente and A. H. Corbett (2010). 'Recognition of polyadenosine RNA by the zinc finger domain of nuclear poly(A) RNA-binding protein 2 (Nab2) is required for correct mRNA 3'-end formation.' *J Biol Chem* **285**(34): 26022-26032.

Kelly, S. M., S. W. Leung, C. Pak, A. Banerjee, K. H. Moberg and A. H. Corbett (2014). 'A conserved role for the zinc finger polyadenosine RNA binding protein, ZC3H14, in control of poly(A) tail length.' *RNA* **20**(5): 681-688.

Kelly, S. M., S. A. Pabit, C. M. Kitchen, P. Guo, K. A. Marfatia, T. J. Murphy, A. H. Corbett and K. M. Berland (2007). 'Recognition of polyadenosine RNA by zinc finger proteins.' *Proc Natl Acad Sci U S A* **104**(30): 12306-12311.

Kelly, S. M., C. Pak, M. Garshasbi, A. Kuss, A. H. Corbett and K. H. Moberg (2012). 'New kid on the ID block.' *RNA Biol* **9**(5): 555-562.

Kim, J. and V. R. Iyer (2004). 'Global role of TATA box-binding protein recruitment to promoters in mediating gene expression profiles.' *Mol Cell Biol* **24**(18): 8104-8112.

Kirchner, S. and Z. Ignatova (2015). 'Emerging roles of tRNA in adaptive translation, signalling dynamics and disease.' *Nat Rev Genet* **16**(2): 98-112.

Kleinschmidt, R. A., K. E. LeBlanc and D. Donze (2011). 'Autoregulation of an RNA polymerase II promoter by the RNA polymerase III transcription factor III C (TF(III)C) complex.' *Proc Natl Acad Sci U S A* **108**(20): 8385-8389.

Knop, M., A. Finger, T. Braun, K. Hellmuth and D. H. Wolf (1996). 'Der1, a novel protein specifically required for endoplasmic reticulum degradation in yeast.' *EMBO J* **15**(4): 753-763.

Knüppel, L. D. (2013). *Nab2 recruitment to RNA-Polymerase III genes in different mutant backgrounds and Generation of the S. pombe homologue*, LMU Munich. **Master thesis**.

Kruppa, M., R. D. Moir, D. Kolodrubetz and I. M. Willis (2001). 'Nhp6, an HMG1 Protein, Functions in SNR6 Transcription by RNA Polymerase III in S. cerevisiae.' *Mol Cell* **7**(2): 309-318.

Kube, S., N. Kapitein, T. Zimniak, F. Herzog, A. Mogk and P. Wendler (2014). 'Structure of the VipA/B type VI secretion complex suggests a contraction-state-specific recycling mechanism.' *Cell Rep* **8**(1): 20-30.

Kubota, T., K. Nishimura, M. T. Kanemaki and A. D. Donaldson (2013). 'The Elg1 replication factor C-like complex functions in PCNA unloading during DNA replication.' *Mol Cell* **50**(2): 273-280.

Kuhlmann, S. I., E. Valkov and M. Stewart (2013). 'Structural basis for the molecular recognition of polyadenosine RNA by Nab2 Zn fingers.' *Nucleic Acids Res* **42**(1): 672-680.

Kuhn, C. D., S. R. Geiger, S. Baumli, M. Gartmann, J. Gerber, S. Jennebach, T. Mielke, H. Tschochner, R. Beckmann and P. Cramer (2007). 'Functional architecture of RNA polymerase I.' *Cell* **131**(7): 1260-1272.

Kuhn, U., M. Gundel, A. Knoth, Y. Kerwitz, S. Rudel and E. Wahle (2009). 'Poly(A) tail length is controlled by the nuclear poly(A)-binding protein regulating the interaction between poly(A) polymerase and the cleavage and polyadenylation specificity factor.' *J Biol Chem* **284**(34): 22803-22814.

Kumar, A., G. A. Kassavetis, E. P. Geiduschek, M. Hambalko and C. J. Brent (1997). 'Functional dissection of the B" component of RNA polymerase III transcription factor IIIB: a scaffolding protein with multiple roles in assembly and initiation of transcription.' *Mol Cell Biol* **17**(4): 1868-1880.

Kumar, Y. and P. Bhargava (2013). 'A unique nucleosome arrangement, maintained actively by chromatin remodelers facilitates transcription of yeast tRNA genes.' *BMC Genomics* **14**: 402.

Kurdistani, S. K., D. Robyr, S. Tavazoie and M. Grunstein (2002). 'Genome-wide binding map of the histone deacetylase Rpd3 in yeast.' *Nat Genet* **31**(3): 248-254.

Laemmli, U. K. (1970). 'Cleavage of structural proteins during the assembly of the head of bacteriophage T4.' *Nature* **227**(5259): 680-685.

Landrieux, E., N. Alic, C. Ducrot, J. Acker, M. Riva and C. Carles (2006). 'A subcomplex of RNA polymerase III subunits involved in transcription termination and reinitiation.' *EMBO J* **25**(1): 118-128.

Layat, E., A. V. Probst and S. Tourmente (2013). 'Structure, function and regulation of Transcription Factor IIIA: From Xenopus to Arabidopsis.' *Biochim Biophys Acta* **1829**(3-4): 274-282.

Lee, D. C. Y. and J. D. Aitchison (1999). 'Kap104p-mediated Nuclear Import.' *J Biol Chem* **274**(41): 29031-29037.

Lee, J. Y., C. E. Rohlman, L. A. Molony and D. R. Engelke (1991). 'Characterization of RPRI, an Essential Gene Encoding the RNA Component of Saccharomyces cerevisiae Nuclear RNase P.' *Mol Cell Biol* **11**(2): 721-730.

Lemieux, C., S. Marguerat, J. Lafontaine, N. Barbezier, J. Bahler and F. Bachand (2011). 'A Pre-mRNA degradation pathway that selectively targets intron-containing genes requires the nuclear poly(A)-binding protein.' *Mol Cell* **44**(1): 108-119.

Leung, S. W., L. H. Apponi, O. E. Cornejo, C. M. Kitchen, S. R. Valentini, G. K. Pavlath, C. M. Dunham and A. H. Corbett (2009). 'Splice variants of the human ZC3H14 gene generate multiple isoforms of a zinc finger polyadenosine RNA binding protein.' *Gene* **439**(1-2): 71-78.

Leveillard, T., G. A. Kassavetis and E. P. Geiduschek (1991). 'Saccharomyces cerevisiae transcription factors IIIB and IIIC bend the DNA of a tRNA(Gln) gene.' *J Biol Chem* **266**(8): 5162-5168.

Li, B., M. Carey and J. L. Workman (2007). 'The role of chromatin during transcription.' *Cell* **128**(4): 707-719.

Lieb, J. D. and N. D. Clarke (2005). 'Control of transcription through intragenic patterns of nucleosome composition.' *Cell* **123**(7): 1187-1190.

Lindstrom, D. L., S. L. Squazzo, N. Muster, T. A. Burckin, K. C. Wachter, C. A. Emigh, J. A. McCleery, J. R. Yates, 3rd and G. A. Hartzog (2003). 'Dual roles for Spt5 in pre-mRNA processing and transcription elongation revealed by identification of Spt5-associated proteins.' *Mol Cell Biol* **23**(4): 1368-1378.

Lionnet, T., J. F. Allemand, A. Revyakin, T. R. Strick, O. A. Saleh, D. Bensimon and V. Croquette (2012). 'Single-molecule studies using magnetic traps.' *Cold Spring Harb Protoc* **2012**(1): 34-49.

Liu, Y., L. Warfield, C. Zhang, J. Luo, J. Allen, W. H. Lang, J. Ranish, K. M. Shokat and S. Hahn (2009). 'Phosphorylation of the transcription elongation factor Spt5 by yeast Bur1 kinase stimulates recruitment of the PAF complex.' *Mol Cell Biol* **29**(17): 4852-4863.

Livak, K. J. and T. D. Schmittgen (2001). 'Analysis of relative gene expression data using real-time quantitative PCR and the 2(-Delta Delta C(T)) Method.' *Methods* **25**(4): 402-408.

Lopez, S., M. Livingstone-Zatchej, S. Jourdain, F. Thoma, A. Sentenac and M. C. Marsolier (2001). 'High-mobility-group proteins NHP6A and NHP6B participate in activation of the RNA polymerase III SNR6 gene.' *Mol Cell Biol* **21**(9): 3096-3104.

Lottspeich, F. and J. W. Engels (2012). Bioanalytik, Springer.

Lüling, R. T. (2014). *Untersuchungen der tRNA Lokalisation in Abhängigkeit von Nab2 sowie der Effekt von Brf1 auf nab2-34 in S. cerevisiae*, LMU Munich. **Bachelor thesis**.

Luna, R., C. Gonzalez-Aguilera and A. Aguilera (2009). 'Transcription at the proximity of the nuclear pore: a role for the THP1-SAC3-SUS1-CDC31 (THSC) complex.' *RNA Biol* **6**(2): 145-148.

Lund, M. K. and C. Guthrie (2005). 'The DEAD-box protein Dbp5p is required to dissociate Mex67p from exported mRNPs at the nuclear rim.' *Mol Cell* **20**(4): 645-651.

Lundblad, V. and H. Zhou (2001). 'Manipulation of plasmids from yeast cells.' *Curr Protoc Mol Biol* **Chapter 13**: Unit13 19.

Mahapatra, S., P. S. Dewari, A. Bhardwaj and P. Bhargava (2011). 'Yeast H2A.Z, FACT complex and RSC regulate transcription of tRNA gene through differential dynamics of flanking nucleosomes.' *Nucleic Acids Res* **39**(10): 4023-4034.

Male, G., A. von Appen, S. Glatt, N. M. Taylor, M. Cristovao, H. Groetsch, M. Beck and C. W. Muller (2015). 'Architecture of TFIIIC and its role in RNA polymerase III pre-initiation complex assembly.' *Nat Commun* **6**: 7387.

Mandel, C. R., Y. Bai and L. Tong (2008). 'Protein factors in pre-mRNA 3'-end processing.' *Cell Mol Life Sci* **65**(7-8): 1099-1122.

Maraia, R. J. (2001). 'La protein and the trafficking of nascent RNA polymerase iii transcripts.' *J Cell Biol* **153**(4): F13-18.

Maraia, R. J., D. J. Kenan and J. D. Keene (1994). 'Eukaryotic transcription termination factor La mediates transcript release and facilitates reinitiation by RNA polymerase III.' *Mol Cell Biol* **14**(3): 2147-2158.

Marck, C., R. Kachouri-Lafond, I. Lafontaine, E. Westhof, B. Dujon and H. Grosjean (2006). 'The RNA polymerase III-dependent family of genes in hemiascomycetes: comparative RNomics, decoding strategies, transcription and evolutionary implications.' *Nucleic Acids Res* **34**(6): 1816-1835.

Marfatia, K. A., E. B. Crafton, D. M. Green and A. H. Corbett (2003). 'Domain analysis of the Saccharomyces cerevisiae heterogeneous nuclear ribonucleoprotein, Nab2p. Dissecting the requirements for Nab2p-facilitated poly(A) RNA export.' *J Biol Chem* **278**(9): 6731-6740.

Martin, F. H. and I. Tinoco, Jr. (1980). 'DNA-RNA hybrid duplexes containing oligo(dA:rU) sequences are exceptionally unstable and may facilitate termination of transcription.' *Nucleic Acids Res* **8**(10): 2295-2299.

Martin, N. C. and A. K. Hopper (1994). 'How single genes provide tRNA processing enzymes to mitochondria, nuclei and the cytosol.' *Biochimie* **76**(12): 1161-1167.

Martinez-Lumbreras, S., C. M. Santiveri, Y. Mirassou, S. Zorrilla and J. M. Perez-Canadillas (2013). 'Two singular types of CCCH tandem zinc finger in Nab2p contribute to polyadenosine RNA recognition.' *Structure* **21**(10): 1800-1811.

Matera, A. G. and Z. Wang (2014). 'A day in the life of the spliceosome.' *Nat Rev Mol Cell Biol* **15**(2): 108-121.

Matsuzaki, H., G. A. Kassavetis and E. P. Geiduschek (1994). 'Analysis of RNA chain elongation and termination by Saccharomyces cerevisiae RNA polymerase III.' *J Mol Biol* **235**(4): 1173-1192.

Matthews, J. M. and M. Sunde (2002). 'Zinc fingers--folds for many occasions.' *IUBMB Life* **54**(6): 351-355.

Mayer, A., M. Lidschreiber, M. Siebert, K. Leike, J. Soding and P. Cramer (2010). 'Uniform transitions of the general RNA polymerase II transcription complex.' *Nat Struct Mol Biol* **17**(10): 1272-1278.

Mayer, A., A. Schreieck, M. Lidschreiber, K. Leike, D. E. Martin and P. Cramer (2012). 'The spt5 C-terminal region recruits yeast 3' RNA cleavage factor I.' *Mol Cell Biol* **32**(7): 1321-1331.

Mei, Y., J. Yong, H. Liu, Y. Shi, J. Meinkoth, G. Dreyfuss and X. Yang (2010). 'tRNA binds to cytochrome c and inhibits caspase activation.' *Mol Cell* **37**(5): 668-678.

Meinel, D. M. (2013). *Genome wide recruitment of TREX reveals a direct interaction with the Rpb1 CTD*, LMU Munich. **Doctoral thesis**.

Meinel, D. M., C. Burkert-Kautzsch, A. Kieser, E. O'Duibhir, M. Siebert, A. Mayer, P. Cramer, J. Soding, F. C. Holstege and K. Strasser (2013). 'Recruitment of TREX to the transcription machinery by its direct binding to the phospho-CTD of RNA polymerase II.' *PLoS Genet* **9**(11): e1003914.

Meinel, D. M. and K. Strasser (2015). 'Co-transcriptional mRNP formation is coordinated within a molecular mRNP packaging station in S. cerevisiae.' *Bioessays* **37**(6): 666-677.

Memet, S., W. Saurin and A. Sentenac (1988). 'RNA Polymerase B ans C Are More Closely Related to Each Other than to RNA Polymerase A.' *J Biol Chem* **263**(21): 10048-10051.

Mitchell, S. F., S. Jain, M. She and R. Parker (2013). 'Global analysis of yeast mRNPs.' *Nat Struct Mol Biol* **20**(1): 127-133.

Moqtaderi, Z. and K. Struhl (2004). 'Genome-Wide Occupancy Profile of the RNA Polymerase III Machinery in Saccharomyces cerevisiae Reveals Loci with Incomplete Transcription Complexes.' *Mol Cell Biol* **24**(10): 4118-4127.

Moqtaderi, Z., J. Wang, D. Raha, R. J. White, M. Snyder, Z. Weng and K. Struhl (2010). 'Genomic binding profiles of functionally distinct RNA polymerase III transcription complexes in human cells.' *Nat Struct Mol Biol* **17**(5): 635-640.

Morawska, M. and H. D. Ulrich (2013). 'An expanded tool kit for the auxin-inducible degron system in budding yeast.' *Yeast* **30**(9): 341-351.

Naar, A. M., B. D. Lemon and R. Tjian (2001). 'Transcriptional coactivator complexes.' *Annu Rev Biochem* **70**: 475-501.

Nguyen, N. T., C. Saguez, C. Conesa, O. Lefebvre and J. Acker (2015). 'Identification of proteins associated with RNA polymerase III using a modified tandem chromatin affinity purification.' *Gene* **556**(1): 51-60.

Nicol, J. W., G. A. Helt, S. G. Blanchard, Jr., A. Raja and A. E. Loraine (2009). 'The Integrated Genome Browser: free software for distribution and exploration of genome-scale datasets.' *Bioinformatics* **25**(20): 2730-2731.

Nino, C. A., L. Herissant, A. Babour and C. Dargemont (2013). 'mRNA nuclear export in yeast.' *Chem Rev* **113**(11): 8523-8545.

Nishimura, K., T. Fukagawa, H. Takisawa, T. Kakimoto and M. Kanemaki (2009). 'An auxin-based degron system for the rapid depletion of proteins in nonplant cells.' *Nat Methods* **6**(12): 917-922.

Noble, K. N., E. J. Tran, A. R. Alcazar-Roman, C. A. Hodge, C. N. Cole and S. R. Wente (2011). 'The Dbp5 cycle at the nuclear pore complex during mRNA export II: nucleotide cycling and mRNP remodeling by Dbp5 are controlled by Nup159 and Gle1.' *Genes Dev* **25**(10): 1065-1077.

Noma, K., H. P. Cam, R. J. Maraia and S. I. Grewal (2006). 'A role for TFIIIC transcription factor complex in genome organization.' *Cell* **125**(5): 859-872.

O'Reilly, D. and D. R. Greaves (2007). 'Cell-type-specific expression of the human CD68 gene is associated with changes in Pol II phosphorylation and short-range intrachromosomal gene looping.' *Genomics* **90**(3): 407-415.

Orioli, A., C. Pascali, A. Pagano, M. Teichmann and G. Dieci (2012). 'RNA polymerase III transcription control elements: themes and variations.' *Gene* **493**(2): 185-194.

O'Sullivan, J. M., S. M. Tan-Wong, A. Morillon, B. Lee, J. Coles, J. Mellor and N. J. Proudfoot (2004). 'Gene loops juxtapose promoters and terminators in yeast.' *Nat Genet* **36**(9): 1014-1018.

Pak, C., M. Garshasbi, K. Kahrizi, C. Gross, L. Apponi, J. J. Noto, S. M. Kelly, S. W. Leung, A. Tzschach, F. Behjati, S. S. Abedini, M. Mohseni, L. R. Jensen, H. Hu, B. Huang, S. N. Stahley, G. Liu, K. R. Williams, S. Burdick, Y. Feng, S. Sanyal, G. J. Bassell, H. Ropers, H. Najmabadi, A. H. Corbett, K. H. Moberg and A. W. Kuss (2011). 'Mutation of the conserved polyadenosine RNA binding protein, ZC3H14/dNab2, impairs neural function in Drosophila and humans.' *Proc Natl Acad Sci U S A* **108**(30): 12390-12395.

Pang, Y. L., K. Poruri and S. A. Martinis (2014). 'tRNA synthetase: tRNA aminoacylation and beyond.' *Wiley Interdiscip Rev RNA* **5**(4): 461-480.

Parker, R. (2012). 'RNA degradation in Saccharomyces cerevisae.' *Genetics* **191**(3): 671-702.

Pascual-García, P., C. K. Govind, E. Queralt, B. Cuenca-Bono, A. Llopis, S. Chavez, A. G. Hinnebusch and S. Rodríguez-Navarro (2008). 'Sus1 is recruited to coding regions and functions during transcription elongation in association with SAGA and TREX2.' *Genes & Development* **22**(20): 2811-2822.

Phizicky, E. M. and A. K. Hopper (2010). 'tRNA biology charges to the front.' *Genes Dev* **24**(17): 1832-1860.

Pluta, K., O. Lefebvre, N. C. Martin, W. J. Smagowicz, D. R. Stanford, S. R. Ellis, A. K. Hopper, A. Sentenac and M. Boguta (2001). 'Maf1p, a negative effector of RNA polymerase III in Saccharomyces cerevisiae.' *Mol Cell Biol* **21**(15): 5031-5040.

Puig, O., F. Caspary, G. Rigaut, B. Rutz, E. Bouveret, E. Bragado-Nilsson, M. Wilm and B. Seraphin (2001). 'The Tandem Affinity Purification (TAP) Method: A General Procedure of Protein Complex Purification.' *Methods* **24**(3): 218-229.

Qian, X., C. Jeon, H. Yoon, K. Agarwal and M. A. Weiss (1993). 'Structure of a new nucleic-acid-binding motif in eukaryotic transcriptional elongation factor TFIIS.' *Nature* **365**(6443): 277-279.

Qu, X., S. Lykke-Andersen, T. Nasser, C. Saguez, E. Bertrand, T. H. Jensen and C. Moore (2009). 'Assembly of an export-competent mRNP is needed for efficient release of the 3'-end processing complex after polyadenylation.' *Mol Cell Biol* **29**(19): 5327-5338.

Raha, D., Z. Wang, Z. Moqtaderi, L. Wu, G. Zhong, M. Gerstein, K. Struhl and M. Snyder (2010). 'Close association of RNA polymerase II and many transcription factors with Pol III genes.' *Proc Natl Acad Sci U S A* **107**(8): 3639-3644.

Raina, M. and M. Ibba (2014). 'tRNAs as regulators of biological processes.' *Frontiers in Genetics* **5**.

Rajyaguru, P. and R. Parker (2012). 'RGG motif proteins: modulators of mRNA functional states.' *Cell Cycle* **11**(14): 2594-2599.

Rameau, G., K. Puglia, A. Crowe, I. Sethy and I. Willis (1994). 'A mutation in the second largest subunit of TFIIIC increases a rate-limiting step in transcription by RNA polymerase III.' *Mol Cell Biol* **14**(1): 822-830.

Rijal, K. and R. J. Maraia (2013). 'RNA polymerase III mutants in TFIIFalpha-like C37 that cause terminator readthrough with no decrease in transcription output.' *Nucleic Acids Res* **41**(1): 139-155.

Roberts, D. N., B. Wilson, J. T. Huff, A. J. Stewart and B. R. Cairns (2006). 'Dephosphorylation and genome-wide association of Maf1 with Pol III-transcribed genes during repression.' *Mol Cell* **22**(5): 633-644.

Roth, K. M., J. Byam, F. Fang and J. S. Butler (2009). 'Regulation of NAB2 mRNA 3'-end formation requires the core exosome and the Trf4p component of the TRAMP complex.' *RNA* **15**(6): 1045-1058.

Roth, K. M., M. K. Wolf, M. Rossi and J. S. Butler (2005). 'The nuclear exosome contributes to autogenous control of NAB2 mRNA levels.' *Mol Cell Biol* **25**(5): 1577-1585.

Rothfels, K., O. Rowland and J. Segall (2007). 'Zinc fingers 1 and 7 of yeast TFIIIA are essential for assembly of a functional transcription complex on the 5 S RNA gene.' *Nucleic Acids Res* **35**(14): 4869-4881.

Sambrook, J. and D. W. Russel (2001). Molecular Cloning - A Laboratory Manual. Cold Spring Habor, New York, CSHL Press.

Santangelo, T. J. and I. Artsimovitch (2011). 'Termination and antitermination: RNA polymerase runs a stop sign.' *Nat Rev Microbiol* **9**(5): 319-329.

Santos-Pereira, J. M., A. B. Herrero, M. L. Garcia-Rubio, A. Marin, S. Moreno and A. Aguilera (2013). 'The Npl3 hnRNP prevents R-loop-mediated transcription-replication conflicts and genome instability.' *Genes Dev* **27**(22): 2445-2458.

Santos-Pereira, J. M., A. B. Herrero, S. Moreno and A. Aguilera (2014). 'Npl3, a new link between RNA-binding proteins and the maintenance of genome integrity.' *Cell Cycle* **13**(10): 1524-1529.

Schmid, M., G. Arib, C. Laemmli, J. Nishikawa, T. Durussel and U. K. Laemmli (2006). 'Nup-PI: the nucleopore-promoter interaction of genes in yeast.' *Mol Cell* **21**(3): 379-391.

Schmid, M., P. Olszewski, V. Pelechano, I. Gupta, L. M. Steinmetz and T. H. Jensen (2015). 'The Nuclear PolyA-Binding Protein Nab2p Is Essential for mRNA Production.' *Cell Rep* **12**(1): 128-139.

Schmid, M., M. B. Poulsen, P. Olszewski, V. Pelechano, C. Saguez, I. Gupta, L. M. Steinmetz, C. Moore and T. H. Jensen (2012). 'Rrp6p controls mRNA poly(A) tail length and its decoration with poly(A) binding proteins.' *Mol Cell* **47**(2): 267-280.

Schneider, C. and D. Tollervey (2013). 'Threading the barrel of the RNA exosome.' *Trends Biochem Sci* **38**(10): 485-493.

Schneider, M., D. Hellerschmied, T. Schubert, S. Amlacher, V. Vinayachandran, R. Reja, B. F. Pugh, T. Clausen and A. Kohler (2015). 'The Nuclear Pore-Associated TREX-2 Complex Employs Mediator to Regulate Gene Expression.' *Cell* **162**(5): 1016-1028.

Schon, A. (1999). 'Ribonuclease P: the diversity of a ubiquitous RNA processing enzyme.' *FEMS Microbiol Rev* **23**(3): 391-406.

Schramm, L. and N. Hernandez (2002). 'Recruitment of RNA polymerase III to its target promoters.' *Genes & Development* **16**(20): 2593-2620.

Schultz, M., R. H. Reeder and S. Hahn (1992). 'Variants of the TATA-Binding Protein Can Distinguish Subsets of RNA Polymerase I, II, and III Promoters.' *Cell* **69**: 697-702.

Schultz, M. C., S. Y. Choe and R. H. Reeder (1991). 'Specific initiation by RNA polymerase I in a whole-cell extract from yeast.' *Proc Natl Acad Sci U S A* **88**(3): 1004-1008.

Schultz, M. C., S. Y. Choe and R. H. Reeder (1991). 'Specific initiation by RNA polymerase I in a whole-cell extract from yeast.' *Proc Natl Acad Sci U S A* **88**(3): 1004-1008.

Scott, K. C., C. V. White and H. F. Willard (2007). 'An RNA polymerase III-dependent heterochromatin barrier at fission yeast centromere 1.' *PLoS One* **2**(10): e1099.

Sentenac, A. and M. Riva (2013). 'Odd RNA polymerases or the A(B)C of eukaryotic transcription.' *Biochim Biophys Acta* **1829**(3-4): 251-257.

Shen, E. C., M. F. Henry, V. H. Weiss, S. R. Vanlentini, P. A. Silver and M. S. Lee (1998). 'Arginine methylation facilitates the nuclear export of hnRNP proteins.' *Genes & Development* **12**(5): 679-691.

Shimada, A., O. Nureki, M. Goto, S. Takahashi and S. Yokoyama (2001). 'Structural and mutational studies of the recognition of the arginine tRNA-specific major identity element, A20, by arginyl-tRNA synthetase.' *Proc Natl Acad Sci U S A* **98**(24): 13537-13542.

Sievers, F., A. Wilm, D. Dineen, T. J. Gibson, K. Karplus, W. Li, R. Lopez, H. McWilliam, M. Remmert, J. Soding, J. D. Thompson and D. G. Higgins (2011). 'Fast, scalable generation of high-quality protein multiple sequence alignments using Clustal Omega.' *Mol Syst Biol* **7**: 539.

Sikorski, R. S. and P. Hieter (1989). 'A system of shuttle vectors and yeast host strains designed for efficient manipulation of DNA in Saccharomyces cerevisiae.' *Genetics* **122**(1): 19-27.

Singh, B. N. and M. Hampsey (2007). 'A transcription-independent role for TFIIB in gene looping.' *Mol Cell* **27**(5): 806-816.

Sonenberg, N. and A. G. Hinnebusch (2009). 'Regulation of translation initiation in eukaryotes: mechanisms and biological targets.' *Cell* **136**(4): 731-745.

Soniat, M., P. Sampathkumar, G. Collett, A. S. Gizzi, R. N. Banu, R. C. Bhosle, S. Chamala, S. Chowdhury, A. Fiser, A. S. Glenn, J. Hammonds, B. Hillerich, K. Khafizov, J. D. Love, B. Matikainen, R. D. Seidel, R. Toro, P. Rajesh Kumar, J. B. Bonanno, Y. M. Chook and S. C. Almo (2013). 'Crystal structure of human Karyopherin beta2 bound to the PY-NLS of Saccharomyces cerevisiae Nab2.' *J Struct Funct Genomics* **14**(2): 31-35.

Soucek, S., A. H. Corbett and M. B. Fasken (2012). 'The long and the short of it: the role of the zinc finger polyadenosine RNA binding protein, Nab2, in control of poly(A) tail length.' *Biochim Biophys Acta* **1819**(6): 546-554.

Sparrer, K. M., C. K. Pfaller and K. K. Conzelmann (2012). 'Measles virus C protein interferes with Beta interferon transcription in the nucleus.' *J Virol* **86**(2): 796-805.

Spingola, M., L. Grate, D. Haussler and M. Ares, Jr. (1999). 'Genome-wide bioinformatic and molecular analysis of introns in Saccharomyces cerevisiae.' *RNA* **5**(2): 221-234.

Steglich, B., S. Sazer and K. Ekwall (2013). 'Transcriptional regulation at the yeast nuclear envelope.' *Nucleus* **4**(5): 379-389.

Stewart, M. (2010). 'Nuclear export of mRNA.' *Trends Biochem Sci* **35**(11): 609-617.

Strambio-de-Castillia, C., G. Blobel and M. P. Rout (1999). 'Proteins Connecting the Nuclear Pore Complex with the Nuclear INterior.' *J Cell Biol* **144**(5).

Strasser, K. and E. Hurt (2000). 'Yra1p, a conserved nuclear RNA-binding protein, interacts directly with Mex67p and is required for mRNA export.' *EMBO J* **19**(3): 410-420.

Strasser, K. and E. Hurt (2001). 'Splicing factor Sub2p is required for nuclear mRNA export through its interaction with Yra1p.' *Nature* **413**(6856): 648-652.

Sträßer, K., S. Masuda, P. Mason, J. Pfannstiel, M. Oppizzi, S. Rodriguez-Navarro, A. G. Rondon, A. Aguilera, K. Struhl, R. Reed and E. Hurt (2002). 'TREX is a conserved complex coupling transcription with messenger RNA export.' *Nature* **417**(6886): 304-308.

Studier, F. W. and B. A. Moffatt (1986). 'Use of bacteriophage T7 RNA polymerase to direct selective high-level expression of cloned genes.' *Journal of Molecular Biology* **189**(1): 113-130

Stutz, F., A. Bachi, T. Doerks, I. C. Braun, B. Seraphin, M. Wilm, P. Bork and E. Izaurralde (2000). 'REF, an evolutionary conserved family of hnRNP-like proteins, interacts with TAP/Mex67p and participates in mRNA nuclear export.' *RNA* **6**(4): 638-650.

Suntharalingam, M., A. R. Alcazar-Roman and S. R. Wente (2004). 'Nuclear export of the yeast mRNA-binding protein Nab2 is linked to a direct interaction with Gfd1 and to Gle1 function.' *J Biol Chem* **279**(34): 35384-35391.

Tan-Wong, S. M., J. D. French, N. J. Proudfoot and M. A. Brown (2008). 'Dynamic interactions between the promoter and terminator regions of the mammalian BRCA1 gene.' *Proc Natl Acad Sci U S A* **105**(13): 5160-5165.

Tavenet, A., A. Suleau, G. Dubreuil, R. Ferrari, C. Ducrot, M. Michaut, J. C. Aude, G. Dieci, O. Lefebvre, C. Conesa and J. Acker (2009). 'Genome-wide location analysis reveals a role for Sub1 in RNA polymerase III transcription.' *Proc Natl Acad Sci U S A* **106**(34): 14265-14270.

Teale, W. D., I. A. Paponov and K. Palme (2006). 'Auxin in action: signalling, transport and the control of plant growth and development.' *Nat Rev Mol Cell Biol* **7**(11): 847-859.

Topisirovic, I., Y. V. Svitkin, N. Sonenberg and A. J. Shatkin (2011). 'Cap and cap-binding proteins in the control of gene expression.' *Wiley Interdiscip Rev RNA* **2**(2): 277-298.

Tran, E. J., Y. Zhou, A. H. Corbett and S. R. Wente (2007). 'The DEAD-box protein Dbp5 controls mRNA export by triggering specific RNA:protein remodeling events.' *Mol Cell* **28**(5): 850-859.

Truant, R., R. A. Fridell, R. E. Benson, H. Bogerd and B. R. Cullen (1998). 'Identification and Functional Characterization of a Novel Nuclear Localization Signal Present in the Yeast Nab2 Poly(A)+ RNA Binding Protein.' *Mol Cell Biol* **18**(3): 1449-1458.

Tuck, A. C. and D. Tollervey (2013). 'A transcriptome-wide atlas of RNP composition reveals diverse classes of mRNAs and lncRNAs.' *Cell* **154**(5): 996-1009.

Ubukata, T., T. Shimizu, N. Adachi, K. Sekimizu and T. Nakanishi (2003). 'Cleavage, but not read-through, stimulation activity is responsible for three biologic functions of transcription elongation factor S-II.' *J Biol Chem* **278**(10): 8580-8585.

Valentini, S. R., V. H. Weiss and P. A. Silver (1999). 'Arginine methylation and binding of Hrp1p to the efficiency element for mRNA 3'-end formation.' *RNA* **5**(2): 272-280.

Vannini, A. and P. Cramer (2012). 'Conservation between the RNA polymerase I, II, and III transcription initiation machineries.' *Mol Cell* **45**(4): 439-446.

Vannini, A., R. Ringel, A. G. Kusser, O. Berninghausen, G. A. Kassavetis and P. Cramer (2010). 'Molecular basis of RNA polymerase III transcription repression by Maf1.' *Cell* **143**(1): 59-70.

Venters, B. J., S. Wachi, T. N. Mavrich, B. E. Andersen, P. Jena, A. J. Sinnamon, P. Jain, N. S. Rolleri, C. Jiang, C. Hemeryck-Walsh and B. F. Pugh (2011). 'A comprehensive genomic binding map of gene and chromatin regulatory proteins in Saccharomyces.' *Mol Cell* **41**(4): 480-492.

Vinciguerra, P., N. Iglesias, J. Camblong, D. Zenklusen and F. Stutz (2005). 'Perinuclear Mlp proteins downregulate gene expression in response to a defect in mRNA export.' *EMBO J* **24**(4): 813-823.

Viphakone, N., F. Voisinet-Hakil and L. Minvielle-Sebastia (2008). 'Molecular dissection of mRNA poly(A) tail length control in yeast.' *Nucleic Acids Res* **36**(7): 2418-2433.

Wang, C. K. and P. A. Weil (1989). 'Purification and characterization of Saccharomyces cerevisiae transcription factor IIIA.' *J Biol Chem* **264**(2): 1092-1099.

Wang, Z. and R. G. Roeder (1997). 'Three human RNA polymerase III-specific subunits form a subcomplex with a selective function in specific transcription initiation.' *Genes & Development* **11**(10): 1315-1326.

Wang, Z. and R. G. Roeder (1998). 'DNA topoisomerase I and PC4 can interact with human TFIIIC to promote both accurate termination and transcription reinitiation by RNA polymerase III.' *Mol Cell* **1**(5): 749-757.

Waterhouse, A. M., J. B. Procter, D. M. Martin, M. Clamp and G. J. Barton (2009). 'Jalview Version 2--a multiple sequence alignment editor and analysis workbench.' *Bioinformatics* **25**(9): 1189-1191.

Werner, M., N. Chaussivert, I. M. Willis and A. Sentenac (1993). 'Interaction between a complex of RNA polymerase III subunits and the 70-kDa component of transcription factor IIIB.' *J Biol Chem* **268**(28): 20721-20724.

Werner, M., P. Thuriaux and J. Soutourina (2009). 'Structure-function analysis of RNA polymerases I and III.' *Curr Opin Struct Biol* **19**(6): 740-745.

White, R. J. (2005). 'RNA polymerases I and III, growth control and cancer.' *Nat Rev Mol Cell Biol* **6**(1): 69-78.

White, R. J. (2011). 'Transcription by RNA polymerase III: more complex than we thought.' *Nat Rev Genet* **12**(7): 459-463.

Wolffe, A. P., E. Jordan and D. D. Brown (1986). 'A bacteriophage RNA polymerase transcribes through a Xenopus 5S RNA gene transcription complex without disrupting it.' *Cell* **44**(3): 381-389.

Woodcock, D. M., P. J. Crowther, J. Doherty, S. Jefferson, E. DeCruz, M. Noyer-Weidner, S. S. Smith, M. Z. Michael and M. W. Graham (1989). 'Quantitative evaluation of *Escherichia coli* host strains for tolerance to cytosine methylation in plasmid and phage recombinants.' *Nucleic Acids Research* **17**(9): 3469-3478.

Xiao, S., F. Scott, C. A. Fierke and D. R. Engelke (2002). 'Eukaryotic ribonuclease P: a plurality of ribonucleoprotein enzymes.' *Annu Rev Biochem* **71**: 165-189.

Xu, C. and M. F. Henry (2004). 'Nuclear export of hnRNP Hrp1p and nuclear export of hnRNP Npl3p are linked and influenced by the methylation state of Npl3p.' *Mol Cell Biol* **24**(24): 10742-10756.

Yamada, T., Y. Yamaguchi, N. Inukai, S. Okamoto, T. Mura and H. Handa (2006). 'P-TEFb-mediated phosphorylation of hSpt5 C-terminal repeats is critical for processive transcription elongation.' *Mol Cell* **21**(2): 227-237.

Yamasaki, S., P. Ivanov, G. F. Hu and P. Anderson (2009). 'Angiogenin cleaves tRNA and promotes stress-induced translational repression.' *J Cell Biol* **185**(1): 35-42.

Yoon, J. H. (2009). 'Effects of spNab2 deletion and over-expression on mRNA export.' *Korean J Microbiol* **45**: 300-305.

Yoon, J. H., K. Abdelmohsen and M. Gorospe (2013). 'Posttranscriptional gene regulation by long noncoding RNA.' *J Mol Biol* **425**(19): 3723-3730.

Yoon, J. H., K. Abdelmohsen, S. Srikantan, X. Yang, J. L. Martindale, S. De, M. Huarte, M. Zhan, K. G. Becker and M. Gorospe (2012). 'LincRNA-p21 suppresses target mRNA translation.' *Mol Cell* **47**(4): 648-655.

Yudkovsky, N., J. A. Ranish and S. Hahn (2000). 'A transcription reinitiation intermediate that is stabilized by activator.' *Nature* **408**(6809): 225-229.

Zaros, C. and P. Thuriaux (2005). 'Rpc25, a conserved RNA polymerase III subunit, is critical for transcription initiation.' *Mol Microbiol* **55**(1): 104-114.

Zhang, D. W., J. B. Rodriguez-Molina, J. R. Tietjen, C. M. Nemec and A. Z. Ansari (2012). 'Emerging Views on the CTD Code.' *Genet Res Int* **2012**: 347214.

Zhao, J., L. Hyman and C. Moore (1999). 'Formation of mRNA 3' ends in eukaryotes: mechanism, regulation, and interrelationships with other steps in mRNA synthesis.' *Microbiol Mol Biol Rev* **63**(2): 405-445.

Zheng, C., M. B. Fasken, N. J. Marshall, C. Brockmann, M. E. Rubinson, S. R. Wente, A. H. Corbett and M. Stewart (2010). 'Structural basis for the function of the Saccharomyces cerevisiae Gfd1 protein in mRNA nuclear export.' *J Biol Chem* **285**(27): 20704-20715.

Acknowledgements

Curriculum vitae

Personal data

Luitpold Maximilian Reuter
born June 27th,1987 in Regensburg
Nationality: german
Single

Education

|	
08/1997 – 06/2006	'Abitur', Gymnasium St. Xaver, Bad Driburg
10/2006 – 08/2011	Study of ´Humanbiologie' (Diploma), Philipps-Universität Marburg
09/2008	'Vordiplom' in 'Humanbiologie', Philipps-Universität Marburg
09/2010	Diploma examinations in biochemistry and cell biology (major) and molecular biology (minor), Philipps-Universität Marburg
10/2010 – 08/2011	Diploma thesis at the 'Institut für Molekularbiologie und Tumorforschung', Philipps-Universität Marburg, AG Brehm Title of the diploma thesis: 'Analysis of Protein Interactions in the dLINT-Complex'
08/2011	Diploma in 'Humanbiologie'
Since 10/2011	Ph.D. student in the laboratory of Prof. Dr. Katja Sträßer, Gene Center, Ludwigs-Maximilian Universität München, Title of the PhD project: 'The poly(A)-binding protein Nab2 functions in RNA Polymerase III transcription'

Grad schools/stipend

|	
Since 10/2011	Student of the 'International Max Planck Research School for Molecular and Cellular Life Sciences' MPI of Biochemistry, Munich
Since 09/2014	Student of the 'The International Research Training Group GRK 1384' JLU Giessen

Appendix
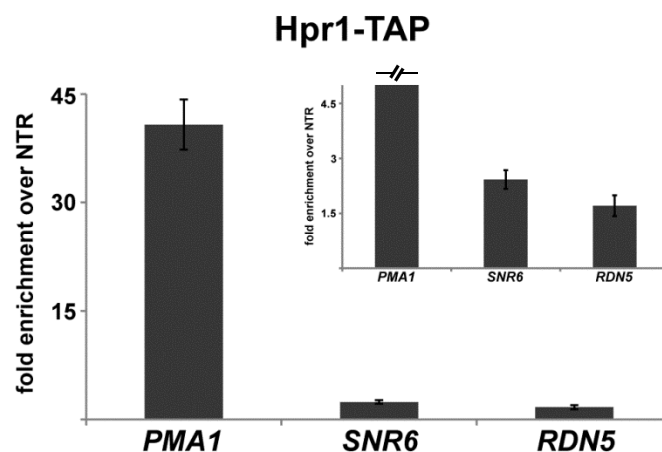
Fig. A1: Hpr1 is recruited to RNAPII but not to RNAPIII transcribed genes. ChIP analysis was done under standard condition with *HPR1-TAP* harboring cells. *PMA1* is a RNAPII transcribed gene, *SNR6* and *RDN5* are RNAPIII transcribed genes (RNAPIII). An enlargement of the low occupancies is given in the right upper corner. Data (n> 3) represent the mean ± SD.
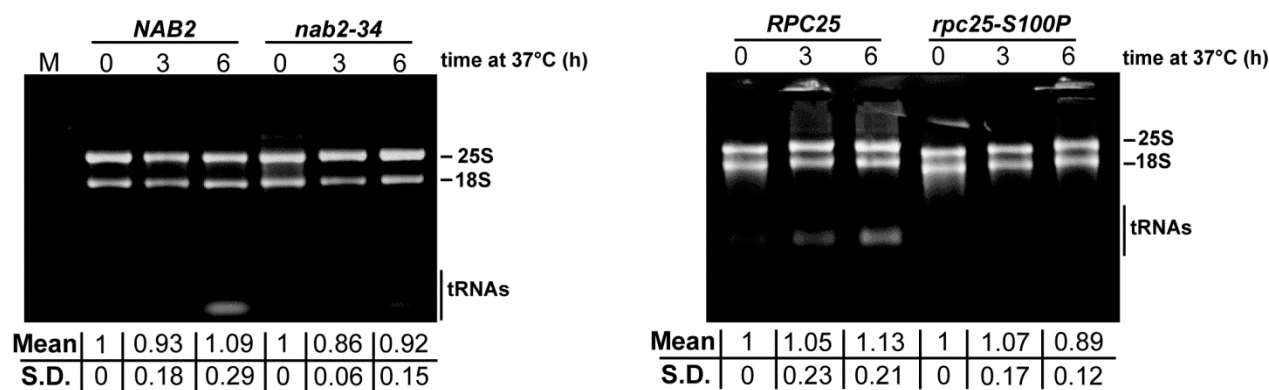
Fig. A2: Nab2 is required for full RNAPIII transcriptional activity *in vivo*. The amount of RNA used in Northern Blots. 1 μg of total RNA of wild-type, *nab2-34*, or *rpc25-S100P* cells, which were shifted to 37 °C for the indicated amount of time, was loaded on 2% Formaldehyde agarose gels. Total RNA was visualized by Ethidium bromide staining. 25S rRNA and 18S rRNA levels were analyzed and quantified. Data represent the mean ± SD of at least 4 independent biological replicates.

A

B
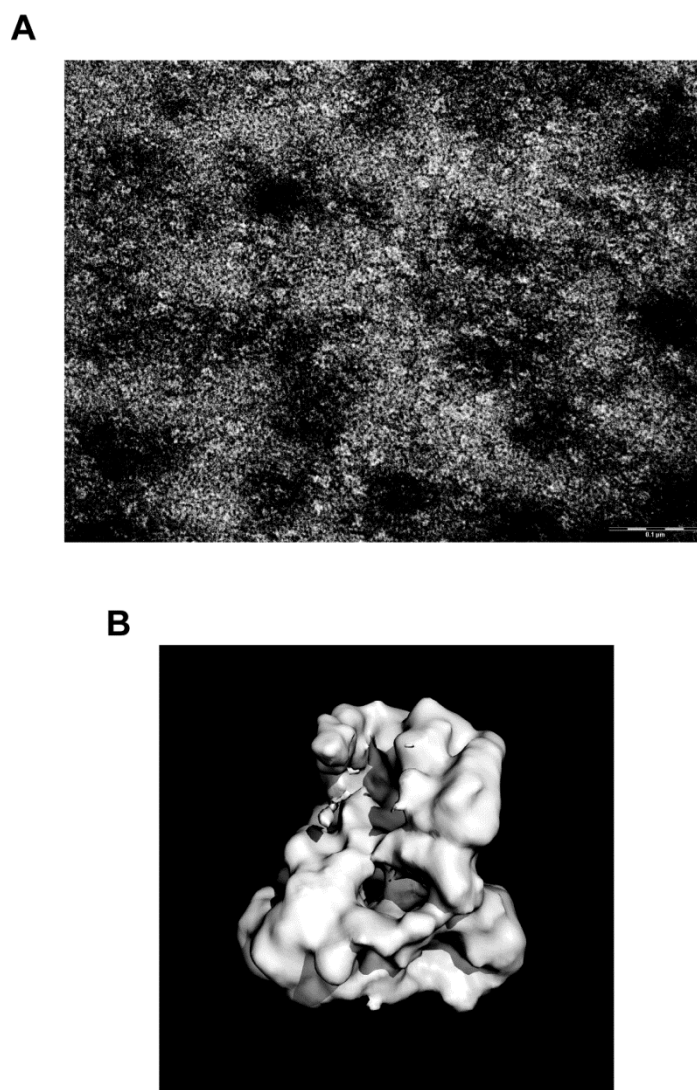
Fig. A3: Reconstruction of an initial 3D RNAPIII model with Nab2 from electron microscopy micrographs. **(A)** A representative electron micrograph showing negatively stained RNAPIII-Nab2 complexes from *S. cerevisiae* spotted on a carbon coated electron microscopy grid. The single, bright complexes were distributed evenly all over the grid and could be picked for analysis. Note that differences in size and shape are due to the orientation of RNAPIII-Nab2 on the grid. **(B)** Initial reconstruction of the core RNAPIII enzyme. Previously compiled class averages were used to generate this 3D reconstruction of the polymerase. Note that the view is the same as in Results 3.9, Fig. 34. No additional and reliable extra density could be identified from this dataset.

Fig. A4: The conservation of Nab2 orthologues in exemplary fungi species. An alignment of *S. cerevisiae* Nab2 and its orthologues from *Chaetomium thermophilum* (Nab2) and *Saccharomyces pombe* (spNab2) is shown. Different shades of blue indicate the degree of conservation between the different organisms. Green bars mark the seven zinc finger in *S. cerevisiae* Nab2. The alignment file was generated with Clustal Omega multiple sequence alignment software (Sievers et al., 2011) and modified using Jalview2 software (Waterhouse et al., 2009).